

Université de Lille  
École Doctorale Biologie-Santé de Lille

**Thèse de Doctorat**  
**Elodie LEBREDONCHEL**

En vue de l'obtention du grade de  
Docteur de l'Université de Lille  
Discipline : Aspects cellulaires et moléculaires de la biologie  
Spécialité : Biochimie et biologie moléculaire  
Laboratoire : Unité de Glycobiologie Structurale et Fonctionnelle UGSF, Villeneuve d'Ascq, France

**Etude de la fonction de TMEM165 dans la glycosylation  
golgienne et de sa dégradation induite par le  
manganèse**

Présentée le 04 septembre 2020 devant la commission d'examen

Président: Pr. Jean-Louis GUEANT (Université de Lorraine, France)  
Rapporteurs: Pr. Rita GERARDY-SCHAHN (Faculté de médecine d'Hanovre, Allemagne)  
Dr. Vincent CANTAGREL (Institut Imagine Paris, France)  
Examineur: Pr. Jaak JAEKEN (KU Leuven, Belgique)  
Directeurs de thèse: Dr. François FOULQUIER (CNRS, Lille, France) et  
Dr. André KLEIN (Centre Hospitalier Universitaire de Lille, France)

Université de Lille  
École Doctorale Biologie-Santé de Lille

**Doctoral Thesis**  
**Elodie LEBREDONCHEL**

To obtain the degree of PhD  
Discipline: Cellular and molecular aspects of biology  
Specialty: Biochemistry and molecular biology

**Insights into TMEM165 function in Golgi glycosylation  
and lysosomal Mn-induced degradation**

Presented on September, the 4<sup>th</sup> 2020 in front of the examination board

President: Pr. Jean-Louis GUEANT (Lorraine University, France)

Reporters: Pr. Rita GERARDY-SCHAHN (Hannover Medical School, Germany)  
Dr. Vincent CANTAGREL (Imagine Institute, France)

Examiner: Pr. Jaak JAEKEN (KU Leuven, Belgium)

PhD supervisors: Dr. François FOULQUIER (CNRS, Lille University, France) and  
Dr. André KLEIN (Lille University Medical Center, France)

## ABSTRACT

Glycobiology is the study of complex sugars, also known as glycans or carbohydrates in biology, including the study of their structure, biosynthesis and functions. These glycans are a major post-translational modification for lipids and/or proteins. Any defects in this finely-regulated process can lead to diseases. Congenital Disorder of Glycosylation (CDG) is an emerging group of rare inherited disorders with an impaired glycan biosynthesis. TMEM165-CDG was characterized in 2012 as a defect in TMEM165 protein, the first member of the Uncharacterized Protein Family 0016 (UPF0016). Although the precise role of TMEM165 in glycosylation is still elusive, our results highly suggest that TMEM165 acts as a Golgi  $\text{Ca}^{2+}/\text{Mn}^{2+}$  antiport transporter regulating both  $\text{Ca}^{2+}$  and  $\text{Mn}^{2+}$  Golgi homeostasis, the latter being required as a cofactor for some Golgi glycosylation enzymes. Interestingly, we recently demonstrated that besides its role in regulating Golgi  $\text{Mn}^{2+}$  homeostasis and consequently Golgi glycosylation, TMEM165 was sensitive to high manganese exposure. Members of the UPF0016 family contain two particularly highly conserved consensus motifs E- $\phi$ -G-D-[KR]-[TS]. We demonstrated the importance of these two conserved motifs and underlined the contribution of some specific amino acids in both Golgi glycosylation and  $\text{Mn}^{2+}$  sensitivity. Another Golgi protein is known to import manganese from the cytosol to the Golgi lumen, SPCA1, which is the Golgi  $\text{Ca}^{2+}/\text{Mn}^{2+}$  ATPase pump. Studying a potential functional link between TMEM165 and SPCA1, we first noticed a nearly complete loss of TMEM165 in SPCA1 deficient HAP1 cells. We demonstrate that TMEM165 was constitutively degraded in lysosomes in the absence of SPCA1. Complementary studies showed that TMEM165 abundance was directly dependent on the function of SPCA1 and more specifically on the capacity to pump  $\text{Mn}^{2+}$  from the cytosol into the Golgi lumen. Among SPCA1 mutants that differentially impair  $\text{Mn}^{2+}$  and  $\text{Ca}^{2+}$  transport, only the Q747A mutant that imports quasi-exclusively  $\text{Mn}^{2+}$ , rescued the abundance and Golgi subcellular localization of TMEM165.

This work provides a new contribution to the cellular and molecular characterization of TMEM165, resulting in the conception of a new model of function of this protein.

## RESUME

La glycobiologie est l'étude des sucres complexes, nommés glycanes ou glucides en biologie. Elle inclue l'étude de leur structure, leur biosynthèse ainsi que leur fonction. Ces glycanes constituent une modification post-traductionnelle majeure des lipides et des protéines ; une anomalie de leur métabolisme peut conduire à des pathologies. Les déficits congénitaux de la glycosylation (CDG) sont un groupe de maladies rares dans lesquelles la biosynthèse des glycanes est altérée. Le TMEM165-CDG a été mis en évidence pour la première fois en 2012, il est causé par une anomalie de la protéine TMEM165, premier membre de la famille UPF0016. Même si son rôle dans la glycosylation reste controversé, nos résultats suggèrent que TMEM165 serait un antiporteur  $\text{Ca}^{2+}/\text{Mn}^{2+}$  golgien régulant l'homéostasie du manganèse au niveau de l'appareil de Golgi. Le manganèse est un cofacteur majeur de nombreuses enzymes de glycosylation, essentiellement des galactosyltransférases responsable du défaut de glycosylation observé dans les cellules des patients. Paradoxalement, nous avons également démontré que TMEM165 est spécifiquement dégradée en cas d'exposition à de fortes concentrations de manganèse.

Les membres de la famille UPF0016 contiennent deux motifs consensus extrêmement conservés E- $\phi$ -G-D-[KR]-[TS]. Nous avons démontré l'importance cruciale de ces deux séquences en soulignant la contribution de certains acides aminés spécifiques à la fois de la fonction de glycosylation et la sensibilité au manganèse de TMEM165.

Parallèlement, nous avons étudié le lien entre TMEM165 et une deuxième protéine connue pour importer du manganèse dans le compartiment golgien : SPCA1, une pompe calcique ATPasique. Notre première observation a été l'absence quasi-totale d'expression de TMEM165 dans les lignées cellulaires KO SPCA1, conséquence d'une dégradation de TMEM165 au niveau du compartiment lysosomal. Des études complémentaires ont montré que l'expression de TMEM165 était directement liée à la capacité de SPCA1 à importer du manganèse.

Parmi les mutants de SPCA1, ayant une anomalie sélective du transport du manganèse et/ou du calcium, seul le mutant Q747A responsable d'un apport quasi-exclusif de manganèse était en mesure de restaurer l'expression et la localisation subcellulaire de TMEM165. Il s'agit de la première mise en évidence d'un lien fonctionnel entre TMEM165 et SPCA1.

Ce travail complète la caractérisation cellulaire et moléculaire de TMEM165 et permet de proposer un nouveau modèle de fonctionnement de la protéine.

This thesis has been supervised by Dr André Klein and Dr François Foulquier and conducted  
in the Unité de Glycobiologie Structurale et Fonctionnelle (UGSF)  
CNRS UMR-8576 laboratory (directed by Pr Yann Guerardel), Villeneuve d'Ascq, France

This work was financed by Lille University Medical Center

## PUBLISHED ARTICLES

- **Dissection of TMEM165 function in Golgi glycosylation and its Mn<sup>2+</sup> sensitivity**  
Lebredonchel, E., Houdou, M., Potelle, S., de Bettignies, G., Schulz, C., Krzewinski Recchi, M.-A., Lupashin, V., Legrand, D., Klein, A., and Foulquier, F. (2019) *Biochimie* 165, 123–130.
- **Investigating the functional link between TMEM165 and SPCA1**  
Lebredonchel, E.\*, Houdou, M.\* , Hoffmann, H.-H., Kondratska, K., Krzewinski, M.-A., Vicogne, D., Rice, C.M., Klein, A., and Foulquier, F. (2019) *Biochem. J.* 476, 3281–3293.
- **Involvement of thapsigargin and cyclopiazonic acid sensitive pumps in the rescue of TMEM165-associated glycosylation defects by Mn<sup>2+</sup>**  
Houdou, M., Lebredonchel, E., Garat, A., Duvet, S., Legrand, D., Decool, V., Klein, A., Ouzzine, M., Gasnier, B., Potelle, S., et al. (2019) *FASEB J.* 33, 2669–2679.
- **Manganese-induced turnover of TMEM165**  
Potelle, S., Dulary, E., Climer, L., Duvet, S., Morelle, W., Vicogne, D., Lebredonchel, E., Houdou, M., Spriet, C., Krzewinski-Recchi, M.-A., et al. (2017) *Biochem. J.* 474, 1481–1493.

## ORAL COMMUNICATIONS

- **CNBBMM seminary Caen, France, September 26-28<sup>th</sup> 2019**  
*“Function of TMEM165 in Glycosylation, Manganese homeostasis and link with SPCA1”*
- **25th International Symposium on Glycoconjugates, Milan, Italy**  
August 25-31<sup>st</sup> 2019 Session: Golgi dynamics in Health and Disease  
*“Function of TMEM165 in Glycosylation, Manganese homeostasis and link with SPCA1”*
- **29<sup>th</sup> Joint of Glycobiology, Ghent, Belgium, October 21-23<sup>rd</sup> 2018**  
*“Dissection of TMEM165 function in Golgi glycosylation and its Mn<sup>2+</sup> sensitivity”*
- **Weekly seminary UGSF IRI C9 Lille, May 25th 2018**  
*“Dissection of TMEM165: function in Golgi glycosylation & Mn<sup>2+</sup>-induced degradation”*
- **Joints Workshop of the International Associated Laboratory, Nancy, France, October 18-19<sup>th</sup> 2017** *“Glycans & Proteoglycans: The Sweet and Smart Molecules of the 21th Century”*. My glycans in 300s, *“Role of the cation antiporter TMEM165 in cellular Golgi N-glycosylation”*

## POSTER COMMUNICATIONS

- **30<sup>th</sup> Joint of Glycobiology, Lille, France, October 27-29<sup>th</sup> 2019**

*“Role of TMEM165 - a protein involved in a CDG type II- in glycosylation, manganese homeostasis and link with SPCA1”*

E. Lebretonchel, M. Houdou, A. Klein, F. Foulquier

- **4<sup>th</sup> World Conference on CDG, Lisbonne, August 25-27<sup>th</sup> 2019**

*“Clues for TMEM165-CDG treatment”*+ flash presentation Poster award

E. Lebretonchel, M. Houdou, E. Morava, J. Jaeken, F. Foulquier

- **3<sup>èmes</sup> journées scientifiques du GDR Gagoscience, Lille, France, September 25<sup>th</sup> 2018**

*“TMEM165, a Golgi protein involved in a CDG-subtype (Congenital Disorders of Glycosylation), function in Golgi glycosylation, Mn<sup>2+</sup> sensitivity & link with SPCA1”*

E. Lebretonchel, M. Houdou, A.S. Roy, F. Foulquier, A. Klein

- **JAV Journée André Verbert, Lille, September 13<sup>th</sup> 2018**

*“TMEM165, a Golgi protein involved in a CDG-subtype (Congenital Disorders of Glycosylation), function in Golgi glycosylation, Mn<sup>2+</sup> sensitivity & link with SPCA1”* + oral flash presentation

E. Lebretonchel, M. Houdou, A.S. Roy, F. Foulquier, A. Klein

- **XIV<sup>th</sup> International Congress of Paediatric Laboratory Medicine & IFCC WorldLab 2017, Durban, South Africa, October 20-25<sup>th</sup> 2017**

*“Role of TMEM165, a Golgi protein involved in a subtype of CDG (Congenital Disorders of Glycosylation) “*

E. Lebretonchel, M. Houdou, S. Potelle, E. Morava, J. Jaeken, A. Klein, F. Foulquier

## LIST OF ABBREVIATIONS

ADCC: Antibody-Dependent Cell-mediated cytotoxicity  
AE2a: Anion Exchanger 2a  
AGA: AspartylGlucosAminidase  
ALG: Asparagine-Linked Glycosylation  
ALS: Amyotrophic Lateral Sclerosis  
ApoC-III: Apolipoprotein C-III  
ARCL: Autosomal Recessive Cutis Laxa  
ASGR: AsialoGlycoprotein Receptor  
Asn: Asparagine  
ATCC: American Type Culture Collection  
ATP: Adenosine TriPhosphate  
ATPase: Adenosine TriPhosphatase  
B4GALT1:  $\beta$ -1,4-galactosyltransferase I  
BBB: Brain-Blood Barrier  
BFA: Brefeldin A  
BSA: Bovin Serum Albumin  
Ca<sup>2+</sup>: Calcium ion  
CAB45: Calcium-Binding Protein 45  
CaCA: Ca<sup>2+</sup>/cation antiporter  
CATCHR: Complexes Associated with Tethering Containing Helical Rods  
CAX: Ca<sup>2+</sup>/H<sup>+</sup> exchanger family  
CAZY: Carbohydrate-Active enZYmes  
CCD: COG Complex-Dependent  
CCDC15: Coiled-Coil Domain-Containing protein 15  
CCT: Coiled-Coiled Tethers  
CD-MPR: Calcium-Dependent MPR  
CD107b: Cluster of Differentiation 107b  
CDDG: Congenital Disorder of DeGlycosylation  
CDG-I: Type I CDG  
CDG-II: Type II CDG  
CDG: Congenital disorders of glycosylation  
CFTR: Cystic fibrosis transmembrane conductance regulator  
CI-MPR: Calcium-Independent MPR  
CMD: Congenital Muscular Dystrophy  
CML: Chronic Myeloid Leukemia  
CMS15: Congenital Myastenic Syndrome 15  
CMT1 : Chloroplast Manganese Transporter 1  
CNS : Central Nervous System  
CNX: Calnexin  
Co<sup>2+</sup>: Divalent cobalt ion  
COG: Conserved Oligomeric Golgi complex  
COP: Coat Protein Complex  
CORVET: Class C Core Vacuole/Endosome Tethering  
COSMC: COre 1  $\beta$ 3-Gal-T-Specific Molecular Chaperone  
CRD: Carbohydrate Recognition Domain

CRISPR-cas9 : Clustered Regularly Interspaced Short Palindromic Repeats-CRISPER associated protein 9  
CRT: Calreticulin  
CTLA4: Cytotoxic T Lymphocyte-Associated protein 4  
CTS: Cytoplasmic Tail-transmembrane Spanning domain  
Cu<sup>2+</sup>: Divalent copper ion  
DAPI: 4',6'-DiAmidino-2-PhenylIndole  
DCT1: Divalent Cation Transporter 1  
DIBD1: Disrupted in Bipolar Disorder protein 1  
DIM: dideoxy-1,4-imino-D-mannitol  
DK1: Dolichol Kinase 1  
DMEM: Dulbecco's Modified Eagle's Medium  
DMT1: Divalent Metal Transporter 1  
Dol-P: Dolichol phosphate  
Dol-PP: Dolichol pyrophosphate  
Dol: Dolichol  
DPAGT1-CDG: Dolichyl-Phosphate N-Acetylglucosaminophosphotransferase 1  
DPBS: Dulbecco's Phosphate Buffer Saline  
DPM: Dolichol-Phosphate Mannosyltransferase  
ECL: Enhanced ChemiLuminescence  
EDEM: ER Degradation-Enhancing  $\alpha$ -Mannosidase-like protein  
EDTA: Ethylene Diamine Tetraacetic Acid  
EE: Early Endosomes  
EGFR: Epidermal Growth Factor Receptor  
EGTA: Ethylene glycol-bis( $\beta$ -aminoethyl ether)-*N,N,N',N'*-tetraacetic acid  
ENGase: Endo- $\beta$ -*N*-Acetylglucosaminidase  
ER: Endoplasmic Reticulum  
ERAD: ER Associated Degradation  
ERES: ER Exit Sites  
ERGIC: ER-Golgi intermediate compartment  
Fab: antigen binding Fragment  
Fc: crystallizable Fragment  
Fuc: Fucose  
GA: Golgi Apparatus  
GAG: Glycosaminoglycans  
Gal: Galactose  
GalNAc: N-acetylgalactosamine  
GALNT2: GalNAc Transferase 2  
GalT:  $\beta$ -1,4-GalactosylTransferase I  
GARP: Glycoprotein A Repetitions Predominant  
GCS1: Glucosidase 1  
Gdt1: Gcr1 Dependent Translation factor 1  
GFP: Green Fluorescent Protein  
GGA1: Golgi Associated, Gamma Adaptin Ear Containing, ARF Binding Protein 1  
GH: GlycosylHydrolase  
GLB1:  $\beta$ -Galactosidase

Glc-6-P: Glucose-6-phosphate  
Glc: Glucose  
GlcNAc-T: GlcNAc transferase  
GlcNAc: N-acetylglucosamine  
GLUT: GLUcose Transporter  
GM: MonosialoGanglioside  
GM130: Golgi Marker protein 130  
GO: Gerodermia Osteodysplastica  
GORAB: Golgin RAB6 Interacting  
GPHR: Golgi pH Regulator  
GPI: GlycosylPhosphatidylInositol  
GPT: GlcNAc-1-P Transferase  
GRASP: Golgi ReAssembly Stacking Protein  
GRP: Glucose-Regulating stress Protein  
GT: GlycosylTransferases  
GWAS: Genome-Wide Association Study  
HDR1: ERAD-associated E3 ubiquitin-protein ligase  
HFRC1: Homolog of FRinge Connection protein 1  
HMT1: protein arginine MethylTransferase 1  
HOPS: Homotypic fusion and Protein Sorting complexes  
HRP: Horse Radish Peroxidase  
HSP: Heat Shock Protein  
ICAM: Intercellular Adhesion Molecule 1  
ICP-MS: Inductively Coupled Plasma Mass Spectrometry  
IEF: IsoElectricoFocusing  
IP3: Inositol-3-Phosphate  
IP3R: IP3 Receptor  
IPD: Idiopathic Parkinson Disease  
IVIg: Intravenous Immunoglobuline  
KD: KnockDown  
KO: KnockOut  
LacNAc: N-acetyllactosamine  
LAD II: Leukocyte Adhesion Deficiency type II  
LAMAN1: Lectin Mannose-Binding 1  
LAMP: Lysosomal-Associated Membrane Protein  
LAS : Low Affinity Systems  
LIMP: Lysosomal Integral Membrane Protein  
LLO: Lipid-Linked Oligosaccharide  
LMP: Lysosomal Membrane Protein  
M6P: Mannose-6-Phosphate  
Man: Mannose  
ManR: Mannose Receptor  
MAN2A1: Alpha-mannosidase 2  
Man2C1: Mannosidase  $\alpha$  class 2C Member 1  
MANBA:  $\beta$ -mannosidase  
MBCD: Methyl- $\beta$ -CycloDextrin

MBP: Mannose Binding Protein  
Mg<sup>2+</sup>: Magnesium ion  
MGAT: Mannosyl  $\alpha$ 1,3-Glycoprotein  $\beta$ 1,2-N-acetylglucosaminyltransferase  
MIM: Mendelian Inheritance in Man  
Mn<sup>2+</sup>: Divalent manganese ion  
MnDPDP: Mangafodipir trisodium  
MnSOD: Manganese SuperOxide Dismutase  
MTOC: Microtubules Organizing Center  
MOGS: Mannosyl-Oligosaccharide Glucosidase  
MOPS: 3-N-morpholino propanesulfonic acid  
MPDU1: Mannose-Phosphate Dolichol Utilization Defect 1  
MPR: Mannose-6-Phosphate Receptor  
mRNA: Messenger RNA  
MS: Multiple Sclerosis  
MTC: Multisubunit Tethering/Trafficking Complexes  
NEU1: Neuraminidase  
Neu5Ac: N-acetylneuraminic acid  
NeuAc: N-acetylneuraminic acid  
NGLY1: N-Glycanase 1  
NHE: Sodium/Hydrogen Exchanger  
NRAMP2: Natural Resistance Associated Macrophage Protein 2  
NST: Nucleotide Sugar Transporter  
OEC: Oxygen Evolving Complex  
OMIM: Online Mendelian Inheritance in Man  
OST: Oligosaccharyltransferase  
PAM71: Photosynthesis Affected Mutant 71  
PAS: Para-AminoSalicylic acid  
PBS: Phosphate Buffer Saline  
PCR: Polymerase chain reaction  
PDGFR: Platelet-Derived Growth Factor Receptors  
PDI: Protein Disulfate Isomerase  
PFA: Paraformaldehyde  
Pi: Inorganic Phosphate  
PI: Phosphatidylinositol  
PLA: Proximity Ligation Assay  
PMCA: Plasma Membrane Calcium ATPase  
Pmr1p: Plasma Membrane ATPase Related  
PPI: Peptidyl Prolyl Isomerase  
PSII: Photosystem II  
PTM: Post-Translational Modification  
RA: Rheumatoid Arthritis  
RFT1: Requiring Fifty Three 1 homolog  
ROS: Reactive Oxygen Species  
RT-qPCR : Reverse Transcription – quantitative Polymerase Chain Reaction  
RyR: Ryanodine Receptor  
SDS-PAGE: Sodium Dodecyl Sulfate Poly-Acrylamide Gel Electrophoresis

Ser: Serine  
SERCA: Sarcoplasmic/Endoplasmic Reticulum Calcium Pump 2  
siRNA: Small interfering RNA  
SLC11A2: Solute Carrier Family 11, member 2  
SLE: Systemic Lupus Erythematosus  
SLGT: Sodium/Glucose Transporters  
SNARE: SNAP (Soluble NSF attachment protein) receptor  
SOC: Store-Operated Calcium  
SOD-2: SuperOxide Dismutase 2  
SPCA1: Secretory Pathway Ca<sup>2+</sup>-ATPase isoform 1  
SRD5A3: Steroid 5 Alpha-Reductase 3  
ST3Gal1:  $\alpha$ 2,3-sialyltransferase I  
ST6Gal1:  $\alpha$ 2,6-sialyltransferase I  
TBS: Tris Buffer Saline  
TCR: T-Cell Receptor  
TGN: *Trans*-Golgi network  
TGN46: Trans-Golgi Network protein 46  
Thr: Threonine  
TM: Transmembrane  
TMBIM: Transmembrane Bax Inhibitor-1 Motif containing  
TMD: Transmembrane Domain  
TMEM165: Transmembrane Protein 165  
TMEM199: TransMembrane Protein 199  
TRAP: TRanslocon-Associated Protein complex  
TRAPP: Transport Protein Particles  
Trp: Tryptophane  
UDP: Uridine DiPhosphate  
UDP: Uridine diphosphate  
UGGT: UDP-glucose: glycoprotein glucosyltransferase  
UGSF: Unité de Glycobiologie Structurale et Fonctionnelle  
UMP: Uridine MonoPhosphate  
VIP36: Vesicular Integral-Membrane Protein 36  
VIPL: VIP36-Like Protein  
WB: Western-Blot  
XDP: Nucleotide DiPhosphate  
XMP: Nucleotide MonoPhosphate  
ZIP8: Zrt- and Irt-like protein 8  
Zn<sup>2+</sup>: Divalent zinc ion

## TABLE OF CONTENTS

### ACKNOWLEDGEMENTS

### ABSTRACT

### ABSTRACT IN FRENCH

### ABREVIATIONS

### TABLE OF CONTENT

### LIST OF FIGURES

### LIST OF TABLES

### GENERAL INTRODUCTION .....1

### CHAPTER 1: *N*-glycoproteins biosynthesis.....3

#### 1.1 *N*-glycans structure.....4

#### 1.2 *N*-glycosylation process.....5

##### 1.2.1 Biosynthesis of the *N*-linked glycan precursor in the ER.....5

###### 1.2.1.1 the dolichol cycle.....7

###### 1.2.1.2 Defects in the precursor synthesis .....8

###### 1.2.1.3 Transfer of the dolichol precursor on a nascent protein.....9

###### 1.2.1.4 The role of chaperones.....11

###### 1.2.1.5 Glucosidases and mannose trimming .....11

###### 1.2.1.6 Glycan-mediated ERQC (ER quality control) .....12

###### 1.2.1.7 ERAD (Endoplasmic Reticulum-Associated Protein Degradation) pathway.....12

###### 1.2.1.8 ER/Golgi Intermediate Compartment (ERGIC), from ER to Golgi back and forth.....14

##### 1.2.2 Sequential maturation of *N*-linked glycans through GA.....15

#### 1.3 Degradation of *N*-glycoconjugates .....16

##### 1.3.1 Lysosomal compartment generalities.....16

##### 1.3.2 Hydrolases targeting.....17

##### 1.3.3 Breakdown of glycoconjugates in the lysosome.....18

#### 1.4 Functions of *N*-glycans.....20

##### 1.4.1 Role of the *N*-glycan during their biosynthesis.....20

###### 1.4.1.1 calnexin/calreticulin cycle.....20

###### 1.4.1.2 Mannose-6-Phosphate.....20

##### 1.4.2 Role of the mature glycoconjugate.....20

###### 1.4.2.1 Role of the *N*-glycan backbone.....20

###### 1.4.2.2 Role of the periphery of the *N*-glycan.....22

##### 1.4.3 Role of the *N*-glycans in the catabolism of glycoconjugates.....25

#### 1.4.4 General approach of the role of glycans.....25

### CHAPTER 2: Regulation of the *N*-glycosylation process.....26

#### 2.1 The role of Golgi structure .....26

##### 2.1.1 Golgi discovery.....26

##### 2.1.2 Golgi architecture.....26

##### 2.1.3 Actors of the maintenance of the Golgi structure.....27

##### 2.1.4 Controversies about Golgi dynamic.....28

###### 2.1.4.1 The cisternal maturation model.....28

###### 2.1.4.2 The intra-Golgi vesicular transport model.....29

#### 2.2 Golgi intravesicular trafficking.....30

##### 2.2.1 COG complex.....31

2.2.1.2 COG complex mechanism in vesicle tethering.....	32
2.2.1.2 COG complex and <i>N</i> -glycosylation.....	33
2.2.1.3 COG-CDGs.....	34
<u>2.4.2 Other membrane trafficking CDGs.....</u>	34
2.2.2.1 TRAPP complexes.....	35
2.2.2.2 Golgin RAB6 Interacting (GORAB) .....	35
<u>2.3 Nucleotide-sugars.....</u>	35
<u>2.3.1 Nucleotide-sugar sources.....</u>	35
2.3.1.1 Import of exogenous sugars.....	35
2.3.1.2 Recycling.....	36
2.3.1.3 Monosaccharides interconversion.....	36
<u>2.3.2 Nucleotide sugar transporters.....</u>	37
2.3.2.1 NST properties.....	37
2.3.2.2 NST-CDGs.....	38
<u>2.4 Glycosylation enzymes.....</u>	39
<u>2.4.1 Classification.....</u>	39
<u>2.4.2 GT structure.....</u>	40
<u>2.4.3 Specificity.....</u>	40
<u>2.4.4 Regulation.....</u>	40
2.4.4.1 Localization.....	41
2.4.4.2 Multimerization.....	41
2.4.4.3 The lipid bilayer sorting model.....	42
<u>2.4.5 Glycosyltransferases-CDG.....</u>	43
<u>2.5 The importance of Golgi pH homeostasis in <i>N</i>-glycosylation.....</u>	43
<u>2.5.1 Regulation of pH homeostasis.....</u>	43
2.5.1.1 The Vacuolar H <sup>+</sup> -ATPase.....	45
2.5.1.2 Counter ion conductance.....	45
2.5.1.3 Proton leak channel.....	45
<u>2.5.2 <i>N</i>-glycosylation abnormalities due to pH misregulation.....</u>	46
2.5.2.1 The Vacuolar- H <sup>+</sup> -ATPase structure.....	46
2.5.2.2 The Vacuolar-type H <sup>+</sup> -ATPase related CDG .....	47
<u>2.6 Divalent cations Golgi homeostasis.....</u>	48
<u>2.6.1 Calcium homeostasis.....</u>	48
2.6.1.1 Calcium concentration.....	48
2.6.1.2 Calcium uptake.....	49
<u>2.6.1.2.1 SERCA .....</u>	49
<u>2.6.1.2.2 SPCA1.....</u>	50
SPCA1 features.....	50
Hailey-Hailey Disease.....	50
2.6.1.3 Channels for Ca <sup>2+</sup> leaks: IP <sub>3</sub> R and RyR.....	51
<u>2.6.2 Other divalent cations homeostasis.....</u>	51
<b>CHAPTER 3: Manganese homeostasis.....</b>	<b>52</b>
<u>3. 1 Manganese on earth.....</u>	<b>52</b>
<u>3.2.1 Manganese sources.....</u>	<b>52</b>
<u>3.2.2 Manganese absorption, distribution, and elimination.....</u>	<b>52</b>
<u>3.2.3 Physiological values and toxicity.....</u>	<b>53</b>

<u>3.2.4 Focus on the influence of manganese on the skeletal system</u> .....	54
<u>3.3 Manganese in the cell</u> .....	54
<u>3.3.1 Manganese transporters</u> .....	54
3.3.1.1 Manganese plasma membrane transporters.....	54
Transferrin	
DMT1	
SLC30A10	
SLC39A8	
SLC39A14	
3.3.1.2 Manganese secretory pathway transporters.....	57
SPCA1/2	
TMEM165	
SERCA2	
<u>3.3.2 Manganese and glycosylation</u> .....	57
3.3.2.1 Manganese-dependent glycosyltransferases.....	58
3.3.2.2 $\beta$ -1,4-galactosyltransferase 1.....	59
<u>3.4 Manganese-linked pathologies</u> .....	61
<u>3.4.1 Manganese deficiency</u> .....	61
SLC39A8	
<u>3.4.2 Manganese excess</u> .....	62
<u>3.4.1 Physiopathology of manganese excess</u> .....	62
<u>3.4.2 Manganism, a chronic pathology due to long-term manganese exposure</u> .....	63
Diagnosis	
Clinical aspects	
Treatment	
<u>3.4.3 Pathologies due to mutations of manganese transporters</u> .....	64
SLC30A10	
SLC39A14	
Treatments	
<b>CHAPTER 4: TMEM165</b> .....	67
<u>4.1 TMEM165 structure, dynamic, stability</u> .....	67
<u>4.1.1 TMEM165, gene, protein, orthologs, and localization</u> .....	67
<u>4.1.2 TMEM165 topology</u> .....	68
<u>4.1.3 TMEM165 stability</u> .....	68
<u>4.2 TMEM165 function</u> .....	70
<u>4.2.1 Role of TMEM165 in glycosylation</u> .....	70
<u>4.2.2 Role of TMEM165 in calcium homeostasis</u> .....	71
<u>4.2.3 Link between TMEM165 and pH</u> .....	72
<u>4.2.4 Role of TMEM165 in manganese homeostasis</u> .....	75
4.2.4.1 Glycosylation defect in Gdt1/TMEM165 deficient cells results of misregulation of Golgi manganese homeostasis	
4.2.4.2 In yeast Gdt1 could be the leak channel of Pmr1	
4.2.4.3 Plant ortholog PAM71 of TMEM165 is a $Mn^{2+}/Ca^{2+}$ antiporter	
<u>4.2.5 Restoration of the glycosylation defect in TMEM165-depleted cells</u> .....	77
4.2.5.1 Restoration of the glycosylation defect in TMEM165-depleted cells by manganese	
4.2.5.2 Restoration of the glycosylation defect in TMEM165-depleted cells by galactose	

<u>4.2.6 Actual model</u> .....	78
<u>4.3 TMEM165-CDG</u> .....	79
<u>4.3.1 Mutations localization in <i>TMEM165</i> gene</u> .....	79
<u>4.3.2 Clinical features</u> .....	80
<u>4.3.3 An experimental animal model for <i>TMEM165</i> deficiency: the zebrafish</u> .....	81
<u>4.3.4 Diagnostic</u> .....	81
<u>4.3.5 Treatment</u> .....	81
<b>OBJECTIVES</b> .....	83
<b>RESULTS</b> .....	84
<b>[1] Dissection of <i>TMEM165</i> function in Golgi glycosylation and its Mn<sup>2+</sup> sensitivity</b>	
1.1 Introduction	
1.1.1 Importance of the signature motifs of the UPF0016 family members	
1.1.2 Identifying amino acids implied in <i>TMEM165</i> function in glycosylation	
1.1.3 The use of LAMP2 as a glycosylation reporter	
1.1.3 Identifying amino acids implied in <i>TMEM165</i> manganese sensitivity	
1.2 Publication.....	86
1.3 Conclusion and discussion.....	105
<b>[2] Investigating the functional link between <i>TMEM165</i> and <i>SPCA1</i></b>	
2.1 Introduction.....	111
2.2 Publication.....	112
2.3 Discussion.....	127
<b>APPENDIX</b>	
<b>[3] Involvement of thapsigargin– and cyclopiazonic acid–sensitive pumps in the rescue of <i>TMEM165</i>-associated glycosylation defects by Mn<sup>2+</sup></b>	
<b>[4] Manganese-induced turnover of <i>TMEM165</i></b>	
<b>GENERAL DISCUSSION</b> .....	185
<u>1. Role of Gdt1 and Pmr1 in yeast</u> .....	185
<u>2. <i>TMEM165</i> function</u> .....	187
<u>3. <i>TMEM165</i> and <i>SPCA1</i></u> .....	187
<u>3.1 Current model of the functionality of <i>TMEM165</i> and <i>SPCA1</i></u> .....	187
<u>3.2 Putative coupling of <i>TMEM165</i> and <i>SPCA1</i> in the late Golgi cisternae</u> .....	188
<u>4. <i>TMEM165</i> is a cytosolic manganese sensor</u> .....	189
<u>5. Unraveling <i>TMEM165</i> degradation pathway</u> .....	189
<u>6. Amino acids implicated in the glycosylation function of <i>TMEM165</i> and in manganese sensitivity</u> .....	190
<u>7. <i>TMEM165</i>-depleted cells glycosylation restoration pathway by manganese</u> .....	193
<u>8. Potential role of <i>TMEM165</i> in the bone phenotype</u> .....	193
<b>BIBLIOGRAPHY</b> .....	195



## LIST OF FIGURES

- Figure 1. Structure of the three human *N*-glycan types (p.4)
- Figure 2. Precursor synthesis, transfer, and associated type I CDG (p.6)
- Figure 3. Protein folding quality control machinery (p.13)
- Figure 4. Golgi steps of *N*-glycans biosynthesis (p.15)
- Figure 5: Schematic representation of the role of lysosome in biomolecules degradation (p.17)
- Figure 6: Figure 6: Endo- and Exo-glycosidases digestion of *N*-glycoproteins (p.18)
- Figure 7. Glycan intrinsic recognition (p.19)
- Figure 8. Structures of the IgG-Fc *N*-glycans attached to Asn297 (p.23)
- Figure 9. Schematic representation of the cisternal maturation model (p.29)
- Figure 10. Schematic representation of the anterograde vesicular trafficking model (p.29)
- Figure 11. Simplified hypothetic function of COG complex in vesicle tethering and fusion (p.32)
- Figure 12 Simplified schematic representation of interconversion reactions of the monosaccharides used in human *N*-glycosylation (p.37)
- Figure 13. Nucleotide sugar transporters required for human Golgi *N*-glycosylation (p.38)
- Figure 14. Glycosyltransferases structure and domains (p.40)
- Figure 15. Glycosyltransferases potential regulatory mechanisms (p.41)
- Figure 16. pH gradient along the secretory pathway (p.44)
- Figure 17. Point mutations on V-ATPase subunits, assembly factor or accessory factor responsible for a glycosylation defect (p.46)
- Figure 18. Calcium concentration gradient along the secretory pathway (p.48)
- Figure 19. Key players of Golgi calcium homeostasis (p.50)
- Figure 20. Schematic representation of manganese absorption from ingestion to cellular internalization (p.53)
- Figure 21 Schematic representation of manganese absorption from ingestion to cellular internalization (p.55)
- Figure 22. 3D representation of  $\beta$ -1,4-galactosyltransferase 1 with cofactor  $Mn^{2+}$  (purple sphere), donor substrate UDP-Gal, acceptor GlcNAc and important amino acids of the pocket reaction site (p.60.)
- Figure 23. History of TMEM165 and TMEM165-CDG major breakthroughs (p.66)
- Figure 24. Alignment of TMEM165 protein sequence and the orthologs PAM71 from *Arabidopsis thaliana* and Gdt1 from *Saccharomyces cerevisiae* (p.68)
- Figure 25. Prediction of TMEM165 topology and the conserved domains (p.69)
- Figure 26. Predicted topology of all the UPF0016 family members based on the phylogenetic comparison (p.70)
- Figure 27. Putative role of TMEM165 and SPCA1 in Golgi lactose biosynthesis (p.74)
- Figure 28. Schematic representation of the hypothetic function of Pmr1 and Gdt1 in yeast (p.76)
- Figure 29. Proposed model for the functionality of TMEM165 in humans (p.78)
- Figure 30. Schematic representations of LAMP2 structure (p.85)
- Figure 31. Summary figure of the localization of TMEM165 amino acids essential in the function in glycosylation and manganese sensitivity (p.105)
- Figure 32. Effect of dominant-negative GGA1 on Mn-induced TMEM165 degradation (p.107)
- Figure 33. Effect of the knockout of Sortilin on TMEM165 manganese-induced degradation (p.108)

**Figure 34: Model of the link between TMEM165 function, conformation change and degradation (p.107)**

**Figure 35. Hypothetical function of Pmr1 and Gdt1 in the yeast model (p.111)**

**Figure 36. Function of the different forms of SPCA1 used on the following publication (p.112)**

**Figure 37. Hypothetic mechanism explaining the loss of expression of TMEM165 in KO SPCA1 cells (p.128)**

**Figure 38. Putative model of TMEM165 and GPP130 as manganese sensors (p.129)**

**Figure 39. The proposed model by Dulary and collaborators showing the importance of Pmr1 in the absence of Gdt1 in yeast (p.176)**

**Figure 40. Current model of the functionality of TMEM165 resulting from our work (p.179)**

**Figure 41. Putative coupling of TMEM165 and SPCA1 in the late Golgi cisternae (p.180)**

## **LIST OF TABLES**

**Table 1. List of type I CDGs and their respective defective genes and proteins (p.8)**

**Table 2. Reported subtypes of CDG type II implying defects in the V-ATPase related components (p.47)**

**Table 3. List of glycosylation enzymes that are manganese-dependent or thought to be manganese-dependent (p.59)**

**Table 4. Principal clinical features observed in TMEM165-CDG patients (p.80)**

**Table 5. Comparison of the link between Gdt1/TMEM165 and Pmr1/SPCA1 (p.177)**

## INTRODUCTION

### GENERAL INTRODUCTION

A cell is composed of four types of macromolecules: nucleic acids, lipids, proteins and carbohydrates, known as sugars or glycans. Always been considered as a lagging science, much time has passed before the advent of glycobiology. Though, many evidences were made of their importance, glycans are present in every single cell in prokaryote and eukaryote organisms and the first steps of their biosynthesis are highly conserved throughout evolution. The biological function of carbohydrates was first restrained to their role as an energy source; however, they are also found as glycoconjugates when linked to lipids or proteins and constitute a major post-translational modification. They are now assigned to many diverse functions, such as the modulation cell-cell interactions and the conformation of the *N*-glycoproteins.

Glycoconjugates are classified in different groups of molecules: glycolipids, lipopolysaccharides, proteoglycans and glycoproteins. The two principal classes of glycoproteins can be distinguished according to the linkage of the oligosaccharide to the peptide backbone; (i) *O*-linked glycoproteins where the carbohydrate is linked through an oxygen atom of a hydroxylated amino acid and (ii) *N*-linked glycoproteins where the carbohydrate is linked through the nitrogen atom of the amido group of the asparagin side chain usually part of a Asn-X-Ser/Thr sequence, called a sequon. Numerous other carbohydrate-peptide linkages have been discovered, P-linkage through the phosphorus group of a phosphoserine, C-linkage, glypiation and more than 40 different saccharide-protein linkages have been described. In this manuscript we will focus on *N*-glycosylation and its regulation in mammals.

The crucial role of the *N*-glycans arose from mutations in genes, KO cells or diseases responsible, coding for glycosylation enzymes or transporters that induce drastic modifications of the structure of the *N*-glycans exiting the Golgi. Clinically, these alterations translate in a group of diseases named Congenital Disorders of Glycosylation (CDG). The index cases were twin sisters presenting a defect in the phosphomannomutase (PMM2), enzyme that converts mannose-6-phosphate into mannose-1-phosphate. The quantity of mannose-1-phosphate available for the formation of the oligosaccharide precursors is diminished, hence resulting in a glycosylation defect. This first CDG was called CDG-Ia. Over the time, this group of rare inherited disorders grew up in a multitude of CDG subtypes,

affecting almost all steps of the glycosylation process. Two types of CDG were distinguished, CDG type I affecting steps occurring before the oligosaccharide precursor transfer and CDG type II affecting steps occurring after the oligosaccharide precursor transfer. Recently, CDG altering the secretory pathway pH and the ion homeostasis were reported. In 2012, the discovery of a glycosylation defect among five patients was characterized in our research group and a gene coding for a completely unknown protein, named Transmembrane protein 165 (TMEM165) was incriminated. TMEM165 is a Golgi transmembrane protein that belongs to the UPF0016 family (Uncharacterized Protein Family). By phylogenetic analogy, TMEM165 was first thought to be a  $\text{Ca}^{2+}/\text{H}^{+}$  antiport transporter. Eight years of research on this unique glycosylation defect shed light on the fascinating aspects of the protein topology and function. Yeast studies and the generation of knockout cell lines, suggested the capability of TMEM165 to transport calcium and manganese. Another breakthrough also linking TMEM165 and manganese, is the ability of manganese to induce the degradation of TMEM165. An increased cytosolic manganese concentration leads to the rapid targeting of TMEM165 to the lysosomes. Our group also demonstrated, in TMEM165-deficient cells, the restoration of the *N*-glycosylation defect by the addition of a slight amount of manganese in the cell culture medium. Very interestingly, galactose supplementation was also able to rescue this defect. In this work, we first wondered which were the domains of the protein responsible for the cation transport and implied in manganese sensitivity.

In a second part of the work we explored the relationship of TMEM165 with another protein known to import manganese into the Golgi lumen, the Secretory pathway calcium ATPase 1 (SPCA1).

## **CHAPTER 1: *N*-glycoproteins biosynthesis**

The biosynthesis of *N*-glycoproteins mainly involves two distinct subcellular compartments, the endoplasmic reticulum (ER) and the Golgi apparatus (GA). The first step occurs in the ER and consists in the biosynthesis of the oligosaccharide precursor on a lipid structure during the dolichol cycle. This precursor is then transferred *en bloc* on a nascent protein by the oligosaccharyltransferase (OST). Then, chaperones ensure that the newly synthesized *N*-glycoproteins are in an ideal conformation during the “quality control” process before the maturation in the GA of the *N*-glycans. Many enzymes are required along the secretory pathway, mainly glycosidases and glycosyltransferases. In order to maintain the optimal function of these *N*-glycosylation contributors, the pH and ions homeostasis inside the two organelles are finely regulated.

### 1.1 N-glycans structure

The pentasaccharide structure, common to every *N*-glycan is called the core (Man<sub>3</sub>GlcNAc<sub>2</sub>). The first GlcNAc residue is linked to the peptide backbone through an amido linkage and is substituted in β1,4 by a second *N*-acetylglucosamine topped by 3 mannose residues, the first residue is β-linked and the two others are α-linked to the first one.

The second domain of the oligosaccharide, called antennae or branches, corresponds to the substitution of the two terminal mannose residues from the core by GlcNAc. The structure is topped with terminal sugars called the periphery (**figure 1**).

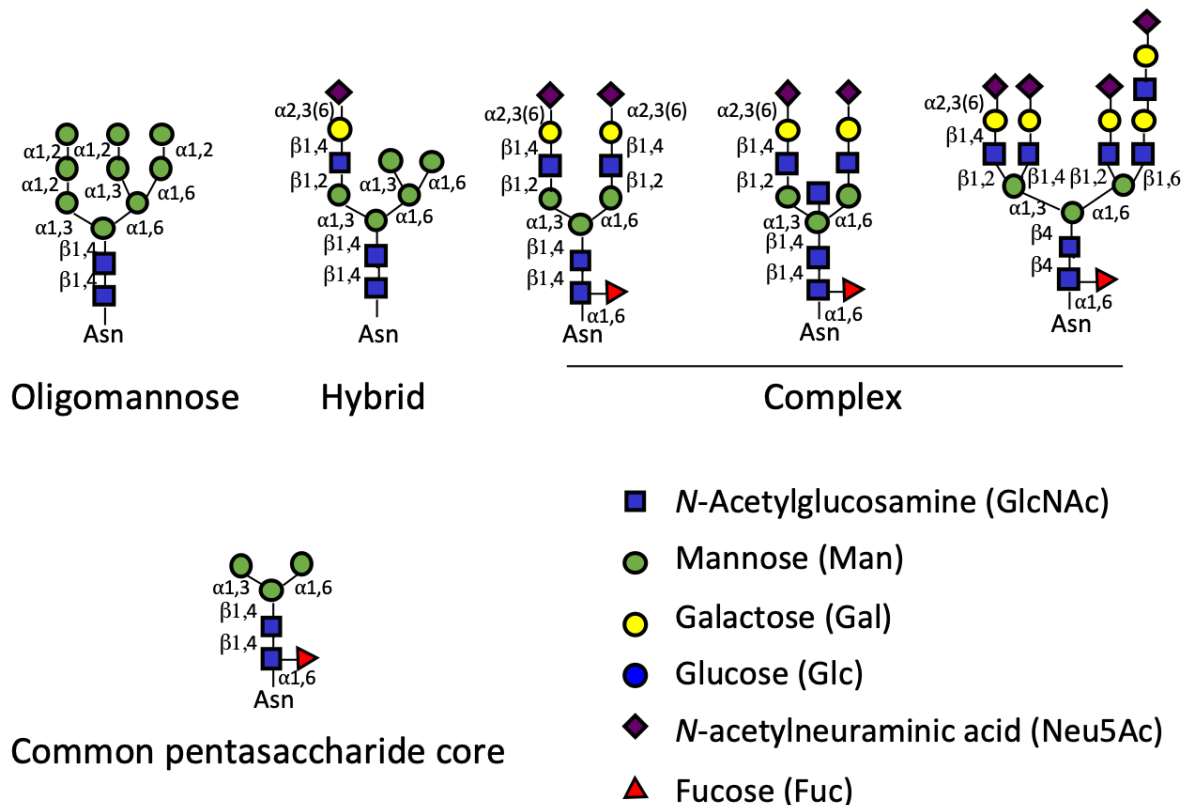


**Figure 1. Structure of the three human *N*-glycan types**

Three different types of *N*-glycans can be distinguished (**figure 1**):

- Oligomannose type: *N*-glycans with a core strictly substituted by mannose residues,
- Complex type or *N*-acetylglucosamine type, with the addition of *N*-acetylglucosamine (Galβ1,4GlcNAc) on α1,3 and α1,6 mannoses leading to mono- to penta-antennary structures,
- Hybrid type: the α1,3 branch is substituted like a complex type whereas the α1,6 branch is substituted like oligomannose type.

Complex and hybrid *N*-glycans can be further modified by addition of terminal sugars. The most frequent substitution in human is the *N*-acetylneuraminic acid (Neu5Ac) a member of the sialic acid family, found principally  $\alpha$ 2,3 or  $\alpha$ 2,6-linked to galactose residues. Fucose (Fuc) residues can be linked in  $\alpha$ 1,6 on the first GlcNAc residue or to an *N*-acetyllactosamine  $\alpha$ 1,3 to the GlcNAc residue and/or  $\alpha$ 1,2 to galactose residues. These structures can be modified with phosphate, sulfate, acetate, or phosphorylcholine. Other modifications such as sulfation, methylation, acetylation, phosphorylation may further diversify the *N*-glycans structures (Muthana et al., 2012; Varki, 2007).

## 1.2 *N*-glycosylation process

### 1.2.1 Biosynthesis of the *N*-linked glycan precursor in the ER

While the Golgi glycosylation differs, ER pathway is highly conserved among eukaryotes, from yeast, *Saccharomyces cerevisiae*, used as a laboratory model to human. The precursor biosynthesis starts co-translationally in the rough endoplasmic reticulum with the transfer of a Lipid-linked tetradecasaccharide precursor on the nascent protein. Similarly, to the synthesis of the protein, the lipid-linked oligosaccharide precursor biosynthesis has a bipartite localization: the cytosolic side of the ER and the ER lumen. The sequential steps of the lipid-linked oligosaccharide (LLO) biosynthesis, its transfer onto the protein, and the first trimming reactions of the oligosaccharide in the ER are summarized on the schematic representation **figure 2**. The first key molecule at the onset of the *N*-glycosylation machinery is the dolichol.

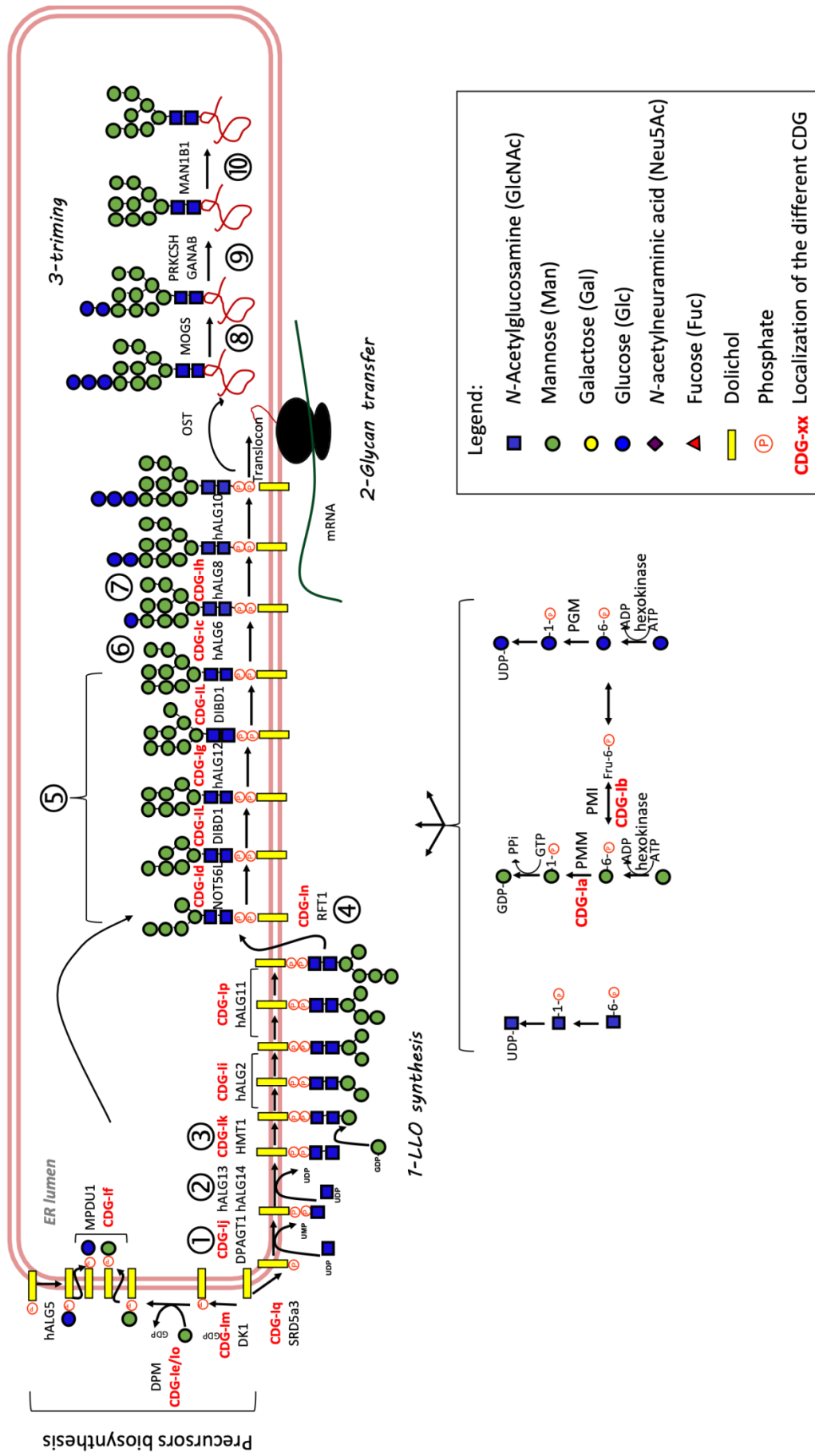


Figure 2. Precursor synthesis, transfer, and associated type I CDG

### 1.2.1.1 The dolichol cycle

The tetradecasaccharide-dolichol precursor,  $\text{Glc}_3\text{Man}_9\text{GlcNAc}_2\text{-P-P-Dol}$ , is synthesized during the dolichol cycle. In mammalian cells, the dolichol is a polyisoprenoid alcohol, a lipid made of 18 to 21  $\alpha$ -isoprene units, enshrined in the ER membrane (Rip et al., 1985). This lipid structure is first phosphorylated (Dol-P) and monosaccharides are added in a highly ordered process. The biosynthetic machinery has been elucidated by the study of knockout yeasts for each enzyme, members of the ER membrane-associated Asparagine-Linked Glycosylation (ALG) glycosyltransferases family (Aebi, 2013). Each of them has a corresponding ortholog in human, mostly encoded by *hALG* genes. The cycle starts at the cytosolic side of the ER with the transfer of a GlcNAc-P residue from a nucleotide-sugar UDP-GlcNAc to the Dol-P by the GlcNAc I phosphotransferase (UDP-GlcNAc:dolichol-P GlcNAc-1-P transferase (GPT)) to obtain the GlcNAc-P-P-Dol, a reaction that releases uridine monophosphate (UMP) molecule (Daran et al., 1995) (**Figure 2** ①). This reaction can be blocked by tunicamycin, an antibiotic, a *N*-glycosylation inhibitor. A second UDP-GlcNAc is added to the GlcNAc-P-P-Dol, releasing a molecule of Uridine diphosphate (UDP) ②. Five mannose residues originated from GDP-Man are then sequentially transferred to this oligosaccharide structure to form  $\text{Man}_5\text{GlcNAc}_2\text{-P-P-Dol}$  ③.

At this point, a phenomenon of transbilayer shift, also known as flipping, translocates this precursor inside the ER lumen *via* an ATP-independent flippase, RFT1 ④ (Helenius, 2002).

Concomitantly, Dol-P-Man and Dol-P-Glc molecules are synthesized on the cytosolic side to provide substrates to further build the oligosaccharide. Both molecules will undergo a translocation in the ER lumen to be available for the respective glycosyltransferases (Heesen et al., 1994; Herscovics and Orlean, 1993; Orlean, 1990) (**figure 2, left part**).

The transfer of 4 more mannose residues on  $\text{Man}_5\text{GlcNAc}_2\text{-P-P-Dol}$  to form  $\text{Man}_9\text{GlcNAc}_2\text{-P-P-Dol}$  ⑤ is achieved with the use of Dol-P-Man as a substrate. The Dol-P-Glc is the substrate for the addition of the 3 last glucose residues to complete the synthesis of the precursor  $\text{Glc}_3\text{Man}_9\text{GlcNAc}_2\text{-P-P-Dol}$ , the so-called lipid-linked oligosaccharide (LLO) (Aebi, 2013) ⑥. Mutations in gene coding for an enzyme with a role in this process usually lead to severe diseases.

### 1.2.1.2 Defects in the precursor synthesis

Name of the disease	Previous name	Defective gene	Defective protein full name	Defective protein usual name
PMM2-CDG	CDG-Ia	PMM2	Phosphomannomutase 2	Phosphomannomutase 2
MPI-CDG	CDG-Ib	MPI	Phosphomannose isomerase	Phosphomannose isomerase
ALG6-CDG	CDG-Ic	hALG6	Dol-P-Glc: Man <sub>9</sub> -GlcNAc <sub>2</sub> -P-P-Dol glucosyltransferase	Glucosyltransferase 1
NOT56L-CDG	CDG-Id	hALG3	Dol-P-Man: Man <sub>5</sub> -GlcNAc <sub>2</sub> -P-P-Dol mannosyltransferase	Mannosyltransferase 6
DPM1-CDG	CDG-Ie	DPM1	GDP-Man:Dol-P-mannosyltransferase (subunit 1)	Dol-P-Man synthase (subunit 1)
MPDU1-CDG	CDG-If	MPDUI	Man-P-Dol utilization 1	Lec35
ALG8-CDG	CDG-Ih	hALG8	Dol-P-Glc: Glc <sub>1</sub> -Man <sub>9</sub> -GlcNAc <sub>2</sub> -P-P-Dol glucosyltransferase	Glucosyltransferase 2
ALG12-CDG	CDG-Ig	hALG12	Dol-P-Man: Man <sub>7</sub> -GlcNAc <sub>2</sub> -P-P-Dol mannosyltransferase	Mannosyltransferase 8
ALG2-CDG	CDG-Ii	hALG2	GDP-Man: Man <sub>1</sub> -GlcNAc <sub>2</sub> -P-P-Dol mannosyltransferase	Mannosyltransferase 2
DPAGT1-CDG	CDG-Ij	DPMI	UDP-GlcNAc: Dol-P-GlcNAc-P transferase	/
HMT1-CDG	CDG-Ik	hALG1	GDP-Man: GlcNAc <sub>2</sub> -P-P-Dol mannosyltransferase	Mannosyltransferase 1
DIBD1-CDG	CDG-Il	hALG9	Dol-P-Man: Man <sub>6</sub> -and Man <sub>8</sub> -GlcNA <sub>2</sub> -P-P-Dol mannosyltransferase	Mannosyltransferase 7-9
DK1-CDG	CDG-Im	DK1	Dolichol Kinase	/
RFT1-CDG	CDG-In	RFT1	Man <sub>5</sub> GlcNAc <sub>2</sub> -P-P-Dol flippase	Flippase
DPM3-CDG	CDG-Io	DPM3	GDP-Man:Dol-P-mannosyltransferase (subunit 3)	Dol-P-Man synthase (subunit 3)
ALG11-CDG	CDG-Ip	hALG11	GDP-Man:Man <sub>3</sub> -GlcNAc <sub>2</sub> -P-P-Dol α1,2-mannosyltransferase	/
SRD5A3-CDG	CDG-Iq	SRD5A3	Steroid-5α reductase type 3	/

**Table 1. List of type I CDGs and their respective defective genes and proteins** (Modified from Jaeken et al., 2009)

In 2018, more than 125 different CDG subtypes have been identified (Ng and Freeze, 2018). These diseases are extremely rare with most of each subtype affecting less than 10 patients in the world. Two groups are distinguished, CDG type I and CDG type II. Disruption of actors of the steps that occur before the LLO transfer lead to diseases called CDG type I. The CDG

nomenclature has changed; they are named by their defective gene but the classification using letters (**figure 2**). CDG type I may result of a defect in glycosyltransferases catalyzing the biosynthesis of the LLO precursor, such as glucosyltransferases and mannosyltransferases, but also in enzymes responsible for the substrates synthesis, such as the dolichol synthesis, among others. The main type I CDGs are reported in **table 1**.

The activated nucleotide-sugars or dolichol-sugars donors that are crucial for the first steps of glycosylation can be a cause of CDG. The first CDG, identified in 1980 by Pr Jaeken is the most common subtype (CDG-Ia), which encompasses 70% of all the CDG cases with an estimated prevalence to 1.5 / 100.000 births. These patients present a deficiency in phosphomannomutase 2 (PMM2) that converts mannose-6-phosphate into mannose-1-phosphate. Phosphomannose isomerase PMI defect (CDG-Ib) blocks the conversion of fructose-6-phosphate into mannose-6-phosphate, the substrate required for PMM2 reaction (Jaeken, 2011).

Other subtypes arise from to a lack of translocation intermediates like the flippase defect with mutations in the *RFT1* gene leading to CDG-In or in the Lec35 protein encoded by *MPDU1* (Mannose-Phosphate Dolichol Utilization Defect 1) gene (CDG-If) (Kranz et al., 2001; Quelhas et al., 2018).

The CDG-type I family is an expanding disease family with a constant discovery of new subtypes. ALG13 encoding a putative bifunctional UDP-*N*-acetylglucosamine transferase/deubiquitinase has been recently reported as CDG-Is. Similarly, ALG14-deficiency, previously considered as a Congenital Myastenic Syndrome 15 (CMS15), is now known as ALG14-CDG (Ferreira et al., 2018). Every organ and system can be affected in this group of inherited diseases; most of them share some clinical features such as psychomotor and developmental delays, seizures, hypotonia, and facial dysmorphism.

#### 1.2.1.3 Transfer of the dolichol precursor on a nascent protein

The translation of proteins transiting in the ER starts with the cytosolic synthesis of a signal peptide recognized by the Signal Recognition Particle (SRP). The SRP receptor localized to the ER membrane recognizes this signal and the protein is translocated into the ER lumen. This translocation occurs through a pore called the translocon complex, principally constituted by the Sec1 transmembrane protein (Blobel and Dobberstein, 1975; Mandon et al., 2013). The

signal sequence is cleaved by a peptidase once localized inside the ER lumen. The ribosome and the translocon are closely associated with the oligosaccharyltransferase (OST).

OST transfers the previously synthesized lipid linked donor LLO (§1.2.1.1) *en bloc* on an asparagine (Asn) residue of an elongating protein ⑦. As mentioned above, this Asn has to be part of a specific sequence N-X-S/T, where X≠P. As a matter of fact, proline would block the loop formation needed for the glycan precursor transfer (Helenius and Aebi, 2004). More rarely, Asn-X-Cys/Val/Gly sequons are glycosylated (Gil et al., 2009; Sun and Zhang, 2015). The OST is the key enzyme in the glycosylation process, localized in the ER membrane in a close proximity with the pore to transfer the LLO on an unfolded peptide with accessible sequons. The yeast OST is a well-described macromolecular complex constituted of 9 subunits that have orthologs in human: ribophorin I (yeast Ost1p) and ribophorin II (yeast Swp1p), DAD1 (yeast Ost2p), OST4 Ost4p), OST48 (Wbp1p), MAGT1 (IAP)/TUSC3 (N33) or DC2/KCP (Ost3p/Ost6p), TMEM258 (Ost5p) and STT3A/STT3B (Stt3p). Every OST subunit is a transmembrane protein made of 1 to 13 domains. Two paralogs of the catalytic subunit exist, STT3A-OST and STT3B-OST, sharing 66% sequence homology. STT3A-OST allows the co-translational transfer of the glycan precursor on the peptide. *N*-glycosylation sites that are missed by STT3A-OST can be post-translationally glycosylated by STT3B-OST. Both catalyze the linkage to the protein releasing a dol-P-P that will be retrotranslocated in the cytosolic side of the ER after dephosphorylation in dol-P.

The precise role of the other subunits has not been completely deciphered; however, each subunit is indispensable for the OST complex function and hence the glycosylation process. They are, for example, required for the interaction of STT3A with the translocon, for the substrate accessibility (Braunger et al., 2018) or for the stabilization of the ribosome and the translocon-associated protein complex (TRAP). This has been demonstrated by yeast studies in which any mutation in genes coding for one of the subunits lowers the global activity of the whole oligosaccharyl transferase resulting in a glycosylation defect. In human, STT3A- and STT3B-CDG have been described and patients present developmental delay. Interestingly, the transferrin of STT3B-CDG patients presents a mild glycosylation abnormalities (Shrimal et al., 2013). Other CDG affecting subunits of the OST such as MAGT1 and TUSC3 have also been identified (Blommaert et al., 2019; Molinari et al., 2008).

#### 1.2.1.4 The role of chaperones

Chaperones are also known as heat shock protein (HSP) due to their action under stress conditions. In the ER lumen chaperones that are regulated by ATPase cycle, have two main functions:

- Due to their flexibility, chaperones are folding assistants that modify protein conformation by recognition and by masking the hydrophobic regions of the newly synthesized glycoproteins.

- Assuming they prevent the aggregation and maintain the solubility of the nascent proteins.

Representing 7% of all of the ER chaperones, the most abundant is the binding immunoglobulin protein (BiP), also known as glucose-regulating stress protein (GRP78) member of the HSP70 family (Lamriben et al., 2016). BiP binds to newly synthesized proteins immediately after translocation and during all the quality process to assist multiple functions: glycoprotein folding and delivery to ERAD. ER also houses calcium dependent-chaperones, that will be described below (Griesemer et al., 2014). Other important chaperones of the ER are GRP94 and the protein disulfide isomerase (PDI) that catalyzes the oxidoreduction of the disulfide bonds between cysteine residues within the protein.

#### 1.2.1.5 Glucosidases and mannose trimming

Immediately after the transfer of the tetradecasaccharide precursor on the Asn residue, a glucose is removed by the glucosidase I (Tannous et al., 2015) ⑧. The  $\alpha$ -(exo)glucosidase I (MOGS) is a 82kDa transmembrane protein with a unique transmembrane domain, the activity is carried by the luminal domain whose activity can be specifically inhibited by castanospermine or deoxynojirimycin (Hempel et al., 1993).

Malectine, an ER membrane protein, recognizes the  $\text{Glc}_2\text{Man}_9\text{GlcNAc}_2$  glycan of misfolded proteins. Though the precise role of this lectin has not been completely elucidated, it is supposed to recruit the (exo)glucosidase II (GANAB) and prevent the aggregation of the nascent protein. The glucosidase II, is an  $\alpha$ 1,2glucosidase able to remove two glucose residues. ⑨. The first removal gives birth to a  $\text{Glc}_1\text{Man}_9\text{GlcNAc}_2$ -protein that will enter the quality control calnexin/calreticulin cycle that will be further detailed in the next paragraph. After this check point, the last glucose residue is removed by the glucosidase II ⑩.

#### 1.2.1.6 Glycan-mediated ER quality control (ERQC) (figure 3)

Following the trimming by glucosidases, the glycoprotein enters the monoglucose calnexin/calreticulin cycle. This checkpoint involves two lectins (Rutishauser, 1975), named calnexin (CNX), also known as calregulin, and the soluble Calreticulin (CRT). Sharing 45% of their sequences, both recognize specifically *N*-glycans with one terminal glucose residue (Glc<sub>1</sub>Man<sub>9</sub>GlcNAc<sub>2</sub>) (Helenius and Aebi, 2004). A cooperation with other proteins such as ERP57, a glycoprotein from the PDI family, contribute to the *N*-glycoprotein folding (Caramelo and Parodi, 2015; Tannous et al., 2015).

After the CNX/CRT cycle, a misfolded glycoprotein can be re-glucosylated by the UDP-glucose glycoprotein glucosyltransferase (UGGT) for another cycle. Then, the correctly folded glycoprotein reaches the ER Exit Sites (ERES). Despite this highly control process, around 30% of the glycoproteins remain misfolded and are targeted to the proteasome for degradation *via* the ERAD system.

#### 1.2.1.7 Endoplasmic Reticulum-Associated Protein Degradation (ERAD) pathway

To avoid congestion in the quality control cycle, ER mannosidases along with EDEM can prevent reglucosylation of the misfolded *N*-glycoprotein by UGGT and orientate them toward ERAD pathway for degradation (Oda et al., 2003). The transport from the ER and through the cytosol is mediated by a degradation signal (Man<sub>8</sub>GlcNAc<sub>2</sub>), generated by the suppression of a mannose residue in  $\alpha$ 1,2 from the oligosaccharide of the misfolded glycoprotein by ER  $\alpha$ -mannosidase.

This signal is specifically recognized by the lectin ER degradation-enhancing  $\alpha$ -mannosidase-like protein 1 (EDEM1) that concomitantly interacts with CNX but not CRT (Molinari, 2003). EDEM1 is one of the three members of the EDEM family, sharing 30% homology with EDEM2 and EDEM3. EDEM proteins and the ER-mannosidase remove up to 4 mannose residues on the glycan of the misfolded glycoprotein which can be taken over by three different ERAD pathways, regarding the protein nature: ERAD-L for luminal, ERAD-M for transmembrane, and ERAD-C for cytosolic glycoproteins.

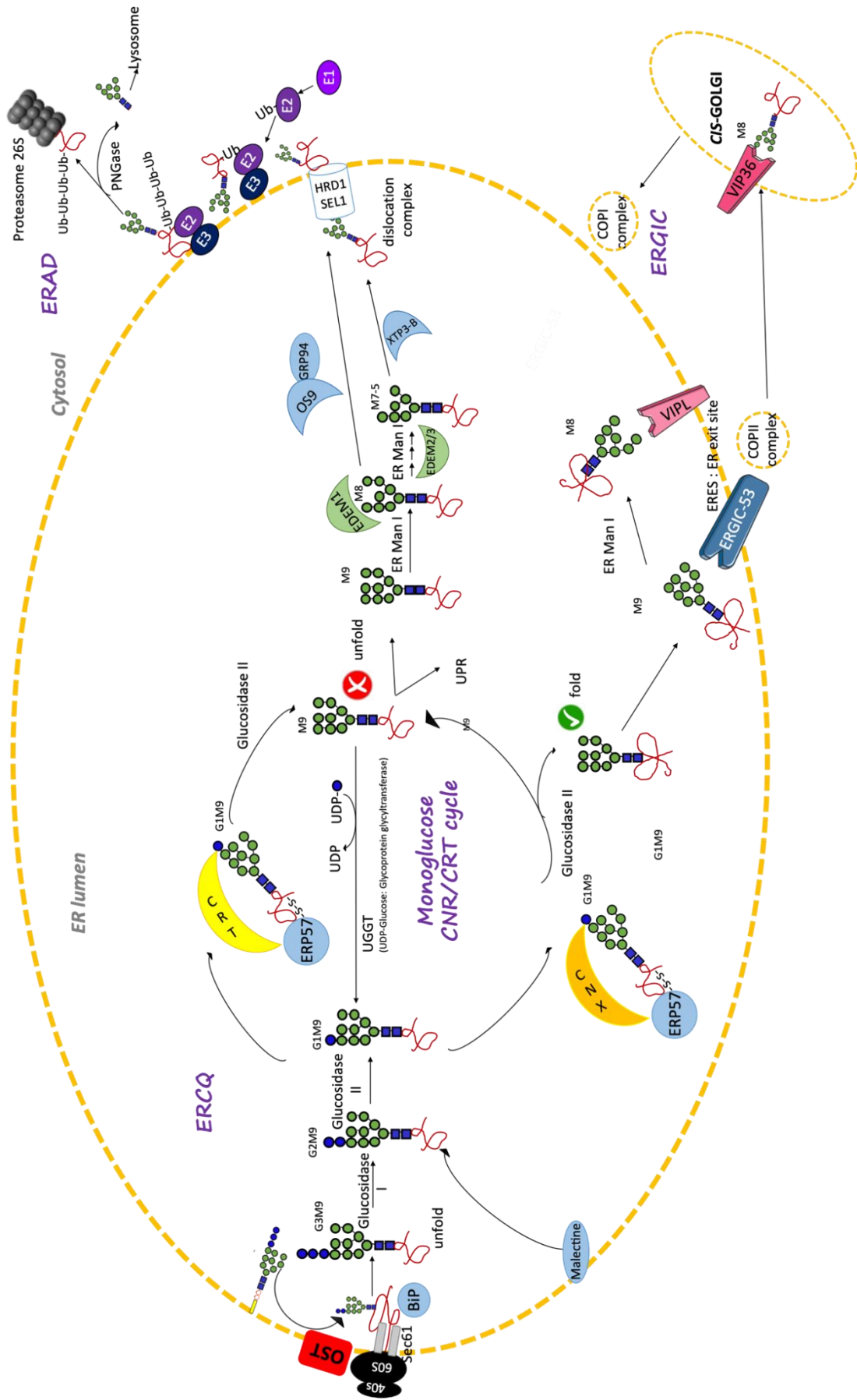


Figure 3. Protein folding quality control machinery

Different structures of the glycan, part of the unfolded protein are recognized by other lectins, OS9 preferentially identifies Man<sub>7</sub> structures while XTP3-B can bind to Man<sub>7-5</sub> structures. Chaperones such GRP94 and BiP are also involved in the ERAD process.

The retrotranslocation occurs via a complex, also known as dislocation complex, made of the ER Sec61 channel linked to HRD1 and SEL1 adaptor. Concomitantly to the dislocation, the glycoprotein undergoes ubiquitination of the lysine residues (**figure 3, right part**). First, E1 (ubiquitin activating enzyme) activates E2 (ubiquitin conjugating enzyme) that binds to a ubiquitin molecule (76AA) *via* a cysteine bond. Then, E3 (ubiquitin ligase enzyme), a transmembrane protein, binds to E2 and provide an optimal stabilization for ubiquitin transfer on the glycoprotein. Several cycles are needed to achieve polyubiquitination, furthermore ubiquitin can itself be ubiquitinated (Meusser et al., 2005; Roth and Zuber, 2017) (**figure 3, upper part**).

The *N*-glycanase (PNGase) separates the *N*-glycan from the peptide. A mutations in NGLY1, an *N*-glycanase, leads to a CDG-related disease, NGLY1-CDDG, a Congenital Disorder of DeGlycosylation (Need et al., 2012; Suzuki et al., 1993, 2016). The ubiquitinated peptide is sent to the proteasome 26S, made of a 20S subunit surrounded by two 19S subunits. The *N*-glycan is then dismantled by the cytosolic endo- $\beta$ -*N*-Acetylglucosaminidase (ENGase) and mannosidase  $\alpha$  class 2C Member 1 (Man2C1) until a limit Man<sub>5</sub>GlcNAc structure which is targeted to lysosomal compartment. There,  $\alpha$ -D-mannosidase and a  $\beta$ -D-mannosidase sequentially end the degradation.

#### 1.2.1.8 ER/Golgi Intermediate Compartment (ERGIC), from ER to Golgi back and forth

Between the ER and the Golgi apparatus, there is an intermediary compartment of very active trafficking called ERGIC. To reach the Golgi apparatus, selected correctly folded proteins are recognized by VIPL (VIP36-Like Protein) and ERGIC-53 (ER-Golgi Intermediate Compartment 53 kDa protein) and loaded into COPII coated vesicles (Bonifacino and Glick, 2004) (**figure 3, lower right part**). A mutation in the gene coding for ERGIC-53, also known as LAMAN1 (Lectin Mannose-Binding 1), leads to a defect in coagulation factors (FV and FVIII) (Peotter et al., 2019).

On the Golgi side, VIP36 (Vesicular Integral-Membrane Protein 36) can return misfolded Golgi *N*-glycoproteins to the ER *via* vesicles coated by coatomer COPI. VIPL and

VIP36 preferentially take over de-glucosylated forms of oligosaccharides like  $\text{Man}_8\text{GlcNAc}_2$  (Fujita et al., 2015).

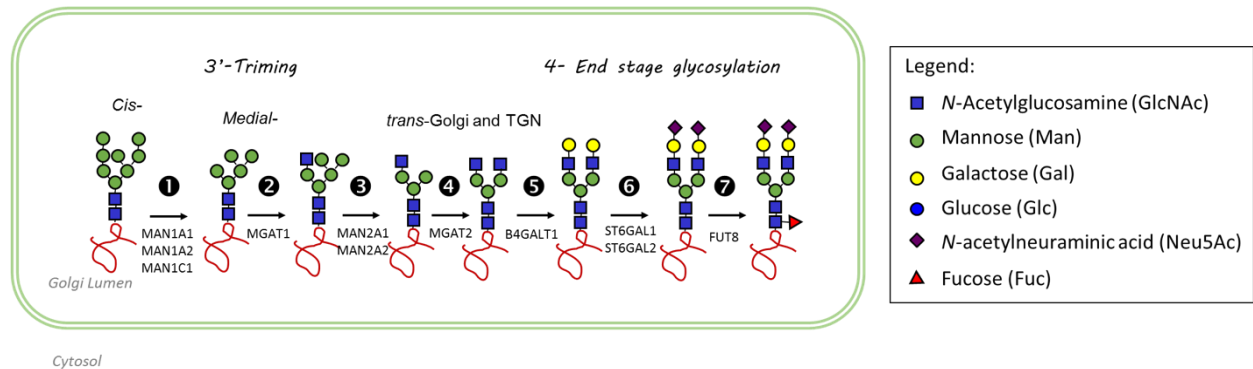


**Figure 4. Golgi steps of *N*-glycans biosynthesis**

### 1.2.2 Sequential maturation of *N*-linked glycans through GA

The sequential action of glycosylhydrolases (GH) and glycosyltransferases (GT) in various loci of the Golgi apparatus give rise to three different categories of *N*-glycans (**figure 1**): oligomannose, hybrid or complex (§1.1, **figure 1**).

The *N*-glycan maturation consists of the sequential modification of their antennae through the Golgi stacks, in a *cis- media- trans-* order. Mannose residues are trimmed while GlcNAc and galactose (Gal) residues forming the *N*-acetylglucosamine chains of the branches are added. Finally, the additions of fucose and sialic acid residues on the periphery further complexify this structure. The addition of a monosaccharide on the growing *N*-glycan requires the presence of a nucleotide-sugar donor imported by a specific nucleotide-sugar transporter and a specific enzyme in the same Golgi cisterna.

First, Golgi  $\alpha$ 1,2-mannosidase IA and B (MAN1A1 and MAN1A2), sensitive to kifunensine, cleaves mannose residues attached in  $\alpha$ 1,2 in a  $\text{Man}_5$  branched structure,  $\text{Man}_5\text{GlcNAc}_2$  (Elbein et al., 1990) (**figure 4**) ❶. In the *medial*-Golgi, the  $\beta$ 1,2 GlcNAc transferase I (GnT-I or MGAT1: Mannosyl  $\alpha$ 1,3-Glycoprotein  $\beta$ 1,2-*N*-Acetylglucosaminyltransferase) adds a GlcNAc on the  $\alpha$ 1,3 linked mannose residue to give  $\text{GlcNAcMan}_5\text{GlcNAc}_2$  ❷. The Golgi  $\alpha$ -mannosidases I and II (MAN2A1, MAN2A2) ❸ that are sensitive to swainsonine and 1,4-dideoxy-1,4-imino-D-mannitol (DIM) (Bashyal et al., 1987), cleave the two terminal  $\alpha$ 1,3- and  $\alpha$ 1,6-linked mannose residues. With the addition of a second GlcNAc in  $\alpha$ 1,6 by MGATII,  $\text{GlcNAc}_2\text{Man}_3\text{GlcNAc}_2$  is obtained ❹.

GlcNAc transferases IV, V and VI (MGAT4A/B, MGAT5) generate the poly-antennary structures of the complex *N*-glycans. Some *N*-glycans may be bisected by a GlcNAc residue on the central  $\beta$  linked-mannose under the action of GlcNAcT-III (MGAT3). In the *trans*-Golgi the  $\beta$ -galactosyltransferase may add galactose residues in  $\beta$ 1,4 to build a *N*-acetyl-lactosamine (LacNAc) and further elongation can occur and results in poly-*N*-acetyl-lactosamine (polyLacNAc) sequence ⑤. Sialyltransferases  $\alpha$ 2,3 or  $\alpha$ 2,6 may cap the terminal galactose residues with *N*-acetylneuraminic acid (Neu5Ac) ⑥. A fucosylation of the core of the *N*-glycan on the GlcNAc linked to Asn might be realized by  $\alpha$ 1,6 fucosyltransferase ⑦. Further addition of fucose residues in  $\alpha$ 1,2,  $\alpha$ 1,3 and  $\alpha$ 1,4 and other post-translational modifications such as sulfation and acetylation can be seen.

### 1.3 Degradation of *N*-glycoconjugates

This step is crucial for the maintenance of cell homeostasis; wide evidence is provided by the existence of lysosomal storage disorders. These diseases are due to mutations in genes coding for proteins involved in glycoprotein lysosomal degradation. A common lysosomal degradation pathway is shared by *N*-glycoproteins, *O*-glycoproteins, proteoglycans and glycolipids; we will only detail the *N*-glycoconjugates degradation.

#### 1.3.1 Lysosomal compartment generalities

Lysosomes are ubiquitous organelles with sizes ranging from 0.2 to 0.5 $\mu$ m found in the cytoplasm of every animal cell. These compartments were unearthed 50 years ago in Belgium by the Physiology and Medicine Nobel prize Christian de Duve. Abundant in osteoclasts for bone formation, they also constitute a defense mechanism against pathogens in neutrophils and macrophage cells. This organelle results from the fusion of vesicles coming from the Golgi and plasma membrane vesicles and is in charge of the digestion and recycling of external and internal components such as lipids, nucleic acids, glycans, and proteins, by hydrolases. They assure the renewal of cytosolic and membrane constituents and cellular nutrition.

The material contained in mature lysosomes results from fusion of endocytic or autophagic pathways with primary lysosomes. The membrane is composed of a phospholipid bilayer enshrined by numerous glycoproteins. In primary lysosomes, three different types of enzymatic transmembrane glycoproteins are distinguished: (i) H<sup>+</sup> pumps that are responsible for the pH between 4.5 and 5.5, (ii) lysosomal membrane proteins (LMPs), and (iii) acid

phosphatases. Lysosomal Integral Membrane Protein (LIMP) and Lysosome Associated Membrane Protein (LAMP) are part of the 25 Lysosomal Membrane Proteins (LMP) (Connus & Simon, 2008) and are responsible for lysosomal acidification, membrane fusion, import of cytosolic proteins, and export of degradation products (Eskelinen et al., 2003). Hence, they may be used as lysosomal markers (Fukuda, 1991). The glycosylation of these proteins is located on the luminal side of the organelle and protect them from the hydrolases. ATP-dependent type V  $H^+$  pump (Forgac, 1989) and ion channels maintain the acidic pH of the lysosome, optimal for the activity of the hydrolases.

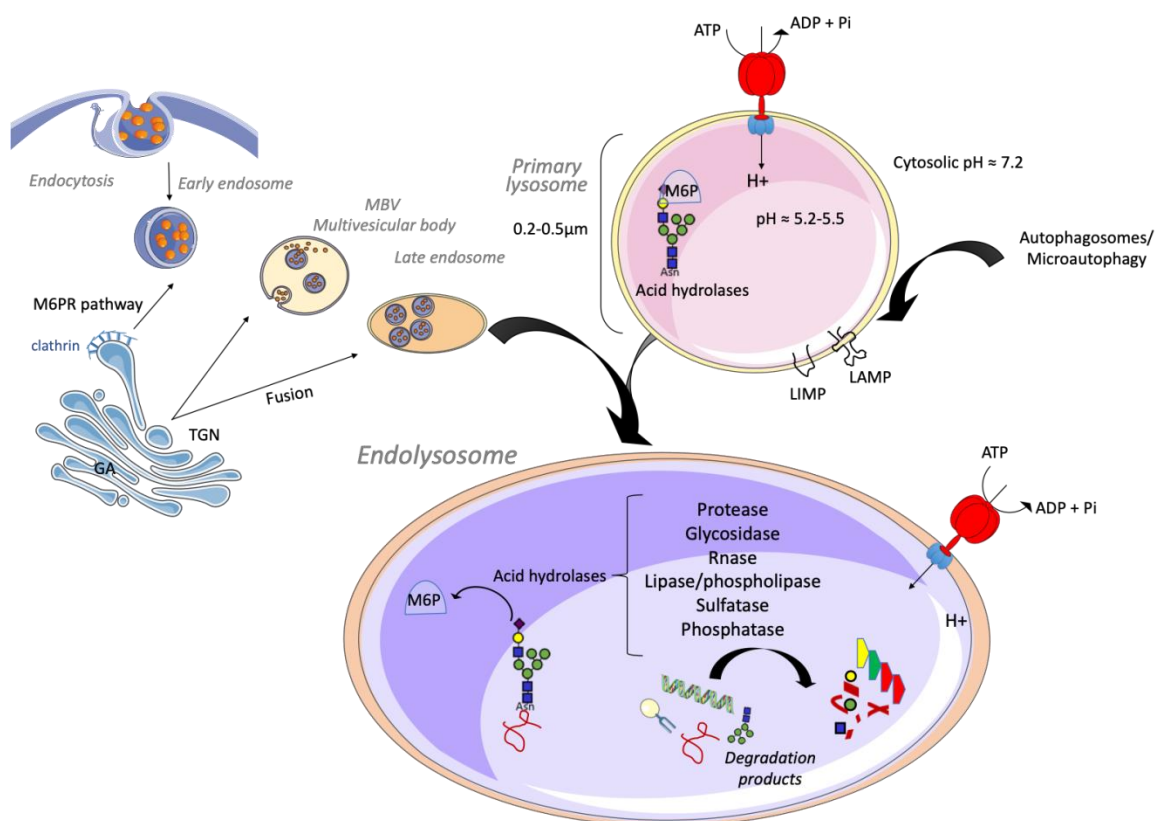


**Figure 5: Schematic representation of the role of lysosome in biomolecules degradation**

### 1.3.2 Hydrolases targeting

These enzymes are addressed from the *cis*-Golgi to the lysosome via the mannose-6-phosphate (M6P) signaling pathway. The UDP-GlcNAc-dependent GlcNAc-1-phosphotransferase transfers a Glc-NAC-1P on the oligomannose type *N*-glycan to the carbon 6 of the two terminal mannose residues of the acid hydrolase. Once the hydrolase reaches the *trans*-Golgi compartment, the GlcNAc is removed by a glycosidase, uncovering the mannose-6-phosphate (M6P) signal that is recognized by a mannose-6-phosphate receptor

(MPR). This glycoprotein capped by the MPR is delivered to the acid endosomes and the MPR is recycled. There are also minor M6P-independent pathways to the lysosome involving proteins such as VPS 10 receptor family (like sortilin) and LIMP2-dependent transport.

Lysosomal enzymes, also referred as acid or lysosomal hydrolases, degrade the glycoproteins, glycolipids and GAGs in every animal cell. Up to 50 different enzymes are now identified.

### 1.3.3 Breakdown of glycoconjugates in the lysosome

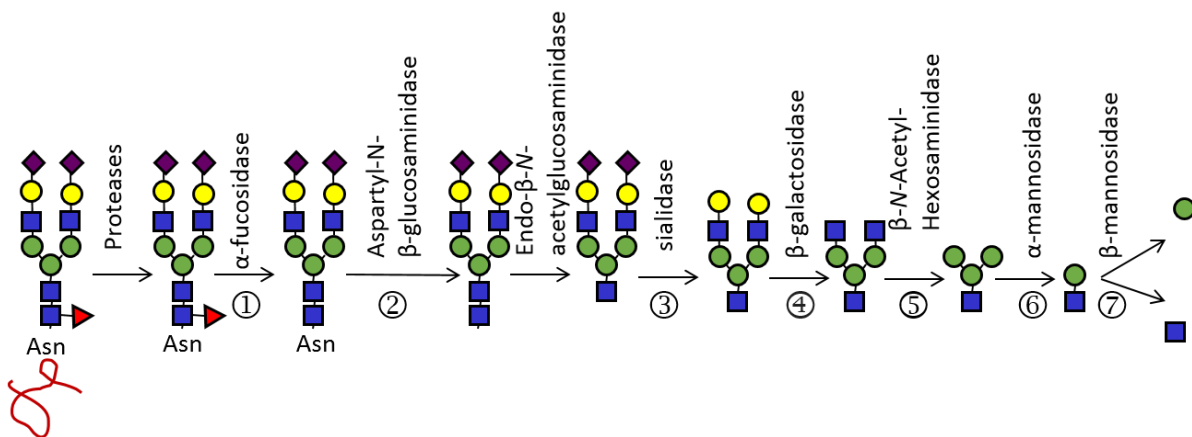


**Figure 6: Endo- and Exo-glycosidases digestion of N-glycoproteins**

Disassembly of N-glycoproteins in the degradation compartment is a well-ordered process where proteases first hydrolyze the polypeptide chain of the glycoprotein into amino acids. They are non-specific and present overlapping functions according to the absence of lysosomal storage disease linked to a peptidase deficiency.

The glycan part is dismantled by glycosidases in a more specific way. Exoglycosidases release monosaccharides of the nonreducing ends whereas endoglycosidases release the carbohydrate moieties on the peptide side of the glycan (Moremen et al., 1994), in a bidirectional catabolism (**figure 6**).

The  $\alpha$ fucosidases encoded by *FUCA1* removes the first fucose of  $\text{Fuca}\alpha 1\text{-6GlcNAc}\beta 1\text{-Asn}$  ① then, the aspartylglucosaminidase (AGA) cleaves the  $\text{GlcNAc}\beta 1\text{-Asn}$  bond between the peptide backbone and the carbohydrates chain ②. The terminal GlcNAc of the previous structure can be released either by exoglycosidases and lysosomal di-N-acetylchitobiase (CTBS). The sialidase, also known as neuraminidase, encoded by *NEU1* ③ release the sialic acid before the removal of galactose residue by  $\beta$ -galactosidase (GLB1) ④. The  $\beta$ -hexosaminidase release the underlying GlcNAc residues ⑤.

For the last steps of the catabolism, two different types of mannosidases are distinguished:

-  $\alpha$ -mannosidase responsible for the mannose trimming of  $(\text{Man}\alpha)_n\text{Man}\beta\text{1-4GlcNAc}$  ( $n= 1$  to 8) into a  $\text{Man}\beta\text{1-4GlcNAc}$  disaccharide ⑥.

- $\beta$ -mannosidase (MANBA) finally cleaves the  $\text{Man}\beta\text{1-4GlcNAc}$  disaccharide ⑦ (Suzuki, 2016).

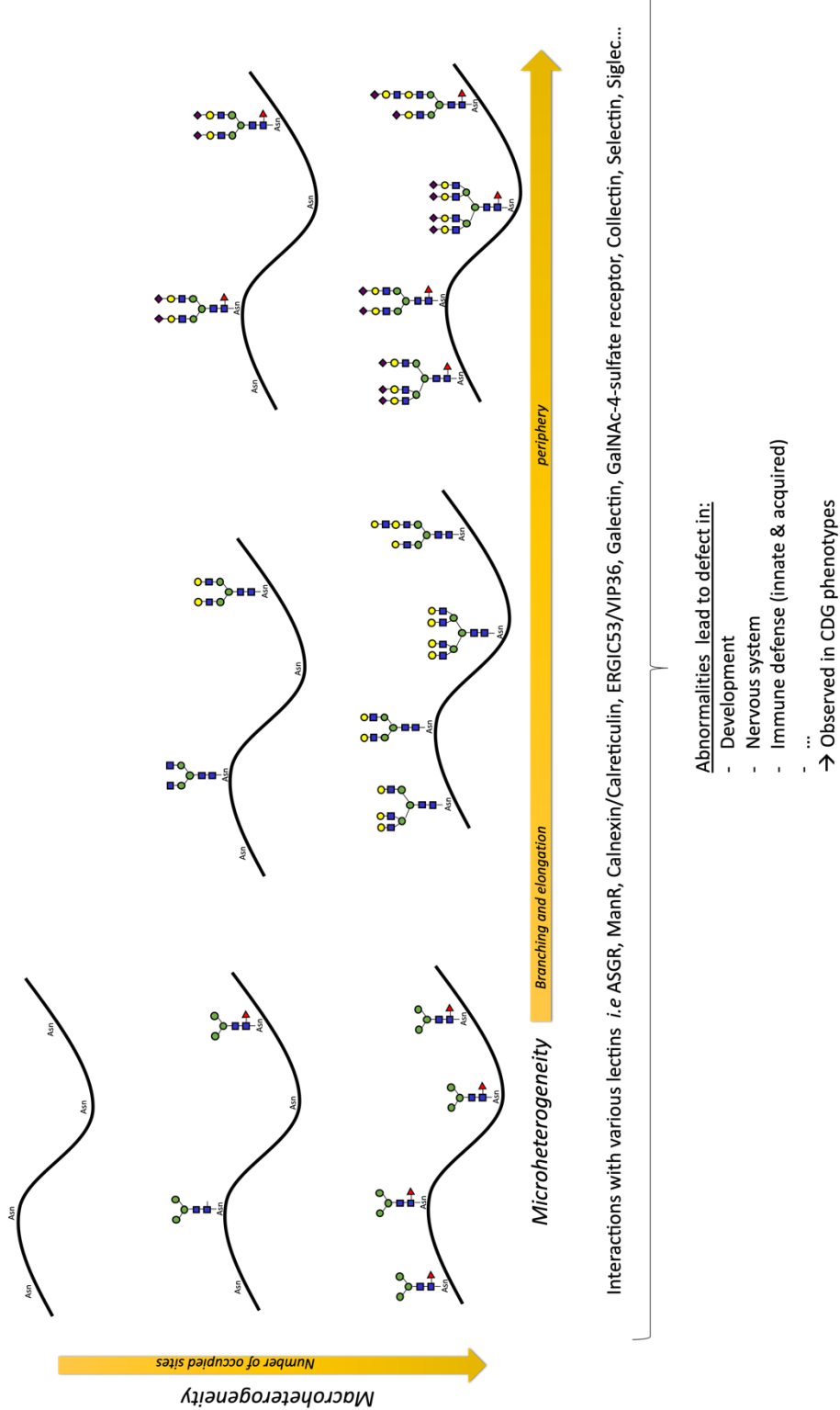


Figure 7. Glycan intrinsic recognition

## 1.4 Functions of *N*-glycans

During the first part of the 20<sup>th</sup> century, glycosylation was only described as a post-translational modification modulating the physicochemical properties of proteins and lipids. During the last decades, models of yeast, mice, and human cell lines knockout for glycosylation enzymes have opened new areas of the functions of glycans. The biological roles of glycosylation have been described and classified in a recent review by Ajit Varki into three categories (i) the structural and modulatory roles (i.e. solubility, rheological properties, protection against proteases....) (ii) extrinsic (interspecies) recognition of glycans (pathogen adherence, toxin fixation....) and (iii) intrinsic (intraspecies) recognition of glycans. In the following chapter, we have focused on the intrinsic recognition and classified the biological functions of *N*-glycosylation into three subgroups, according to the evolution of the *N*-glycosylprotein: the birth, the maturation and the death of the glycoconjugate. We will give some examples illustrating their roles in cellular communication, in molecular targeting and in the modulation of the function of the glycoconjugates (Varki, 2017).

### 1.4.1 Role of the *N*-glycan during their biosynthesis

#### 1.4.1.1 Calnexin/calreticulin cycle

In the ER the *N*-glycosylation occurs co-translationally and one of the main roles of *N*-glycans is the recognition by lectins implied in the optimal conformation of the nascent protein. A description of the ER lectins and specially of the Calnexin-Calreticulin cycle checkpoint is made in §1.2.1.5, §1.2.1.7.

#### 1.4.1.2 Mannose-6-Phosphate

Mannose-6-phosphate is the targeting signal to the lysosome for enzymes (Kundra and Kornfeld, 1999). *N*-glycoproteins possessing mannose-6-phosphate residues will be recognized by two different groups of MPR: CD-MPR or CI-MPR regarding whether this receptor is calcium-dependent or independent, previously described in §1.3.2.

### 1.4.2 Role of the mature glycoconjugate

#### 1.4.2.1 Role of the *N*-glycan backbone

During the last decade, the work of Jim Dennis group described the importance of the interaction of *N*-glycan with the galectin network at the surface of the cell. At the cell surface,

multimeric galectin 3 interacts with the *N*-acetylglucosamine groups of the *N*-glycan forming a lattice with the glycoconjugates. The strength of the interaction is quantitative and increases with the number of glycans, the number of branches and the length of the glycans.

The branching of *N*-glycan is governed by specific *N*-acetylglucosaminyltransferases, and is regulated by the metabolic flux; when *N*-acetylglucosamine, glucose and secondary UDP-GlcNAc concentrations increase the number of branches of the glycan increases (Dennis et al., 2009). This interaction regulates the surface level of transmembrane receptors and of solute transporters, and has a great number of physiological consequences (Nabi et al., 2015). Galectin 3 binds to the *N*-glycan of the epidermal growth factor receptor (EGFR) and reduces the lateral diffusion and the endocytosis of the receptor. The more the glycans of the receptor are branched, the less it is removed from the cell surface to endocytic domains. An interesting observation is the difference of glycosylation between growth promoting receptors possessing a great number of glycans and arrest promoting receptors possessing a low number of glycans, this results in a differential arrival at the cell surface of the receptors when there is an increased metabolic flux (increase of GlcNAc). The first to arrive at the cell surface at low UDP-GlcNAc concentrations are the growth promoting receptors (*i.e.*: EGFR, PDGFR, insulin receptor) with a hyperbolic kinetic response and the arrest promoting receptors (*i.e.*: transforming growth factor  $\beta$  receptor) arrive in a sigmoidal response (switch-like response) with the increase of UDP-GlcNAc concentration. The metabolic flux stimulates first the growth and, at higher flux, the arrest and the cellular differentiation.

In the galectin network, the retention of the receptor and solute transporters by the number of glycans and their branching is implicated in a great number of pathophysiological effects. We will describe as examples the glucose transporters (GLUT1, 2 and 4) and the T-cell Receptor (TCR).

The glucose transporters GLUT2 and 4 possess a single *N*-glycan and are dependent of the branching (and of the metabolic flux) for cell surface retention; the insulin receptor has 18 potential sites of *N*-glycosylation. In this regard, deficient mice in the branching enzyme *Mgat5*<sup>-/-</sup> present a phenotype with hypoglycemia, resistance to weight gain on a high fat diet, and deficient mice in *Mgat4a*<sup>-/-</sup> present a phenotype with hypoinsulinemia and hyperglycemia (Cheung and Dennis, 2007). *Mgat4a* induced the branching of the *N*-glycan of the GLUT2 (SLC2A2) and consequently induced glucose transport and insulin secretion of in the pancreatic  $\beta$  cells (Ohtsubo et al., 2005). *Mgat5* induced the branching of the *N*-glycan

localized on the glucagon receptor and increased the glucagon response in hepatocytes (Johswich et al., 2014). These mechanisms link the UDP-GlcNAc flux to the complex glucose homeostasis through *N*-glycan structures that are present at the cell surface.

Another example of the importance of the galectin molecular lattice at the cell surface and the branching of *N*-glycans concerns the immunity and the autoimmunity sensitivity. Knockout mice for *Mgat5* branching enzymes are more susceptible to autoimmune diseases; one of the physiopathological mechanism implied the role of cytotoxic T lymphocyte-associated protein 4 (CTLA-4) that regulates the T-cell receptor (TCR) clustering. The metabolic flux and secondary the branching of the *N*-glycan, increases the expression of surface CTLA-4 by interaction with galectins that reduces the endocytose and consequently increases the threshold of TCR activation (Lau et al., 2007). A more recent study, has demonstrated the influence of *N*-glycan branching in multiple sclerosis (MS), through environmental and genetic factors, among them vitamin D and sunshine that increases the branching of *N*-glycans and consequently reduces MS risks. This is confirmed by Genome-Wide Association Study (GWAS) of MS that has shown the influence of *MGAT5* gene in the disease prognosis (Brynedal et al., 2010; Mkhikian et al., 2011).

In general, the *N*-glycan backbone is important and has to be considered as a number of *N*-acetylglucosamine groups reacting with galectins, the affinity of the interaction increasing with branching and with the length of the glycan chain. A recent study has shown that further reducing of the branching (*Mgat2* knockout) was compensated by elongation of the glycan (Mkhikian et al., 2016).

Finally, these *N*-acetylglucosamine groups are the support of the peripheral “decoration” of the *N*-glycans (*i.e.* sialylation, fucosylation and sulphation) that modifies or fine-tunes the properties of the glycoconjugates.

#### 1.4.2.2 Role of the periphery of the *N*-glycan

The importance of the periphery of the *N*-glycan has been demonstrated through numerous biological examples; the modulation of immunoglobulin G crystallizable (Fc) fragment functions by glycosylation is one of the most interesting recently opened fields of glycobiology.

Immunoglobulin G (IgG) is a heterotetrameric glycoprotein consisting of two light chains and two heavy chains. Papain digestion cleaves IgG into two fragments, the antigen binding

fragment (Fab) and the crystallizable fragment (Fc). The Asn at position 297 is substituted by a *N*-glycan, which structure can be described as a core of seven monosaccharides substituted by different sugars (**figure 8**). The various substitutions by galactose, sialic acid, fucose and bisecting GlcNAc residues can generate 36 different structures; the five majors that represent 90% of the glycans are described in (**figure 8**).

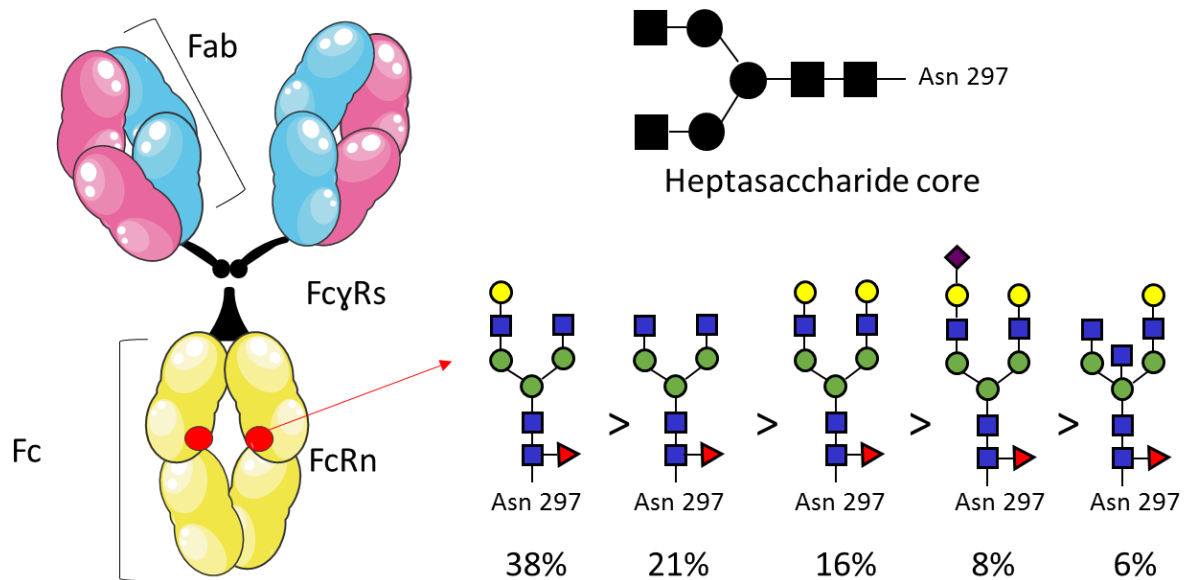


**Figure 8. Structures of the IgG-Fc *N*-glycans attached to Asn297** (adapted from Kiyoshi et al., 2017).

While the Fab fragment recognizes the antigen, the Fc carries the effector properties of the molecule by interactions with the Fcγ receptors (FcγR) on the surface of different cells (leucocytes, dendritic cells, platelet...) or with the complement system. IgG is involved the defense against pathogens and toxins and contributes to their efficient neutralization and elimination. They are also implicated in the pathophysiology of numerous autoimmune diseases (*i.e.* rheumatoid arthritis (RA), systemic lupus erythematosus (SLE), myasthenia gravis...). Glycosylation of IgG has been shown to be important for the tuning of the biological properties of IgG (antibody-dependent phagocytosis, antibody-dependent cell-mediated cytotoxicity (ADCC), and complement-dependent toxicity). The various substitutions of the heptasaccharide core by different monosaccharides affect differently the function of the Fc part of IgG (**figure 8**).

Decreased galactosylation and sialylation has been first observed in rheumatoid arthritis (Parekh et al., 1985) and in various autoimmune disorders. Furthermore, a decrease in galactosylation has been observed during the humoral immune response (Lastra et al., 1998). The absence of galactose induces an increased mobility of the underlying GlcNAc residues,

allowing an easier interaction with the mannose binding protein (MBP) and consequently facilitates activation of the complement pathway through the C1q that contributes to the inflammation (Malhotra et al., 1995).

Sialylation change the properties of the IgG from inflammatory to anti-inflammatory. This has also been shown by the therapeutic use of intravenous immunoglobulin (IVIg) and by the production of tetrasialylated IVIg in the treatment of acute inflammatory access of autoimmune diseases (Kaneko et al., 2006; Washburn et al., 2015).

Sialic acid mechanisms of action are complex and depend on Fc $\gamma$ R on which they react (type I or type II) and on the diversity of the cells in which they are expressed. Type II Fc $\gamma$ R are C-type lectin receptors, with two members CD23 and DSC-SIGN. An increase of sialylation of Fc increased the interaction with CD23 on B cell. This mechanism has been shown to improve the influenza vaccination efficacy, sialylated Fc abundance predicting the quality of the vaccine response (Wang et al., 2015b).

Fucosylation is important for the modulation of the pro-inflammatory activity of IgG as fucose removal increases the ADCC. Antibodies lacking fucose have an increased affinity for Fc $\gamma$ RIIIa, and an increased efficiency of ADCC (Ferrara et al., 2011). These findings have been applied to therapeutic antibody for the treatment of cancers (Liu et al., 2015).

Bisecting GlcNAc residue has been shown to enhance the ADCC (Umana et al., 1999) but to a lesser extent compared to the absence of fucose residue (Shinkawa et al., 2003)

This example shows how the different monosaccharides of the *N*-glycan periphery can influence the function of a glycoconjugate, by modifying the accessibility of the underlying protein or by interacting with different Carbohydrate recognition Domain (CRD) of receptor proteins.

The diversity of *N*-glycan functions is correlated to the diversity of glycan binding proteins and establishing a list of the different human lectins with fundamental biological properties would be tedious. Among them we can cite the selectins, the Siglecs, the man/ GalNAc-4-sulfate receptor, collectins...

The function of a *N*-glycan might be summarized to the addition of the backbone and the periphery properties. The resulting biological effect might reflect the diversity of the structure(s) present on a glycoprotein and is a much more complex language than the genetic code or the protein amino-acid sequence and remains to be elucidated.

### 1.4.3 Role of the *N*-glycans in the half-life of circulating glycoproteins

Desialylated glycoconjugates are eliminated from the blood stream by two liver receptors, possessing C-type CRD, (i) the asialoglycoprotein receptor (ASGR) made of two units (Asgr1, Asgr2), and (ii) the mannose receptor (ManR) (Zhou and Qiu, 2019). These endocytic receptors remove glycoproteins with terminal Gal and GalNAc residues, for the ASGR in the liver parenchyme, and containing Man, GlcNAc, or SO<sub>4</sub>-4-GalNAc residues, for the ManR in the liver sinusoidal endothelial cells. These receptors regulate the half-life of numerous circulating glycoproteins. The knockout of these receptors in mice demonstrated their importance in the regulation of reproductive hormones, blood coagulation factors and in controlling the serum level of glycoproteins (Mi et al., 2016).

### 1.4.4 General approach of the role of glycans

The roles of glycans still remains poorly understood, under certain circumstances the removal of the *N*-glycan from a glycoconjugate does not change the properties of the glycoconjugate (*i.e* transferrin) (Zhao and Enns, 2013), at the opposite the complete knockdown of certain GT is not compatible with life.

Hudson Freeze in 2001 published an article in which he hypothesized that during evolution there has been an advantage to reduce glycosylation to the minimal but necessary functions (Freeze and Westphal, 2001). The diminished glycosylation conferred an advantage by reducing the numbers of fixation sites for pathogens.

The glycans in general are extracellular at the surface of cells or in the extracellular media their roles are consequently principally in the cell-cell communication (immune cells, tissue development, nervous communication) and represent a language that is far to be fully understood.

## **CHAPTER 2: Regulation of the *N*-glycosylation process**

The first CDG described affected the supply of the secretory pathway in precursors required in the *N*-glycoconjugate biosynthesis. Every steps of the lipid-linked oligosaccharide precursor biosynthesis abnormalities were discovered over the time. Dissimilarly, affection of steps following the precursor transfer lead to glycosylation defect categorized as CDG type II. Mutations in genes encoding Golgi enzymes (glycosyltransferases and glycosylhydrolases) involved in the maturation and trimming of the *N*-glycans, or in the nucleotide sugar transporters, have been reported and abundantly reviewed. More recently, mutations in proteins involved in the secretory pathway homeostasis, affecting vesicular trafficking, pH and ionic environment of the ER and the Golgi apparatus were reported as type II CDG. Understanding the regulation mechanisms of each aspect of the secretory pathway complex machinery is the first step toward therapeutic development.

### 2.1 The role of Golgi structure

The comprehension of the Golgi architecture and the secretory pathway vesicular trafficking is important to understand how any disruption might impact the whole *N*-glycosylation process. The view is even more complex as there are different controversial models of the Golgi dynamics.

#### 2.1.1 Golgi discovery

The Golgi apparatus was discovered by Camillo Golgi (1843-1926) in Pavia, Italy. This medical neuropathologist focused his studies on the central nervous system. In 1889, he ended the Golgi controversy shedding light on the organelle *via* the so-called “black reaction” histological staining technique. This *reazione nera* based on silver staining allowed the visualization of the Golgi apparatus in neurons. For this discovery, Camillo Golgi received the Nobel Prize of physiology and medicine in 1906 together with Santiago Ramón y Cajal. Their finding was assessed in the early 1950s with the first electron microscopy image of the organelle (Berger and roth 1997, Dröscher 1998).

#### 2.1.2 Golgi architecture

In invertebrates, like in the budding yeast model *Saccharomyces cerevisiae*, Golgi stacks are sparse and distinct compartments in the cytosol (Preuss et al., 1992). Dissimilarly, in most

vertebrates as in humans, the Golgi apparatus appears as a ribbon with perinuclear localization during the interphase. In these higher eukaryotic organisms, the Golgi ribbon is made of the fusion of 3 to 20 individual flattened stacks, called cisternae. These cisternae are polarized from *cis* to *trans* and are compartmentalized in several networks: the CGN (*cis*-Golgi Network), the *cis*-Golgi, the *medial*-Golgi, the *trans*-Golgi and the TGN (*Trans*-Golgi Network) (Makaraci and Kim, 2018). Localized near the centrosome or MTOC (Microtubules Organizing Center) this structure is in constant remodeling. This plasticity is mainly due to interactions with the cytoskeleton *via* many intermediates such as dynein, a microtubule-associated motor protein (Zhu and Kaverina, 2013). Indeed, a dispersion of the Golgi architecture has been assessed for a long time by means of experiments of microtubules depolymerization using a drug, Nocodazole (Shima et al., 1998). These interactions with the cytoskeleton govern the balance between Golgi mini-stacks structure required for the mitosis and the ribbon structure observed in G<sub>0</sub>.

### 2.1.3 Actors of the maintenance of the Golgi structure

The architectural organization of the Golgi apparatus is mediated by two main families of proteins: GRAPS (Golgi Reassembly Stacking Protein), a Golgi matrix proteins family, and Golgins, a tether proteins family. They maintain the balance between the ribbon and mini-stacks organizations of the GA. The first Golgi stacking protein family to be identified was GRASP, that encounters two members GRASP65 (GORASP1) and GRASP55 (GORASP2) in human (Barr et al., 1997). GRASP65 is localized at the *cis*-Golgi cisterna while GRASP55 is in the *medial*-Golgi. They are oriented and tethered inside the Golgi membrane by two phenomena: myristoylation of their N-terminal tail and linkage of their C-terminal tail to Golgin proteins. GM130 golgin binds to GRASP65 whereas Golgin-45 preferentially links to GRASP55 (Barinaga-Rementería Ramirez and Lowe, 2009; Rabouille and Linstedt, 2016). Golgins are members of the CCT (Coiled-Coiled Tethers), characterized by a large coiled-coil structure also called superhelix that enables interactions with the cytoskeleton and nearby membranes. Other members of the CCT family will be further approached in this section.

As Golgi functions have been mainly conserved throughout evolution, the benefit of the emergence of a ribbon structure among vertebrates remains elusive. One can hypothesize that it allows a more accurate regulation of cellular processes (Makhoul et al., 2018).

Interestingly, in many neurodegenerative pathologies such as Amyotrophic Lateral Sclerosis (ALS) (Sundaramoorthy et al., 2015), Parkinson disease, Alzheimer disease, and Huntington's chorea, a fragmentation of Golgi architecture in neuronal cells can be observed concomitantly to protein aggregation. This further assesses the crucial importance of the Golgi ribbon structure; however, the underlying relationship between this subcellular aspect and neurodegeneration remain elusive (Jie Fan IJDN 2008).

#### 2.1.4 Controversies about Golgi dynamic

The mechanism by which glycoproteins and/or glycolipids move through the GA has been a long-standing source of controversies. The first hypothesis lies in a model of the progressive movement of the Golgi stacks with maturation during the process. The second hypothesis resides in the potential existence of an anterograde transit of vesicles from a static cisterna to another. These two hypotheses may not be exclusive; furthermore, emerging concepts have recently emerged to complexify these models.

##### 2.1.4.1 The cisternal maturation model

Golgi is thought to be a conveyor belt. Vesicles from ER are fusing to the *cis*-Golgi network. A *cis*-Golgi cisterna will mature into a *medial*- one and then move forward and become a *trans*-Golgi stack. Finally, this stack bubbles into TGN vesicles that will be sorted and dispatched to their final destination (Farquhar and Palade, 1981). The *cis*-Golgi contains enzymes needed at the onset of the maturation process, while the *trans*-Golgi cisterna houses enzymes like galactosyltransferases, fucosyltransferases, and sialyltransferases that are in charge of the latest steps of this process. As a cisterna progresses, Golgi resident proteins are loaded into the rims of COPI vesicles in order to send them back to a younger cisterna (**figure 9**). This retrograde transport would maintain the localization of each resident protein in their intended cisterna. In this model, cargoes are not leaving the cisterna membrane and lumen (Glick and Nakano, 2009; Kurokawa et al., 2019) and these proteins, as Carroll Lewis wrote in *Alice in Wonderland*, “*must run as fast as they can, just to stay in place* ».

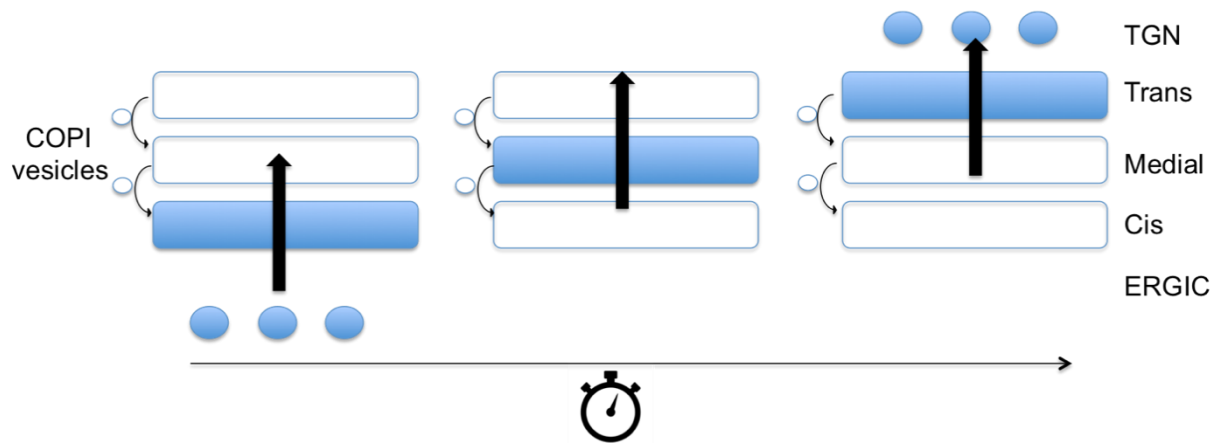


**Figure 9. Schematic representation of the cisternal maturation model**

#### 2.1.4.2 The intra-Golgi vesicular transport model

A second scenario hypothesizes the stability of the cisternae over time. Cargo molecules are ferried from the ER to the TGN undergoing distinct processing and sorting in a strictly ordered sequence along Golgi cisternae (Rothman and Wieland, 1996). Vesicles would transit gradually in the *cis-trans* direction carrying their protein content with them. They move from one cisterna to another in an anterograde manner, excluding Golgi resident enzymes that remain in their workplace (Dunlop et al., 2017). A supplementary argument for this model is the rapid crossing of small soluble proteins through the Golgi stacks. For instance, it takes 15 minutes for pro-collagen to go from the *cis*- to the *trans*-Golgi and only 2 minutes for albumin. This speed might be due to an anterograde movement of the vesicles (Beznoussenko et al., 2014).

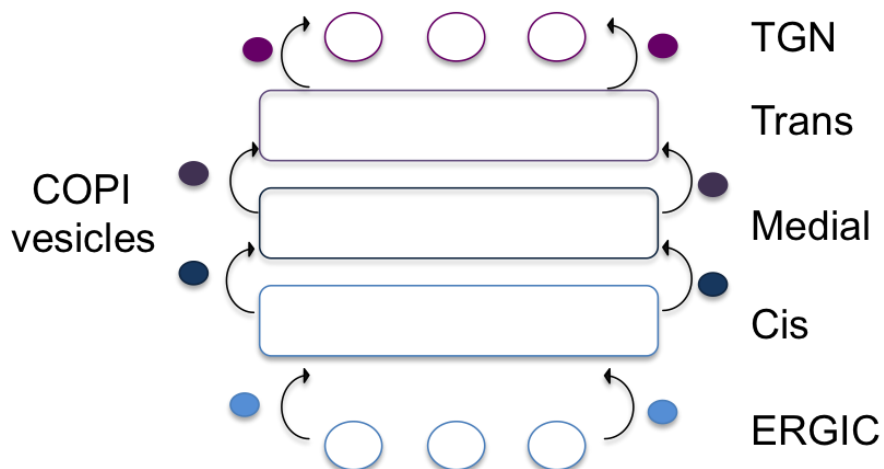


**Figure 10. Schematic representation of the anterograde vesicular trafficking model**

Nowadays, these two models are still a source of controversies (Boncompain and Weigel, 2018). The truth might reside in the possible coexistence of several models. Parashuraman's team recently made controlled aggregation studies showing that aggregated glycosylation enzymes, not entering in carriers, are still moving forward in Golgi stacks reinforcing the maturation model hypothesis (Rizzo et al., 2013). Conversely, Lavieu and collaborators "staples" proteins in compartments showing that they were not able to move forward comparatively to soluble aggregates, consolidating the second model (Lavieu et al., 2013). These two publications can be argued as they are conducted in non-physiological conditions. Moreover, other models have raised with the notion of a tubular vertical continuity between cisternae (Glick and Luini, 2011) and a rapid-partitioning. This model of rapid-partitioning was proposed by Patterson and collaborators in 2008. The existence of different sections in each cisterna, retaining more or less resident enzymes regarding the lipid composition of the section, is hypothesized. For example, sphingolipids proportion will be the highest in *trans*-Golgi, whereas glycerophospholipids would concentrate on the ER, *cis*- and *medial*- cisternae (Patterson et al., 2008). There would be a *cis-trans* polarity coupled to a lateral one.

## 2.2 Golgi intra-vesicular trafficking

In 2013 James E. Rothman, Randy Schekman, and Thomas Südhof received the Nobel Prize in Physiology or Medicine for their work on vesicular trafficking. The Golgi is the central hub of membrane trafficking where vesicles are shuttled achieving transport from a donor compartment to an acceptor compartment.

As exposed in chapter one, a great number of molecular players are needed for soluble or membrane glycoproteins distribution, the membrane curvature, and vesicle budding. A signal sequence for the retrieval pathway of resident ER membranes proteins lays in the sequence KKXX (Lysine-Lysine-X-X) which is recognized by COPI coat proteins. In a different way, ER-resident soluble proteins are retrieved to the ER by their KDEL sequence before entering COPI vesicles.

The cargo recruitment implies protein-protein interactions by coat proteins such as clathrin or COP proteins (COatomer Protein complex). Clathrin coat is required for the secretory vesicles sorting from the TGN and will not be further detailed here. However, the following

information about vesicular trafficking effectors may be helpful to better understand the overall Golgi functions regulation. In human, COPII-covered vesicles initiate the anterograde transport while the heptameric COPI can be implied in both retrograde and anterograde transport mechanism between ERGIC and *cis*-Golgi (Appenzeller-Herzog and Hauri, 2006).

The budding step engaging COP proteins is governed by Arf (ADP Ribosylation Factor)/Sar1 proteins from the RAS superfamily (Rat Sarcoma). This highly conserved superfamily includes Arf, Sar, Rac, Ras, Rho, Sar, dynamin Rab family. These proteins exist under two forms: the active form is linked to GTP while the inactive form is linked to GDP. When Arf/Sar1 is under its GTP form, the hydrophobic tail enshrines in the membrane of the vesicle initiating COP proteins assembly around the membrane to form a sphere (Dodonova et al., 2017).

Following this budding step, the anchoring and fusion of the vesicle will require the cooperation of many factors such as GTPases, tethering factors and fusogenic SNAREs. There are two groups of tethering factors in the maintenance of Golgi vesicular trafficking, the first consists of the Multisubunit Tethering/Trafficking Complexes (MTCs) (Brunet and Sacher, 2014) and the second is represented by the Coiled-Coil Tethers (CCT). The CCT are long structures including Golgins (GM130, Giantin...). The MTCs consists of two different complexes, (i) Complexes Associated with Tethering Containing Helical Rods (CATCHR) including the Conserved Oligomeric Golgi complex (COG) and GARP (Glycoprotein A repetitions predominant), and (ii) NON-CATCHR including Transport Protein Particles (TRAPPs), the Homotypic fusion and Protein Sorting complexes (HOPS) and class C Core Vacuole/Endosome Tethering complex CORVET. Here we will focus on the vesicle trafficking steps implying MTCs whose defects are responsible for CDG such as COG complex that is now well documented.

### 2.2.1 COG complex

The COG complex is a cytosolic hetero-octameric structure expressed in every eukaryote cell and highly conserved from yeast to human. This complex operates as a vesicular tether in the COPI-initiated retrograde trafficking of the COG complex-Dependent (CCD) vesicles. It retrieves compounds from the distal compartments back to their site of function (Foulquier, 2009).

This complex is made of two subcomplexes called lobe A and lobe B, each made of 4 subunits. Lobe A is composed of COG1 to COG4 while lobe B is made of COG5 to COG8. Each COG has a

molecular weight between 70 and 110 kDa for a total of approximately 800 kDa for the global complex (Ungar et al., 2002). By the mean of knockdown experiments, each of these subunits was shown to be essential for the global function of the COG complex and also these lobes are codependent, *i.e* a disruption of one subunit destabilizes the entire lobe (Smith and Lupashin, 2008).

### 2.2.1.2 COG complex mechanism in vesicle tethering

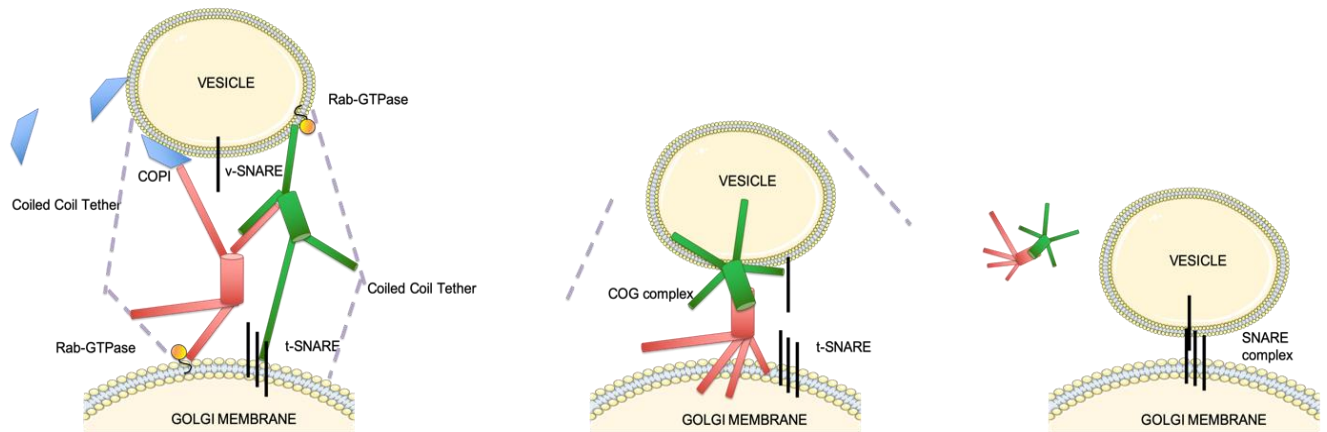


**Figure 11. Simplified hypothetical function of COG complex in vesicle tethering and fusion** (Inspired from several publications from the work of V. Lupashin and D. Ungar REF)

COG complex interacts with core components of the vesicles: COPI coat protein, Ras-Associated protein found in Brain (Rab)-GTPases, coiled coil tethers (CCT), fusogenic Soluble N-Ethylmaleimide-sensitive factor-activating protein Receptors (SNAREs) and SNARE-interacting proteins for the tethering docking and fusion machinery. These interactions occur sequentially to achieve the approach, tether, docking and fusion steps.

Several hypotheses about this ordered process recently arose through with the possibility of the spatial separation of the 2 lobes (Foulquier, 2008). The model proposed by Pr Lupashin is the most commonly admitted (Blackburn et al., 2019) and consists of the following steps, as soon as a COPI vesicle buds off, Rab proteins, acting as a molecular switch, bind to it. Rab family is a group of 70 protein members of the Ras superfamily. In humans, Rab-GTPases, also called small GTPases, have different localizations. In the case of a COG complex-dependent vesicle, Rab proteins form a “signaling platform” at the vesicle surface.

It is proposed that the two lobes interaction is transient. There are two different types of SNAREs implied in this process, v-SNARE localized to the vesicle surface and t-SNARE, “t” for target, localized to the acceptor compartment, a Golgi cisterna. Lobe B on the vesicle side

interacts with the v-SNARE and Rabs. Conversely, lobe A on the Golgi membrane interacts with t-SNAREs, Coiled-coil tethering factors and Golgi Rabs. Among the 20 Rab proteins that are associated with the GA, the COG complex can bind 12 different members (Willett et al., 2013). As a vesicle approaches the Golgi membrane by means long CCTs, the two COG lobes can stick together. As the in-between space reduces, lobe A localized on the acceptor membrane can fix to the lobe B. The transient interaction of the two COG lobes increases their proximity between the donor and acceptor membrane and induces a correct alignment of the SNAREs. At this step, v-SNARE and three t-SNARE molecules rearrange in the correct orientation to form a bundle of four SNAREs called the *trans*-SNARE complex. SNAREs proteins and the energy released by their assembly cause the *bonafide* fusion. The COG complex then unties and can start over a new cycle (Willett et al., 2016).

#### 2.2.1.2 COG complex and N-glycosylation

The knockdown of COG subunits one by one lead to the spread of vesicles surrounding the Golgi, to the formation of a distorted Golgi apparatus in mini-stacks and to the apparition of a large vacuole in human cells. Due to the inhibition of the fusion process of vesicles with Golgi stacks, these vesicles are directly targeted to the lysosome. This fusion results in the formation of a vacuole called Enlarged Endo-Lysosomal Structure (EELS), in which acidity is maintained by the V-ATPase pump. This COG-deficient cells specific phenotype does not alter the viability of the cells and is completely restored by the reintroduction of each WT form.

One hypothesis to link COG complex and glycosylation is, that the disturbance of the Golgi architecture abolishes the close contacts between COG and the Golgi cisternae, hence separating glycosyltransferases from their substrates. The mistargeting of the cargo also results in faster degradation of the GT, and consequently the Golgi is deprived of resident enzymes (D'Souza et al., 2019).

In HeLa cells, the knockdown (KD) of lobe A lead to the disturbance of the overall Golgi architecture while the KD of lobe B showed a destabilization and/or mislocalization of two enzymes implied in the late Golgi N-glycosylation process:  $\beta$ 1,4-galactosyltransferase 1 (B4GALT1) and 2,6-sialyltransferase 1 (ST6GAL1) (Haijes et al., 2018; Peanne et al., 2011).

Another recent study, conducted in CrispR/Cas9 COG KO HEK293T cells, demonstrated an increase of hypermannosylated N-glycans. To detect immatures N-glycoconjugates, Bailey-Blackburn and collaborators used a lectin, *Galanthus nivalus* lectin (GNL), that

recognizes the terminal  $\alpha$ 1,3 linked mannose residues. Their results demonstrated the impairment of the MAN1A1, MAN1A2, MAN1C1, MAN2A that are *cis/medial*-Golgi mannosidases and a GlcNAc transferases MGAT1 (Bailey Blackburn et al., 2016). These enzymes were already classified as COG complex-dependent enzymes in previous studies (Pokrovskaya et al., 2011).

Immunoprecipitation experiments demonstrated that COGs have a great number of partners interacting with the whole COG complex or with a single subunit. TMEM165, another protein involved in a CDG type II, was found to be one of the proteins able to interact with the COG complex. Interestingly no modification of TMEM165 expression was observed in COG knockout cells and reciprocally (Blackburn et al., 2018).

These results explain the altered glycosylation pattern observed in COG-CDGs patients; that will be discussed in the next paragraph.

#### 2.2.1.3 COG-CDGs

COG defects in patients lead to type II CDGs, called COG-CDG. The first described was COG7-CDG (Wu et al., 2004). All the different subunits have been involved in a COG-CDG at the exception of COG3 (Foulquier et al., 2007; Paesold-Burda et al., 2009; Reynders et al., 2009; Zeevaert et al., 2008, 2009) and these CDG represent approximatively 70 cases in 2019 (Blackburn et al., 2019). Clinically, alterations of the CNS, liver, spleen, eyes, heart and skeletal functions have been reported (Climer et al., 2018). The observed phenotypes are diverse and can be either due to *O*-, *N*- and lipid glycosylation abnormalities or to an isolated impairment of the *N*-glycosylation. Mass spectrometry reveals a predominant modification of the *N*-glycans sialylation but also galactosylation and fucosylation (cf § 2.2.1.2) (Blackburn et al., 2019).

These pathologies demonstrate the importance of vesicular trafficking regulation in *N*-glycosylation and more specifically of the COG complex-dependent trafficking regulation where every single subunit is essential.

#### 2.4.2 Other membrane trafficking CDGs

Many other CDG type II linked to an alteration of the retrograde or anterograde Golgi vesicular trafficking have been reported during the last years. Two examples among others are described in the next paragraphs. It is worth noting that new diseases with phenotypes related

to CDG syndrome have also been reported with mutations in genes coding for coatamer protein subunits, for instance *COPA*, *COP2B* and *ARCN1* for COPI and *SEC23A*, *SEC23B*, *SEC24D*, *SAR1B* for COPII (Ferreira et al., 2018).

#### 2.2.2.1 TRAPP complexes

The Transport Protein Particle complexes (TRAPP) are another tethering protein family. Recently mutations in genes coding for TRAPP II and III complexes subunits have been involved in type II CDGs. Patients presented a defect in both *N*- and *O*-glycosylation and delayed vesicular trafficking, but compared to COG-CDG, TRAPP-CDG, they have very divergent phenotypes (Sacher et al., 2019).

#### 2.2.2.2 Golgin RAB6 Interacting (GORAB)

COPI proteins are recruited at the Golgi membrane by GTPase proteins, such as Arf, to assemble as a coat. Recently disruptions of other intermediates between these main actors have been identified like GORAB, a protein required in the *trans*-Golgi cisternae for Arf recruitment. It results in a dermatological affection called Geroderma Osteodysplastica (GO). GO is now considered as a CDG type II-like affection presenting similarities with COG defects such as the presence of an *N*-glycosylation defect (Witkos et al., 2019).

### 2.3 Nucleotide-sugars

Although the NST are a key element for the Golgi glycosylation machinery, they have not been yet shown to be a component involved with COG or any vesicular trafficking defect.

#### 2.3.1 Nucleotide-sugar sources

Monosaccharides may originate from external or internal sugar sources. We distinguished the exogenous import from the internal recycling and activation/interconversion of monosaccharides. The percentages of sugars of each origin used in the Golgi for glycosylation remain unknown.

##### 2.3.1.1 Import of exogenous sugars

In human monosaccharides enter the enterocytes via two different pathways. The first one is the facilitated diffusion which is energy-independent. For instance, it can be conducted by a

family of glucose transporters (GLUT) encoded by *Solute Carrier A2 (SLCA2)* genes. This family is constituted of 14 members that harbor a signature amino acid sequences for GLUT. Their barrel shape allows the import of hexoses with different affinity according to the transporter and the sugar. On the contrary, other transporters are energy-consuming. As examples, Sodium/Glucose Transporters (SLGT) encoded by *SLC5* genes are localized at the epithelium of guts and kidneys.

#### 2.3.1.2 Recycling

The contribution of the lysosome salvage pathway is consequent regarding the cell type and the implicated sugar. For instance, liver cell lysosomes are recycling 80% of their GlcNAc into UDP-GlcNAc of which 30% is reused for the biosynthesis of *N*-glycans. On the opposite, mannose is poorly recycled. Recycled monosaccharides are using many specific carriers from the lysosome to the cytoplasm (Varki, 2015).

#### 2.3.1.3 Monosaccharides interconversion

Golgi glycosyltransferases require a continuous supply in monosaccharides that have to be activated. This activated form consists of a single carbohydrate linked to a nucleotide diphosphate or monophosphate *via* a phosphodiester bond. Mannose and fucose are attached to a guanosine diphosphate (GDP) molecule, sialic acid is linked to a cytosine monophosphate (CMP) molecule, whereas the other sugars are attached to uridine diphosphate (UDP). The synthesis of the nucleotide sugars occurs in the cytosol with the exception of CMP-Sia synthesized in the nucleus (Parker et al., 2019). Nucleotide sugars can also be the result of interconversion reactions as represented in **figure 12**. Hexokinases can phosphorylate the carbon 6 of Man, Fru, Glc and Gal, but sugar-specific kinases also exist. During the reaction of sugar addition to the growing glycan chain by GT, the hydrolysis of the phosphodiester bond furnishes enough energy for the creation of a glycosidic bond (Lairson et al., 2008). Before this step, nucleotide-sugars have to reach the Golgi and ER lumen by means of transporters called nucleotide-sugar transporters (NST) (Freeze and Elbein, 2009) (**figure 13**).



(Hadley et al., 2019). These transporters are temperature-dependent and present a  $K_m$  approximately 1 to  $10\mu M$  for their substrate. They work as antiporters exchanging an equal number of their corresponding nucleotide-monophosphate in an electroneutral manner (Ahuja and Whorton, 2019). Hence, mono or diphosphate nucleosides are competitive inhibitors of NSTs.

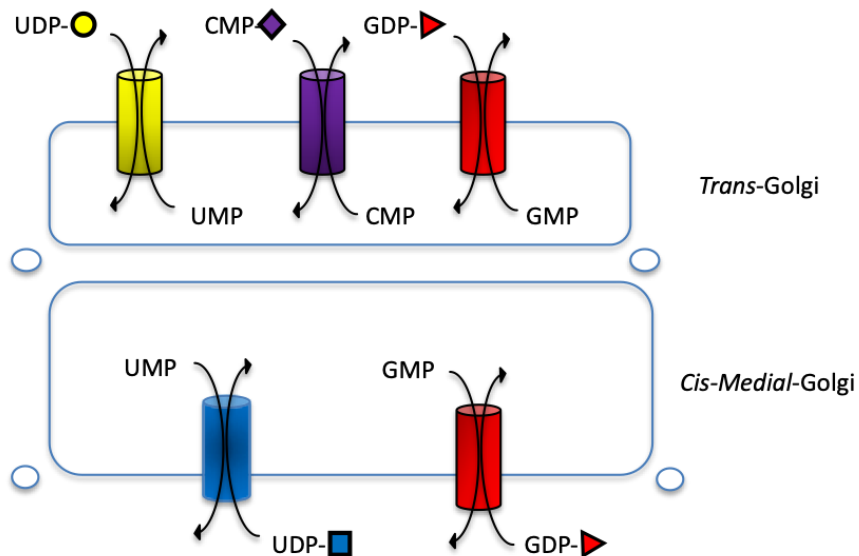


**Figure 13. Nucleotide sugar transporters required for human Golgi N-glycosylation** (inspired from Varki 2015)

The Golgi distribution of the NST is described in **figure 13**. In both ER and Golgi, SLC35A2 imports UDP-Gal while SLC35A3 imports UDP-GlcNAc. Some of them are specific, whereas some are multisubstrate transporters. For instance, SLC35D2 also known as HFRC1 is able to import UDP-GlcNAc, UDP-Glucose or GDP-Man with different affinity constants, respectively 8.0, 2.1 and 0.14 (Suda et al., 2004). Conversely, SLC35C1 imports specifically GDP-Fucose.

#### 2.3.2.2. NST-CDGs

- The defect in SLC35C1 was the first CDG described in this group of diseases. Leukocyte Adhesion Deficiency type II (LAD II) or previously CDG-IIc, now called SLC35C1-CDG, is due to a mutation affecting a nucleotide-fucose transporter in the *medial*-Golgi cisternae. A direct consequence is the underfucosylation of glycoconjugates, defect of expression of sialyl lewis X determinants with an impairment of interactions with selectins leading to immunodeficiency (Lühn et al., 2001). Oral fucose supplementation is available as a promising therapy for these patients. After nine months of treatment, the expression of fucosylated

selectin ligands on neutrophilic cells was induced as well as the presence of a fucosylated core in patient serum glycoproteins. Clinically, there is a reduction of infections and an improvement of psychomotricity (Brasil et al., 2018; Marquardt et al., 1999).

- In humans, UDP-Gal transporter (SLC35A2) shares 43% homology with CMP-Sia transporter (SCL35A1) which is also monospecific (Hadley et al., 2014). SLC35A1 translocates specifically CMP-Sia from the cytoplasm to the *trans*-Golgi stacks lumen. A defect in SLC35A1 is responsible for CDG-II<sub>f</sub>.

- More recently, NST defects such as SCL35A2-CDG (UDP-Gal transporter), SLC35A3-CDG (UDP-GlcNAc transporter) and Schneckenbecken dysplasia due to SLC35D1 (UDP-GlcA/UDP-GalNAc transporter) defect have been reported (Edvardson et al., 2013; Hiraoka et al., 2007; Ng et al., 2013). In the future, one can expect this family of CDG subtypes to further expand.

## 2.4 Glycosylation enzymes

In the human ER/Golgi *N*-glycosylation biosynthesis, six different nucleotide-sugars UDP-glucose, UDP-galactose, UDP-GalNAc, GDP-mannose, GDP-fucose and CMP-Sia are used by glycosyltransferases. Beside glycosyltransferases, trimming enzymes such as glycosidases or glycosylhydrolases are also needed in the *N*-glycan build, however, in this paragraph, we will focus on the first category. Glycosyltransferases are enzymes catalyzing the addition of a donor carbohydrate attached to a nucleotide phosphate on an acceptor, usually a peptide or a lipid backbone.

### 2.4.1 Classification

The enzyme classification nomenclature for glycosyltransferases is E.C.2.4.x.y and has been established by IUBMB (International Union of Biochemistry and Molecular Biology) for every glycosyltransferase regarding their specificity for the glycan they build, for their acceptor, the anomeric, and the nature of the glycosylation reaction. Another classification, the CAZY (Carbohydrate-Active Enzymes) database divided the overall GT in about 106 different families according to the homologies of their short N-terminal sequence, for a total of 480,000 GT identified in 2019 in nature (Mestrom et al., 2019).

### 2.4.2 GT structure

There are about 250 different Golgi GT that mostly share a type II membrane protein structure with a transmembrane domain (TM), a short cytosolic N-terminal tail and a long luminal C-terminal enzymatic tail. The topology of these GT is important to determine their enzymatic activity, localization, and regulation by recognition of their cytoplasmic tail-transmembrane spanning domain (CTS), Stem/Stalk region. These regulation mechanisms will be detailed below (Tu and Banfield, 2010).

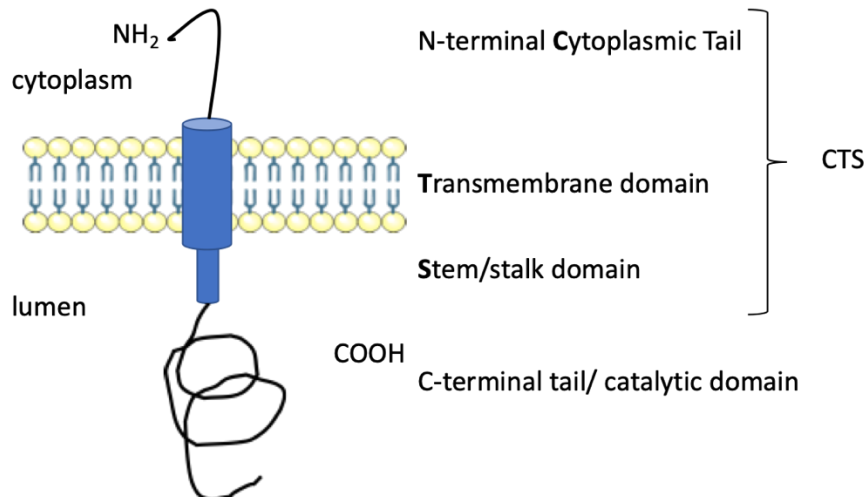
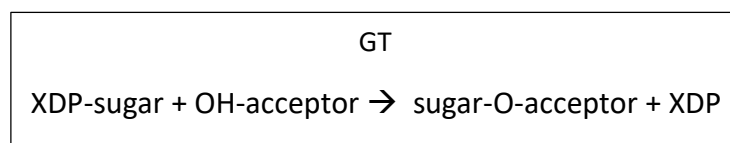


**Figure 14. Glycosyltransferases structure and domains**

GT can also be classified regarding to their 3D structures. According to their folding, most human GT can be classified in GT-A or GT-B structures, both containing Rossmann domains. Their structure will be detailed in chapter 3. Both nucleotide-dependent enzymes GT-A and GT-B catalyze the following reaction (Chemical Glycobiology, 2018).



### 2.4.3 Specificity

As mentioned above, the formal nomenclature of the GT contains the name of the transferred sugar, the nature of the linkage, the name of the acceptor and the isomer number. GT are mostly specific of one reaction and the dogma “one enzyme, one linkage” is virtually always verified. They may be specific of an acceptor as OST for Asn-X-Ser/Thr protein sequence or not, as the  $\beta$ 1-4 galactosyltransferase that can switch from *N*-acetylglucosamine to glucose.

#### 2.4.4 Regulation

*N*-glycosylation is dependent of the activity and the expression level of the enzymes. GT depletion seen in COG-CDG and mutations affecting GT encoding genes dramatically impair the global cell or organism glycosylation profile, and will be detailed in a paragraph below.

##### 2.4.4.1 Localization

The sugar addition to built the *N*-glycan in the Golgi is characterized, first by the localization of both nucleotide-sugar, enzyme and the sugar acceptor in the same compartment at the same time and by the sequential distribution of the sugar added in the different compartment. The *cis*- and *medial*-Golgi compartments are generally the regions of GlcNAc and fucose addition whereas, in the *trans*-Golgi and the TGN, terminal sugars such as sialic acids, fucose, and galactose under the form of their nucleotide sugars are usually transferred (**figure 13**). The mechanisms, by which the distribution of the respective glycosyltransferases is realized and maintained, might be driven by the properties of their transmembrane domain to multimerize and to interact with membrane lipids.

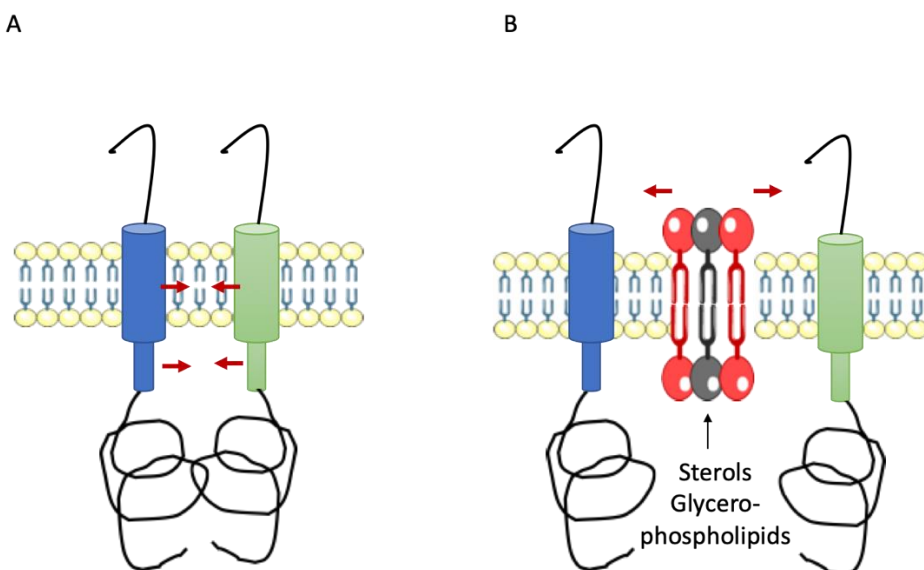


**Figure 15. Glycosyltransferases potential regulatory mechanisms. A.** Multimer association of GT by disulfide bonds or uncharged AA interactions between their TM or stalk domains **B.** Lipid-based partitioning model representation (adapted from Tu et al., 2010)

##### 2.4.4.2 Multimerization

The hypothesis that GT can be found as monomers, homodimers or heterodimers, or oligomers in yeast of enzymes catalyzing the transfer of successive sugars has been first proposed by Machamer in 1991. The existence of neighbor enzymes such as

*N*-acetylglucosaminyl transferase and mannosidase forming heterodimers by their TM domain in the same Golgi cisternae support this paradigm (Banfield, 2011). The kin-recognition model of Nilson claims that GT aggregation in clusters allows the retention at their workplace by preventing their entrance in transport vesicles due to their large size. The oligomerization may result from the formation of disulfide bonds between two enzymes transmembrane domains or interactions between uncharged polar amino acids in the sequence of their CTS site. It is worth noting that, that some peculiar nucleotide-sugar transporters can also form heterodimers; this phenomenon probably regulates their localization (Parker and Newstead, 2019). This kin-recognition model has been criticized since the knockout of the neighbor GT has not shown any effect on the potential interacting partners.

#### 2.4.4.3 The lipid bilayer sorting model

This model arises from three historical observations:

- The size of the transmembrane domain of Golgi GT is shorter than the one found in plasma membrane proteins without any consensus signature sequence of secretory pathway GT.
- The membrane of the Golgi apparatus is thinner than the plasma membrane.
- The lipid composition is different between the plasma membrane and the compartments of the secretory pathway (Bretscher and Munro, 1993).

Moreover, the lipid composition of the early and late cisternae is changing as specific lipids concentrate in the later compartments. *Cis*- and *medial*-Golgi stacks have a composition close to the ER with a majority of phospholipids and few sphingolipids and sterols resulting in a thinner and less ordered membrane than the *trans*-Golgi membrane.

These features are thought to be one reason for the maintenance of the Golgi enzymes at their workplace by their CTS domains. Conversely, the *trans*-Golgi compartments bilayer is rich in sphingolipid and sterols resulting in a thicker and rigid membrane (Welch and Munro, 2019). The potential interaction or repulsion of the GT transmembrane domains amino acids with these bilayer components is called the lipid-based partitioning and complete the model of GT localization regulation processes.

A more recent argument, reinforcing this hypothesis is the dependence of the regulation of the vesicular Golgi trafficking, such as the one found for COG, by the lipid bilayer composition (Blackburn et al., 2019).

To conclude, the retention of GT is due to the length of the transmembrane domain, their CTS

amino acid sequence, their ability to oligomerize together and the lipid composition of the cisternae bilayer. Recognition sequence for vesicular trafficking proteins and adaptors has also been recently discussed in recent studies (Welch and Munro, 2019).

#### 2.4.5 Glycosyltransferases-CDG

CDG-type II are characterized by the presence of truncated glycan structures due to a defect in Golgi maturation steps either caused by a reduction of glycosyltransferases, glycosylhydrolases and/or nucleotide sugars transporters amounts/activity.

Among these GT defects, the first described was MGAT2-CDG in the early 90s. Formerly named CDG-IIa, this affection is due to mutations in GlcNAc transferase II inducing the presence of monoantennary *N*-glycans in the sera of patients (Jaeken et al., 1994). Similarly, B4GALT1-CDG patients have a decreased activity of the  $\beta$ 1,4-galactosyltransferase 1 with a loss of galactose and sialic acid residues on their serum transferrin glycans (Hansske et al., 2002). Other families of GlcNAc-transferases, Gal-transferases and sialyltransferases defects may also lead to the apparition of truncated glycan structures in some specific glycoconjugates or cell types (Joshi et al., 2018).

Concerning glycosylhydrolases, mutations in Golgi trimming glycans enzymes, such as glucosidase I and  $\alpha$ 1,2 mannosidases are responsible for respectively GCS1-CDG, previously CDG-IIb and MAN1B1-CDG (De Praeter CM et al., 2000; Rymen et al., 2013).

Mutations in ER and Golgi enzymes are the cause of most CDG cases, but the reports of type II CDG due to disruption of pH, ion concentration and vesicular trafficking of the secretory pathway are now flourishing.

### 2.5 The importance of Golgi pH homeostasis in *N*-glycosylation

CDGs due to an impairment of Golgi homeostasis have recently arisen. For instance, ATPV<sub>0a2</sub>-CDG is linking *N*-glycosylation and Golgi pH regulation. The mechanism, as well as Golgi pH-related diseases, will be detailed here.

#### 2.5.1 Regulation of pH homeostasis

Compared to prokaryotes, eukaryote cells are characterized by compartmentalization of their functionalities into organelles. Separated from the cytosol by a lipid layer, each organelle has a distinct role that requires an appropriate pH. While mitochondria need a basic environment,

the Golgi apparatus is mildly acidic. By means of pH-sensitive green fluorescent protein approaches like pHluorin, a pH gradient across the Golgi has been measured. Starting from 6.7 pH units in the *cis*-Golgi, the *trans*-Golgi network is more acidic with a pH around 6.0 (figure 16) (Paroutis et al., 2004) (Schapiro and Grinstein, 2000).

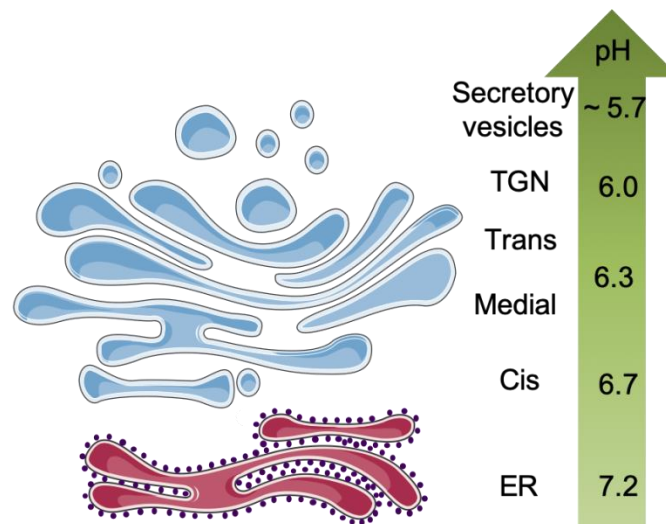


**Figure 16. pH gradient along the secretory pathway**

It has been shown that slight modifications of pH of the secretory pathway alter glycosylation and delays vesicle transport.

A recent study demonstrates that an increase of 0.2 pH unit in the Golgi lumen, by the action of chloroquine, was sufficient to impair the last steps of *N*-glycosylation, delocalizing glycosyltransferases, especially sialyltransferases and galactosyltransferases (Rivinoja et al., 2009).

Another effect of a pH change on Golgi glycosylation is due to modifications of the vesicular trafficking mechanism. The  $V_0$  domain, more specifically the  $\alpha 1$  subunit, would be indeed involved in the membrane fusion with a role in the regulation/formation of a fusion pore (Morel et al., 2014).

The importance of Golgi pH in glycosylation is illustrated by recent reports of diseases, similar to type II CDGs, caused by mutations in genes coding for the  $H^+$  regulators. The pH relies on three different ion movements across the membrane: the vacuolar-type proton ATPase, the counter ion channel and a presumed proton leak channel (Rivinoja et al., 2012).

#### 2.5.1.1 The Vacuolar H<sup>+</sup>-ATPase

The Golgi mildly acidic pH is generated by the energy consuming V-type H<sup>+</sup>-ATPase pump. The other effectors are rather dissipating an excessive membrane potential induced by this pump. In eukaryote cells this V-ATPase, V<sub>1</sub>V<sub>0</sub>-ATPase, uses the hydrolysis of ATP to import H<sup>+</sup> from the cytosol into the Golgi lumen, hence creating an electrochemical potential difference across the membrane and is the latest discovered family of ATP-driven enzymes after the F-type and P-type ATPase family (Pedersen and Carafoli, 1987). The families share homologies but while the F-type is localized at the mitochondrion inner membrane, the V-ATPase is found in intracellular vesicles and plasma membrane. The location has been highlighted by specific V-ATPase inhibition experiments using two macrolide antibiotics: Concanamycin A (Muroi et al., 1993) and Bafilomycin A1 (Bowman et al., 1988).

Beside intravesicular acidification, this pump also has a role as a pH sensor, recruiting vesicle coat components required for vesicle trafficking (Brown et al., 2009).

#### 2.5.1.2 Counter ion conductance

An excessive membrane potential difference would lead to the inhibition of the V-ATPase pump. Therefore H<sup>+</sup> import has to be counterbalanced by the influx of anions or efflux of cations usually by energy-consuming pumps. The Golgi pH regulator (GPHR), a chloride ion channel, is thought to be the main balance of V-ATPase. Maeda and collaborator showed that mutations in GPHR decreased Golgi pH from nearly 0.5 units (Maeda, 2011).

The Cystic Fibrosis Transmembrane conductance Regulator (CFTR), a cAMP-regulated chloride channel is presumed to counterbalance positive charges in the *trans*-Golgi and the TGN. The presence of other chloride channels as the voltage-gated chloride channels ClC-3B, members ClC-family has been recently proposed to have a role in this process. Similarly, a K<sup>+</sup> efflux or the presence of a Na<sup>+</sup>/K<sup>+</sup>-ATPase pump has been discussed.

HCO<sub>3</sub><sup>-</sup> is a soluble buffering molecule that has recently been shown to be imported by anion exchanger AE2a (SLC4A2a) to prevent Golgi over-acidification (Kellokumpu, 2019).

#### 2.5.1.3 Proton leak channel

A proton leak channel system would retrieve back H<sup>+</sup> from the Golgi to the cytosol; the existence of this mechanism remains elusive. The Golgi-localized Na<sup>+</sup>/H<sup>+</sup> exchangers NHE7

belonging to the NHE (Sodium/Hydrogen Exchanger) family could be candidates (Numata and Orlowski, 2001). The orchestration of regulators of the Golgi ions and pH environments are currently far from being completely understood (Kellokumpu, 2019).

## 2.5.2 N-glycosylation abnormalities due to pH regulation defect

### 2.5.2.1 The Vacuolar- H<sup>+</sup>-ATPase structure

V-ATPase is a multimeric complex forming a molecular nano-motor made of two parts, V<sub>1</sub> and V<sub>0</sub>. The cytoplasmic domain V<sub>1</sub> is constituted of 8 different subunits (A<sub>3</sub>B<sub>3</sub>CDE<sub>3</sub>FG<sub>3</sub>H<sub>1-2</sub>) divided in a catalytic part responsible for the ATP hydrolysis (stator) and a stalk part (subunits DF) (rotor). This reaction provides energy for the clockwise rotary of V<sub>0</sub>, the proton pore. The transmembrane domain V<sub>0</sub>, made of 6 different subunits (ac<sub>4</sub>c''de), translocates protons from the cytosol into the lumen of the vesicles or outside the cell in the case of plasma membrane V-ATPases. The regulation of the V-ATPase consists of a reversible disassembly of V<sub>0</sub> and V<sub>1</sub> (Marshansky and Futai, 2008; Oot et al., 2017). Mutations in genes coding for the V-ATPase subunits induce a CDG-type II.

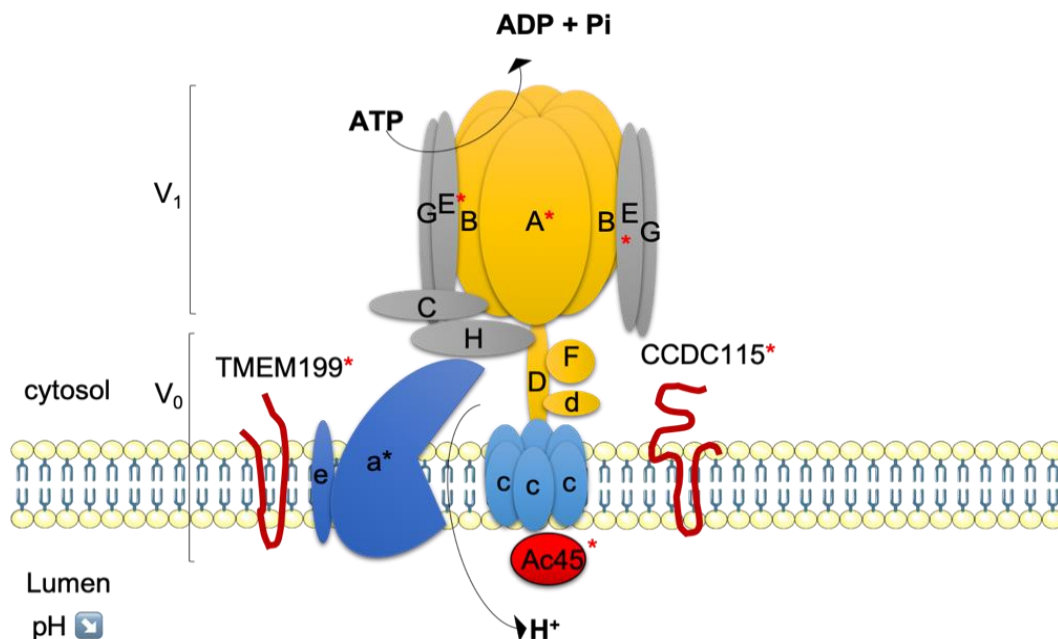


**Figure 17. Point mutations on V-ATPase subunits, assembly factor or accessory factor responsible of a glycosylation defect** (inspired from Rivinoja et al., 2012; Sun-Wada and Wada, 2015) Mutations (depicted with red asterisk) in V<sub>1</sub> subunit E and A, V<sub>0</sub> a subunit as well as assembly (TMEM199, CCDC115) and accessory (Ac45) components of the pump have been so far reported.

### 2.5.2.2 The Vacuolar-type H<sup>+</sup>-ATPase related CDG

Patients affected by the wrinkled skin syndrome, also known as ARCL (Autosomal Recessive Cutis Laxa) [MIM: 219200], present mutations in the gene coding for the  $\alpha 2$  subunit of the V<sub>0</sub> domain of the V-type H<sup>+</sup> ATPase. This translates in a glycosylation defect and an impairment of Golgi trafficking in the fibroblasts which is clinically characterized by a wrinkled skin together with various neurological and developmental impairments (Kornak et al., 2008).

Patients with defects in other subunits of the proton pump have been recently identified. Mutations in the A subunit (ATP6V1A) and the E1 subunit of the (ATP6V1E1) of the V<sub>1</sub> part induce a mild phenotype of the ARCL (Van Damme et al., 2017). The multimeric complex V<sub>1</sub>V<sub>0</sub>-ATPase biosynthesis starts in the ER with the assembly of the V<sub>0</sub> domain orchestrated by numerous proteins. Also, in the last 3 years, mutations in an accessory factor (Ac45) and in assembly factors of the proton pump (TMEM199 and CCDC115) have also been reported to be responsible for CDG-type glycosylation defects (**table 2**).

Gene	Protein	Ortholog in yeast	Potential role	Affected families reported to date	Clinical features	Publication
ATP6V0A2	$\alpha 2$ subunit of V0	Vph1	$\alpha 2$ subunit of V0	>16	ARCLII : wrinkled skin, developmental delay, skeletal abnormalities	(Kornak et al., 2008)
ATP6V1E1	E1 subunit of V1	Vma4	E1 subunit of V1	2	mild to severe ARCL, facial dysmorphism, cardiopulmonary	(Van Damme et al., 2017)
ATP6V1A	A subunit of V1	Vma1	A subunit of V1	3	mild to severe ARCL, facial dysmorphism, cardiopulmonary	(Van Damme et al., 2017)
ATP6AP1	Ac45	possibly Voa1	assembly of V0 pore in the ER	6	hepatopathy, immunodeficiency, epilepsy, intellectual disability	(Rujano et al., 2017)
ATP6AP2	ATPAP2/[pro]renin receptor	No equivalent but interact with Voa1	assembly of V0 pore in the ER together with ATPAP1	2	hepatopathy, immunodeficiency, <i>cutis laxa</i> , psychomotor delay	(Jansen et al., 2018)
TMEM199	TMEM199 / C17orf32,	Vma12	assembly of a subunit to the V0 pore	3	hepatopathy, few patients with intellectual disability	(Jansen et al., 2016a)
CCDC115	Coiled-Coil Domain-Containing Protein	Vma22	assembly of a subunit to the V0 pore	5	hepatopathy, epilepsy, intellectual disability	(Jansen et al., 2016b)

**Table 2. Reported subtypes of CDG type II due to defects in the V-ATPase related components**

Patients with a mutation in a gene encoding these assembly factors present both *N*- and *O*-glycosylation defects of their blood serum. A milder phenotype has been displayed in patients with mutations in *TMEM199* [MIM:616829] (CDG-IIp). This newly identified transmembrane protein, also known as C17orf32, is the human ortholog of Vma1p in yeast, a Golgi iron homeostasis regulator and an important assembly component of the Golgi Vacuolar H<sup>+</sup>-ATPase. *TMEM199* colocalizes with ER, ERGIC and COPI markers. The four patients presented a defect in galactosylation and hence in sialylation, resulting in an hepatopathy (Jansen et al., 2016a).

2.6 Divalent cations Golgi homeostasis

2.6.1 Calcium homeostasis

2.6.1.1 Calcium concentration

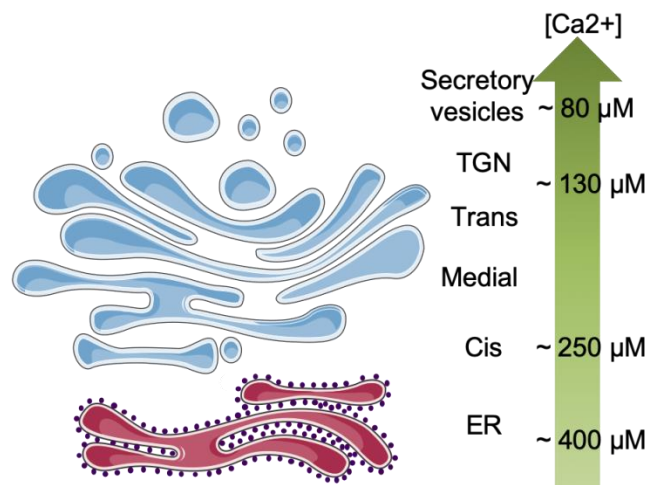


**Figure 18. Calcium concentration gradient along the secretory pathway**

There is a steep calcium concentration difference between the extracellular space (~1.3 mM), the cytosol (~100 nM), and the lumen of organelles may be significantly more concentrated. ER is a compartment of major calcium storage (~400 μM) tightly regulated, however, more recently the Golgi apparatus gained interest as an intracellular calcium store (**figure 18**). The Golgi calcium concentration is variable regarding the sacks; there is a concentration gradient decreasing from the *cis*-Golgi (~250 μM) to the secretory vesicles (~80 μM) (Pizzo et al., 2010). Nowadays, the compartmental calcium concentration of Golgi can be finely appreciated by

means of  $\text{Ca}^{2+}$  dependent fluorescence technique using Fura-2 and Mag-Fluo-4 (Gallegos-Gómez et al., 2018).

Certain glycosylation enzymes also bind to  $\text{Ca}^{2+}$  such as glycosidases of the  $\alpha$ 1,2 mannosidases family (Tempel et al., 2004),  $\beta$ 1,4-galactosyltransferase (Boeggeman and Qasba, 2002) and potentially multiple enzymes implied in glycosaminoglycans biosynthesis (Barré et al., 2006; Cheng and DeVries, 1986). Calcium is an ubiquitous second messenger and also as membrane vesicular trafficking tethers are calcium-dependent, especially SNARE fusion proteins, it may have an indirect role in Golgi glycosylation (Micaroni, 2012).

There are two major calcium pumps, Secretory Pathway Calcium ATPase 1 (SPCA1) and Sarcoplasmic/Endoplasmic Reticulum Calcium Pump 2 (SERCA2) that maintain a high luminal  $\text{Ca}^{2+}$  concentration in the secretory pathway compartments and a low cytosolic  $\text{Ca}^{2+}$  concentration together with Plasma Membrane Calcium ATPase (PMCA) (**figure 19**). The major effector of calcium release are  $\text{IP}_3$  receptor and Ryanodin receptor. These ion transporters have different cisternae localizations, saliently; the *trans*-Golgi cisternae are enriched in SPCA1 pumps and devoid of SERCA2.

#### 2.6.1.2 Calcium uptake

##### 2.6.1.2.1 SERCA

In vertebrates, 3 paralogous genes code for SERCA: *ATP2A1*, *ATP2A2* and *ATP2A3*. Alternative splicing gives birth to up to ten different isoforms with different affinities for calcium, depending on the cell type. SERCA is highly expressed in the sarcoplasmic reticulum of muscle cells, in the ER of other cells and also in *cis*-Golgi with the presence of SERCA2b isoform (Li et al., 2013). This pump is able to import two calcium molecules for every hydrolysis of one ATP molecule. This pump is specifically inhibited by thapsigargin, a plant sesquiterpene lactone that is also a tumor promoter in mammalian cells. Heterozygous mutations of *ATP2A2* lead to a dermatological pathology known as Darier disease (Li et al., 2013).

##### 2.6.1.2.2 SPCA1

- SPCA1 features

SERCA probably contributes to the major proportion of  $\text{Ca}^{2+}$  uptake with the exception of human keratinocytes where 67% of the Golgi  $\text{Ca}^{2+}$  is loaded by SPCA1. This could explain the

physiopathology of the dermatological affection, Hailey-Hailey disease (HHD), due to monoallelic loss of SPCA1 (Callewaert et al., 2003).

Two genes code for SPCA pump: *ATP2C1* for SPCA1 and *ATP2C2* for SPCA2. Their structure is close to SERCA pump and contains all the highly conserved domains that are the signature of the P-ATPase pumps (He and Hu, 2012). With ten transmembrane helix domains, this *trans*-Golgi membrane-localized protein has a molecular weight of around 115 kDa. While *ATP2C2* is localized in epithelial cells from the whole digestive system except the esophagus, and in the secretory glands localized in lungs and breast, SPCA1 is ubiquitous with increased expression in epidermal keratinocytes (Missiaen et al., 2004). There are four different isoforms of SPCA1 (a-d) resulting from the alternative splicing of 28 exons. Whereas overexpression of SPCA1 is linked with breast cancer (Grice et al., 2010), SPCA1 knockout and knockdown have been shown to imbalance the Golgi architecture and trafficking. Indeed, a recent study has shed light on the possible indirect interaction of the tail of a particular SPCA2 isoform with COPI and/or GRASPs proteins (Micaroni et al., 2016).

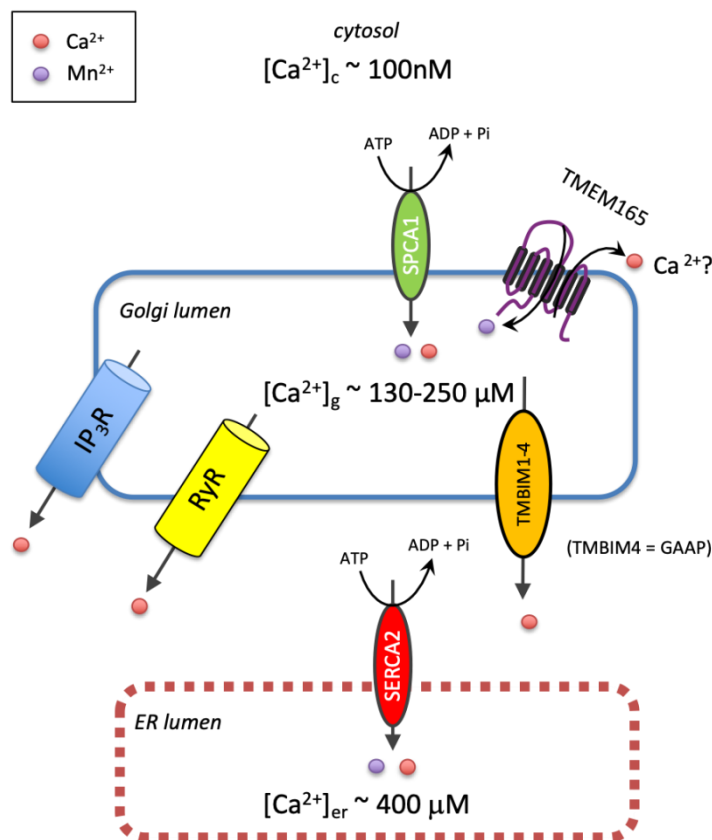


Figure 19. Key players of Golgi calcium homeostasis

### 2.6.1.3 Channels for Ca<sup>2+</sup> leaks

IP<sub>3</sub>R and RyR proteins bind calcium with a high affinity. In accordance with the current cytoplasmic calcium concentration, the fixation of IP<sub>3</sub> to its receptor allowing the outing of calcium ions from the ER/Golgi lumen to the cytosol and generating intracellular Ca<sup>2+</sup> signals that regulates numerous cellular processes (Parys and Vervliet, 2019).

RyR, the ryanodine receptor, is also a Golgi calcium leak homotrimer channel that contains two calcium fixation sites on the cytosolic side (Lacampagne et al., 2008).

Other recently studied proteins may also have a role in Golgi calcium regulation such as:

- Among the TMBIM (Transmembrane Box Inhibitor-1 Motif containing) protein family, TMBIM 1 to 4 are Golgi and ER-localized. This highly conserved transmembrane protein family is involved in cell death and calcium homeostasis of the organelles by calcium release (Liu, 2017).
- On the other hand, CAB45 which is calcium-binding protein, has recently gained interest due to its ability to act as a buffer for this ion (Blank and von Blume, 2017).

TMEM165 is a recently described cations antiport transporter that is a major Golgi Mn<sup>2+</sup> importer. In yeast, it is considered to be the leak channel of SPCA1 but the counterion nature in humans is still a controversial topic (Dulary et al., 2018).

### 2.6.2 Other divalent cations homeostasis

Other ions such as Mg<sup>2+</sup>, Zn<sup>2+</sup>, and Fe<sup>2+</sup> have recently gained interest in Golgi homeostasis. Their influence compared to calcium and manganese seems to be less important but their precise roles remain unclear.

## CHAPTER 3: Manganese homeostasis

### 3.1 Manganese on earth

Manganese is the 12<sup>th</sup> most abundant element and the 5<sup>th</sup> most abundant metal on earth, representing 0.085% of the terrestrial crust (Lanham-New et al., 2019). Found in pyrolusite that contained manganese dioxide, it was studied in the middle of the 18<sup>th</sup> century by chemist Carl Wilhelm Scheele. Then, it was isolated for the first time by Johan Gottlieb Gahn in 1774 (Lide, 2004). Anecdotally, paleolithic cave paintings in Lascaux, France, were drawn using manganese-based pigments (Chalmin et al., 2006). Thirty different known hydro/oxide minerals are known to encompass this element on earth.

This trace element with atomic number 25 has a molar weight around 54.94 g.mol<sup>-1</sup> and the closest metal in the periodic table of the elements is iron (Fe), with atomic number 26 and a 55.84 g.mol<sup>-1</sup> molar mass which will be important to understand the global manganese transport mechanism. Despite this essential transition metal has eleven possible oxidation states; Mn<sup>2+</sup>, manganese (II) and Mn<sup>3+</sup> manganese (III) are the main oxidation states found in bio-organisms. Manganese plays a role in many physiological functions such as immunity, reproduction, bone formation, coagulation, digestion and at a cellular level, a role in energy machinery, cell stress, and at the molecular level, on glycosylation processes (Erikson and Aschner, 2019). The sources of exposition are air, soil, water, food and industrial products (Lanham-New et al., 2019).

### 3.2 Manganese in human organism

#### 3.2.1 Manganese sources

The main source of intake for humans is water and food, especially nuts (pine nuts, hazelnuts, walnuts), seafood (mussels, oysters), whole grains (oat flakes), leafy greens vegetables (spinach), legumes (soy, beans), brown rice, pineapple, pumpkin, sesame seeds, tea and dietary supplements (Baker et al., 2014).

#### 3.2.2 Manganese absorption, distribution, and elimination

One to 5% of the manganese brought into the gastrointestinal tract is effectively absorbed. The absorption route first involved in the manganese-induced toxicity is inhalation, which allows a rapid entrance of manganese in the blood that reaches the brain *via* olfactory bulb (Chen et al., 2018) (**figure 20**). Dermal absorption has also been reported with a limited

contribution. The elimination pathway is biliary and, to a smaller extent, urinary; hence hepato-insufficiency leads to an increase of manganese blood levels (Erikson and Aschner, 2019).

Circulating manganese is bound to transferrin under  $Mn^{3+}$ , citrate, albumin and  $\alpha_2$ macroglobulin (Harischandra et al., 2015). Manganese ensures a structural role for metalloproteins and is a cofactor for: (i) superoxide dismutase (SOD-2), an antioxidant, (ii) astrocytes glutamine synthase, (iii) alkaline phosphatases of liver and bone and (iv) arginase localized in the hepatocytes (Zhang et al., 2003).

The whole-body half-life of manganese in human and monkey is approximately 50 days, while the brain half-life elimination in monkey exceeds 220 days reflecting the specific affinity of this metal for the central nervous system (CNS) (Aschner, 2006; Aschner et al., 2005).

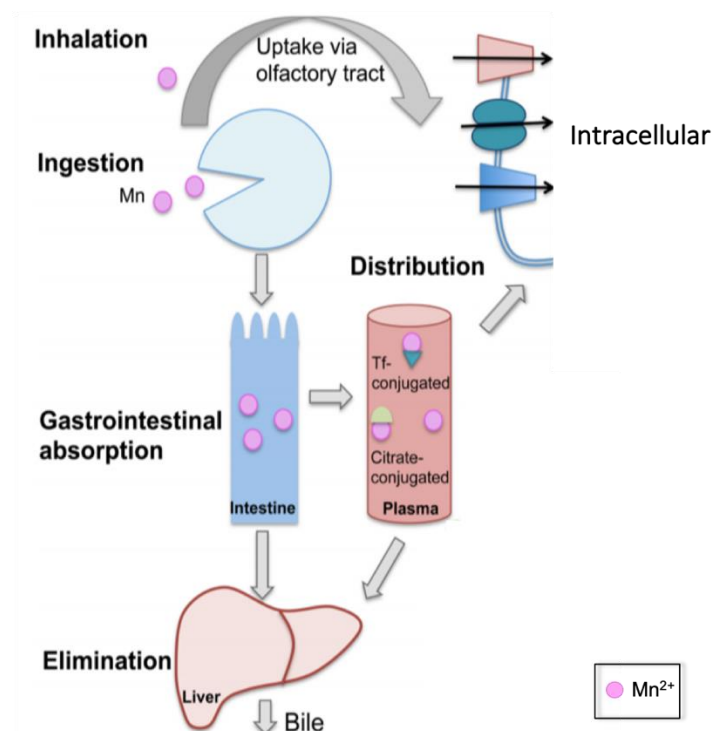


**Figure 20. Schematic representation of manganese absorption from ingestion to cellular internalization** (Modified from Peres et al., 2016)

### 3.2.3 Physiological values and toxicity

The whole human body burden of manganese is approximately 15 mg, mainly stored in bone, liver, pancreas, kidney, adrenal glands and brain in pituitary glands (Rahil-Khazen et al., 2002). The Drinking Water Guideline recommendation for water manganese content is 60  $\mu\text{g/L}$  (Valcke et al., 2018). Regarding the total everyday intake, the recommendation for an

adult female is 1.8mg and 2.3mg for an adult male (Lanham-New et al., 2019). In clinical biology, a manganese concentration between 4 and 15 µg/L in blood, 1–8 µg/L in urine, and 0.4–0.85 µg/L in serum is considered normal. The difference between blood and serum concentration is due to the fact that 85 % of manganese is linked to the hemoglobin of the erythrocytes (Furbee, 2009). The methods used in laboratories to assess these concentrations are Inductively Coupled Plasma Mass Spectrometry (ICP-MS) and atomic absorption spectrometry. A concentration over the upper limit of blood level (15 µg/L) is considered toxic even if manganesemia is not a reliable reporter of the manganese whole-body burden.

#### 3.2.4 Focus on the influence of manganese on the skeletal system

The skeletal system contains up to 40 % of the whole manganese burden of the human body with a half-life of around 8 years (O’Neal and Zheng, 2015). This osteotropic metal is important for bone metabolism, cartilage matrix synthesis, and calcification. This trace element, a cofactor of many enzymes implied in skeletal integrity, has a key role in bone mineral density in adult. For instance, low manganesemia tends to aggravate osteoporosis, increasing the bone fracture frequency among women after menopause. No similar correlation could be established among men, probably due to a link between estrogen and manganese bone deposition (Wang et al., 2015a; Zofkova et al., 2017). These observations are important to understand the pathophysiological mechanisms of manganese-induced pathologies that are discussed at the end of this chapter.

### 3.3 Manganese in the cell

The cellular manganese concentration is not clearly defined but a recent study has evaluated the intracellular concentration in HEK293 cells by means of ICP-MS to 400 ppb (400 µg/L or ~8 µM) including both cytosolic and organelles concentrations (Harischandra et al., 2015). Manganese is an essential cofactor for a wide range of enzymes cited above, nevertheless, little is known about the exact the concentration regulation and the transport mechanism of this metal and new insights are published every year (Aydemir and Cousins, 2018).

#### 3.3.1 Manganese transporters

Elements that may explain homologies between manganese and iron transport might be their similar molecular weights and atomic numbers.

### 3.3.1.1 Manganese plasma membrane transporters

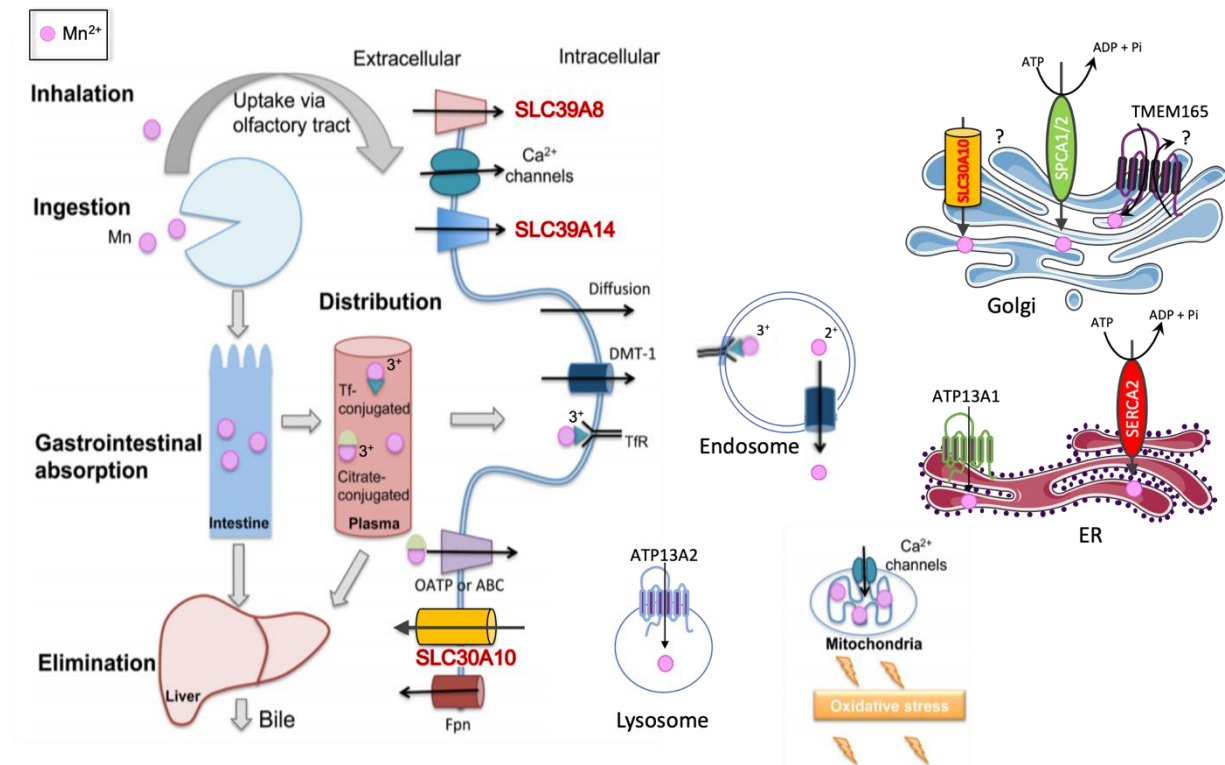


**Figure 21. Schematic representation of manganese absorption from ingestion to cellular internalization** (Modified from Peres et al., 2016)

- Transferrin

In the blood, ceruloplasmin first converts Mn<sup>2+</sup> into Mn<sup>3+</sup>. This ferroxidase protein, better known to transport copper is usually implied in the iron ion oxidation. Manganic (Mn<sup>3+</sup>) manganese ions can subsequently bind to transferrin that enters the cell *via* the transferrin receptor by endocytosis. Finally, endosomal Mn<sup>3+</sup> is reduced in Mn<sup>2+</sup> and taken over by DMT1 to reach the cytoplasm. Transferrin-linked endocytosis is the main manganese pathway, even if its first function is to import iron (Anagianni and Tuschl, 2019; Gunter et al., 2013) (**figure 21, center**).

- DMT1

The Divalent Metal Transporter 1 (DMT1) has many denominations: Natural Resistance Associated Macrophage Protein 2 (NRAMP2), Divalent Cation Transporter 1 (DCT1) and now Solute Carrier Family 11, member 2 (SLC11A2). This major Fe<sup>2+</sup> transporter is localized in the plasma and endosome membrane. DMT1 also binds seven other divalent metal ions: Mn<sup>2+</sup>,

$Cd^{2+}$ ,  $Cu^{2+}$ ,  $Co^{2+}$ ,  $Ni^{2+}$ ,  $Pb^{2+}$  and  $Zn^{2+}$  with a high affinity for manganese (Garrick et al., 2003, 2006).

- SLC30A10

SLC30A10 (or Zn transporter 10 or ZnT-10) is expressed in the liver and the brain cells. While other SLC30 transport zinc, SLC30A10 transports manganese but not zinc due to differences in the structure of the metal-binding site (Zogzas and Mukhopadhyay, 2018). Localized to the plasma membrane, SLC30A10 mediates manganese efflux from the cytosol to the extracellular medium. SLC30A10 is also localized at the membrane of the Golgi apparatus and endosomes probably and participates to the maintenance of manganese cellular homeostasis (Quadri et al., 2012) (**figure 21**).

- SLC39A8

SLC39A8, also named Zrt- and Irt-like protein 8 (ZIP8), is an evolutionary conserved, ubiquitous, plasma membrane-localized manganese uptake transporter. This transporter is not manganese-specific as it also imports  $Zn^{2+}$ ,  $Fe^{2+}$ ,  $Se^{4+}$  and  $Co^{2+}$ . Genetically, SLC39A8 is closely related to another manganese transporter SLC39A14 (Nebert and Liu, 2019).

- SLC39A14

SLC39A14, known as ZIP14 can either transport  $Zn^{2+}$ ,  $Mn^{2+}$ ,  $Fe^{2+}$ , and  $Cd^{2+}$ , with a higher affinity for Zn. The highest expression of this transporter is observed in the liver and the brain. Both knockdowns of SLC39A8 and SLC39A14 impair the plasma membrane manganese uptake but SLC39A14 has been recently shown to be also localized in the endosome of HEK293. This endosomal localization indicates a function in the intracellular  $Mn^{2+}$  transport, similar to the role of in zinc transport (Maxel et al., 2019; Thompson and Wessling-Resnick, 2019).

Other transporters might influence manganese import with various degree of involvement, among these, citrate, choline, dopamine, glutamate transporters, store-operated calcium channel (SOC) and voltage regulator calcium channel can be cited (O'Neal and Zheng, 2015). Mutations in Ferroportin (SLC40A10), responsible for the plasma membrane manganese efflux and in DMT1 have been reported but none of the patients were presenting neither an increase in blood manganese level nor a brain accumulation. Similarly, intracellular transporters

displaying an affinity for manganese such as ATP13A1 and ATP13A2 participate to the manganese uptake respectively in the ER and lysosomes are not implied in any manganese disorder (**figure 21**).

### 3.3.1.2 Manganese secretory pathway transporters

- SPCA1/2

Two SPCA P-type ATPase pumps have been described in chapter 2 (§.6.1.2.2). SPCA1 has an ubiquitous localization, while SPCA2 is more specifically localized in the gastrointestinal tract. By means of yeast ortholog studies, Pmr1/SPCA1 is now considered as the major calcium importer in the Golgi lumen and a key manganese pump (Dulary et al., 2018).

- TMEM165

This transmembrane protein, localized in the Golgi apparatus, has been identified in 2012 and is now thought to be one of the main Golgi manganese importer. Compared to SPCA1, TMEM165 would be an ATP-independent antiport transporter whose counterion still remains controversial (cf Chapter 4).

- SERCA2

The sarco/endoplasmic reticulum Ca<sup>2+</sup>-ATPase, described in chapter 3 (§6.1.2.1), is a well-known major ER calcium ATP-dependent pump, highly sensitive to thapsigargin and potentially also localized in the *cis*-Golgi. SERCA2 was demonstrated to be an actor of the glycosylation restoration of TMEM165-deficient cells by manganese under certain conditions (Houdou et al., 2019). The function and regulation of these three transporters will be further discussed in this essay.

SLC30A10 (chapter 3 §.3.1.1) has recently been proposed to be a Golgi manganese importer in addition to its role in manganese cellular efflux to the plasma membrane (**figure 21**).

### 3.3.2 Manganese and glycosylation

Manganese concentration in the Golgi lumen in physiologic conditions represents 60 % of the total cellular manganese; 20 % is contained in the nucleus and 20 % in the cytosol. The mass of manganese contained in the GA in normal conditions is inferior to 0.72x10<sup>-6</sup> g/g of dry cell

mass. A concentration of 100  $\mu\text{M}$   $\text{MnCl}_2$  applied for 4 hours is still physiological for the cells. In these conditions again, 60 % of whole manganese lies in the GA ( $2.4 \times 10^{-6}$  g/g of dry cell mass) of the cell. A toxic concentration of 300  $\mu\text{M}$   $\text{MnCl}_2$  changes the repartition of manganese in the cell with 40 % ( $12 \times 10^{-6}$  g/g of dry cell mass) in the GA, 20 % in the nucleus and 40 % in the cytosol (Carmona, 2011).

A slight concentration decrease of manganese concentration in the GA has also been shown to have critical consequences on glycosylation due to the requirement of this metal for the normal function of certain glycosyltransferases, principally galactosyltransferases.

### 3.3.2.1 Manganese-dependent glycosyltransferases

The glycosylation enzymes known or thought to require manganese for their function are listed in **table 3**.

Among these, MGAT1 (Mannosyl  $\alpha$ 1,3-Glycoprotein  $\beta$ 1,2-*N*-acetylglucosaminyltransferase 1), known as GlcNAcT-1 (EC 2.4.1.101), interacts with both UDP-GlcNAc and  $\text{Mn}^{2+}$  in rabbit and probably in human too (Chen et al., 2001). Another enzyme, UGGT (UDP-Glucose Glycoprotein Glucosyltransferase 1 and 2), responsible for the folding of the *N*-glycoprotein during the ER quality control, also requires manganese (Arnold et al., 2000). We will focus on the most studied glycosylation enzyme,  $\beta$ -1,4-galactosyltransferase 1.

### 3.3.2.2 $\beta$ -1,4-galactosyltransferase 1

Nineteen galactosyltransferases have been identified in mammals. In the presence of metal ions, they catalyze the addition of galactose from UDP-Galactose donor to the glycoconjugate acceptor in a specific linkage ( $\alpha$ 1,3-,  $\alpha$ 1,4-,  $\beta$ 1,4-, or  $\beta$ 1,3-). There are at least seven members of the B4GALT subfamily (T1 to T7) sharing 25% to 55% similarities and T1 to T5 are ubiquitous (Hennet, 2002). Their specificity towards the nucleotide sugar UDP-Gal is determined by a tyrosine residue of the binding pocket, highly conserved among the family members from different species.

Glycosylation type	Manganese-dependent glycosylation enzymes	Reference
--------------------	---	-----------

<b>GAG</b>	<ul style="list-style-type: none"> <li>• Xylosyltransferase 1 (XYLT1)</li> <li>• Chondroitin Sulfate Synthase 1 (CHSY1)</li> <li>• Chondroitin Polymerizing Factor/Chondroitin Sulfate Synthase 2 (CHPF)</li> <li>• Chondroitin Sulfate Synthase 3 (CHSY3)</li> <li>• <math>\beta</math>1,3-Glucuronyltransferase 3 (B3GAT3)</li> <li>• <math>\beta</math>1,3-Glucuronyltransferase 1 (B3GAT1)</li> <li>• <math>\beta</math>1,4-Galactosyltransferase 7 (B4GALT7)</li> <li>• <i>Xylosyltransferase 2 XYLT2</i> Mn<sup>2+</sup> by similarity with XYLT1 Glycosaminoglycans</li> <li>• <i>Exostosin-1 and 2 EXT1/EXT2</i></li> <li>• <i>Exostosin-like glycosyltransferases 1, 2 and 3 EXTL1/EXTL2/EXTL3</i></li> </ul>	(Götting et al., 2004) (Yada et al., 2003) (Yada et al., 2003) (Kakuda et al., 2004) (Tsutsui et al., 2013) (Hinsdale, 2014) (Pedersen et al., 2003)
<b>Glycolipids</b>	<ul style="list-style-type: none"> <li>• <math>\beta</math>1,4-N-Acetyl-Galactosaminyltransferase 1 (B4GALNT1)</li> <li>• <math>\beta</math>1,4-Galactosyltransferase 6 (B4GALT6)</li> <li>• <math>\beta</math>1,3-N-Acetylgalactosaminyltransferase 1 (B3GALNT1)</li> <li>• <i>Globoside <math>\alpha</math>1,3-N-Acetylgalactosaminyltransferase 1 (GBGT1)</i></li> <li>• <i><math>\alpha</math>1,3-Galactosyltransferase 2 (A3GALT2)</i></li> </ul>	(Li et al., 2001) (Okajima et al., 2000) (Amado et al., 1998) (Honke, 2014) (Boix et al., 2002)
<b>O-glycosylation</b>	<ul style="list-style-type: none"> <li>• Polypeptide N-Acetylgalactosaminyltransferase 1, 2, 3 (GALNT1-3)</li> <li>• Polypeptide N-Acetylgalactosaminyltransferase 10 (GALNT10)</li> <li>• Fucosyltransferases 3, 5, 7 (FUT3, FUT5, FUT7)</li> <li>• <math>\beta</math>1,4-N-Acetyl-Galactosaminyltransferase 2 (B4GALNT2)</li> <li>• <math>\alpha</math>1,3-N-Acetylgalactosaminyltransferase (GTA)</li> <li>• <math>\alpha</math>1,3-Galactosyltransferase (GTB) (ABO system)</li> <li>• <i>Glycosyltransferase 6 Domain Containing 1 (GLT6D1)</i></li> <li>• <i>Polypeptide N-Acetylgalactosaminyltransferases GALNT(X)</i></li> </ul>	(Wandall et al., 1997) (Kubota et al., 2006) (de Vries et al., 2001) (Murray et al., 1996) (Palma et al., 2004) (Kaufman et al., 1994) (Persson et al., 2007) (Saito et al., 2016) (Kubota et al., 2006)
<b>O-mannosylation</b>	<ul style="list-style-type: none"> <li>• <math>\beta</math>1,4-glucuronyltransferase 1 (B4GAT1)</li> <li>• LARGE Xylosyl- And Glucuronyltransferase 1 (LARGE 1)</li> <li>• LARGE Xylosyl- And Glucuronyltransferase 2 (LARGE 2)</li> <li>• <i>Protein O-Linked Mannose N-Acetylglucosaminyltransferase 1 (POMGNT1)</i></li> </ul>	(Willer et al., 2014) (Kakuda et al., 2004) (Inamori et al., 2014) (Manya et al., 2004)
<b>O-glucosylation</b>	<ul style="list-style-type: none"> <li>• Xyloside Xylosyltransferase 1 (XXYLT1)</li> </ul>	(Minamida et al., 1996)
<b>O-fucosylation</b>	<ul style="list-style-type: none"> <li>• <math>\beta</math>1,3-N-acetylglucosaminyltransferase lunatic fringe, manic fringe and radical fringe (LFNG, MFNG, RFNG)</li> </ul>	(Zhou et al., 1999)
<b>N-glycosylation</b>	<ul style="list-style-type: none"> <li>• <math>\beta</math>1,4-Galactosyltransferase 1 (B4GALT1)</li> <li>• UDP-Glucose Glycoprotein Glucosyltransferase 1 and 2 (UGGT1 / UGGT2)</li> <li>• <i>Mannosyl (<math>\alpha</math>1,3)-Glycoprotein <math>\beta</math>1,2-N-Acetylglucosaminyltransferase (MGAT1)</i></li> <li>• <i><math>\beta</math>1,4-Galactosyltransferase 2, 3, 4, 5 (B4GALT2-5)</i></li> <li>• <i>Mannosyl (Alpha-1,3-)-Glycoprotein <math>\beta</math>1,2-N-Acetylglucosaminyltransferase 4A, 4B, 4C (MGAT4A, 4B and 4C)</i></li> </ul>	(Arnold et al., 2000) (Chen et al., 2001) (Qasba et al., 2008) (Spahn et al., 2017)
<b>Other/Multiple pathways</b>	<ul style="list-style-type: none"> <li>• UDP-GlcNAc <math>\beta</math>1,3-N-Acetylglucosaminyltransferase 2 (B3GNT2) (poly-N-acetyllactosamine biosynthesis)</li> <li>• Glycogenin 1 (GYG1), Glycogenin 2 (GYG2) (autoglucosylation)</li> <li>• <i><math>\beta</math>1,3-Glucuronyltransferase 2 (B3GAT2)</i></li> <li>• <i><math>\beta</math>1,3-Galactosyltransferase 1 and 2 (B3GALT1/B3GALT2)</i></li> </ul>	(Okajima et al., 2000) (Nilsson et al., 2014) (Kizuka and Oka, 2014) (Amado et al., 1998)

**Table 3. List of glycosylation enzymes that are manganese-dependent or thought to be manganese dependent (italics).** These suppositions are due to studies made on orthologs or glycosylation enzymes with structural similarities.

The first described and first cloned galactosyltransferase is B4GALT1 ( $\beta$ 1,4-galactosyltransferase 1) (EC 2.4.1.38) (Shaper et al., 1986). This is the most studied galactosyltransferase, responsible for the formation of the disaccharide *N*-acetyllactosamine (Gal $\beta$ 1,4-GlcNAc) on the growing carbohydrate chain. There are two metal binding sites in the catalytic site of B4GALT1, site I binds specifically to manganese whereas site II can bind to calcium and multiple other metal ions (Boeggeman et Qasba 2002).

Combined with  $\alpha$ lactalbumin, it is part of the lactose synthase which catalyzes the addition of a UDP-galactose on a glucose residue to form lactose. This *trans*-Golgi glycosyltransferase is also localized at the cell surface.

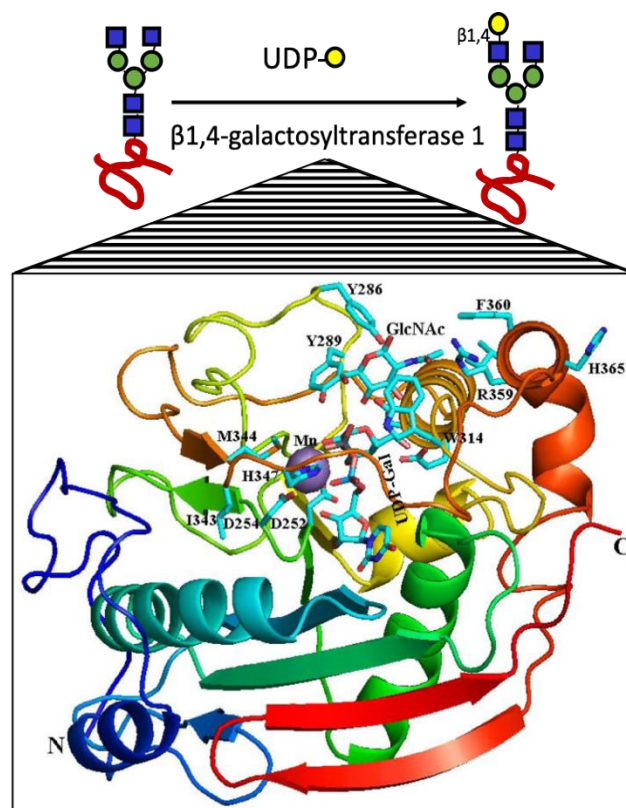


**Figure 22. 3D representation of  $\beta$ -1,4-galactosyltransferase 1 with cofactor  $Mn^{2+}$  (purple sphere), donor substrate UDP-Gal, acceptor GlcNAc and important amino acids of the pocket reaction site (Adapted from Qasba et al., 2008)**

There are two main structural groups of glycosyltransferases in humans, GT-A and GT-B. GT-A fold enzymes are divalent metal cations-dependent enzymes harboring a Asp-X-Asp (where X can be any amino-acid except Proline) amino acid signature sequence, also called D-X-D, where the two carboxyl groups coordinate the divalent metal cation, essential for the stabilization of the pyrophosphate of the nucleotide sugar. The metallic ion is usually manganese. GT-B, devoid of this D-X-D motif, does not require metal ions but have two

Rossmann domains separated by a deep cleft. First described in 1970 by Michael Rossmann, the Rossmann-like domain, also known as “nucleotide-binding domain”, is an alternation of  $\beta$ -strands and  $\alpha$ -helix units (Albesa-Jové et al., 2014).

The catalytic domain of the globular protein  $\beta$ 1,4-galactosyltransferase 1 has a GT-A fold containing two flexible loops: a short and a long, undergoing a conformational change during the reaction. Between the two domains, the active site is a cleft where the metal cofactor binds. In an open conformation, the N-terminal domain of the long loop binds to  $Mn^{2+}$  and reorganizes the positions of water molecules. Consequently, the substrate donor UDP-Gal binds and a second conformational change occurs regarding the presence of an acceptor molecule (GlcNAc-glycoprotein) in the C-terminal domain (Qasba et al., 2008) (**figure 22**).

The view is even more complex as GT-A protein can transfer the glycosyl groups to the acceptor with either retention or inversion of the anomeric conformation. In retaining enzymes, the two D of the DXD motif interact with manganese, whereas the Asp254 of the DXD motif together with oxygen atoms of the two phosphates for the UDP molecule have a crucial role in  $Mn^{2+}$  binding in inverting enzyme (Breton et al., 2006). REF

### 3.4 Manganese-linked pathologies

#### 3.4.1 Manganese deficiency

No severe case of manganese deficiency has been reported so far in human due to an adequate supply by water and food. However, in depletion experiment studies made on animals, induced reproductive, growth and metabolism impairments (Institute of Medicine (US) Panel on Micronutrients, 2001). In adult men, a 3-weeks depletion showed the apparition of cutaneous rash called *Milaria crystallina* that was reversible (Friedman et al., 1987). Few studies suggest that certain patients with epilepsy and osteoporosis had lower manganese levels (Aschner et al., 2005). In addition, mutations in specific manganese transporters may induce clinical features related to a manganese deficiency.

- SLC39A8

The first patient with homozygous mutation in *SLC39A8* was described in 2015 and presented a CDG syndrome, called SLC39A8-CDG (previously CDG-II<sub>n</sub>) (OMIM 616721). The cellular manganese depletion reduces the activity of mitochondrial manganese superoxide dismutase (MnSOD) and hinders glycosylation enzymes such as of  $\beta$ 1,4-galactosyltransferases. This

explains the hypoglycosylation pattern observed in this severe inborn error of metabolism that is clinically characterized by dwarfism, hepatopathy, deafness, seizures together with psychomotor delay.

Regarding this CDG, treatments, with galactose oral supplementation was promising with the normalization of one patient hypoglycosylation pattern (Park et al., 2015). More recently, a high-dose of 10 to 15mg/kg improved motor abilities of two patients (Park et al., 2018).

### 3.4.2 Manganese excess

The central nervous system is the major target of manganese toxicity and the second more sensitive organ is lung. Other systems such as cardiovascular, hematological (decrease of red blood cells and granulocytes), reproductive (sterility) and immune (decrease of immunoglobulin G) can also be affected but only through chronic manganese exposure. Due to a slow elimination of manganese from the brain, only the CNS toxicity will be discussed here.

#### 3.4.2.1 Physiopathology of manganese excess

Manganese can cross the blood-brain barrier (BBB) *via* facilitated diffusion or active transport by, (*i.e* the divalent metal transporter 1 (DMT1)) or transferrin mediated transport (Milatovic et al., 2011). Recent studies have also proposed SLC39A8 and SLC39A14, ATP13A2 and SPCAs transporters to be responsible for the brain transport (Keith M. Erikson, 2019).

Once in the CNS, neurodegeneration is induced by three deleterious effects of manganese:

- Oxidative stress: production of free radicals and reactive oxygen species (ROS)
- Disturbance of mitochondria functions, *i.e* ATP production, due to the inactivation of particular enzymes by competition of  $Mn^{2+}$  with  $Ca^{2+}$  and  $Mg^{2+}$  and their replacement as a cofactor
- Potential aggregation of a protein called  $\alpha$ -synuclein.

This soluble protein expressed in erythrocytes and brain has the property to form fibrils and possesses a high affinity for metal ions. Manganese binding is thought to modified  $\alpha$ -synuclein folding leading to aggregation. Nonetheless, the role of this protein is a controversial issue as it is considered either protective or harmful for the brain, regarding publications (Peres et al., 2016).

#### 3.4.2.2 Manganism, a chronic pathology due to long-term manganese exposure

Manganism, also named hypermanganesaemia, a Parkinson-like disease, or chronic manganese poisoning was first described by John Couper in 1837 among pyrolusite mill workers. Later it has been highlighted among, welders, miners and dry-cell battery, steel or ferroalloy factories workers. More recent risks of manganese exposure are electronic factories, fungicides and manganese-containing contrast agents like mangafodipir trisodium (MnDPDP). However, the clinical use of this molecule would be relatively safe if repeated exposure is avoided (Crossgrove and Zheng, 2004).

- Diagnosis

Blood levels higher than 15 µg/L are considered toxic even if the exact dose inducing brain damage is not known. For example, Beijing welders affected by manganism presented blood levels between 3 and 36 µg/L not reflecting the metal accumulation (Wang et al., 2015a)

As considered the *in vivo* neurotoxicity, values in the whole brain have been estimated in the range of 60 µM–150 µM (Kumar et al., 2015).

- Clinical aspects

The increase of Mn concentration in the brain is responsible for neurological disorders analogous to Parkinsonism. Nonetheless, histologically affected neurological areas are different between manganism and Idiopathic Parkinson Disease (IPD) (Avila et al., 2013). In the first stage, the neurological picture is made of unspecific symptoms like mood alteration such as irritability, asthenia and headache. In the following stages, anxiety, apathy, aggressiveness, hallucinations, inability to concentrate, rigidity, tremor, reduced coordination, paresthesia, dystonia, facial muscle spasm, speech disturbance, amnesia, and other symptoms are observed. The late psychiatric stage of the disease is called manganese mania, psychosis or madness. A pathognomonic sign is called “cock-walk” where patients can hardly walk backward.

- Treatment

The first treatment is to stop the manganese exposure at the onset of the intoxication; unfortunately for long-time exposure, the toxicity is irreversible due to the slow elimination of this metal from the brain as compared to other organs (Mergler and Baldwin, 1997).

Treatments with divalent ion chelators  $\text{CaNa}_2\text{EDTA}$  or with para-aminosalicylic acid (PAS) are available. Despite promising results for some patients, their efficiency remains transient and limited (Jiang et al., 2006; Nelson et al., 2010; Rivera-Mancía et al., 2011). On the other hand, it has been also shown that the increase of ferroportin expression in HEK293 cells was able to lower intracellular  $\text{Mn}^{2+}$  concentration and thus its toxicity (Yin et al., 2010).

#### 3.4.4 Pathologies due to mutations of manganese transporters

- SLC30A10

Recent studies indicate that homozygous mutations in *SLC30A10* gene cause hypermanganesemia, hepatopathy and polycythemia (Tuschl et al., 2012). The observation of a manganese fixation in the basal ganglia area of the brain is visible in Magnetic Resonance Imaging (MRI), as observed in manganism. The patients affected by this new form of familial parkinsonism presented at least a 10-fold increase of their  $\text{Mn}^{2+}$  blood concentration. This observation lead to the assumption that plasma membrane transporter SLC30A10 would be a protector against Mn cellular overload (Chen et al., 2018).

By fluorescence microscopy and synchrotron X-ray fluorescence imaging, Ortega and collaborators were able to visualize manganese accumulation in the Golgi apparatus in the absence of SLC30A10, more precisely in vesicles rather in cisternae (Carmona et al., 2019).

- SLC39A14

While SLC39A8 deficiency is linked to a CDG, SLC39A14 deficiency manifests by an autosomal recessive Parkinson-like dystonia resembling the Mn-efflux SLC30A10 transporter defect. Strikingly, SLC39A14 deficiency does not show polycythemia neither liver impairment observed in Mn overload (Steimle et al., 2019; Tuschl et al., 2016).

Recent studies tried to explain this phenomenon by the role of SLC39A14 transporter in liver detoxification of manganese. A loss-of-function of this transporter impairs the liver uptake of  $\text{Mn}^{2+}$  by SLC30A10. The lack of hepatic detoxification lead to an elevation of the manganese blood concentration and to the accumulation of manganese in brain and bone tissues. SLC39A14 is able to transport three other metal ions, nevertheless the deficiency has not been correlated with a major change in these metal concentrations. This transporter, alongside with SLC30A10 would hence be crucial for Mn homeostasis and clearance in humans.

SLC39A14 as well as TMEM165 are sensitive to supraphysiologic manganese exposure leading to lysosomal degradation. In other words, SLC39A14 would have a role of cellular protection against hypermanganesemia (Aydemir and Cousins, 2018; Thompson and Wessling-Resnick, 2019).

- Treatments

Chelation with disodium calcium edetate  $\text{Na}_2\text{CaEDTA}$  has been shown to significantly lower blood Mn levels increasing the urinary excretion in patients affected by SLC39A14 mutations with various clinical improvements. This variability can be explained by the different range of severity of the affection and also by the specific roles of SLC39A14 distinct isoforms.

These new discoveries about SLC39A14 have to be further expanded for a better understanding of proteinopathies induced by manganese. Despite manganism, the idiopathic Parkinson disease also presents an increased susceptibility to manganese toxicity (Anagianni and Tuschl, 2019).

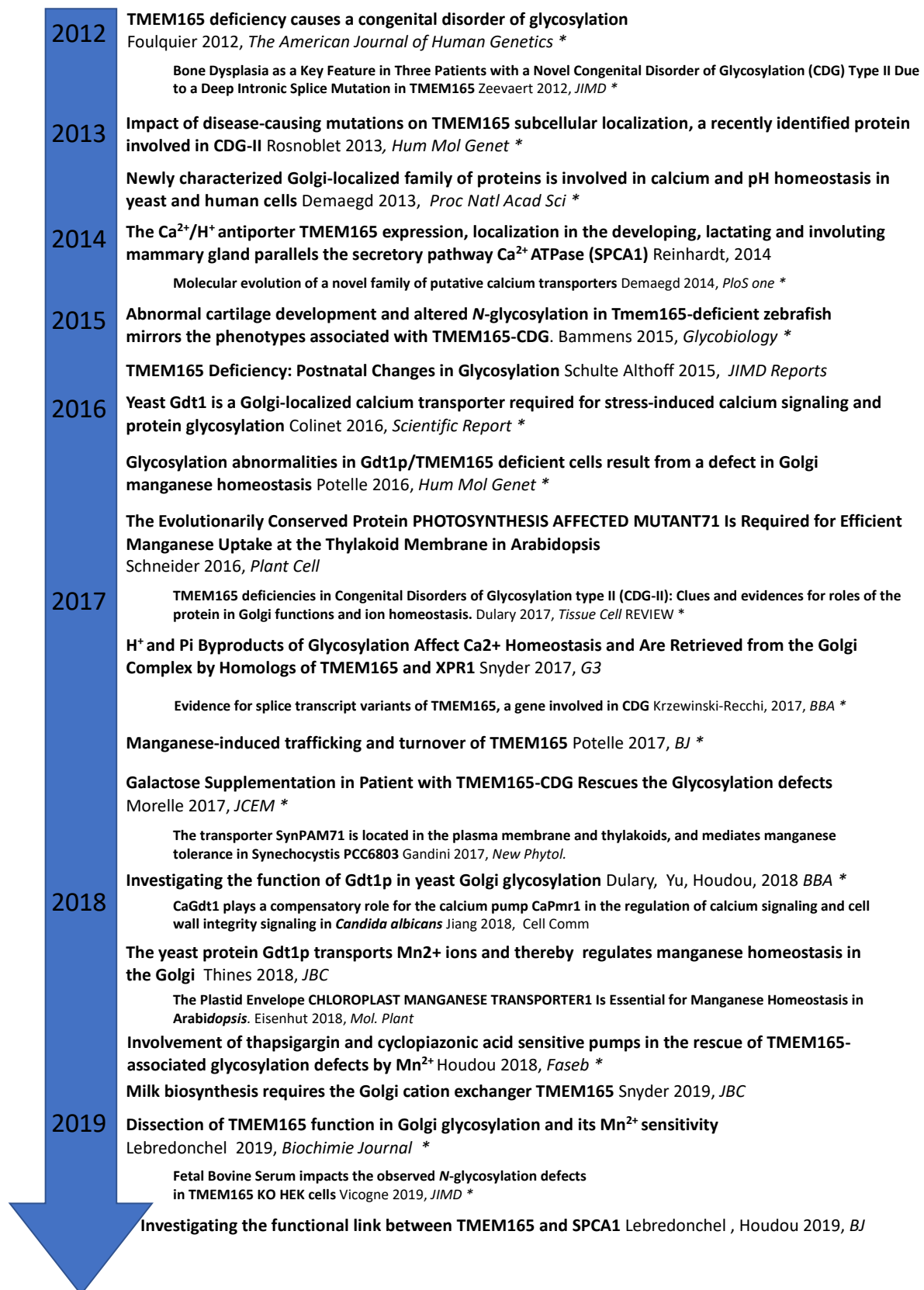


**Figure 23. History of TMEM165 and TMEM165-CDG major breakthroughs**  
Publications with asterisks are related to our laboratory

## CHAPTER 4: TMEM165

TMEM165 was identified in 2012 in patients affected by a new CDG type II called TMEM165-CDG. To date, many research groups have worked on the elucidation of the structure, cellular localization, regulation and functions of this protein. The chronology of these discoveries is summarized in **figure 23**.

### 4.1 TMEM165 structure, dynamic, stability

#### 4.1.1 TMEM165, gene, protein, orthologs, and localization

*TMEM165*, Transmembrane protein 165, is known under different names: *TPARL*, *TMPT27*, *FT27*, *GDT1*, *CDG2K*, and sometimes *TM165*. This gene, localized on chromosome section 4q12, made of 6 exons, generates a mRNA of 1312 bp. It encodes a 324 amino acids protein, member of the Uncharacterized Protein Family 0016 (UPF0016; Pfam accession number: PF001169). This family includes 6 subfamilies in prokaryotes (I to VI) and in eukaryotes (VII to XII), that are highly conserved throughout evolution, (919 different species in the prokaryotes and 405 species in eukaryotes), especially 230 amino acids.

In budding yeast, *Saccharomyces cerevisiae*, the ortholog of *TMEM165* is *GDT1* (Gcr1-dependent translation factor). Gdt1 is shorter than TMEM165 with only 280 amino acids, however, both EXGDK/R motifs and the transmembrane domains are conserved with a 38% sequence identity between the two orthologs. The first transmembrane domain is absent in Gdt1 and the central loop is 10 amino acids longer (Demaegd et al., 2014).

Plants possess 5 protein members of the UPF0016 family. Among them, the protein that shares the higher sequence homologies with TMEM165 is PAM71 (PHOTOSYNTHESIS AFFECTED MUTANT71) (Schneider et al., 2016) (**figure 24**).

The cellular localization of the protein, Gdt1, is strictly in the Golgi apparatus, while PAM71 is localized at the thylakoid membrane of the chloroplasts. The Golgi apparatus is the main localization of human TMEM165 (Foulquier et al., 2012a), however, a small proportion can be found at the plasma membrane and in lysosomes, especially in the case of an overexpression ((Rosnoblet et al., 2013) Demaegd et al., 2013) .

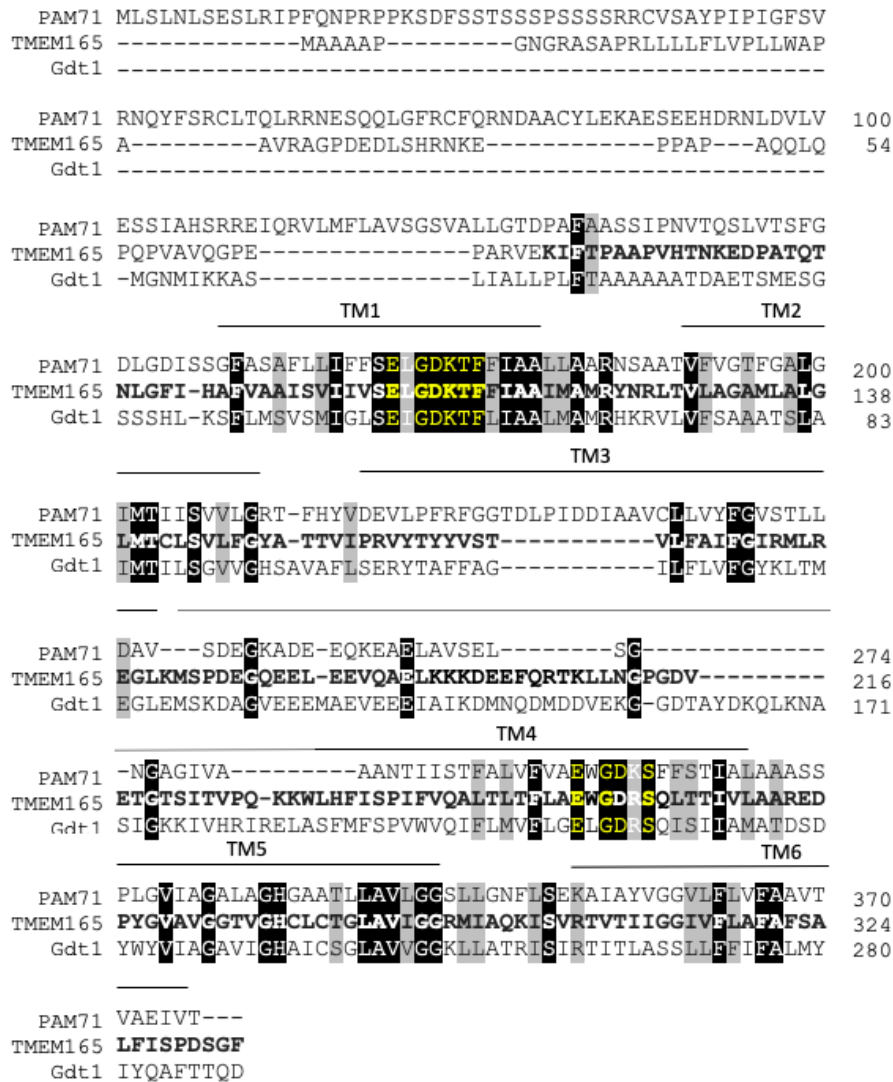


**Figure 24. Alignment of TMEM165 protein sequence and the orthologs PAM71 from *Arabidopsis thaliana* and Gdt1 from *Saccharomyces cerevisiae*** (Mammalian TMEM165 sequence (bold characters), identical residues (black boxes), homologous amino acids (gray boxes), transmembrane domains (black horizontal bars), cytosolic central loop (dotted line)).

#### 4.1.2 TMEM165 topology

TMEM165 has been predicted to form 7 transmembrane domains, with a signal-peptide cleavage site on the 33<sup>rd</sup> amino acid, and two specific amino acid sequences EXGDK/R, that are the signature motifs of the UPF0016 family. Besides these motifs, TMEM165 protein presents a cytoplasmic loop of 52 amino acids shaped in a coiled-coil domain (Rosnoblet et al., 2013) (figure 25).

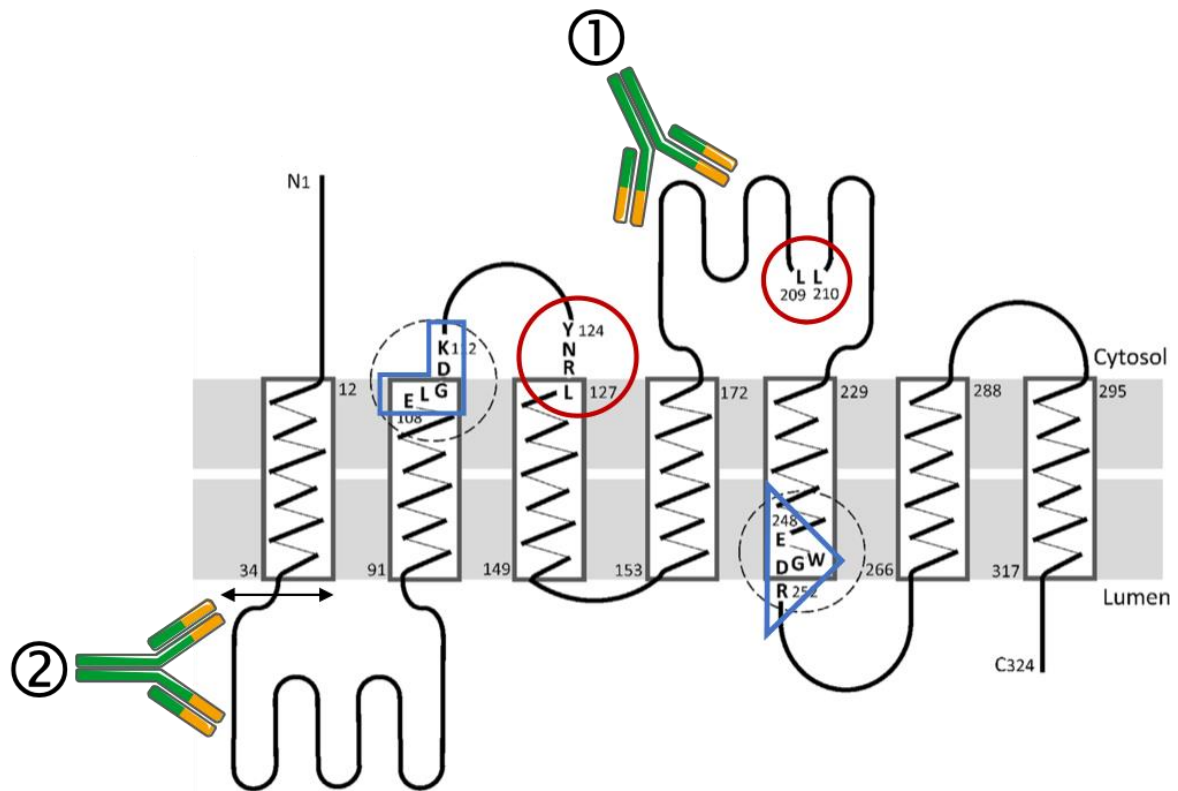


**Figure 25. Prediction of TMEM165 topology and the conserved domains** (modified from Dulary et al., 2017) The two EXGDK/R motifs of the UPF0016 family are delineated with blue frames, the two putative lysosomal targeting sequences YNRL and [DE]XXXL[LI] with red circles. The two antibodies used to recognize the protein are depicted in green. The black arrow indicates the cleavage point.

Two putative lysosomal-targeting sequences, YNRL and [DE]XXXL[LI] were proposed (**figure 25**). [DE]XXXL[LI] with two leucine residues in the large cytoplasmic loop, was shown not to be relevant for TMEM165 localization. YNRL belongs to the classical YXX $\Phi$  lysosomal-targeting signal and mutations in this domain have brought new insights on TMEM165 trafficking.

From the Golgi, there are two main pathways for a protein to reach the lysosome, one direct and the second indirect *via* the plasma membrane before reinternalization. Mutations in the Y124 amino acid prevent the transport of the protein to the plasma membrane. In cells expressing R126 mutant, a delay in the internalization of TMEM165 from the plasma membrane was demonstrated. These mutations assess the crucial importance of the YNRL motif for the targeting of TMEM165 to the lysosome (Rosnoblet et al., 2013).

The loop contains also, many acidic amino acids initially proposed to constitute a cation-binding site.

Moreover, in 2014, a bioinformatic phylogeny study of TMEM165 hypothesized that TMEM165 would be made of two homologous domains with an antiparallel orientation

resulting from a genetic duplication event, separated by a positively charged cytoplasmic loop. The characteristics of the human extra N-terminal domain remains unclear (Demaegd et al., 2014) (**figure 26**).

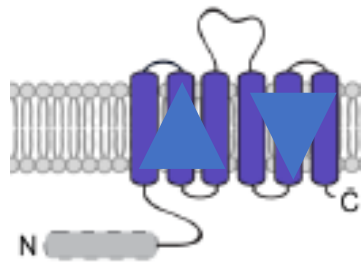


**Figure 26. Predicted topology of all the UPF0016 family members based on the phylogenetic comparison** (modified from Demaeagd et al., 2014)

The cytosolic localization of E-X-G-D-K-[S-T] and the luminal localization of E-X-G-D-R-[S-Q] has been proven in 2016 by our research group (REF POTELLE). This has been demonstrated with two antibodies that recognize respectively the cytosolic loop sequence (aa176–aa229) and the luminal loop sequence (aa17–aa45) of TMEM165. In the presence of digitonine, a molecule able to permeabilize plasma and mitochondrial membranes or in the presence of Triton X-100 that permeabilizes all the subcellular compartments, we were able to assess the orientation of TMEM165 protein (**figure 25**).

#### 4.1.3 TMEM165 stability

The high sensitivity of TMEM165 to manganese exposure was a major breakthrough. Indeed, the addition of high manganese concentration to the cell medium induced a rapid loss of TMEM165 expression in human control cells. The lysosomal degradation was proven to be manganese specific. Immunofluorescence experiments demonstrated the inhibition of lysosomal Mn<sup>2+</sup>-induced degradation of TMEM165 by chloroquine (Result part, article 4, Potelle et al, 2017).

#### 4.2 TMEM165 function

##### 4.2.1 Role of TMEM165 in glycosylation

When TMEM165 was discovered, the N-glycosylation defect was observed on patients serum transferrin by IEF. The glycosylation defect was also assessed in patient fibroblasts. The first

knockdown experiments (Foulquier et al., 2012a), and later the use of KO TMEM165 HEK293 cell lines confirmed the *N*-glycosylation defects.

Mass spectrometry analyses of the sera of TMEM165-deficient individuals and KO TMEM165 HEK293 cells, characterized the defect with an elevation of hyposialylated and hypogalactosylated *N*-glycans. The truncated glycoconjugates presented the same proportion of species lacking sialic acid and galactose moieties on their branches, attesting that the galactose addition was impaired (Morelle et al., 2017). The observed *N*-glycosylation defect would mostly be due to the impairment of the activity of the  $\beta$ 1,4-galactosyltransferase.

Four classes of glycosylation might be impaired in CDG, *N*-glycosylation, *O*-glycosylation, glycolipids and proteoglycans (Moremen, 2014), in TMEM165-CDG, the four of them can be defective. The *O*-glycosylation abnormalities was translated by the increase of the asialo-forms of Apo CIII (Foulquier et al., 2012). Apo CIII is a glycoprotein with a unique *O*-glycosylation site presenting up to two terminal sialic acids.

Using MALDI-MS, our team also demonstrated an alteration of the glycolipids. As the  $\beta$ 1,4*N*-acetylgalactosaminyltransferase, also known as GM2/GD2 synthase, also requires manganese as cofactor, a drastic decrease of gangliosides expressions was observed in KO TMEM165 cells (Morelle et al., 2017).

Concerning GAG synthesis, the zebra fish model experiments demonstrated the alteration of the chondroitin sulfate proteoglycan of the cartilage; this study will be further detailed in §4.3.3 (Bammens, 2015).

#### 4.2.2 Role of TMEM165 in calcium homeostasis

The deleterious effect of high calcium concentration in yeast studies is assessed by a delayed or a halted growth. Gdt1 was proposed to be implied in the calcium transport into the secretory pathway after experiments with Gdt1 KO cells that were intolerant to extremely high calcium concentration (500-700mM). The initial yeast study, conducted by Demaegd and collaborators in 2014, demonstrated that (i) the calcium sensitivity of the KO Pmr1 strain was compensated by Gdt1 and reciprocally; (ii) the double KO *pmr1Δ* / *gdt1Δ* was more deleterious than the single *pmr1Δ*. However, (iii) the single KO Pmr1 was shown to be more deleterious than the Gdt1 knockout.

There were evidences that UPF0016 family members had a role in manganese transport but no direct proof. For instance, in *Lactococcus lactis* heterologous expression of Gdt1 induced a

manganese influx in the bacteria (Thines et al., 2018), in addition to the previously shown calcium transport faculty (Colinet et al., 2016). Pmr1 was shown to supply the secretory pathway in  $\text{Ca}^{2+}$ , and to a lesser extent  $\text{Mn}^{2+}$ .

Finally, data pointed out that despite structural and functional common properties Gdt1 and TMEM165 did not share enough sequence homology with CaCA superfamily and probably belong to a new group of cation transporter.

Based on these results, pmr1 and Gdt1 were thought to be two calcium transporters of distinct pathways with a related function. It leads to the assumption that Gdt1 and TMEM165 would be the first members of the same new  $\text{Ca}^{2+}/\text{H}^+$  antiporter family.

A yeast study further explored Gdt1 function. In this model, the vacuolar  $\text{H}^+$  pool brought by V-ATPase is used by the CAX-family  $\text{H}^+/\text{Ca}^{2+}$  exchangers to import  $\text{Ca}^{2+}$  into the vacuole lumen. One member of this family is Vcx1 and Gdt1 would have the corresponding role in the Golgi apparatus retrieving  $\text{H}^+$  in exchange of  $\text{Ca}^{2+}$ . A further argument for this concept is the calcium hypersensitivity of *gdt1Δ* and *vcx1Δ* strains. In the case of a disruption of the V-ATPase pump, an elevated cytoplasmic calcium concentration is observed and Gdt1 works in reverse mode. Vcx1 and Gdt1 would enhance calcium storage only if the Golgi presents a correct acidification by the proton pump. Vcx1 function is inhibited by calcineurin and Gdt1 forward mode too. Surprisingly both Gdt1 and Vcx1 can also inhibit calcineurin.

Gdt1 calcium transport is shown to be independent of Pmr1, Pmc1, and Vxc1 (Snyder et al., 2017).

#### 4.2.3 Link between TMEM165 and pH

Experiments, using a fluorescent pH-sensitive marker, demonstrated an increased lysosomal acidity in TMEM165-CDG patient fibroblasts (Demaegd et al., 2013). On this basis, several teams tried to establish a direct link between TMEM165 and Golgi/lysosomal pH.

The expression of TMEM165 is enhanced in specific tissues, like in the mammary epithelial cells, while calcium concentration in the blood is between 2 and 2.5 mM, milk concentrates calcium up to 30-80 mM. The evaluation of the gene expression by mRNA quantification assessed a 25-fold increase peak of TMEM165 expression during lactation as compared to the prepartum period. In mice, TMEM165 expression was reduced by 50 %, 24 hours after a total stop of the breastfeeding and by 95% after 96 hours (Reinhardt et al., 2014a). TMEM165 is

thought to import  $\text{Ca}^{2+}$  into the mammary epithelial cell and to remove proton excess (Reinhardt et al., 2014a). This demonstrated that  $\text{Ca}^{2+}$ , pH and also  $\text{Mn}^{2+}$  environments are crucial for milk production efficiency in the Golgi of mammary epithelial cell. Manganese appears as an important cofactor for lactose synthase.

The high expression of TMEM165 in mammary gland cells leads to the hypothesis that it would represent a proton pump responsible for the Golgi apparatus to the cytosol proton leakage. One of the arguments was that the biosynthesis of one lactose molecule leads to the release of two  $\text{H}^+$  in the Golgi that need to exit the compartment.

TMEM165 would have a role in pH and calcium metabolism that could be consistent with the osteoporosis observed in patients. In 2016, the calcium uptake of Gdt1 was assessed to be a pH-dependent phenomenon (Colinet et al., 2016).

Carbohydrate moieties of glycoconjugates originate from nucleotide mono- or diphosphate sugars in the Golgi. The byproducts of the glycosylation reaction are sent back to the cytosol for recycling. The nucleotides are retrieved through the same nucleotide-sugar transporter by which they arrived, while  $\text{H}^+$  and inorganic phosphate (Pi) present an unclear recycling mechanism. In 2017, the role of Gdt1 in proton export and Erd1, an ortholog of human XPR1, in Pi retrieval was studied (Snyder et al., 2017). The authors demonstrated that (i) Erd1 can inhibit Gdt1, (ii) both Erd1 and Gdt1 exhibit unrelated function in the Golgi apparatus and (iii) that they may have an indirect role on byproducts recycling, regulating unidentified transporters.

The same group, in 2019 managed to generate TMEM165-deficient mice and demonstrated that their milk contains low levels of  $\text{Ca}^{2+}$  and  $\text{Mn}^{2+}$  and that their progeny grew up slower than control mice. The decrease in lactose production is thought to be linked to the dysfunction of manganese-dependent B4GALT1 required, together with  $\alpha$ lactalbumin, to form lactose synthase (Snyder et al., 2019).

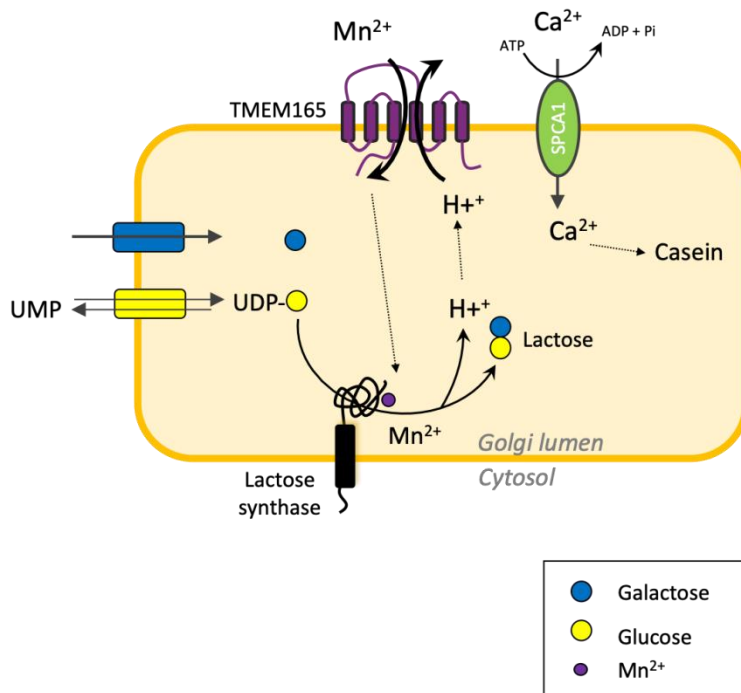


**Figure 27. Putative role of TMEM165 and SPCA1 in Golgi lactose biosynthesis**

Snyder and collaborators shed light on the particular role of TMEM165 in epithelial cells of the mammary gland. A considerable increase in the level of expression of TMEM165 during lactation was observed. The role of TMEM165 in this tissue is the supply of manganese as a cofactor for lactose synthase enzyme, composed of  $\alpha$ -lactalbumin and N-acetyllactosamine synthase, categorized as a  $\beta$ 1,4-galactosyltransferase. A second argument is the fact that lactose synthesis releases a significant number of protons that have to exit the Golgi apparatus to maintain an optimal pH for the resident enzymes. In this compartment, TMEM165 would be a candidate for proton export (**figure 27**). In the model proposed by Snyder, TMEM165 calcium import would be neglectable, this role being dedicated to SPCA1 and other calcium pumps (Snyder et al., 2019).

Nowadays, questions about the link between Gdt1/TMEM165 and pH, the direct or indirect mechanism of the impact of Gdt1/TMEM165 on calcium store, the direction of the presumed calcium transport performed by Gdt1 and the nature of TMEM165 counterion exchanged against of  $\text{Ca}^{2+}$  and/or  $\text{Mn}^{2+}$  remain unsolved.

#### 4.2.4 Role of TMEM165 in manganese homeostasis

##### 4.2.4.1 Glycosylation defect in Gdt1/TMEM165 deficient cells results of misregulation of Golgi manganese homeostasis

The electrophoretic study of secreted invertase, a marker Golgi *N*-glycosylation in yeast, is used to study the influence of  $Mn^{2+}$  and  $Ca^{2+}$  on the glycosylation process in yeast mutants *pmr1Δ*, *gdt1Δ* and double KO *pmr1Δ/gdt1Δ* was assessed in our laboratory in 2016 (Potelle et al., 2016). First, *gdt1Δ* showed an invertase electrophoretic shift under high calcium concentration conditions, consistent with previous yeast studies (Demaegd et al., 2013). Regarding the calcium supplementation, a strong glycosylation defect in *gdt1Δ* strain was induced, while in *pmr1Δ* a beneficial effect rescuing the preexistent glycosylation deficiency was shown. This opposite response confirms a different mechanism of action of the two ion transporters. Interestingly, manganese supplementation was able to restore *pmr1Δ* glycosylation defects and *gdt1Δ* glycosylation defect induced by calcium pressure.

These results suggest that in high calcium concentration, in the absence of Gdt1, the excess of calcium ions will compete with manganese to enter the cell via Pmr1 and decrease Golgi manganese concentration. Once in the Golgi, calcium can compete with manganese and inhibit the manganese-dependent glycosyltransferases leading to the observed glycosylation defect. This also explains the glycosylation rescue by manganese addition.

Moreover, in the absence of *pmr1*, overexpression of Gdt1 respond to  $Ca^{2+}$  stress storing calcium in the GA and thus acts on a reverse-mode in *pmr1Δ/gdt1Δ strain* (Colinet et al., 2016).

##### 4.2.4.2 In yeast Gdt1 could be the leak channel of Pmr1

In 2018, Dulary and collaborators demonstrated that  $Ca^{2+}$  and also  $Mn^{2+}$  were both able to restore the glycosylation defect created by the inactivation of Pmr1. In the double KO yeast for Gdt1 and Pmr1, manganese was able to restore the induced glycosylation defect but not calcium. Moreover, when a mutated strain of Pmr1 was able to import only calcium (*Pmr1pQ783A*), Gdt1 was required to import  $Mn^{2+}$  inside the Golgi lumen to restore glycosylation. The aspartic acid of conserved EXGDK/R motifs was considered as a cation-binding site, crucial for Golgi glycosylation (Dulary et al., 2018).

The same year,  $Ca^{2+}$  and  $Mn^{2+}$  affinity constants of Gdt1 were determined and despite the highest affinity of Pmr1 for  $Mn^{2+}$  compared to Gdt1, *gdt1Δ* strain exhibited a misregulation of

manganese cytoplasmic concentration leading to the disruption of SOD activity. This study reinforces the previous hypothesis based on the direct regulation of yeast calcium and manganese concentration by Pmr1 for Gdt1. They may share the same ion transport direction, namely the import of cation from the cytosol to the Golgi lumen (Thines et al., 2018).

These recent results suggest that Gdt1 could be a  $Mn^{2+}/Ca^{2+}$  antiport transporter able to import  $Mn^{2+}$  inside the Golgi lumen concomitantly with the export of  $Ca^{2+}$  in the cytosol. Gdt1 would represent a “leak channel” of Pmr1 (figure 28) and this was the first evidence of a functional link between these two proteins.

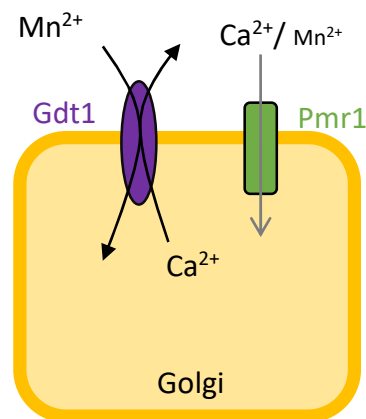


**Figure 28. Schematic representation of the hypothetical function of Pmr1 and Gdt1 in yeast** Gdt1 would represent the leak channel of Pmr1 in order to maintain the Golgi ion homeostasis

#### 4.2.4.3 Plant ortholog PAM71 of TMEM165 is a $Mn^{2+}/Ca^{2+}$ antiporter

In 2016, a study was conducted in *Arabidopsis thaliana*, a plant whose chloroplastic ortholog of TMEM165 is the PAM71, one out of five members of UPF0016 family represented in plants. PAM71 is localized to the thylakoid membrane of plants and algae chloroplasts. This plastid, like mitochondria, has its own DNA and can be compared to the Golgi apparatus of mammals. The plastid composed of a stroma and thylakoids that are stacks of disks, also named grana, containing the photosynthetic pigments. PAM71 is required for a correct function of the Oxygen Evolving Complex (OEC) a catalytic center of water oxidation of the Photosystem II (PSII) complex (Ferreira, 2004) made of an inorganic  $Mn_4CaO_5$  cluster. *pam71Δ* induced an imbalanced partitioning of  $Ca^{2+}$ ,  $Mn^{2+}$ , and protons. Plants need calcium as a macronutrient and  $Mn^{2+}$  as a micronutrient. While this KO resulted in a lack of manganese in the OEC, the stroma calcium concentration increased, moreover, manganese supplementation could rescue the photosynthesis; furthermore, the expression of *pam71* in *pmr1Δ* yeast induced manganese tolerance.

PAM71 is proposed to be a divalent cation exchanger, essential for calcium, manganese homeostasis and pH maintenance. PAM71 would act as the transporter that sustains thylakoid  $Mn^{2+}$  need, in exchange of  $Ca^{2+}$  (Schneider et al., 2016), however, the exact role has to be further explored. A year later, experiments in a cyanobacterium, *Synechocystis spp*, proposed SynPAM71 (PAM71 ortholog) to be a  $Mn^{2+}/ H^+$  antiporter mediating manganese tolerance (Gandini et al., 2017). In a recent study in *Arabidopsis thaliana*, CMT1 (Chloroplast Manganese Transporter 1) was shown to be the chloroplast envelope homolog of PAM71 that is localized at the thylakoid membrane. They are thought to both transport manganese to the PSII (Eisenhut et al., 2018).

#### 4.2.5 Restoration of the glycosylation defect in TMEM165-depleted cells

##### 4.2.5.1 Restoration of the glycosylation defect in TMEM165-depleted cells by manganese

Multiple treatments were tested on KO cells to restore the glycosylation defect. According to previous yeast studies linking Gdt1 with manganese uptake into the Golgi apparatus, the addition of  $Mn^{2+}$  in the medium of human KO TMEM165 cells was conducted. Surprisingly,  $Mn^{2+}$  addition was able to restore glycosylation as observed by mass spectrometry and in LAMP2 electrophoretic profile and is consistent with previously observed results (Potelle et al., 2016; 2017 and Dulary et al., 2018). A concentration of  $1\mu M$  of manganese for 48 hours was sufficient for the restoration of galactosylated and sialylated *N*-glycans (Morelle et al., 2017).

##### 4.2.5.2 Restoration of the glycosylation defect in TMEM165-depleted cells by galactose

As the galactosylation step of the glycosylation process is disrupted in TMEM165 KO cells, the idea of a galactose supplementation rose. Remarkably, mass spectrometry assessed that 1 mM galactose concentration was able to restore fully glycosylated glycans species in KO TMEM165 HEK293 cells experiments. Western blot also showed a rescue of fully glycosylated forms of LAMP2. Other monosaccharides, such as GlcNAc and  $GlcNH_2$ , were also tested, but none induced any benefit (Morelle et al., 2017). Galactose is the sole monosaccharide capable of rescuing a normal glycosylation.

#### 4.2.6 Actual model

These experiments conducted during the past 8 years lead us to hypothesize a model of TMEM165 function in which this transmembrane protein is a passive transporter. The nature

of the imported cation can either be calcium or manganese. However, the direction of calcium transport has not clearly been established. In addition to this, yeast Gdt1 and human TMEM165 may have different functionalities and a switch in reverse-mode is conceivable under certain conditions. From this statement, the nature of the counterion remains unsolved. Due to the continuous link between pH and TMEM165/Gdt1, this transporter could actually be responsible for the proton leakage of the Golgi apparatus as shown in **figure 29**. The study of the functional link between TMEM165/Gdt1 with SPCA1/Pmr1 will be a key element to further understand the cooperation between these two transporters in the Golgi ion homeostasis regulation.

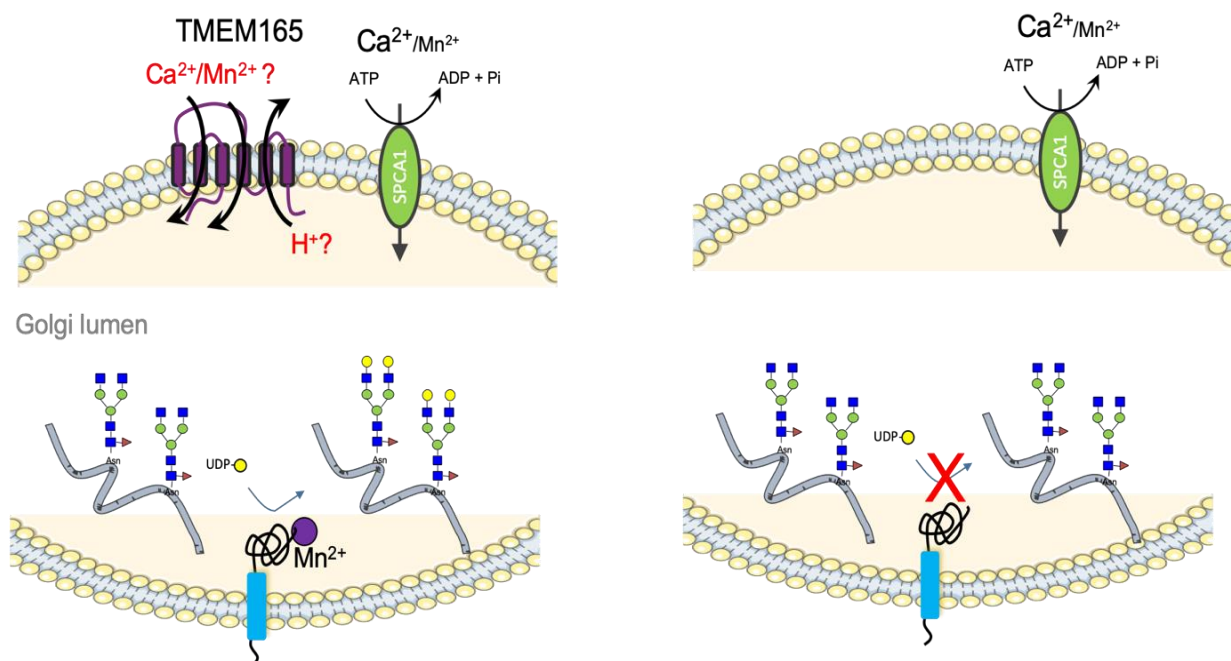


**Figure 29. Proposed model for the functionality of TMEM165 in humans**

The putative function of TMEM165 can be the import of  $\text{Ca}^{2+}$  or  $\text{Mn}^{2+}$  and the counterion would be  $\text{H}^+$ . In the absence of TMEM165, the Golgi  $\text{Mn}^{2+}$  concentration is insufficient to supply the  $\text{Mn}^{2+}$  to manganese-dependent galactosyltransferases that leads to glycosylation defect.

The demonstration of this model is necessary to understand the physiopathology of TMEM165-CDG.

#### 4.3 TMEM165-CDG

In 2012, by means of autozygosity mapping coupled to expression analysis, Foulquier and collaborators linked for the first time a glycosylation defect to TMEM165, a newly discovered

protein (Foulquier et al., 2012). Autozygosity mapping is a genetic technique used to identify homozygosity of ancestral genes found in related affected individuals in a context of consanguinity. Mutations in *TMEM165* gene were found in five patients, two of them being siblings, in a cohort of undiagnosed CDG cases. These patients shared an abnormal IEF, typical of type II CDG phenotype, and clinical features such as psychomotor retardation, developmental delay and skeletal abnormalities. This was the first mention of a new CDG subtype, TMEM165-CDG.

#### 4.3.1 Localization of the *TMEM165* gene mutations

Seven patients out of four families harboring different mutations have been identified in four different families and reported in literature.

The index case reported in 2012, as well as two other patients, harbored a homozygous intronic mutation c.792+182G>A, (IVS4+182G). The mutation activates a cryptic splice donor site and leads to two transcripts: a wild type form in addition to a modified form resulting in the loss of exon 4 that is replaced by a 117 bp intronic sequence, this shorten the protein of 94 amino acids after translation with a change in 27 amino acids at the C-terminus. A decreased level of TMEM165 protein expression was observed in the fibroblasts of three patients. The expression of the mutated form of in yeast model confirmed the inability of intronic splice mutated-TMEM165 to rescue yeast growth impairment in *gdt1Δ* strain.

A missense homozygous mutation, c.377G>A resulting in the substitution of an arginine by an histidine residue ([p.Arg126His] or R126H), also decreased the expression level of TMEM165 in the patient fibroblast probably due to an impaired targeting of TMEM165 from the Golgi to the lysosomal/endosomal compartments. A heterozygous missense mutation affecting the same amino acid, c.376C>T [p.Arg126Cys] (R126C), associated with a missense mutation of the other allele c.910G>A [p.Gly304Arg] (G304R) has also been reported in another patient. The arginine 126 and the glycine 304 are found to be highly conserved throughout evolution and are likely to be responsible for the phenotype. In the fibroblasts of the fifth patient, TMEM165 remains localized in the Golgi apparatus membrane but the expression was slightly decreased (Foulquier et al., 2012; Rosnoblet et al., 2013; Zeevaert et al., 2013).

The last two patients harbored a homozygous missense mutation c.323A>G [p.Glu108Gly] (E108G), responsible for a partial resistance to a manganese-induced lysosomal degradation.

It should be noted that patients with the splice mutation leading to a complete loss of TMEM165 expression present the most severe phenotypes.

#### 4.3.2 Clinical features

The main feature of TMEM165-CDG is the skeletal disorder, a clinical sign present in only 20% of all the described CDG subtypes (*i.e* EXT1/ EXT2-CDG, B4GALT7-CDG, B3GAT3-CDG, GALNT3-CDG, SLC35D1-CDG, LFNG-CDG, PIGV-CDG, ATP6V<sub>0</sub>A2-CDG). The link between the glycosylation defect and these skeletal abnormalities is not clearly uncovered yet. The main clinical features of TMEM165 are resumed in **table 4**.

General development	<ul style="list-style-type: none"> <li>▪ Psychomotor retardation, failure to thrive</li> </ul>
Muscular/skeletal system	<ul style="list-style-type: none"> <li>▪ Dwarfism resistant to growth hormone</li> <li>▪ Spondylo-, epi- and metaphyseal skeletal dysplasia</li> <li>▪ Joint hyperlaxity</li> <li>▪ Muscular hypotrophy</li> <li>▪ Midface hypoplasia</li> <li>▪ Low-set ears</li> <li>▪ Early osteoporosis</li> <li>▪ Scoliosis</li> </ul>
Liver	<ul style="list-style-type: none"> <li>▪ Hepatosplenomegaly</li> <li>▪ ↗ transaminases, especially aspartate transaminase ASAT</li> <li>▪ ↗ Creatine Kinase (CK), ↗ Lactate Deshydrogenase (LDH)</li> <li>▪ ↘ FVIII, IX, XI, protein C (coagulation factors)</li> </ul>
Central nervous system	<ul style="list-style-type: none"> <li>▪ White matter abnormalities</li> <li>▪ Absence of neural pituitary gland</li> </ul>
Eye	<ul style="list-style-type: none"> <li>▪ Macular epithelial pigment alterations</li> </ul>

**Table 4. Principal clinical features observed in TMEM165-CDG patients** (Zeevaert et al., 2013)

#### 4.3.3 An experimental animal model for TMEM165 deficiency: the zebrafish

An experiment, conducted on zebrafish morpholino-based approach, studied the impact of a reduced expression of TMEM165 on fish development. Tmem165, the zebrafish ortholog protein, presents 79% identity with human TMEM165. Craniofacial morphology, cartilage/bone maturation and development abnormalities found in the morphants were

consistent with patients TMEM165-CDG phenotypes. At a cellular level, the inhibition of Tmem165 actually alters chondrocytes and osteoblasts differentiation.

Zebrafish is validated as an interesting model to study TMEM165-CDG and maybe other CDG implying skeletal alterations similar to those found in human (Bammens et al., 2015a). In the future, a mouse model should also be generated.

#### 4.3.4 Diagnostic

The biochemical diagnosis of CDG can be made either by transferrin isoelectrofocusing (IEF), capillary zone electrophoresis, and/or mass spectrometry total serum *N*-glycome.

The genetic identification of the mutated gene by sequencing is required to categorize the CDG.

In 2015, the first perinatal glycosylation pattern assessment of a TMEM165-CDG newborn was carried out due to the preexistence of a homozygous mutation in a sibling. The prenatal diagnostic was realized by genetic analysis on an amniocentesis sample at six months of pregnancy (Schulte Althoff et al., 2015).

#### 4.3.5 Treatment

For the deep intronic changes of TMEM165, c.792+182G>A mutation, the use of an antisense oligonucleotide-mediated pseudo exon skipping on TMEM165 mRNA to correct the aberrant insertion in patient fibroblasts was performed. A restoration up to 60% of TMEM165 expression of the control cells was observed in the patient fibroblasts. This is a promising track for TMEM165-CDG despite the non-applicability for missense mutations (Yuste-Checa et al., 2015).

As patients presented a normal manganese blood level, manganese supplementation was not tested to prevent a potential toxicity induced by elevation of manganesemia. However, as the galactosylation step of the glycosylation process is disrupted in TMEM165 KO cells, the idea of an oral galactose supplementation for TMEM165-CDG patients arose. In 2017, the first clinical trial on TMEM165-CDG patients possessing the deep intronic mutation c.792+182G>A was conducted. Oral supplementation by D-galactose, with the use of a dose of 1 g/kg/day during 18 weeks, showed a slight restoration of fully glycosylated glycans in serum and an improvement of the biochemical parameters of patients. However, the benefit on biochemical parameters is variable among individuals and the cellular action mechanism remains unclear

(Brasil et al., 2018; Ferreira et al., 2018; Morelle et al., 2017).

## OBJECTIVES

Since the discovery in 2012, the elucidation of the function of TMEM165 has been challenged and the more we have learned, the more questions emerged about this protein implied in a newly identified type II CDG.

Members of our group recently linked TMEM165 and manganese twice. First, TMEM165-CDG glycosylation defect is due to a Golgi manganese impaired homeostasis. Second, TMEM165 is a manganese-sensitive protein which is specifically targeted to the lysosome under an elevation of the cytosolic manganese concentration.

The first issue of my essay was to dissect the topological localization of the amino acids sequence involved in the glycosylation function of TMEM165 and its manganese sensitivity.

As the link was proposed in yeast with Gdt1/Pmr1, the second aim was to further understand the link between TMEM165 and SPCA1, the unique other known  $\text{Ca}^{2+}/\text{Mn}^{2+}$  Golgi pump in human.

All these studies are at the onset of a characterization of the cellular and molecular mechanisms of TMEM165 to propose *in fine* a potential therapeutic option for TMEM165-CDG and other manganese-related CDG patients.

## RESULTS

### [1] Dissection of TMEM165 function in Golgi glycosylation and its Mn<sup>2+</sup> sensitivity

In 2012, the first link between a novel CDG subtype and the newly discovered protein, TMEM165, was established (Foulquier et al., 2012). At the beginning of my PhD, little was known about TMEM165 function. During the last eight years, interesting breakthroughs were made and TMEM165 is now proposed to be one of the main regulators of Golgi manganese homeostasis acting as a potential Mn<sup>2+</sup>/Ca<sup>2+</sup> exchanger.

#### 1.1.1 Importance of the signature motifs of the UPF0016 family members

TMEM165 is now known to be a 324 amino acids-, Golgi-localized transmembrane protein that belongs to the Uncharacterized Protein Family 0016 (UPF0016). Members of this family are highly conserved throughout evolution, especially in two specific motifs E-ϕ-G-D-K-T and E-ϕ-G-D-R-S-Q, which are the signature of the UPF0016 family. According to a phylogenetic study, TMEM165 would be the result of a duplication of two homologous clusters of 3 transmembrane domains with opposite orientation. Hence, these motifs are facing each other, one is luminal and one is cytosolic, and may be responsible for ion transport (Demaegd et al., 2014). In this study, we aimed to further understand the role of the two signature motifs in glycosylation and in TMEM165 sensitivity to manganese-induced degradation.

#### 1.1.2 Identifying amino acids implied in TMEM165 function in glycosylation

First, as TMEM165 was involved in a CDG, its role in Golgi glycosylation was first studied. The glycosylation pattern of TMEM165-depleted cells and TMEM165-deficient patient sera demonstrated an extensive abnormal glycosylation (Morelle et al., 2017; Potelle et al., 2016, 2017), characterized by a hypogalactosylation combined with a hyposialylation. In this study, we wondered which amino acids are responsible for the function of TMEM165 in glycosylation. The associated glycosylation defect of KO TMEM165 HEK293 cells after TMEM165-mutants transfection can be assessed by mass spectrometry but also by analysis of lysosome-associated membrane protein 2 (LAMP2) gel mobility in Western Blot. LAMP2 is a highly glycosylated protein used as a glycosylation reporter in our studies.



hours exposition to a supraphysiologic concentration of manganese to attest the sensitivity of the different TMEM165 mutants.

In this study, highly conserved amino acids were chosen and 25 mutated-forms and a WT-form of TMEM165 were generated, including some patient mutations (Foulquier et al., 2012a; Schulte Althoff et al., 2016). The amino acids were modified into glycine, this amino acid was chosen for the small steric hindrance, neutrality and the absence of asymmetric carbon. Transient transfection of KO TMEM165 HEK293 by the different constructs allows the identification of the important amino acids for TMEM165 function in glycosylation. We then focused on the E- $\phi$ -G-D-K-T and E- $\phi$ -G-D-R-S-Q motifs to better delineate their role in manganese-induced TMEM165 degradation.

## **1.2 Publication**



Published in final edited form as:

*Biochimie*. 2019 October ; 165: 123–130. doi:10.1016/j.biochi.2019.07.016.

## Dissection of TMEM165 function in Golgi glycosylation and its Mn<sup>2+</sup> sensitivity

Elodie Lebretonchel<sup>a,b</sup>, Marine Houdou<sup>a</sup>, Sven Potelle<sup>a</sup>, Geoffroy de Bettignies<sup>a</sup>, Céline Schulz<sup>a</sup>, Marie-Ange Krzewinski Recchi<sup>a</sup>, Vladimir Lupashin<sup>c</sup>, Dominique Legrand<sup>a</sup>, André Klein<sup>a,b</sup>, François Foulquier<sup>a,\*</sup>

<sup>a</sup>Univ. Lille, CNRS, UMR 8576 – UGSF - Unité de Glycobiologie Structurale et Fonctionnelle, F-59000, Lille, France

<sup>b</sup>Centre de Biologie et Pathologie, UAM de Glycopathologies, Lille Medical Center, University of Lille, 59000, Lille, France

<sup>c</sup>Department of Physiology and Biophysics, College of Medicine, University of Arkansas for Medical Sciences, Biomed 261-2, Slot 505, 200 South Cedar St., Little Rock, AR, 72205, USA

### Abstract

Since 2012, the interest for TMEM165 increased due to its implication in a rare genetic human disease named TMEM165-CDG (Congenital Disorder(s) of Glycosylation). TMEM165 is a Golgi localized protein, highly conserved through evolution and belonging to the uncharacterized protein family 0016 (UPF0016). Although the precise function of TMEM165 in glycosylation is still controversial, our results highly suggest that TMEM165 would act as a Golgi Ca<sup>2+</sup>/Mn<sup>2+</sup> transporter regulating both Ca<sup>2+</sup> and Mn<sup>2+</sup> Golgi homeostasis, the latter is required as a major cofactor of many Golgi glycosylation enzymes. Strikingly, we recently demonstrated that besides its role in regulating Golgi Mn<sup>2+</sup> homeostasis and consequently Golgi glycosylation, TMEM165 is sensitive to high manganese exposure. Members of the UPF0016 family contain two particularly highly conserved consensus motifs E-φ-G-D-[KR]-[TS] predicted to be involved in the ion transport function of UPF0016 members. We investigate the contribution of these two specific motifs in the function of TMEM165 in Golgi glycosylation and in its Mn<sup>2+</sup> sensitivity.

Our results show the crucial importance of these two conserved motifs and underline the contribution of some specific amino acids in both Golgi glycosylation and Mn<sup>2+</sup> sensitivity.

---

\*Corresponding author. francois.foulquier@univ-lille.fr (F. Foulquier).

#### Authors contribution

Conceived and designed experiments: F.F., A.K., and D.L. Performed experiments: E.L., M.H. and S.P. Contributed reagents/materials: V.L., C.S. Analyzed data: E.L., M.H., G.D.B., and M.K.R. Wrote the paper: F.F., A.K., and D.L.

#### Competing interests

The author(s) declare no competing interests.

#### Declaration of interests

The authors declare that they have no known competing financial interests or personal relationships that could have appeared to influence the work reported in this paper.

#### Appendix A. Supplementary data

Supplementary data to this article can be found online at <https://doi.org/10.1016/j.biochi.2019.07.016>.

## Keywords

TMEM165; CDG; UPF0016; Golgi glycosylation; Mn<sup>2+</sup>

---

## 1. Introduction

Congenital Disorders of Glycosylation (CDG) are a rapidly expanding family of genetic diseases. The first patient cases were reported 38 years ago; today more than hundred different CDG have been reported [1]. The frequency of most CDG is unknown but they are probably underestimated. The genetic transmission is mostly autosomal recessive [1]. Congenital disorders of protein glycosylation are classified in two groups. CDG-I are assembly defects in the cytosol and the endoplasmic reticulum (ER), while CDG-II are defects in glycan remodeling in the Golgi [2]. They are multisystem disorders with a broad spectrum of severity and mostly comprising neurological involvement.

In 2012, a new CDG called TMEM165-CDG or CDG-IIk (OMIM #614727) has been described [3]. To date, a dozen of TMEM165-CDG patients have been worldwide diagnosed with a common semiology. The most severe phenotypes present a growth retardation resistant to human growth hormone, associated with a psychomotor disability, microcephaly, facial hypoplasia, hypotonia, seizures and hepatosplenomegaly with increased serum transaminases [4]. Some patients also harbor cardiac defects [5] but the pathognomonic signs remain bone and cartilage dysplasia with early and severe osteoporosis. All TMEM165-CDG present a strong defect in the Golgi glycosylation characterized by hypogalactosylation of total serum *N*-glycoproteins [3].

This CDG is due to a deficiency in TMEM165 protein, also named TPARL [3], a 324 amino-acids transmembrane protein member of the UPF family 0016 (Uncharacterized Protein Family 0016; Pfam PF01169). This protein is mainly localized in Golgi membranes [3,6], predominantly in the *trans*-Golgi subcompartment. Similarly to other UPF0016 family members, TMEM165 is highly conserved throughout evolution (919 different species in prokaryotes and 405 species in eukaryotes) [7].

The cellular and molecular functions of UPF0016 family members remain controversial. Gdt1p (Grc1 dependent translation factor 1), the yeast ortholog of TMEM165 in *Saccharomyces cerevisiae* was initially postulated to be a Ca<sup>2+</sup>/H<sup>+</sup> exchanger [8]. Recent results however question the nature of the exchanged ions. Unexpectedly, PAM71 (Photosynthesis Affected Mutant 71), the *Arabidopsis thaliana* plant ortholog of TMEM165 has been shown to function as a Ca<sup>2+</sup>/Mn<sup>2+</sup> cation antiport transporter localized in the thylakoid membranes system and crucial for the regulation of chloroplastic Mn<sup>2+</sup> homeostasis [9]. In addition, we recently demonstrated that the Golgi glycosylation defect due to TMEM165 deficiency also results from a defect in Golgi Mn<sup>2+</sup> homeostasis [10]. Very importantly, a slight Mn<sup>2+</sup> supplementation is sufficient to suppress the observed Golgi glycosylation defect in both deficient yeasts and human cells [11]. Furthermore, our recent studies suggested the function of Gdt1p as a Ca<sup>2+</sup>/Mn<sup>2+</sup> cation antiport transporter [12]. In agreement with these results, Thines and collaborators have recently demonstrated that the

$\beta$

Serum Albumin (BSA), 2% FBS (Lonza) in PBS], followed by the incubation for 1 h with primary antibody diluted at 1:100 in blocking buffer, except for GPP130 that was diluted at 1:300. After washing with PBS, cells were incubated for 1 h with Alexa 488- or Alexa 568-secondary antibody (Life Technologies) diluted at 1:600 in blocking buffer. After three washes with PBS, nuclei were labeled with DAPI 1:300 for 15 min and then coverslips were mounted on glass slides with Mowiol. Fluorescence was detected through an inverted Zeiss LSM700 confocal microscope. Acquisitions were done with ZEN pro 2.1 software (Zeiss, Oberkochen, Germany).

## 2.6. Image analyses

Immunofluorescent images were edited using imageJ software (<http://imagej.nih.gov/ij>) developed by Fiji<sup>®</sup>.

## 2.7. Western blotting

Cells were collected in PBS after 2 washes and centrifuged at 6000 rpm for 10 min. Cells were lysed in RIPA buffer [Tris/HCl 50 mM pH 7.9, NaCl 120 mM, NP40 0.5%, EDTA 1 mM, Na<sub>3</sub>VO<sub>4</sub> 1 mM, NaF 5 mM] supplemented with a protease inhibitors mix (Roche Diagnostics, Penzberg, Germany) by a 30 min centrifugation at 14 000 rpm. Concentration of extracted proteins was determined with the Micro BCA™ Protein Assay Reagent kit (Thermo Fisher Scientific, Waltham, MA USA). For LAMP2 study only samples were preheated 10 min at 95 °C. 10 or 20 µg of total proteins of each sample were dissolved in reducing NuPage® Sample buffer and resolved by MOPS 4–12% Bis–Tris gel (Thermo Fisher Scientific, Waltham, MA USA) and then transferred with iBlot 2 Dry Blotting System (Thermo Fisher Scientific, Waltham, MA USA). Nitrocellulose membranes were blocked 1 h in TBS (Tris Buffer Saline) containing 0.05% Tween 20 5% (w/v) non-fat dried milk for at least 1 h at room temperature, then incubated 1 h with primary antibodies (used at a dilution of 1:2000 for TMEM165, 1: 20 000 for β Actin) and overnight for LAMP2 primary antibody 1:20 000. After three 5 min-TBS-T washes, membranes were incubated with respective secondary antibodies for 1 h (1:10 000 dilution for polyclonal goat anti-rabbit IgG and 1:20 000 for goat anti-mouse IgG Horse Radish Peroxidase-conjugated).

Signal was detected using chemiluminescence reagent Pierce™ Pico Plus Western Blotting Substrate (Thermo Fisher Scientific, Waltham, MA USA) on imaging film (GE Healthcare, Buckinghamshire, UK) or Camera Fusion® (Vilber Lourmat) and its software.

## 3. Results

### 3.1. Functionality of TMEM165 mutants in Golgi glycosylation

The ability for TMEM165 to rescue LAMP2 glycosylation defect in TMEM165 KO HEK293T cells was used to investigate the involvement each amino acid of the two highly conserved sequences. To explore this, 10 different mutations in the most conserved amino acids that lay in the two signature-motifs were generated (Fig. 1). The wild type (wt-) and mutated forms of TMEM165 were then transiently expressed in TMEM165 KO HEK293T cells and the Golgi glycosylation of LAMP2 was followed by Western blot experiments as previously described [14] (Fig. 2A). Compared to untransfected cells (KO), the expression

of the wt-TMEM165 rescued fully glycosylated forms of LAMP2 similar to control cells. Even though the mutated forms of TMEM165 transfection gave heterogeneous results (Fig. 2A), only 3 mutants showed a partial restoration of LAMP2 glycosylation: E108G-, K112G-, R252G-TMEM165, E108G and R252G giving the mildest restorations. Interestingly among all our mutants, 6 of the conserved E-x-GDKT/E-x-GDRSQ motifs are unable to restore LAMP2 glycosylation (Fig. 2B). The mutants (D111G-, T113G-, F114G-, E248G-, D251G-, S253G-, Q254G) were found unable to restore LAMP2 glycosylation (Fig. 2B). This result is characteristic from these two motifs as most of the TMEM165 mutated forms, except G304R (patient mutation), were able to rescue LAMP2 glycosylation (Supp. Fig. 1).

To assess these results, the expression level among the mutated forms of TMEM165 was then investigated by Western blot experiments. Although the TMEM165 profile is found heterogeneous with two major bands, there was no major difference in TMEM165 expression level (Fig. 2A). Altogether these results emphasize the importance of some specific amino acids of the two conserved motifs in TMEM165 function in Golgi glycosylation.

### 3.2. Subcellular localization of TMEM165 mutants

The functionality of TMEM165 mutants in Golgi glycosylation depends of the TMEM165 mutants' expression but also on their subcellular Golgi localization. To reinforce the above results, the Golgi localization of the mutated forms of TMEM165 was then investigated by immunofluorescence and confocal microscopy experiments.

Most of the mutated forms of TMEM165 displayed a Golgi localization as observed by colocalization experiments using the GM130 Golgi marker (Fig. 2C and D). Very interestingly, the D251G- and S253G-TMEM165 mutants, did not entirely colocalize with GM130 as vesicular structures localized throughout the cytoplasm could be detected. To further assess the subcellular localization of these mutants, immunofluorescence staining using the lysosomal/endosomal intracellular marker LAMP2 was performed. A partial colocalization was observed with LAMP2 demonstrating the differential subcellular localization for these mutated forms (Supplementary Figs. 2A and B). For these mutants, it is likely that the observed lack of Golgi glycosylation restoration results from a subcellular mislocalization.

### 3.3. Sensitivity of TMEM165 mutants to manganese exposure

We recently highlighted that, when exposed to high manganese concentration, TMEM165 was efficiently targeted to lysosomes for degradation [15]. As for the glycosylation study, we investigated the  $Mn^{2+}$  sensitivity of these different mutants. To assess this point, the wild-type and mutated forms of TMEM165 were transiently transfected in KO cells. The impact of high  $Mn^{2+}$  concentration supplementation on the stability and subcellular localization was investigated during a 4 and 8 h time course by Western blot (Fig. 3) and immunofluorescence experiments (data not shown). Diagrams under each mutant's Western blot describe the quantification of the remaining TMEM165 after 4 and 8 h of  $Mn^{2+}$  treatment. As previously published [15] we observed that TMEM165 in normal HEK293T

cells is highly sensitive to manganese, with a complete loss of this protein after 8 h treatment (Fig. 3A). Same observation is made after transfection of the wild-type form of TMEM165 in HEK293T KO TMEM165 cells with a loss over 75% of TMEM165 expression after 4 h manganese treatment (Fig. 3A).

Concerning the mutated forms of TMEM165, 5 are found partially resistant, E108G, D111G, T113G, D251G and S253G. At the opposite, K112G, F114G, E248G, R252G and Q254G are sensitive to manganese treatment. These results were confirmed by immunofluorescence confocal microscopy (data not shown) and demonstrate the crucial importance of specific amino acids in the differential Mn induced sensitivity of TMEM165.

### 3.4. The functional mutants are targeted and degraded into lysosomes

We recently established that the  $Mn^{2+}$  induced degradation of TMEM165 was inhibited by chloroquine treatment [15]. To assess whether the mutated forms of TMEM165 fall under the same regulation, the stability of wt- and mutated forms of TMEM165 were analyzed by Western blot and immunofluorescence after  $Mn^{2+}$  exposure, in the presence or the absence of chloroquine. The degradation of every mutated forms of TMEM165 was completely blocked by chloroquine (data not shown). The molecular mechanism by which TMEM165 is sent to lysosomes following  $Mn^{2+}$  exposure is currently unknown. Monoubiquitination is known to be a very efficient mechanism to target proteins for lysosomal degradation. It appears that the cytosolic loop of TMEM165 contains 4 lysine residues K198, K199, K200 and K208 that could be involved in the  $Mn^{2+}$  induced lysosomal targeting. In order to investigate the role of these lysines, TMEM165 mutants (K198R, K199R, K200R, K208R and K198–K200R) were generated and analyzed by Western blot and immunofluorescence after  $Mn^{2+}$  exposure, in the presence or in the absence of chloroquine (Supp. Figure 3). We observed that after  $Mn^{2+}$  exposure, the lysine mutants of TMEM165 were localized in the Golgi and were degraded similarly to what is observed for wt-TMEM165. Altogether, these results indicate that the lysine residues of the cytosolic loop are not involved in the expression, neither in the Golgi localization nor in its  $Mn^{2+}$ -induced degradation of TMEM165.

## 4. Discussion

Although the precise molecular and cellular functions of TMEM165 are still under debate, its functional role in Golgi glycosylation is now clearly established. The link between TMEM165 and cellular/Golgi  $Mn^{2+}$  homeostasis maintenance is shown by (i) the alteration of GPP130  $Mn^{2+}$  induced degradation in TMEM165 depleted cells, (ii) the restoration of Golgi glycosylation by  $Mn^{2+}$  supplementation [11], and (iii) the TMEM165  $Mn^{2+}$  sensitivity [15]. It is now highly suspected that TMEM165 functions as a Golgi  $Ca^{2+}/Mn^{2+}$  transporter regulating both  $Ca^{2+}/Mn^{2+}$  Golgi homeostasis. As observed in yeasts, the Golgi glycosylation defect due to a lack of TMEM165 would result in an alteration of the Golgi  $Mn^{2+}$  homeostasis crucial for the activities of Golgi glycosyltransferases using UDP-sugars as donors [11]. TMEM165 is a member of the UPF0016 family characterized by two highly conserved consensus motifs E- $\Phi$ -G-D-[KR]-[TS]. Our previous results showed that the E- $\Phi$ -G-D-K-T motif (motif 1) was facing the cytosol while the E- $\Phi$ -G-D-R-S (motif 2) was

exposed to the Golgi luminal side and hence are predicted to be involved in the transport function of UPF0016 members [15]. In this paper we wanted to further understand the contribution of these two highly conserved motifs in the role of TMEM165 in Golgi glycosylation and also in its sensitivity to high  $Mn^{2+}$  concentration.

Our results first emphasized that some of the mutated forms of TMEM165 are unable to rescue Golgi glycosylation. The mutation of the amino acid E108G does not seem to strongly affect the function of TMEM165 in Golgi glycosylation as a slight restoration of LAMP2 glycosylation is observed. At the opposite, the E248G mutation (second motif) cannot rescue Golgi glycosylation. Interestingly, the polar amino acids (T113 and S253) are found crucial for the function of TMEM165 in Golgi glycosylation while basic amino acids (K112 and R252) are dispensable. We hypothesize that these polar amino acids, via post-translational modifications, play a crucial role in the regulation of TMEM165 functionality.

As proposed for yeasts, it is most likely that amino acids of the two conserved motifs constitute the cation binding sites of TMEM165. In such hypothesis, mutations in specific amino acids of the two conserved motifs alter the transport function of TMEM165 by impairing cation affinity or pocket conformation changes.

The other particularity of TMEM165 is its sensitivity to high  $Mn^{2+}$  concentrations. We recently demonstrated that following high  $Mn^{2+}$  exposure, TMEM165 was targeted to lysosomes for its degradation [15]. The targeting molecular mechanism is unclear but recent investigations propose the requirement of Sortilin in the  $Mn^{2+}$  induced degradation of TMEM165 [16]. The  $Mn^{2+}$  sensitivity of the mutated forms of TMEM165 was evaluated. As pointed out for the glycosylation, most of the generated mutated forms of TMEM165 are resistant to  $Mn^{2+}$  exposure and only few are sensitive. Our results demonstrate that the acidic amino acids (E and D) of the first conserved motif are crucial in conferring the  $Mn^{2+}$  sensitivity to TMEM165. The two resistant mutants D251G and S253G of the second motif are insensitive to manganese presumably due to their mislocalization. Another interesting observation deals with the T113G that is also clearly found resistant to Mn exposure while correctly Golgi localized. The roles of these amino acids in the  $Mn^{2+}$  induced degradation mechanism/Golgi subcellular localization are not clear but one can imagine that they are part of a regulatory mechanism that delicately governs the Golgi ion homeostasis.

In conclusion, this paper highlights the importance of the two very conserved regions for the functionality of TMEM165 in Golgi glycosylation, its subcellular Golgi localization and  $Mn^{2+}$  sensitivity.

## Supplementary Material

Refer to Web version on PubMed Central for supplementary material.

## Acknowledgements

This work was supported by grants from Agence Nationale de la Recherche (SOLV-CDG project to F.F.), and EURO-CDG-2 that has received a funding from the European Union's Horizon 2020 research and innovation program under the ERA-NET Cofund action N° 643578. We are also indebted to Dr Dominique Legrand for the Research Federation FRABio (Univ. Lille, CNRS, FR 3688, FRABio, Biochimie Structurale et Fonctionnelle des

Assemblages Biomoléculaires) for providing the scientific and technical environment conducive to achieving this work. We thank the BioImaging Center of Lille, especially Christian Slomianny and Elodie Richard, for the use of the Leica LSM700.

## Abbreviations

<b>CQ</b>	Chloroquine
<b>CDG</b>	Congenital Disorder(s) of Glycosylation
<b>GPP130</b>	Golgi Phosphoprotein 4
<b>ER</b>	Endoplasmic Reticulum
<b>LAMP2</b>	Lysosomal-associated membrane protein 2
<b>Mn</b>	Manganese
<b>Mn<sup>2+</sup></b>	Manganese, ion (2+)
<b>MnCl<sub>2</sub></b>	Manganese (II) chloride tetrahydratex
<b>TMEM165</b>	Transmembrane Protein 165
<b>SPCA1</b>	Secretory-Pathway Ca <sup>2+</sup> -ATPase 1
<b>PAM71</b>	Photosynthesis Affected Mutant 71
<b>UPF</b>	Uncharacterized Protein Family

## References

- [1]. Jaeken J, Péanne R, What is new in CDG? *J. Inherit. Metab. Dis* 40 (2017) 569–586, 10.1007/s10545-017-0050-6. [PubMed: 28484880]
- [2]. Aebi M, Helenius A, Schenk B, Barone R, Fiumara A, Berger EG, Hennet T, Imbach T, Stutz A, Bjursell C, Uller A, Wahlström JG, Briones P, Cardo E, Clayton P, Winchester B, Cormier-Dalre V, de Lonlay P, Cuer M, Dupré T, Seta N, de Koning T, Dorland L, de Loos F, Kupers L, Carbohydrate-deficient glycoprotein syndromes become congenital disorders of glycosylation: an updated nomenclature for CDG. *First International Workshop on CDGS, Glycoconj. J* 16 (1999) 669–671. [PubMed: 11003549]
- [3]. Foulquier F, Amyere M, Jaeken J, Zeevaert R, Schollen E, Race V, Bammens R, Morelle W, Rosnoblet C, Legrand D, Demaegd D, Buist N, Cheillan D, Guffon N, Morsomme P, Annaert W, Freeze HH, Van Schaftingen E, Vikkula M, Matthijs G, TMEM165 deficiency causes a congenital disorder of glycosylation, *Am. J. Hum. Genet* 91 (2012) 15–26, 10.1016/j.ajhg.2012.05.002. [PubMed: 22683087]
- [4]. Marques-da-Silva D, Francisco R, Webster D, dos Reis Ferreira V, Jaeken J, Pulinilkunnit T, Cardiac complications of congenital disorders of glycosylation (CDG): a systematic review of the literature, *J. Inherit. Metab. Dis* 40 (2017) 657–672, 10.1007/s10545-017-0066-y. [PubMed: 28726068]
- [5]. Marques-da-Silva D, dos Reis Ferreira V, Monticelli M, Janeiro P, Videira PA, Witters P, Jaeken J, Cassiman D, Liver involvement in congenital disorders of glycosylation (CDG). A systematic review of the literature, *J. Inherit. Metab. Dis* 40 (2017) 195–207, 10.1007/s10545-016-0012-4. [PubMed: 28108845]
- [6]. Rosnoblet C, Legrand D, Demaegd D, Hacine-Gherbi H, de Bettignies G, Bammens R, Borrego C, Duvet S, Morsomme P, Matthijs G, Foulquier F, Impact of disease-causing mutations on

- TMEM165 subcellular localization, a recently identified protein involved in CDG-II, *Hum. Mol. Genet* 22 (2013) 2914–2928, 10.1093/hmg/ddt146. [PubMed: 23575229]
- [7]. Demaegd D, Colinet A-S, Deschamps A, Morsomme P, Molecular evolution of a novel family of putative calcium transporters, *PLoS One* 9 (2014) e100851, 10.1371/journal.pone.0100851. [PubMed: 24955841]
- [8]. Demaegd D, Foulquier F, Colinet A-S, Gremillon L, Legrand D, Mariot P, Peiter E, Van Schaftingen E, Matthijs G, Morsomme P, Newly characterized Golgi-localized family of proteins is involved in calcium and pH homeostasis in yeast and human cells, *Proc. Natl. Acad. Sci* 110 (2013) 6859–6864. [PubMed: 23569283]
- [9]. Schneider A, Steinberger I, Herdean A, Gandini C, Eisenhut M, Kurz S, Morper A, Hoecker N, Rühle T, Labs M, Flügge UI, Geimer S, Schmidt SB, Husted S, Weber APM, Spetea C, Leister D, The evolutionarily conserved protein PHOTOSYNTHESIS AFFECTED MUTANT71 is required for efficient manganese uptake at the thylakoid membrane in Arabidopsis, *Plant Cell* 2015 (2016) 00812, 10.1105/tpc.15.00812.
- [10]. Potelle S, Morelle W, Dulary E, Duvet S, Vicogne D, Spriet C, Krzewinski-Recchi M-A, Morsomme P, Jaeken J, Matthijs G, De Bettignies G, Foulquier F, Glycosylation abnormalities in Gdt1p/TMEM165 deficient cells result from a defect in Golgi manganese homeostasis, *Hum. Mol. Genet* 25 (2016) 1489–1500, 10.1093/hmg/ddw026. [PubMed: 27008884]
- [11]. Morelle W, Potelle S, Witters P, Wong S, Climer L, Lupashin V, Matthijs G, Gadomski T, Jaeken J, Cassiman D, Morava E, Foulquier F, Galactose supplementation in patients with TMEM165-CDG rescues the glycosylation defects, *J. Clin. Endocrinol. Metab* 102 (2017) 1375–1386, 10.1210/jc.2016-3443. [PubMed: 28323990]
- [12]. Dulary E, Potelle S, Legrand D, Foulquier F, TMEM165 deficiencies in Congenital Disorders of Glycosylation type II (CDG-II): clues and evidences for roles of the protein in Golgi functions and ion homeostasis, *Tissue Cell* 49 (2017) 150–156, 10.1016/j.tice.2016.06.006. [PubMed: 27401145]
- [13]. Thines L, Deschamps A, Sengottaiyan P, Savel O, Stribny J, Morsomme P, The yeast protein Gdt1p transports  $Mn^{2+}$  ions and thereby regulates manganese homeostasis in the Golgi, *J. Biol. Chem* 293 (2018) 8048–8055, 10.1074/jbc.RA118.002324. [PubMed: 29632074]
- [14]. Houdou M, Lebredonchel E, Garat A, Duvet S, Legrand D, Decool V, Klein A, Ouzzine M, Gasnier B, Potelle S, Foulquier F, Involvement of thapsigargin- and cyclopiazonic acid-sensitive pumps in the rescue of TMEM165-associated glycosylation defects by  $Mn^{2+}$ , *FASEB J* 33 (2019) 2669–2679, 10.1096/fj.201800387R. [PubMed: 30307768]
- [15]. Potelle S, Dulary E, Climer L, Duvet S, Morelle W, Vicogne D, Lebredonchel E, Houdou M, Spriet C, Krzewinski-Recchi M-A, Peanne R, Klein A, de Bettignies G, Morsomme P, Matthijs G, Marquardt T, Lupashin V, Foulquier F, Manganese-induced turnover of TMEM165, *Biochem. J* 474 (2017) 1481–1493, 10.1042/BCJ20160910. [PubMed: 28270545]
- [16]. Venkat S, Linstedt AD, Manganese-induced trafficking and turnover of GPP130 is mediated by sortilin, *Mol. Biol. Cell* (2017), 10.1091/mbc.E17-05-0326 mbc.E17-05-0326.

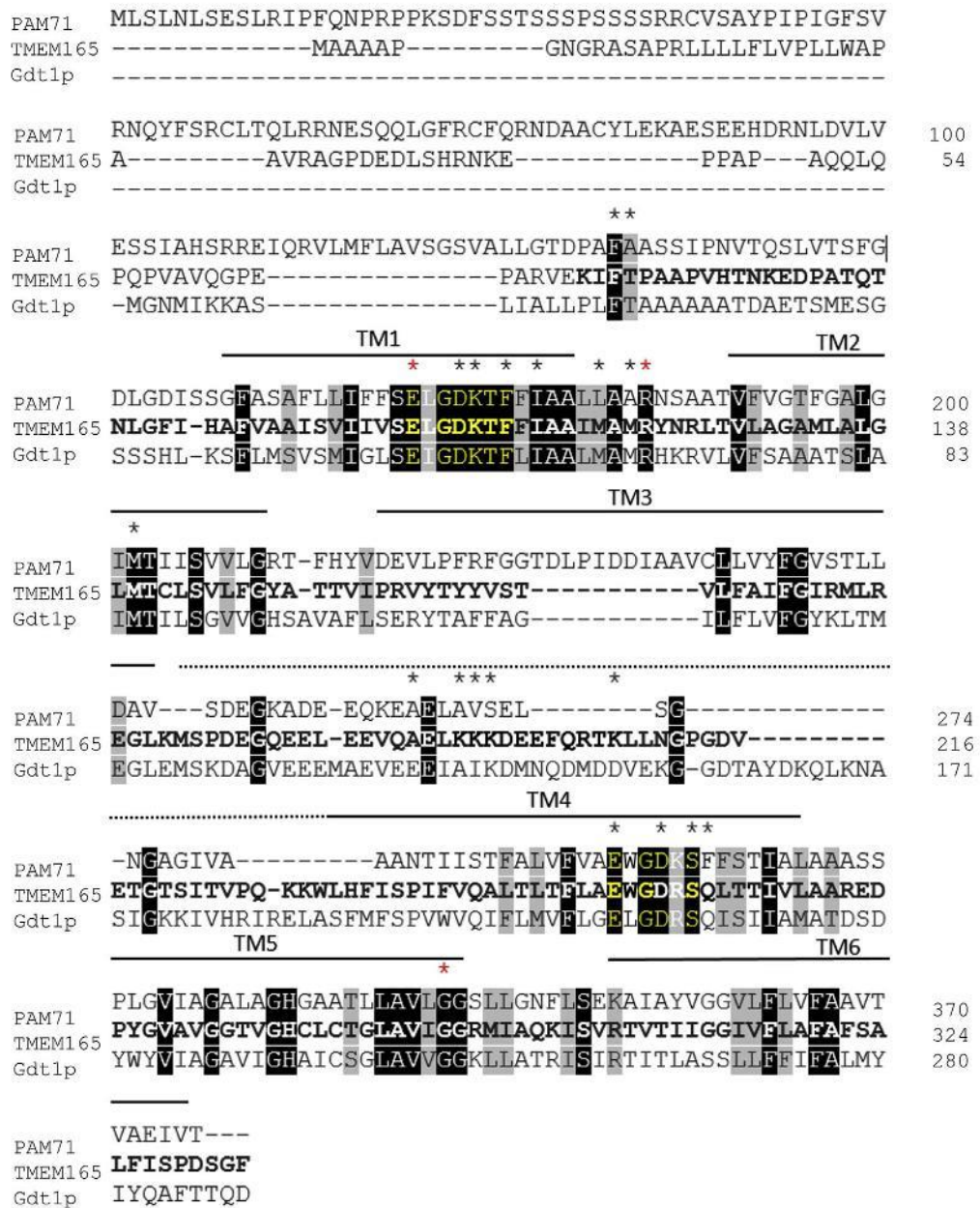
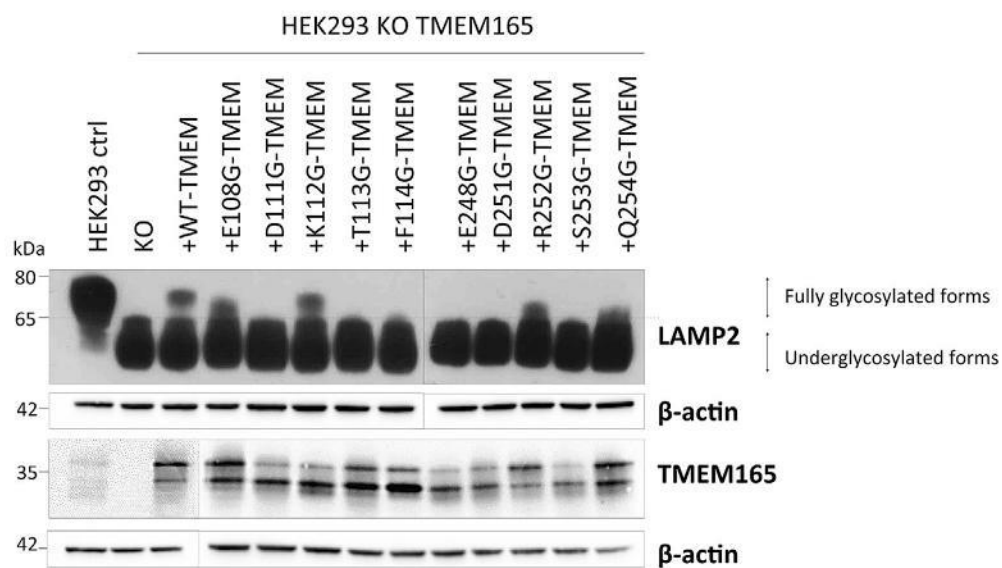


**Fig. 1. Protein sequence alignment of TMEM165 and its orthologs PAM71 from *Arabidopsis thaliana* and Gdt1p from *Saccharomyces cerevisiae*.**

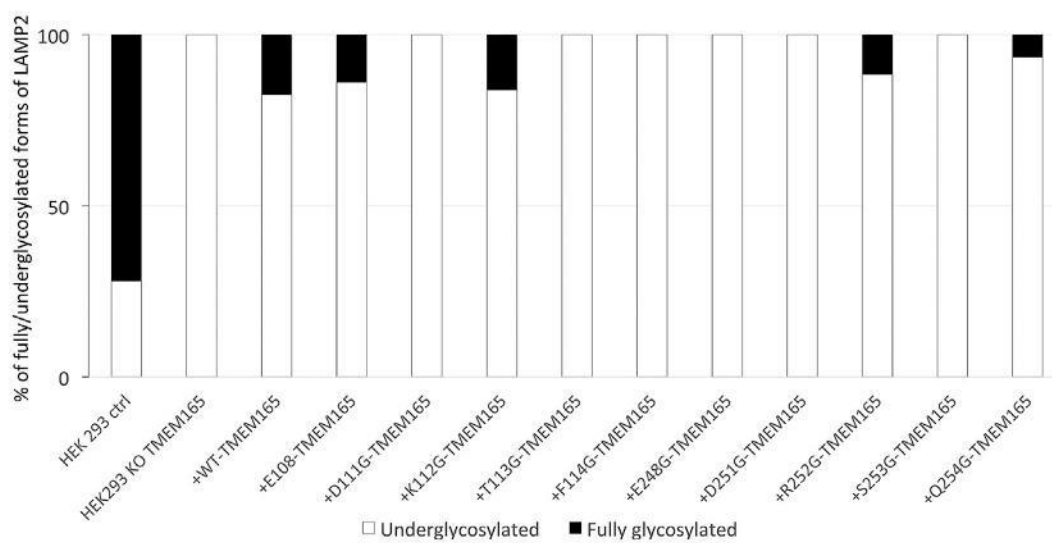
The sequences were found in Uniprot database ([www.uniprot.org](http://www.uniprot.org)) and the protein sequence alignment was generated using Clustal Omega (<https://www.ebi.ac.uk/Tools/msa/clustalo>). Black boxes indicate the amino acid residues that are identical whereas gray boxes show the homologous amino acid residues. The black asterisks indicate the position of the generated mutated amino acids. The red asterisks indicate the mutated amino acids found in TMEM165-CDG patients' proteins. The bold characters correspond to the amino acid residues that are found conserved in the mammalian TMEM165 sequence (SwissProt Database) using the Cobalt-NCBI multiple alignment tool (NCBI). Conserved domains (motif 1 and 2) are highlighted in yellow. Black horizontal bars on the top of the sequences

indicate the amino acids within the predictive transmembrane domains (TMHMM v2.0 server tool). The dotted line indicates the cytosolic central loop.

A.



B.



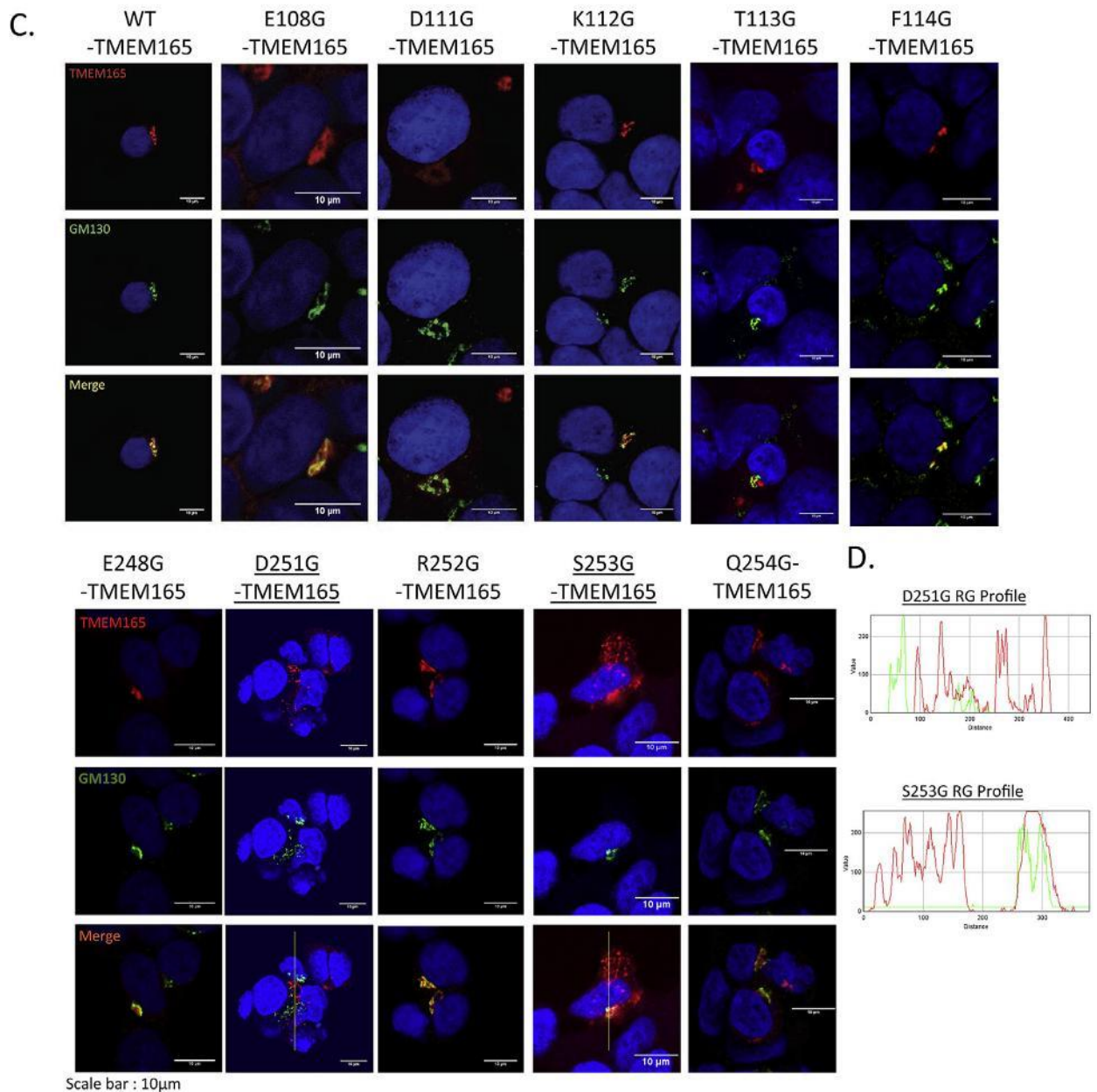


**Fig. 2. LAMP2 glycosylation profile after TMEM165 mutants transfection.**

HEK293T KO TMEM165 cells were transfected with empty-vector, wild-type or TMEM165 constructs. Total cells lysates were obtained, subjected to SDS-PAGE, Western blot was performed with the respective antibodies. **A.** LAMP2 and TMEM165 profiles obtained 24 h after transfection. **B.** Ratio of fully glycosylated forms of LAMP2 (percentage of fully glycosylated forms versus the total LAMP2). **C.** Immunofluorescence analysis of the expression and localization of TMEM165 in transfected cells with mutated forms of TMEM165 in conserved amino-acids. (GM130 = Golgi marker) **D.** Illustration of red and green fluorescence merge with RGB Profiler (ImageJ Fiji®).

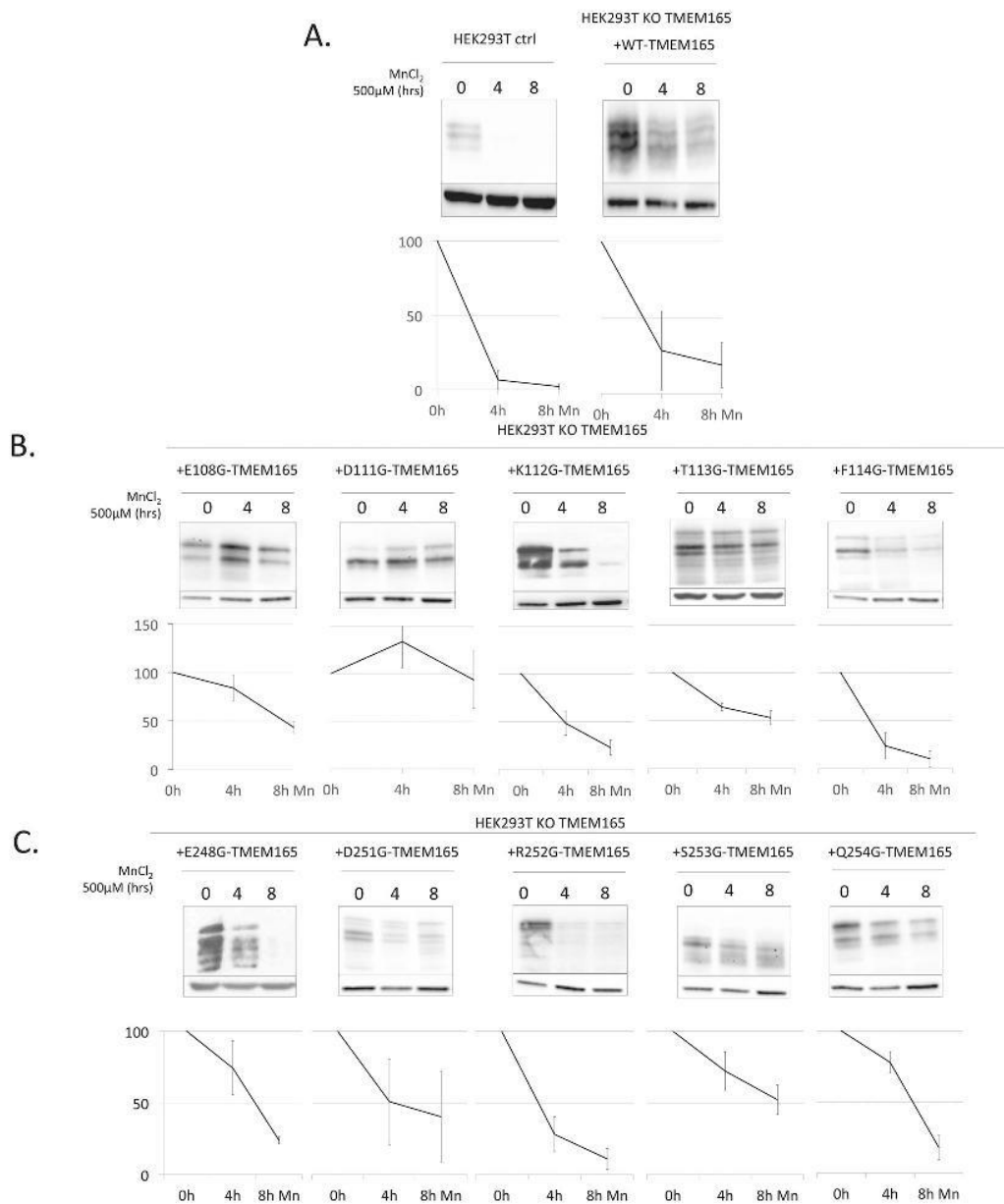
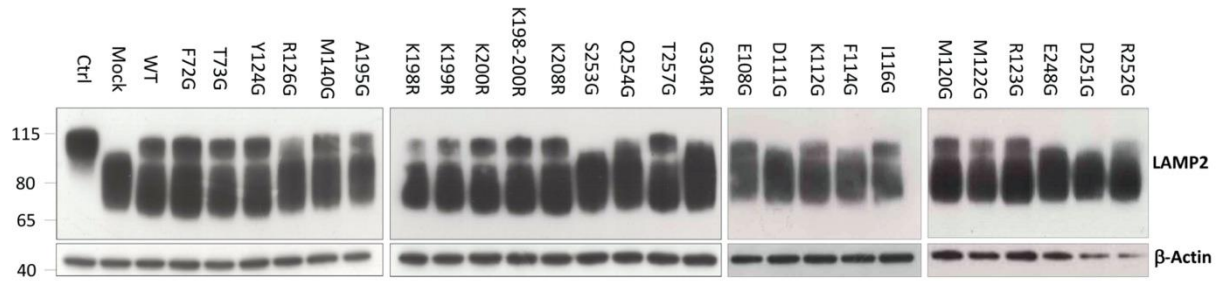


**Fig. 3. Sensitivity of TMEM165 mutants to manganese exposure.**

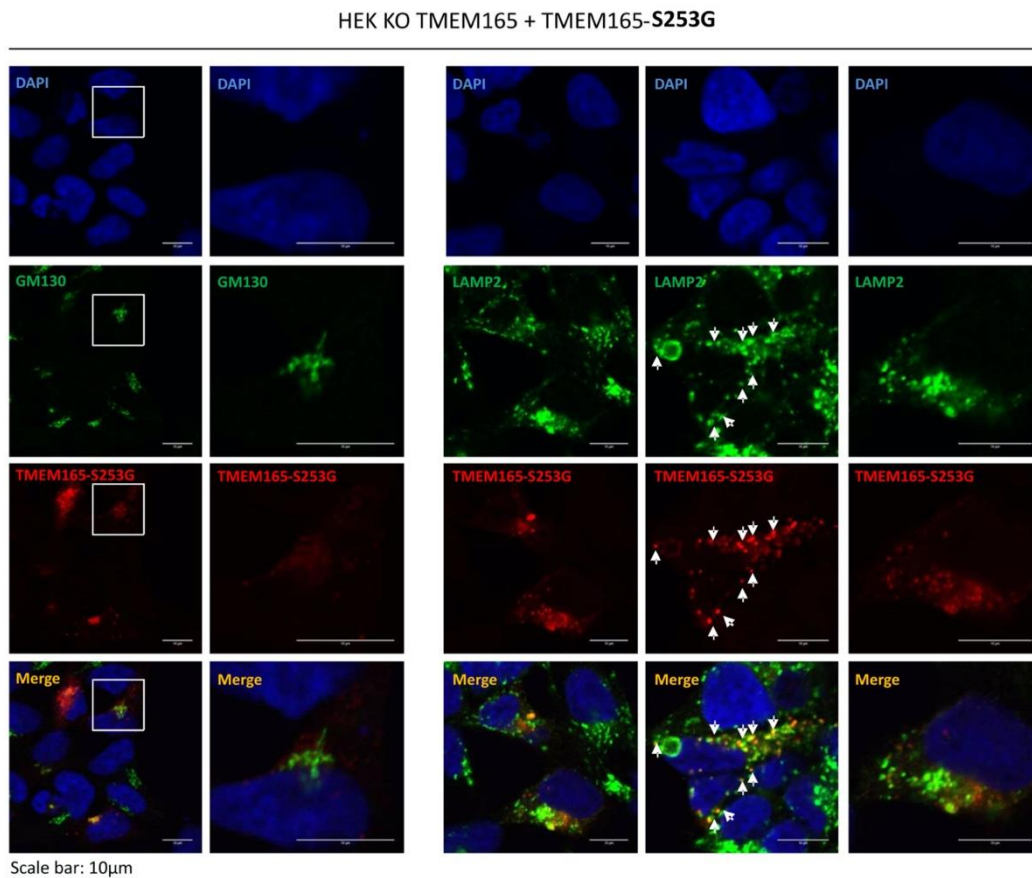
TMEM165 expression in cells transfected with transfected cells forms of TMEM165 in the conserved sequences with or without manganese (N ≥ 3) **A.** In control cells and transfected cells with WT-TMEM165. **B.** In the cytosolic E-x-G-D-K-[TF] motif. **C.** In the luminal E-x-G-D-R-[SQ] motif. Relative quantification of TMEM165 degradation at 4 and 8 h manganese treatment below each respective Western blot.

Supp. Fig. 1



**Supplementary figure 1:** HEK293T KO TMEM165 cells were transfected with empty-vector, wild-type or TMEM165 constructs. Total cell lysates were obtained, subjected to SDS-PAGE, Western blot was performed with the respective antibodies. **A.** LAMP2 profiles were obtained 24 h after transfection.

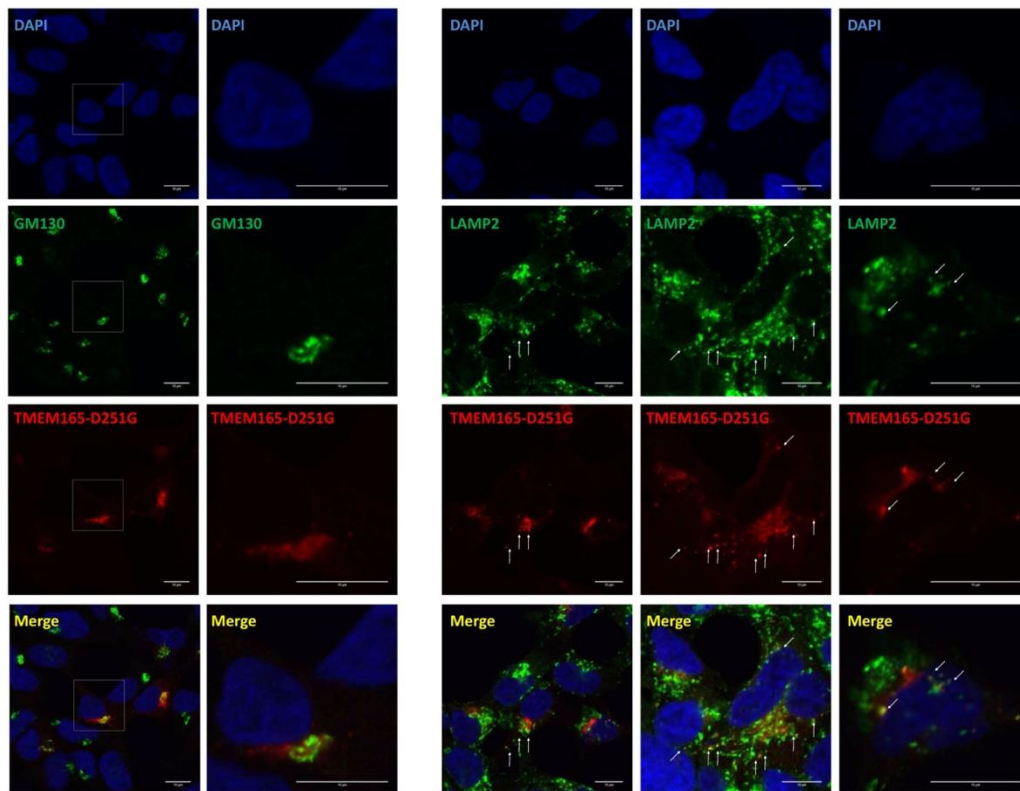
Supp. Fig. 2A



**Supplementary figure 2A. Subcellular localization of S253G-TMEM165.** Localization of S253G-TMEM165 mutants and LAMP2 by immunofluorescence analysis. HEK293T cells were fixed and labeled with antibodies against LAMP2 and TMEM165 before confocal microscopy. Nuclei are labeled with DAPI staining. White arrows point co-localization of TMEM165 and LAMP2 in lysosome vesicles.

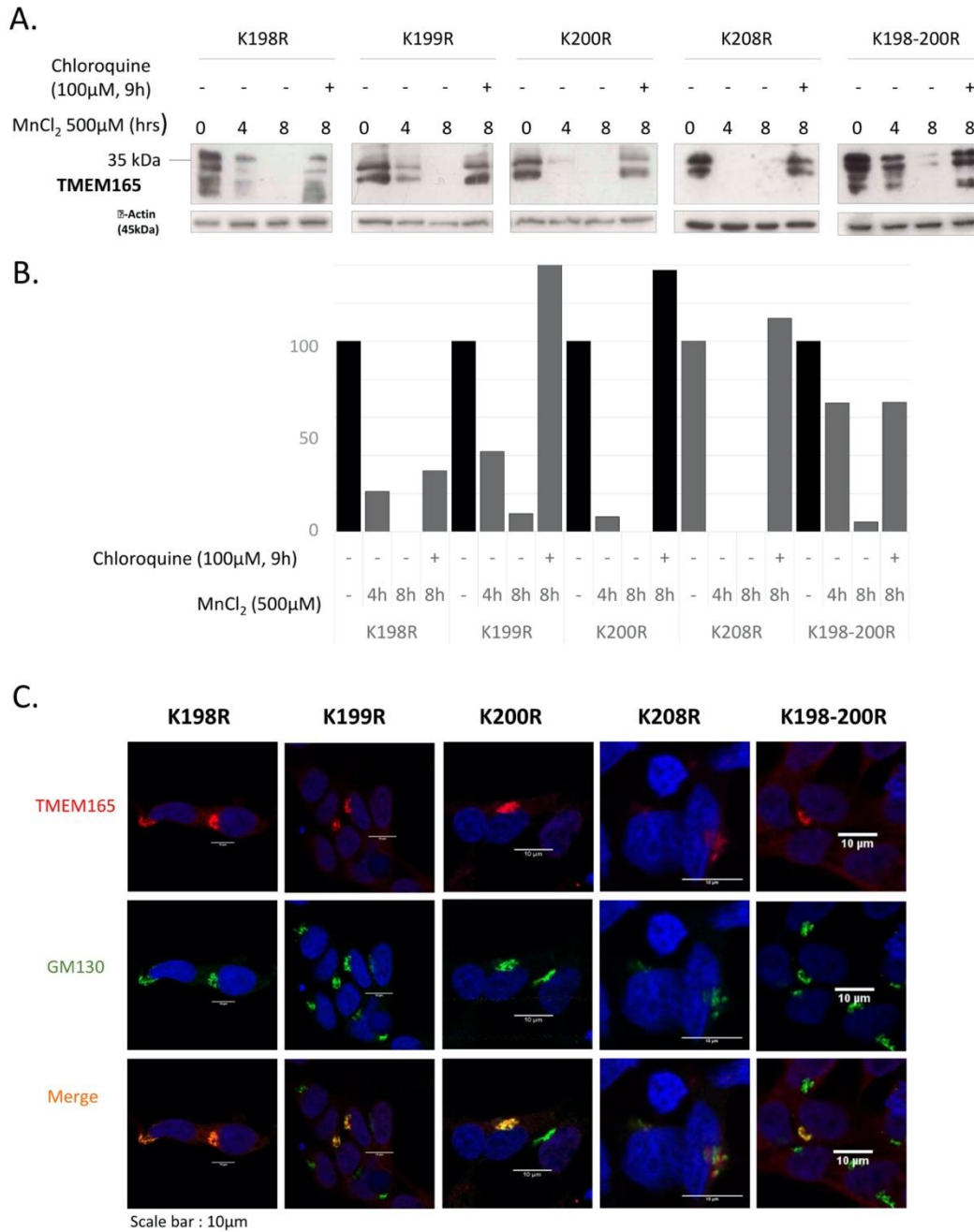
Supp. Fig. 2B

HEK KO TMEM165 + TMEM165-D251G



**Supplementary figure 2B. Subcellular localization of D251G-TMEM165.** Localization of D251G-TMEM165 mutants and LAMP2 by immunofluorescence analysis. HEK293T cells were fixed and labeled with antibodies against LAMP2 and TMEM165 before confocal microscopy. Nuclei are labeled with DAPI staining. White arrows point co-localization of TMEM165 and LAMP2 in lysosome vesicles.

Supp. Fig. 3



**Supplementary figure 3. Effect of chloroquine (CQ) on manganese-induced degradation of lysine mutated forms of TMEM165.** **A.** TMEM165 KO HEK293T cells transfected with K198R, K199R, K200R, K2008R, K199-200R mutants. Cells were incubated with 500 µM of MnCl<sub>2</sub> for 4 h, 8 h and in combination of 8 h of MnCl<sub>2</sub> and CQ 100 µM. Total cell lysates were prepared, subjected to SDS-PAGE and Western blot with TMEM165 antibodies. Black bars indicate percentage of TMEM165 without any treatment. Gray bars indicate percentage of TMEM165 left after 500 µM of MnCl<sub>2</sub> for 4 h, 8 h or a combination of 8 h of MnCl<sub>2</sub> and CQ 100 µM with 1 h of CQ pretreatment. **B.** Quantification of TMEM165 protein expression with or without treatments mentioned above. **C.** Localization of lysine residues TMEM165 mutants by immunofluorescence experiments.

### 3. Conclusion and Discussion

In this study, we first showed that (i) mutations of specific conserved amino acids lead to the loss of function of TMEM165 in glycosylation; (ii) these amino acids are more likely to be localized in the two signature motifs of the UPF0016 family, (iii) most of these amino acids were also shown to be crucial for the manganese-induced degradation of TMEM165 (**figure 31**).

★ Mutation

★ Mutant unable to restore glycosylation

★ Mutant with a partial resistance to manganese

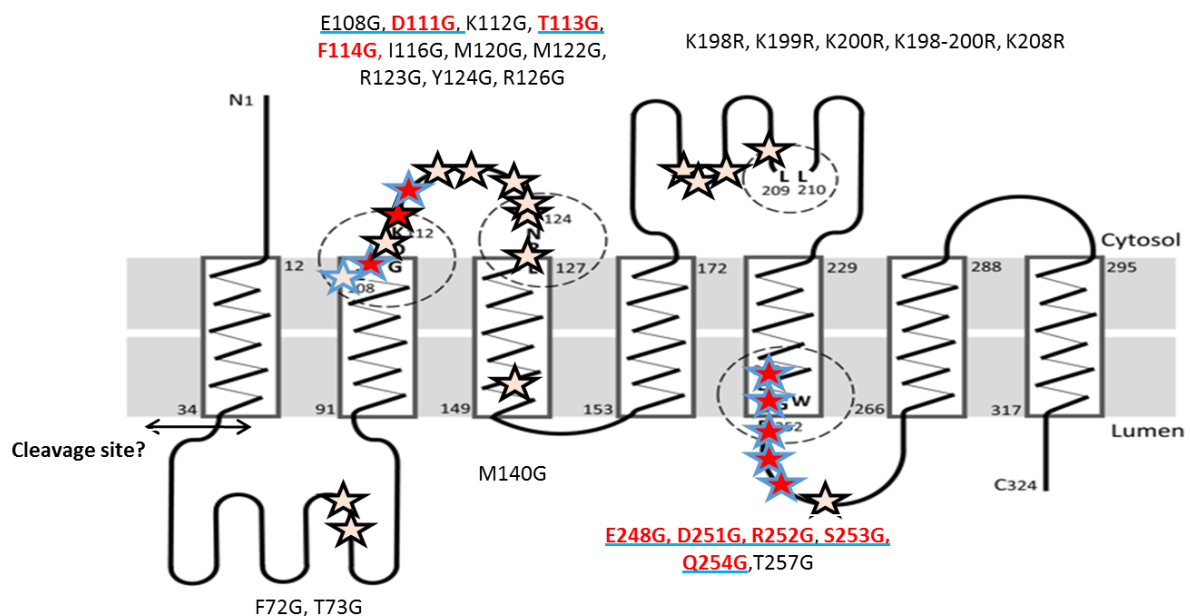


**Figure 31. Summary of the localization of TMEM165 amino acids essential in the function in glycosylation and manganese sensitivity**

This cartography of TMEM165 was essential to delineate the regions implied in the different aspects of TMEM165 regulation.

#### Molecular mechanisms of TMEM165 Mn<sup>2+</sup>-induced degradation.

Although the observation of high sensitivity of TMEM165 to extracellular Mn<sup>2+</sup> exposure was obvious, the molecular mechanisms involved are absolutely not depicted. In order to tackle this point, we knockdown proteins involved in the vesicular trafficking such as Rab proteins (cf chapter 2 §2.2). By means of siRNA, our research group previously showed that TMEM165 degradation was neither Rab5 nor Rab7 dependent (data not shown).

The possible degradation of TMEM165 by the proteasome through monoubiquitylation of lysine residues was tested, four lysine residues of the cytosolic acidic loop were mutated (**Supplementary figure 3, article [1]**). No difference was observed. Another Golgi-localized protein, Golgi Phosphoprotein 30 (GPP130), presents a similar manganese-induced degradation (Mukhopadhyay et al., 2010). It was first hypothesized that GPP130 and TMEM165 had a common degradation pathway. Lindsted research group investigated the Mn<sup>2+</sup>-induced GPP130 degradation and demonstrated the involvement of two proteins: ARF Binding Protein 1 (GGA1) and Sortilin (Venkat and Lindstedt, 2017). They showed that sortilin was involved in the Mn<sup>2+</sup> induced degradation TMEM165 mechanisms.

To reproduce these results, we first used a GGA1 dominant-negative mutant that inhibits the recruitment of clathrin. By using this tool, we showed that the Mn<sup>2+</sup>-induced degradation of TMEM165 was not GGA1-dependent and hence not clathrin-mediated. In **figure 32** and after the transfection of a GGA1 DN GFP form, no difference is observed on the Mn<sup>2+</sup>-induced TMEM165 degradation. Immunofluorescence microscopy confirmed the western blot result.

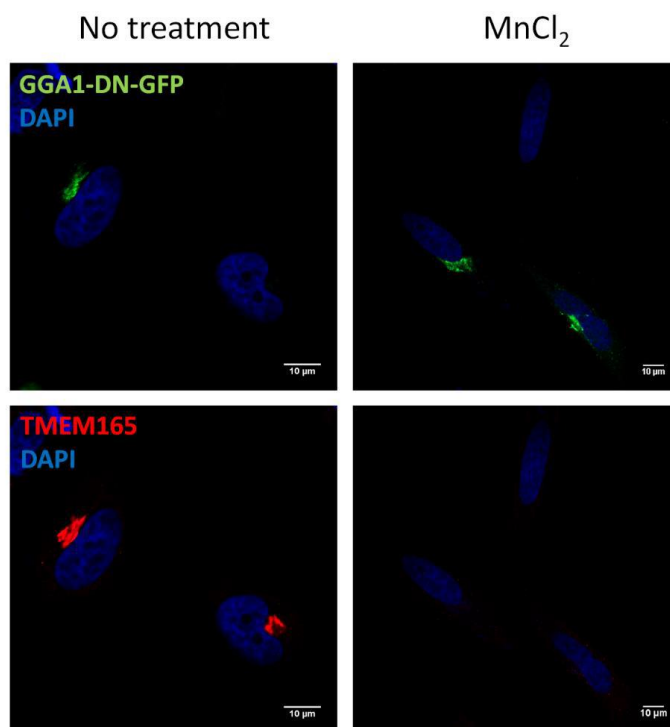
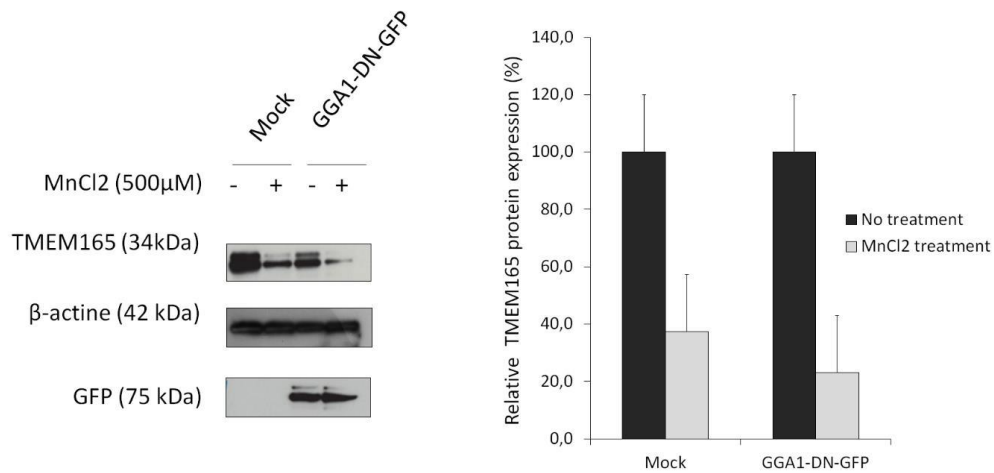


**Figure 32. Effect of dominant-negative GGA1 on Mn-induced TMEM165 degradation** HeLa cells were transfected with pEGFP-C2 GGA1 encoding dominant-negative mutant GGA1. Manganese treatment was conducted with MnCl<sub>2</sub> 500  $\mu$ M for 4 hours, after 36 hours post-transfection. **A.** Western blot and quantification of TMEM165, GFP and actin expression. **B.** Immunofluorescence analysis by confocal microscopy of the experiment described above.

As GGA1 binds to sortilin in the degradation process of GPP130, we then analyzed the influence of the knockout of sortilin on TMEM165 manganese-induced degradation (**figure 32**).

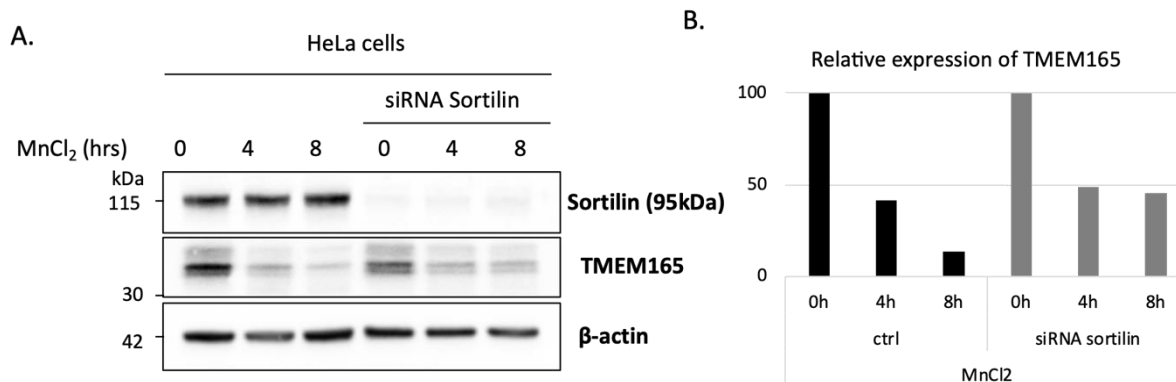


**Figure 33. Effect of the knockout of Sortilin on TMEM165 manganese-induced degradation**  
 A. Expression of Sortilin, TMEM165, and actin in the presence or the absence of MnCl<sub>2</sub> 500 μM for 4 and 8 hours in HeLa cells with or without silencing of Sortilin by siRNA. B. Quantification of the relative expression of TMEM165 in the indicated conditions.

As shown in **figure 33**, the knockout of Sortilin protein is not sufficient to prevent the manganese-induced degradation of TMEM165. Beside a correct knockdown of sortilin, we were unable to reproduce the results obtained by Venkat and Linstedt.

Compared to GPP130, TMEM165 is rapidly degraded in the presence of high manganese concentrations; this difference suggests that the degradation pathway of TMEM165 may be completely different from the one involved for GPP130.

Altogether, these data suggest that lysosomal TMEM165 targeting under Mn<sup>2+</sup> exposure may involve a completely new mechanism with unidentified intermediary proteins. In the near future, our aim would be to unveil the molecular pathway in charge of TMEM165 manganese-induced degradation. In this publication, we have delineated the essential amino acid sequences for TMEM165 degradation; a further study of these specific mutants would be a key to achieve this goal.

#### Can we link the function of TMEM165 to its Mn<sup>2+</sup> sensitivity?

Interestingly, the existence of a link between the function and the stability of TMEM165 is proposed, as amino acids involved in the glycosylation function of TMEM165 present the strongest resistance to manganese-induced degradation. If we compare the proportion of fully glycosylated forms of LAMP2 restored after transfection of each mutant in KO TMEM165 HEK293 cells, to the level of degradation of TMEM165 after a manganese treatment during 8 hours, a link can be hypothesized. The inability to restore glycosylation mirrors manganese resistance.

As seen in figure 30, both the cytosolic motif 1 and the luminal motif 2 are responsible for TMEM165 function and  $Mn^{2+}$  sensitivity. How could we explain this relation? In physiological conditions, we could hypothesize that the functionality of TMEM165 is linked to its lysosomal degradation. The mechanism behind this is not known so far but is certainly based on conformational changes (Figure 33). We can imagine that the ion transport requires pocket conformational changes that make the protein competent for lysosomal targeting and degradation. In such conditions,  $Mn^{2+}$  pressure favors the conformation compatible for the lysosomal degradation of TMEM165. Based on this model, in the case where TMEM165 is mutated in amino acids implied in the ion channel, the protein is not functional, the conformation change cannot be achieved, and the protein become resistant to a targeting to the lysosome. Sortilin could be the protein recognizing these conformational changes and promote TMEM165 for lysosomal targeting.

This model is schematized **figure 34**.

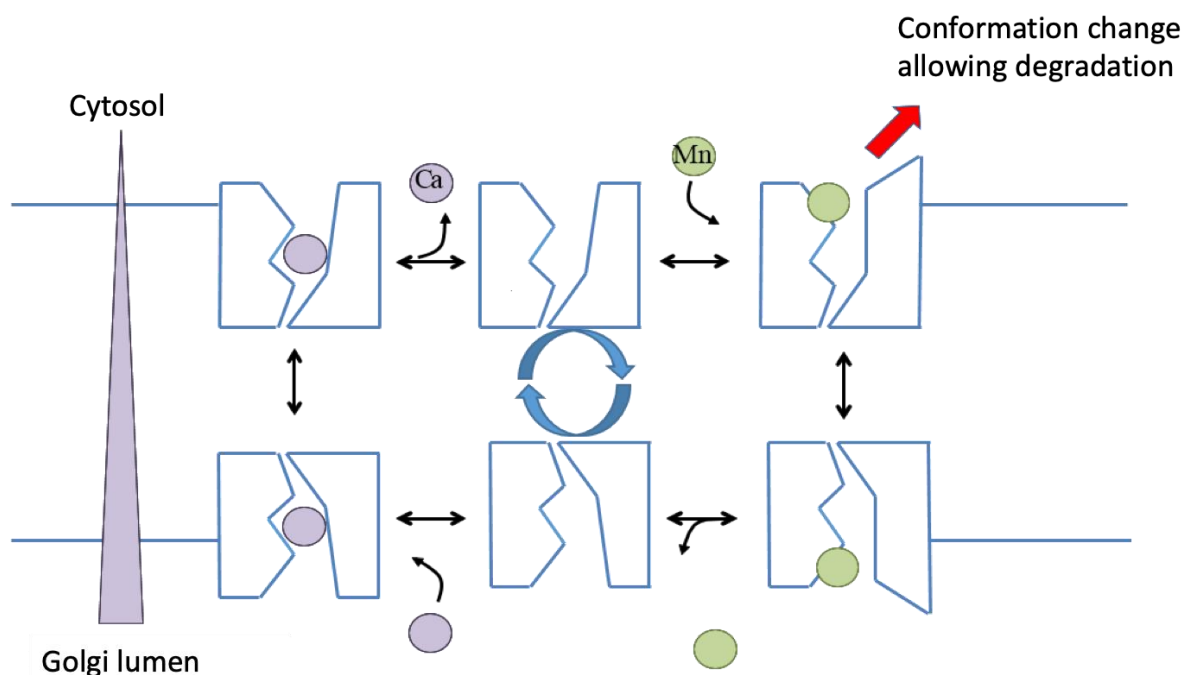


**Figure 34: Model of the link between TMEM165 function, conformation change and degradation.**

This article is the first evidence of a link between TMEM165 function and manganese sensitivity. A question remains, why TMEM165 as to be degradable to be functional? And

which system related to the Golgi apparatus is responsible for the specific degradation of TMEM165?

## [2] Investigating the functional link between TMEM165 and SPCA1

### 2.1 Introduction

The characterization of TMEM165, since its discovery, has been made along with another Golgi membrane cation transporter SPCA1. SPCA1 and TMEM165 are the only proteins known to import manganese in the Golgi lumen. Curiously, the defects in TMEM165 or in SPCA1 are responsible for extremely different diseases respectively a CDG syndrome and a dermatological disease, this difference of expression remains unexplained.

In 2018, yeast studies demonstrated that  $\text{Ca}^{2+}$  and  $\text{Mn}^{2+}$  were both able to restore the glycosylation deficiency induced by the knockout of Pmr1, the ortholog of SPCA1. Only manganese could rescue a glycosylation defect induced by a double KO for Gdt1 (yeast ortholog of TMEM165) and Pmr1 in yeast (Dulary, Yu, Houdou et al., 2018). A mutated strain of Pmr1 able only to import calcium (Pmr1pQ783A) was used to show the requirement of  $\text{Mn}^{2+}$  import in the Golgi lumen by Gdt1 to restore glycosylation. This led to a model in which Gdt1 would be a  $\text{Mn}^{2+}/\text{Ca}^{2+}$  antiport transporter and a “leak channel” of Pmr1 (**figure 35**).

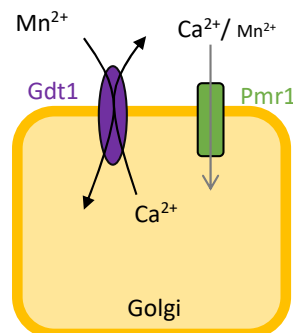


**Figure 35. Hypothetical function of Pmr1 and Gdt1 in the yeast model**

This potential evidence of a functional link between these two proteins in yeast conducted our research group to approach the link between human TMEM165 and SPCA1. To achieve this, we first used KO SPCA1 HAP1 cells to study TMEM165 expression. Then, TMEM165 expression was studied in stable cell lines expressing different forms of SPCA1, (i) one with the ability to import only calcium (G309C-SPCA1), (ii) one inactive form (D742Y-SPCA1), and a WT-form (Hoffmann et al., 2017). Finally, a mutated form of SPCA1 with the ability to import manganese only was stably expressed in KO SPCA1 HAP1 was tested (**figure 36**).

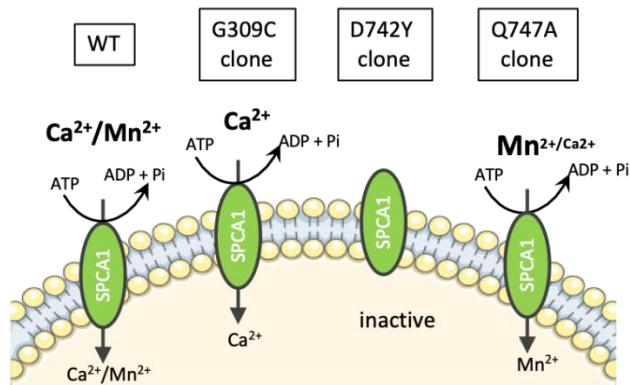


Figure 36. Function of the different forms of SPCA1 used on the following publication

## 2.2 Publication

Research Article

# Investigating the functional link between TMEM165 and SPCA1

Elodie Lebreton<sup>1,2,\*</sup>, Marine Houdou<sup>1,\*</sup>, Hans-Heinrich Hoffmann<sup>3</sup>, Kateryna Kondratska<sup>4,5</sup>, Marie-Ange Krzewinski<sup>1</sup>, Dorothée Vicogne<sup>1</sup>, Charles M. Rice<sup>3</sup>, André Klein<sup>1,2</sup> and François Foulquier<sup>1</sup>

<sup>1</sup>Univ. Lille, CNRS, UMR 8576 – UGSF - Unité de Glycobiologie Structurale et Fonctionnelle, F-59000 Lille, France; <sup>2</sup>Univ. Lille, CHU Lille, Centre de Biologie et Pathologie, UAM de glycopathologies, Centre de Biologie et Pathologie, F-59000 Lille, France; <sup>3</sup>Laboratory of Virology and Infectious Disease, The Rockefeller University, New York, NY 10065, U.S.A; <sup>4</sup>Univ. Lille, INSERM U1003 - PHYCEL - Physiology Cellulaire, F-59000 Lille, France; <sup>5</sup>Laboratory of Excellence, Ion Channels Science and Therapeutics, Université de Lille, Villeneuve d'Ascq, France

**Correspondence:** François Foulquier (francois.foulquier@univ-lille.fr)

TMEM165 was highlighted in 2012 as the first member of the Uncharacterized Protein Family 0016 (UPF0016) related to human glycosylation diseases. Defects in TMEM165 are associated with strong Golgi glycosylation abnormalities. Our previous work has shown that TMEM165 rapidly degrades with supraphysiological manganese supplementation. In this paper, we establish a functional link between TMEM165 and SPCA1, the Golgi  $\text{Ca}^{2+}/\text{Mn}^{2+}$  P-type ATPase pump. A nearly complete loss of TMEM165 was observed in SPCA1-deficient Hap1 cells. We demonstrate that TMEM165 was constitutively degraded in lysosomes in the absence of SPCA1. Complementation studies showed that TMEM165 abundance was directly dependent on SPCA1's function and more specifically its capacity to pump  $\text{Mn}^{2+}$  from the cytosol into the Golgi lumen. Among SPCA1 mutants that differentially impair  $\text{Mn}^{2+}$  and  $\text{Ca}^{2+}$  transport, only the Q747A mutant that favors  $\text{Mn}^{2+}$  pumping rescues the abundance and Golgi subcellular localization of TMEM165. Interestingly, the overexpression of SERCA2b also rescues the expression of TMEM165. Finally, this paper highlights that TMEM165 expression is linked to the function of SPCA1.

## Introduction

Organelle ionic homeostasis within the secretory pathway is regulated by  $\text{Ca}^{2+}$  and  $\text{Mn}^{2+}$  ion concentrations through the action of transporters and pumps. Cation homeostasis is known to be crucial for many cellular processes including vesicular fusion events, the secretion of proteins as well as for the activity of Golgi glycosyltransferases and glycosidases [1]. This cation homeostasis stems from a balance between  $\text{Ca}^{2+}$  influx and efflux but its molecular mechanisms have not been completely defined nor have the different actors been identified [2,3]. A major regulator of  $\text{Ca}^{2+}/\text{Mn}^{2+}$  homeostasis in the Golgi compartment is the P-type ATPase SPCA1 encoded by *ATP2C1* [4,5]. While the function of SPCA1 in regulating Golgi  $\text{Ca}^{2+}$  homeostasis has been well documented, less is known about its role in  $\text{Mn}^{2+}$  homeostasis. It has been hypothesized that SPCA1 might play a role in  $\text{Mn}^{2+}$  detoxification given that cytosolic  $\text{Mn}^{2+}$  accumulation [6] is detrimental for many cellular processes, resulting in neurological disorders similar to Parkinson's disease [7]. In 2012, we described TMEM165 as the first member of the Uncharacterized Protein Family 0016 (UPF0016) related to human diseases [8]. TMEM165 is believed to be a  $\text{Ca}^{2+}/\text{H}^{+}$  transporter located in the Golgi and in lysosomes, where it participates in the homeostasis of pH and  $\text{Ca}^{2+}$  ion concentration. This protein is highly conserved through evolution and defects in TMEM165 lead to strong Golgi glycosylation abnormalities responsible for a congenital disorder of glycosylation (TMEM165-CDG or CDG-IIk) [9,10]. Interestingly, these defects are completely rescued by  $\text{Mn}^{2+}$  supplementation in the culture medium, suggesting the involvement of TMEM165 in Golgi  $\text{Mn}^{2+}$  homeostasis [11,12]. Similar functions have been observed

\*These authors equally contributed to this work.

Received: 26 June 2019  
Revised: 7 October 2019  
Accepted: 17 October 2019

Accepted Manuscript online:  
17 October 2019  
Version of Record published:  
11 November 2019

for TMEM165 orthologs of plants, bacteria and yeast. In *Arabidopsis thaliana*, PAM71 (photosynthesis affected mutant 71) has been shown to be required for efficient  $Mn^{2+}$  uptake at the thylakoid membrane [13]. In the cyanobacterial model strain *Synechocystis sp.* PCC 6803, the Mnx protein was also determined to be a  $Mn^{2+}$  ion exporter [14]. When expressed in the bacterial model *Lactococcus lactis*, the yeast ortholog of TMEM165 (Gdt1p) was shown to be involved in  $Mn^{2+}$  transport [15]. Interestingly, we also found that TMEM165 is specifically degraded in lysosomes in response to high extracellular  $Mn^{2+}$  concentration, reinforcing the link between this protein and cellular  $Mn^{2+}$  homeostasis [16]. The cellular function of other UPF0016 members is certainly more complex as it has been previously reported that Gdt1p is also involved in  $Ca^{2+}$  transport [16]. Gdt1p might act as  $Ca^{2+}/Mn^{2+}$  antiporter in the Golgi apparatus. However, this model has been challenged by recent results showing that Gdt1p was necessary to retrieve  $H^+$  and Pi products generated during glycosylation in the Golgi lumen [2,17].

Our recent work in yeast suggested a link between Gdt1p and Pmr1p (ortholog of SPCA1 in yeast), the P-type ATPase ortholog of SPCA1 and one of the main  $Ca^{2+}/Mn^{2+}$  pump in the Golgi. We indeed demonstrated that the activity of Gdt1p in Golgi glycosylation maintenance depends on the ion transported by Pmr1p [18].

In this paper, we investigated the functional link between TMEM165 and SPCA1. We show that TMEM165 expression depends on SPCA1 as a lack of SPCA1 led to the complete loss of TMEM165. Complementation studies showed that TMEM165 abundance was directly dependent on the nature of the ion transported by SPCA1.

## Experimental Antibodies

Anti-TMEM165 and anti- $\beta$ -actin antibodies were purchased from Millipore Sigma (Burlington, MA, U.S.A.), anti-LAMP2 antibody from Santa Cruz Biotechnology (Dallas, TX, U.S.A.), anti-GM130 antibody from BD Biosciences (Franklin Lakes, NJ, U.S.A.), anti-SPCA1 from Abnova (Taipei City, Taiwan), anti-TGN46 from Bio-Rad (U.S.A.), anti-SERCA2 antibody was purchased from Millipore (Darmstadt, Germany) and anti-GPP130 (GOLPH4) antibody from Abcam (Cambridge, U.K.). Polyclonal goat anti-rabbit IgG and goat anti-mouse IgG horseradish peroxidase-conjugated were from Dako (Denmark) and donkey anti-sheep IgG horseradish peroxidase-conjugated was purchased from R&D Systems (Minneapolis, U.S.A.). Alexa 488- or Alexa 568-conjugated secondary antibodies were from Molecular Probes (Thermo Fisher Scientific, Waltham, MA, U.S.A.).

## Cell culture, transfection and other reagents

Hap1 cells were kindly provided by Pr C.M. Rice (Laboratory of Virology and Infectious Disease, The Rockefeller University, New York, NY, U.S.A.) [19] and maintained at 37°C in humidity-saturated 5%  $CO_2$  atmosphere in Iscove's modified Dulbecco's medium (IMDM) supplemented with 10% fetal bovine serum. For the complementation studies, SPCA1 isoform 1D was chosen for all experiments, as it has no truncated N- or C-terminus compared with the 1A-F isoforms. When used, MG132 (Sigma) was added for 8 h at the final concentration of 10  $\mu$ M and chloroquine (ICN Biomedicals) for 8 /24 h at 100  $\mu$ M. MG132 efficacy was assessed by Western blot using an anti-ubiquitin mouse antibody. All other chemicals were from Sigma–Aldrich unless otherwise specified.

HeLa cells were maintained in Dulbecco's modified eagle's medium (DMEM) supplemented with 10% FBS, at 37°C in humidity-saturated 5%  $CO_2$  atmosphere. The HeLa SPCA1 KO cells were provided by Dr. Charles Rice (The Rockefeller University) and generated as described in Hoffmann et al., (<https://www.ncbi.nlm.nih.gov/pubmed/29024641>). Transfections were performed using Lipofectamine 2000® (Thermo Scientific) according to the manufacturer's guidelines. Human SERCA2b plasmid (pcDNA3.1+) was purchased from Addgene.

## Vector construction and generation of stable cell line

Q747A-SPCA1 plasmid vector was generated by E-Zyvec® (Lille, France). Hap1 SPCA1 KO cells were transfected in a six-well plate at 70% confluence with SPCA1 (Q747A) plasmid using TurboFectin™ 8.0 (Origene) at a ratio of 4 : 1 ( $\mu$ l TurboFectin: $\mu$ g plasmid) in IMDM supplemented with 10% FBS. Cells were incubated with the lipid–DNA complexes for 24 h and then ten times diluted in culture medium containing 0.5  $\mu$ g/ml puromycin (Gibco Life Technologies) as the selective agent. The medium was changed every 3 days for

12 days, maintaining puromycin pressure at 0.5 µg/ml. Cells were then screened for Q747A-SPCA1 expression via Western blot and immunofluorescence.

### Western blotting

Cells were pelleted and lysed in RIPA Buffer (50 mM Tris-HCl pH 7.9, 120 mM NaCl, 1% NP-40, 1 mM EDTA, 1 mM Na<sub>3</sub>VO<sub>4</sub>, 5 mM NaF) supplemented with a cocktail of protease inhibitors (Roche, Meylan, France) and lysed by ultrasonic treatment for 2 min. The concentration of extracted proteins was determined with the Micro BCA™ Protein Assay Reagent kit (Thermo Fisher Scientific, Waltham, MA U.S.A.). Ten or twenty microgram of total proteins of each sample were dissolved in reducing NuPage® Sample buffer and resolved by MOPS 4–12% Bis-Tris gel (Thermo Fisher Scientific, Waltham, MA, U.S.A.). After transfer with iBlot 2 Dry Blotting System (Thermo Fisher Scientific, Waltham, MA, U.S.A.), nitrocellulose membranes were blocked using TBS (tris buffer saline) containing 0.05% Tween 20 and either 5% (w/v) bovine serum albumin (BSA) or 5% (w/v) non-fat dried milk for at least 1 h. Primary antibodies rabbit anti-TMEM165, mouse anti-SPCA1, mouse anti-LAMP2 and sheep anti-TGN46 were incubated at least 1 h at room temperature (RT) or overnight at 4°C in TBS, 0.05% Tween 20 (TBS-T) and 5% (w/v) BSA or 5% (w/v) non-fat dried milk at respectively, 1 : 3 000, 1 : 4 000 and 1 : 2 000 dilution. Anti-β-actin mouse antibody was used for quantification at 1 : 20 000 in TBS-T and 5% (w/v) non-fat dried milk. All the membranes were washed three times 5 min in TBS-T after the addition of the primary and the secondary antibodies. Either goat anti-rabbit IgG, goat anti-mouse IgG (Dako, Agilent technologies, Santa Clara, U.S.A.) or donkey anti-sheep HRP-conjugated were used as secondary antibodies at a dilution of 1 : 10 000 or 1 : 20 000. Signal was detected using chemiluminescence reagent (Pierce™ Pico Plus Western Blotting Substrate (Thermo Fisher Scientific, Waltham, MA, U.S.A.) on imaging film (GE Healthcare, Buckinghamshire, U.K.) or Camera Fusion® (Vilber Lourmat) and its software.

### Immunofluorescence imaging

Twenty-four hours after transfection, cells were seeded on coverslips, washed once with DPBS+/+ (Dulbecco's phosphate saline buffer with calcium and manganese) fixed with methanol for 10 min or 4% paraformaldehyde (PFA) in 0.1 M sodium phosphate buffer (PBS, pH 7.2) for 30 min at RT, and then washed twice with PBS. Cells fixed with PFA were permeabilized in 0.5% Triton X100 for 15 min. Fixed cells were saturated 1 h in blocking buffer (0.2% gelatin, 2% BSA and 2% fetal bovine serum (Lonza) in PBS) and then incubated with primary antibody diluted at 1 : 100 in blocking buffer for 1 h.

After three washes with PBS, cells were incubated with Alexa 488- or Alexa 568-conjugated secondary antibodies diluted at 1 : 600 in blocking buffer for 1 h. Fifteen minutes of DAPI 1 : 200 in PBS were used to stain cells nuclei. Coverslips were mounted on glass slides with 6 µl of Mowiol. Immunostaining and fluorescent proteins were detected through an inverted Zeiss LSM700 confocal microscope. Data acquisition was done using ZEN pro 2.3 SP1 software (Carl Zeiss GmbH, Jena, Germany) and quantifications were done using ImageJ (Fiji) plugin (National Institutes of Health, Bethesda, MD, U.S.A.; <http://imagej.nih.gov/ij>) developed by the local TisBio (<http://tisbio.wixsite.com/tisbio>) facility.

### qRT-PCR analysis

Total RNA was extracted using NucleoSpin® RNA Plus Kit (Macherey-Nagel) following manufacturer protocol. cDNA was synthesized by reverse transcription. Two microgram of total RNA was reverse transcribed into cDNA at 42°C using random hexamer primers (PerkinElmer) and MuLV reverse transcriptase (PerkinElmer) in a 20 µl final volume. qRT-PCR was performed in triplicate in 96-well plates in a real-time thermal cycler Cfx C1000 (Bio-Rad) using EvaGreen Supermix (Bio-Rad). Primers used for hTMEM165 (forward GGGATTGGCAGTAATTGGAGGA; reverse AGCCGGCCCGGGTCGAGGACCCC); hGAPDH (forward TTCGTCATG-GCTGTGAACCA, reverse CAGTGATGCGCATGGACTGT); hHPRT (forward GGCGTCGTGATTAGTGATGAT, reverse CGAGCAAGACGTTTCAGTCCT).

### Proximity ligation assay (PLA) and microscopy analysis

Duolink® PLA Kit (Sigma-Aldrich) was used with red (DUO92008) detection reagents, anti-mouse MINUS probe (DUO92004) and anti-rabbit PLUS probe (DUO92002). Cells were fixed, blocked and incubated with primary antibodies as for standard immunofluorescence except that the mouse anti-SPCA1 antibody was from Abcam (Cambridge, U.K.) dilution 1 : 50. The protocol was followed according to the manufacturer recommendations. Coverslips were mounted on glass slides with Mounting Medium including DAPI (DUO82040). The

acquisition was made with Zeiss LSM700 confocal microscope. PLA was quantified as the total number of spots was normalized on the number of cells. All the analyses were performed by TisGolgi.

## Results

### TMEM165 expression is altered in SPCA1 KO cells

Our previous work on yeast strongly indicated a potential link between Gdt1p and Pmr1p, the yeast orthologs of the mammalian proteins TMEM165 and SPCA1 [18]. To test this hypothesis in mammalian cells, the expression of TMEM165 was first evaluated in Hap1 cells deficient for SPCA1 by Western blot and immunofluorescence. As shown in Figure 1A, a nearly complete loss of TMEM165 is observed in SPCA1 KO cells compared with control cells. Quantification indicated that the decrease of TMEM165 exceeded 90% (Figure 1B). The lack of TMEM165 was also seen by immunofluorescence where a decrease in Golgi-associated TMEM165 was observed (Figure 1C). As defects in TMEM165 lead to strong Golgi glycosylation abnormalities, we assessed the glycosylation status of LAMP2 and TGN46 by Western blot in WT and SPCA1 KO cells. Surprisingly, there was no change in LAMP2 or TGN46 gel mobility suggesting that the lack of SPCA1 and subsequently TMEM165 did not lead to major glycosylation alterations (Figure 1D).

Interestingly, despite the decrease of TMEM165 in the Golgi, weak peripheral punctate structures were apparent, suggesting that TMEM165 was re-located and potentially targeted for lysosomal degradation in the absence of SPCA1 (data not shown). To address whether TMEM165 is subjected to lysosomal degradation in SPCA1 KO cells, we tested the impact of the lysosomotropic agent chloroquine (CQ) on its cellular abundance by Western blot at different times. As shown in Figure 1E and Supplementary Figure S1A,B, the abundance of TMEM165 was recovered in CQ treated SPCA1 KO cells. Quantification indicated an 80% rescue of TMEM165 levels in SPCA1 KO cells treated with CQ for 24 h (Figure 1F). The lysosomal degradation of TMEM165 was also confirmed by immunofluorescence where co-localization of TMEM165 ( $63 \pm 1\%$ ) with LAMP2 is observed in CQ treated SPCA1 KO cells (Figure 1G). The degradation of TMEM165 in SPCA1 KO cells occurs specifically in lysosomes as we demonstrated the absence of proteasomal degradation by using MG132, a proteasomal inhibitor (Supplementary Figure S1C,D). Altogether these results suggest that lack of SPCA1 leads to lysosomal degradation of TMEM165.

### TMEM165 stability depends on the function of SPCA1

To determine whether the observed instability of TMEM165 was dependent on specific functions of SPCA1, we reconstituted SPCA1 KO Hap1 cells with either SPCA1 WT (isoform 1D) or SPCA1 harboring point mutations that impair its ion transport activities. While G309C blocks primarily  $Mn^{2+}$  pumping, D742Y impairs both  $Ca^{2+}$  and  $Mn^{2+}$  pumping [19]. First, to test the inability of the mutated SPCA1 to import  $Mn^{2+}$  inside the Golgi lumen, the stability of GPP130 was followed under  $Mn^{2+}$  pressure by Western blot. In accordance with the literature [20], we showed that the quantity of GPP130 was reduced when SPCA1 KO Hap1 cells reconstituted with wild-type SPCA1 isoform 1D were cultured in the presence of  $500 \mu M Mn^{2+}$ . A 60% decrease is observed after 2 h  $Mn^{2+}$  treatment in control cells (Figure 2A, quantification not shown). Interestingly, in SPCA1 KO cells and SPCA1 KO HAP1 cells reconstituted with either G309C or D742Y, the  $Mn^{2+}$  induced degradation of GPP130 is either blocked or strongly delayed (Figure 2A, quantification not shown). We can indeed see a slight effect of the  $Mn^{2+}$  induced degradation of GPP130 in G309C-SPCA1 cells where a 40% decrease is observed. Altogether these results demonstrate a severe impairment of the  $Mn^{2+}$  import inside the Golgi lumen when cells are subjected to high  $Mn^{2+}$  exposure. The stability of TMEM165 was then investigated in these cells. While the abundance of TMEM165 was fully recovered in SPCA1 KO cells reconstituted with WT-SPCA1 isoform 1D (Figure 2A,C), the expression of the two mutant constructs (G309C and D742Y) had no effect on TMEM165 abundance (Figure 2A,C). The real-time PCR analysis was also performed and no difference in TMEM165 mRNA expression could be observed (Supplementary Figure S1E). We then analyzed the subcellular localization of TMEM165 in SPCA1 KO cells complemented with the different SPCA1 constructs (Figure 2C). Only the expression of WT-SPCA1 isoform 1D rescued the Golgi subcellular localization of TMEM165, while expression of the mutated forms of SPCA1 had no effect (Figure 2C). The glycosylation status of LAMP2 and TGN46 was assessed by Western blot in reconstituted SPCA1 KO cells and no defects were observed in their gel mobility (Supplementary Figure S1F).

We then wondered whether CQ might rescue TMEM165 levels in SPCA1 KO cells. As shown in Figure 3, levels of TMEM165 were restored in CQ treated cells. As in SPCA1 KO cells treated with CQ (Figure 1F),

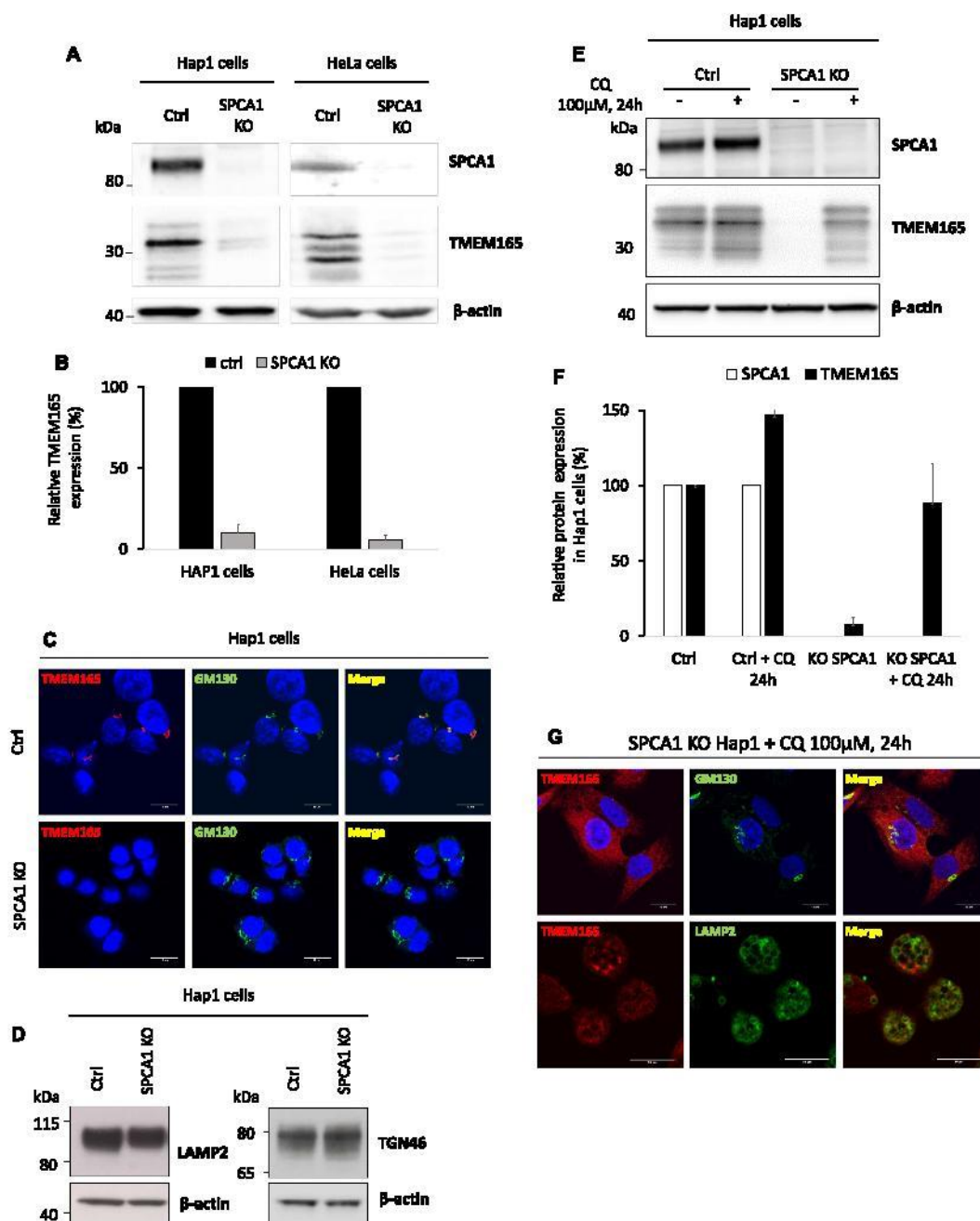


**Figure 1. TMEM165 expression in SPCA1 KO cells.**

(A) Expression of TMEM165 and SPCA1 in Hap1 and HeLa control cells versus SPCA1 KO cells. Total cell lysates were prepared, subjected to SDS-PAGE and Western blot with the indicated antibodies. (B) Quantification of TMEM165 protein expression ( $N = 3$ ) in Hap1 and HeLa control cells versus SPCA1 KO cells. (C) Subcellular localization and abundance of TMEM165 in Hap1 control and SPCA1 KO cells. (D) Expression of LAMP2 and TGN46 in Hap1 control cells versus SPCA1 KO cells. (E) Expression of TMEM165 and SPCA1 in Hap1 control cells versus SPCA1 KO cells with or without chloroquine (CQ) treatment (100  $\mu$ M, 24 h). (F) Quantification of TMEM165 and SPCA1 proteins expression ( $N = 3$ ) in Hap1 control and SPCA1 KO cells. (G) Subcellular localization and abundance of TMEM165 in Hap1 control and SPCA1 KO cells with CQ treatment (100  $\mu$ M, 24 h). LAMP2 is used as a lysosomal marker and nuclei are stained with DAPI staining (blue). Scale bars, 10  $\mu$ m.

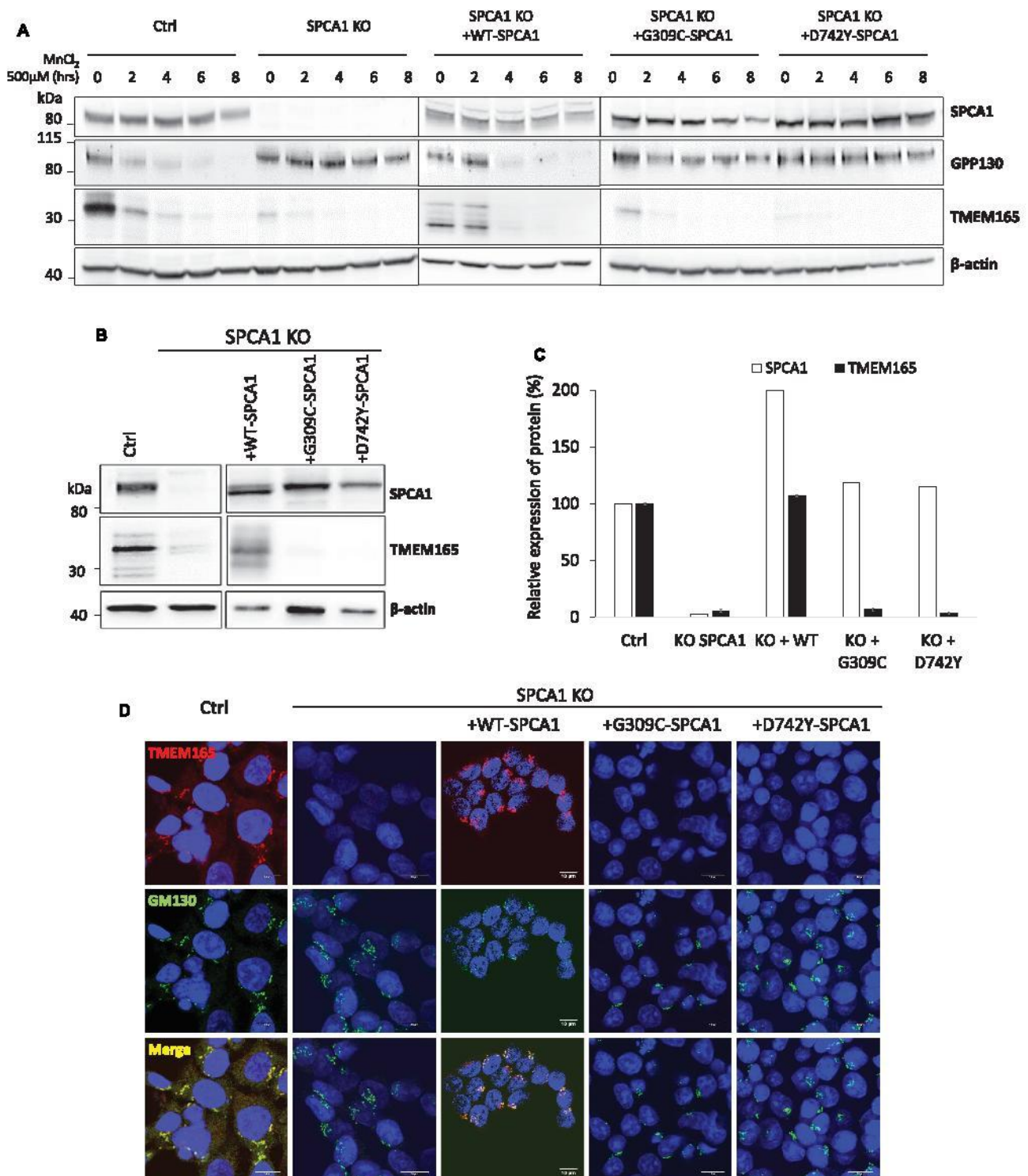


**Figure 2. TMEM165 expression in complemented Hap1 SPCA1 KO cells.**

(A) Expression of TMEM165, GPP130 and SPCA1 in Hap1 SPCA1 KO cells complemented with WT-SPCA1 and mutated SPCA1 constructs: G309C-SPCA1 and D742Y-SPCA1. Total cell lysates were prepared, subjected to SDS-PAGE and Western blot with the indicated antibodies. (B) Expression of TMEM165 and SPCA1 in Hap1 SPCA1 KO cells complemented with WT-SPCA1 and mutated SPCA1 constructs: G309C-SPCA1 and D742Y-SPCA1. Total cell lysates were prepared, subjected to SDS-PAGE and Western blot with the indicated antibodies. (C) Quantification of TMEM165 and SPCA1 proteins expression ( $N=3$ ). (D) Subcellular localization and abundance of TMEM165 in Hap1 SPCA1 KO cells complemented with WT-SPCA1, G309C-SPCA1 and D742Y-SPCA1. GM130 is used as Golgi marker and nuclei are stained with DAPI staining (blue).

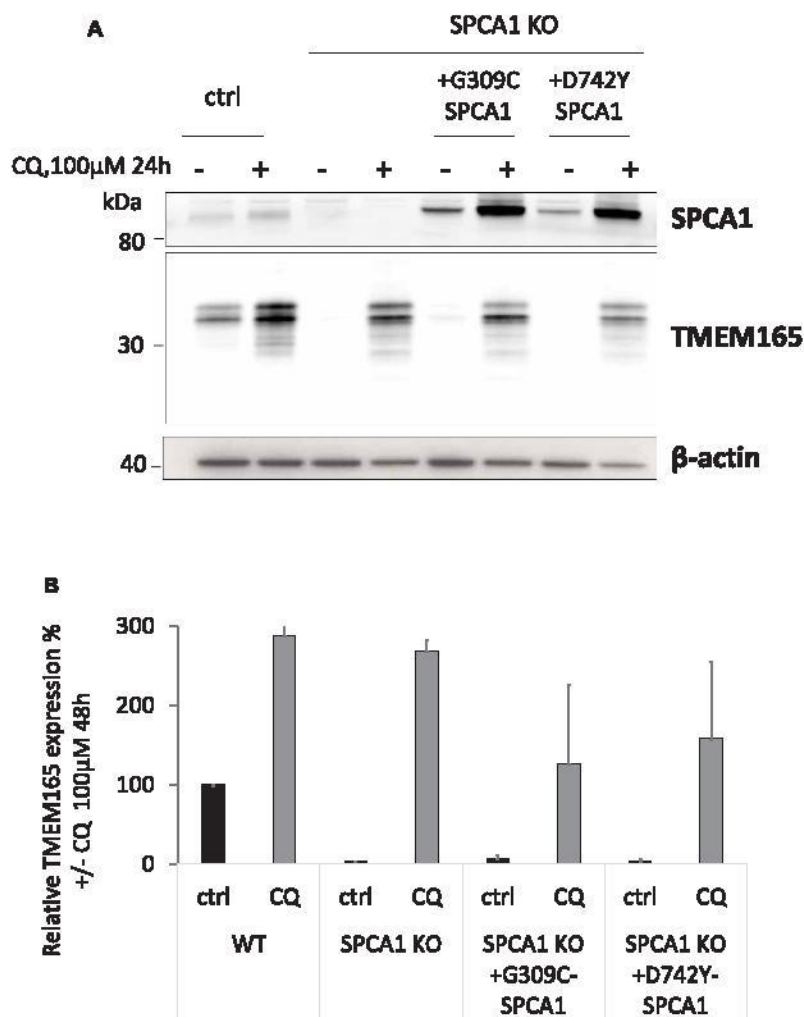


**Figure 3. Effect of chloroquine (CQ) on TMEM165 expression in complemented Hap1 SPCA1 KO cells.**

(A) Expression of TMEM165 and SPCA1 in Hap1 control and SPCA1 KO cells and KO cells complemented with G309C-SPCA1 and D742Y-SPCA1, with or without chloroquine (CQ) treatment (100 µM, 24 h). (B) Quantification of TMEM165 protein expression in Hap1 control and SPCA1 KO cells and KO cells complemented with G309C-SPCA1 and D742Y-SPCA1, with or without chloroquine (CQ) treatment (100 µM, 24 h).

lysosomal subcellular localization of TMEM165 was observed after CQ treatment in all complemented SPCA1 KO Hap1 cells (data not shown). These results demonstrate that the level and subcellular Golgi localization of TMEM165 is not dependent on the Ca<sup>2+</sup> transport function of SPCA1 or its presence.

### TMEM165 stability depends on the Mn<sup>2+</sup> pumping function of SPCA1

Our previous results suggest that the stability of TMEM165 is dependent on SPCA1's ion transport function. It has been observed that TMEM165 and Gdt1p are degraded in response to high manganese concentration. We reason that SPCA1 mutants unable to transport Mn<sup>2+</sup> cause a Mn<sup>2+</sup> build-up and therefore TMEM165 degradation. This result converges with the observation that TMEM165 and Gdt1p are degraded in response to high Mn<sup>2+</sup> concentrations [20,21]. When cells were cultured in the presence of high Mn<sup>2+</sup>, a Mn-induced lysosomal degradation of TMEM165 was observed. To confirm this point, we took advantage of the Q747A-SPCA1 mutant identified to favor Mn<sup>2+</sup> transport [22]. Transient expression experiments were first performed in Hap1 SPCA1 KO cells (Figure 4A). As shown in Figure 4A, the transient expression of Q747A-SPCA1 fully rescues the abundance and the Golgi subcellular localization of TMEM165. We also observed co-localization between

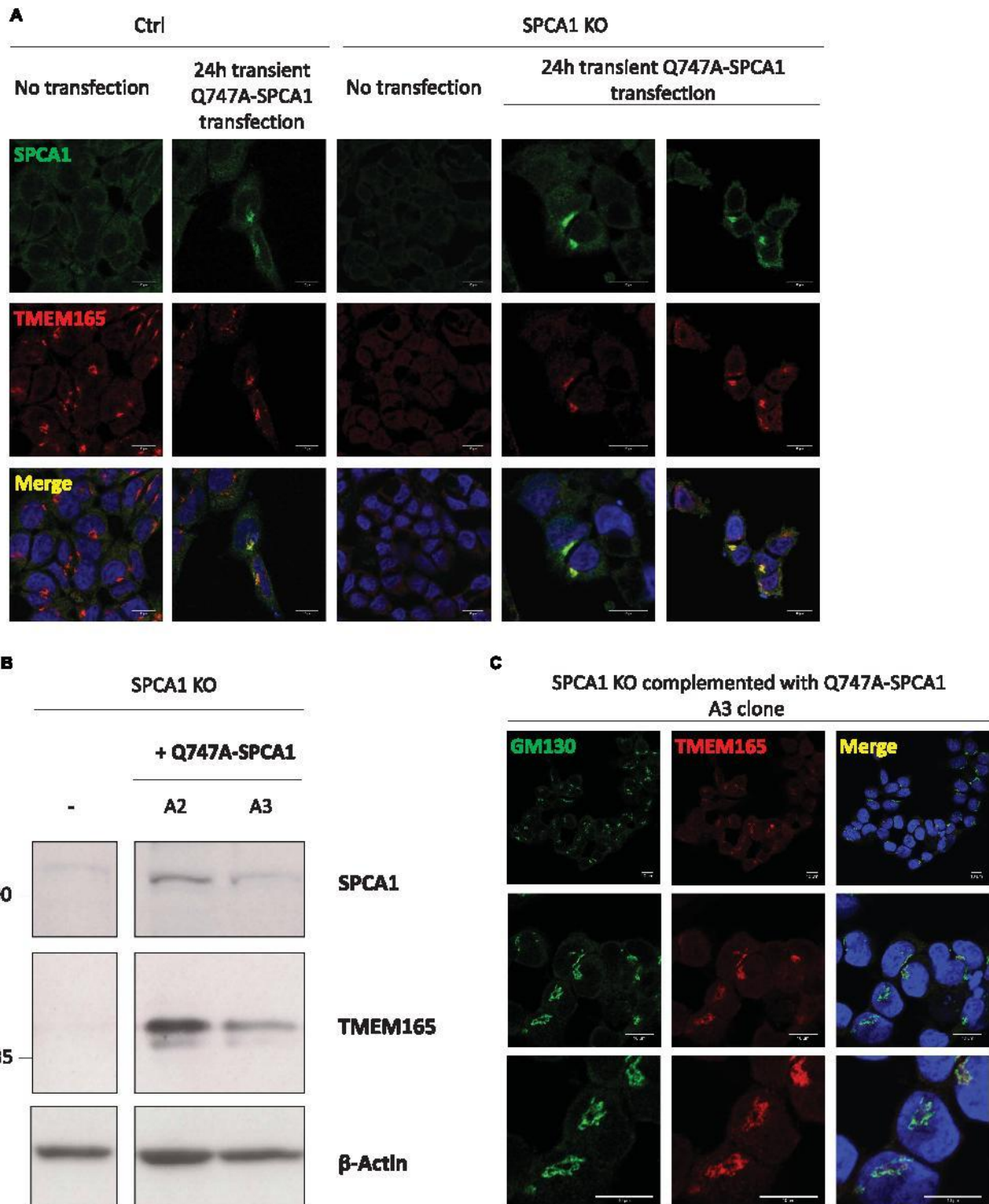


**Figure 4. Q747A-SPCA1 expression stabilizes TMEM165 expression.**

Part 1 of 2

(A) Hap1 control and SPCA1 KO cells were transiently transfected with Q747A-SPCA1 for 24 h in IMDM supplemented with 10% FBS B. Cells were then fixed, permeabilized and labeled with antibodies against TMEM165 and SPCA1 before confocal microscopy visualization. DAPI staining (blue) was performed, showing nuclei. Scale bars, 10  $\mu$ m. (B) Hap1 SPCA1 KO cells were transfected with Q747A-SPCA1 for 24 h in IMDM supplemented with 10% FBS B. Cells were diluted ten times in culture medium containing 0.5  $\mu$ g/ml puromycin as the selective agent and cultured for several days. Four polyclonal populations were then screened by Western blot. Total cell lysates were prepared, subjected to SDS-PAGE and Western blot

**Figure 4. Q747A-SPCA1 expression stabilizes TMEM165 expression.**

Part 2 of 2

with the indicated antibodies. (C) Immunofluorescence analysis of A3 clone. Cells were fixed, permeabilized and labeled with antibodies against TMEM165 and GM130 before confocal microscopy visualization. DAPI staining (blue) was performed, showing nuclei. Scale bars, 10  $\mu\text{m}$ .

TMEM165 and SPCA1 in both control and SPCA1 KO cells reconstituted with Q747A-SPCA1. In non-transfected cells, the Golgi subcellular localization of SPCA1 was not observed possibly due to low antibody sensitivity. These results were then confirmed in Hap1 cells stably expressing Q747A-SPCA1 mutant. Western blot experiments showed rescued protein levels of TMEM165 in two different tested clones (A2, A3) compared with SPCA1 KO cells (Figure 4B). Additionally, immunofluorescence experiments of the A3 clone confirmed TMEM165's subcellular Golgi localization (Figure 4C). These results link the stability of TMEM165 to SPCA1's function in pumping  $\text{Mn}^{2+}$  from the cytosol into the Golgi lumen and highlight TMEM165's sensitivity to high cytosolic manganese concentrations.

We then exploited our recent results demonstrating the involvement of the sarco/endoplasmic reticulum  $\text{Ca}^{2+}$ -ATPase (SERCA) pumps in the rescue of the Golgi N-glycosylation defects in TMEM165 KO cells by extracellular  $\text{Mn}^{2+}$  [23]. The hypothesis underlying this result strongly suggested that SERCA pumps were capable to pump  $\text{Mn}^{2+}$  from the cytosol to the ER lumen. In line with this, we then wondered whether an over-expression of SERCA in KO SPCA1 cells could rescue the abundance and Golgi subcellular localization of TMEM165 by decreasing the cytosolic Mn accumulation. To address this point, HeLa SPCA1 KO cells were used to transiently overexpressed SERCA2b. As shown in Figure 5A, the transient expression of SERCA2b in HeLa SPCA1 KO cells rescues the abundance of TMEM165. Immunofluorescence experiments were then performed in order to confirm the Western blot results. We showed that TMEM165 Golgi subcellular localization is specifically rescued in cells overexpressing SERCA2b (Figure 5B).

### Proximity between TMEM165 and SPCA1

To evaluate a potential interaction between SPCA1 and TMEM165, proximity ligation assays (PLA) using Hap1 control cells and SPCA1 KO cells as negative controls were performed. Endogenous interactions of TMEM165 with SPCA1 were clearly visible in control cells with an average of 35 dots per cell; however, the interaction was strongly reduced in SPCA1 KO cells (Figure 6). This result suggests a potential interaction between TMEM165 and SPCA1 or at least their close localization since both proteins reside in the Golgi compartment.

## Discussion

The regulation of  $\text{Mn}^{2+}$  homeostasis in the secretory pathway is fundamental as many ER/Golgi glycosyltransferases are  $\text{Mn}^{2+}$  dependent [24]. The underlying molecular mechanisms involved in such regulation are not completely understood. Our previous work uncovered a role for TMEM165, a member of the Uncharacterized Protein Family 0016 (UPF0016), in Golgi  $\text{Mn}^{2+}$  homeostasis [12]. Defects in TMEM165 and its yeast ortholog Gdt1p have been shown to be associated with strong Golgi glycosylation abnormalities [20]. Furthermore, the stability of both proteins is dependent on  $\text{Mn}^{2+}$  ion levels as high  $\text{Mn}^{2+}$  concentration targets them for degradation in lysosomes (TMEM165) or vacuoles (Gdt1p) [21,25]. Another Golgi protein is known to be involved in  $\text{Ca}^{2+}/\text{Mn}^{2+}$  pumping named SPCA1 (Secretory pathway  $\text{Ca}^{2+}$ -ATPase pump type 1). In this paper, we investigated the functional link between TMEM165 and SPCA1. We demonstrate that TMEM165 expression was dependent on SPCA1 as a lack of SPCA1 led to a nearly complete loss of TMEM165. TMEM165 was localized to and specifically degraded in lysosomes of SPCA1-deficient cells, which could be stabilized by the lysosomotropic agent CQ. Complementation studies showed that TMEM165 abundance was dependent on the ion pumped by SPCA1, specifically  $\text{Mn}^{2+}$ . Among SPCA1 mutants, only the Q747A mutant, which exhibits an enhanced  $\text{Mn}^{2+}$  pumping activity, fully rescued TMEM165 stability and Golgi subcellular localization. Two other SPCA1 mutants, G309C which blocks  $\text{Mn}^{2+}$  but not  $\text{Ca}^{2+}$  pump activity and D742Y that alters both  $\text{Ca}^{2+}$  and  $\text{Mn}^{2+}$  binding [19] did not rescue the stability of TMEM165. These results are in strong concordance with the observed  $\text{Mn}^{2+}$  sensitivity of TMEM165 and its lysosomal targeting at high  $\text{Mn}^{2+}$  culture conditions [21]. It is possible that the lack of SPCA1 results in cytosolic manganese accumulation, which then mimicks conditions where cells are exposed to high extracellular manganese concentrations. These results suggest that the stability

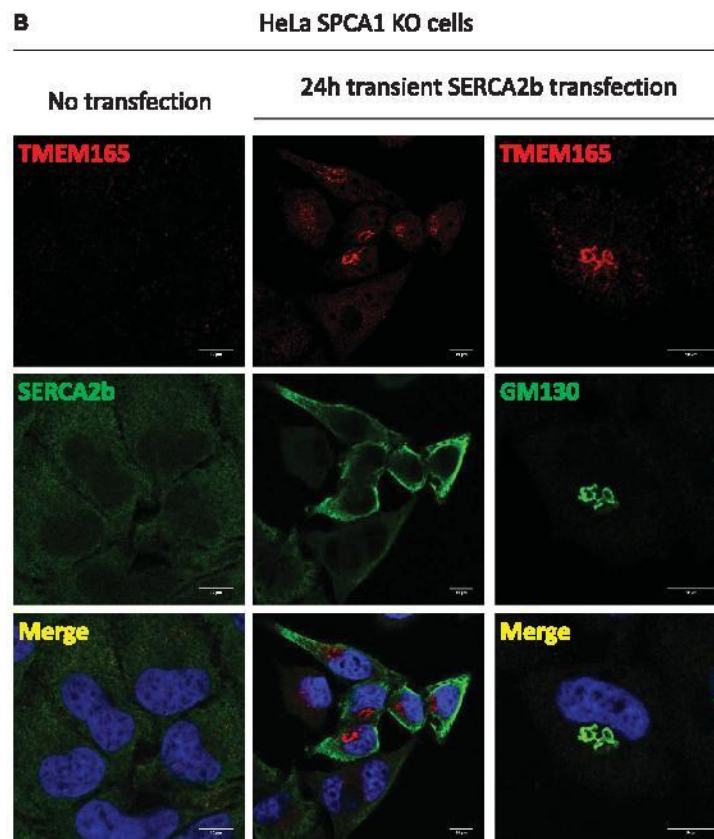
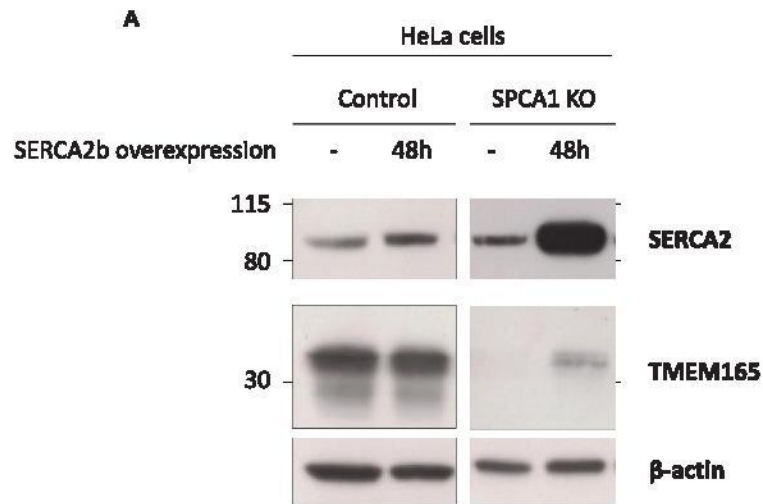


**Figure 5. TMEM165 expression is rescued in the Golgi apparatus when overexpressing SERCA2b in HeLa SPCA1 KO cells.**

(A) HeLa control and SPCA1 KO cells were transiently transfected with SERCA2b for 48 h. Total cell lysates were prepared, subjected to SDS–PAGE and Western blot with the indicated antibodies. (B) Subcellular localization of TMEM165 in HeLa SPCA1 KO cells overexpressing SERCA2b. Cells were fixed, permeabilized and labeled with antibodies against TMEM165, SERCA2 and GM130 before confocal microscopy visualization. DAPI staining (blue) was performed, showing nuclei. Scale bars, 10  $\mu$ m.

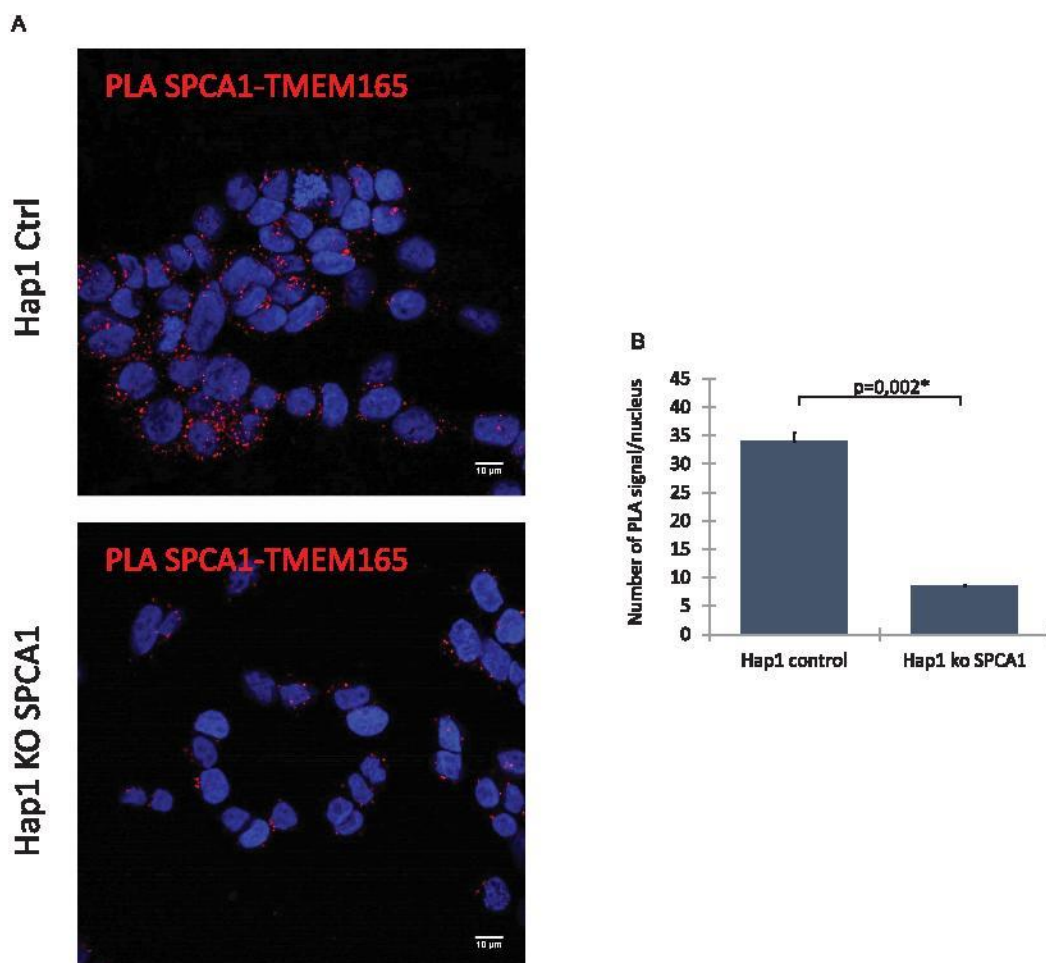


**Figure 6. A. Representative image of Proximity Ligation Assay of protein–protein proximity between TMEM165 and SPCA1.**

(A) Hap1 control and SPCA1 KO cells were stained with anti-TMEM165 rabbit polyclonal antibody 1 : 100 and anti-SPCA1 mouse polyclonal antibody 1 : 100. Each red dot represents a positive signal of protein–protein interaction and nuclei were counterstained with DAPI (blue). (B) Quantification of the red dots per nucleus in Hap1 control versus SPCA1 KO cells ( $N=2$ , 100 cells analyzed).

of TMEM165 may depend on cytosolic  $Mn^{2+}$  ion changes rather than luminal changes in the Golgi. The manganese sensitive region(s) of TMEM165 have not been identified. TMEM165 possesses two highly conserved consensus motifs; an E-x-G-D-K-T motifs facing the cytosol and an E-x-G-D-R-S-Q motif exposed in the Golgi lumen, both predicted to be implicated in the transport function of UPF0016 members [12,16]. While the exact functions of these two motifs in Golgi glycosylation and  $Mn^{2+}$  ion sensitivity are not yet clear, previous work indicated that the E108G TMEM165-CDG mutant [16,25] was resistant to manganese supplementation. As this acidic amino acid is present in the first conserved motif, it seems likely that the E-x-G-D-K-T motif facing the cytosol plays a role in the  $Mn^{2+}$  ion sensitivity of TMEM165.

The importance of TMEM165 in Golgi glycosylation has been established in humans, yeast and mammalian cells. Strong Golgi glycosylation defects are observed when TMEM165 is absent [8]. Interestingly, this is not the case for SPCA1 KO cells. The molecular mechanisms by which SPCA1 KO cells maintain their apparent glycosylation is not understood. This could be linked to recent observations that in absence of TMEM165, glycosylation defects are rescued by exogenous  $Mn^{2+}$  and involve SERCA pump activity [23]. In SPCA1-deficient cells, it is likely that cytosolic  $Mn^{2+}$  accesses the Golgi via the activity of SERCA pumps. Given SERCA pumps do not transport  $Mn^{2+}$  as efficiently as SPCA1, we can't exclude the fact that other mechanisms may compensate for a lack of  $Mn^{2+}$  transport via SPCA1.

Additionally, it is well known that SPCA1 is involved in manganese detoxification when cells are exposed to high manganese concentrations [6]. This process is considered to be essential by decreasing cytosolic manganese concentrations, which would otherwise impair many cytosolic processes by competing with other divalent ions. Our results reinforce a model in which both SPCA1 and TMEM165 participate in manganese detoxification. According to recent studies, the direction of  $Mn^{2+}$  transport is the same for these two proteins [15]. As such, TMEM165 could act in concert with SPCA1 to conduct detoxification. The question of why TMEM165 is degraded during cytosolic manganese accumulation remains open. It is likely that the transport function of TMEM165 is yet to be fully elucidated. Some results suggest that TMEM165 might function as an antiporter using a Golgi luminal ion gradient (where the counter ion can be  $Ca^{2+}$ ,  $H^+$  or Pi) to either import  $Mn^{2+}$  and/or  $Ca^{2+}$  to the Golgi lumen [2,18]. The degradation of TMEM165 could be required to prevent the collapse of a Golgi luminal gradient essential for maintaining other critical Golgi functions. As secondary transporters exhibit a high capacity for transport with low ion affinity, it is likely that TMEM165 could also work in reverse. In this scenario, the degradation of TMEM165 would prevent the accumulation of  $Mn^{2+}$  in the Golgi lumen due to the activity of SPCA1. The observed proximity of TMEM165 and SPCA1 might be important for regulating their activities. This unambiguously demonstrates the role of these two proteins in the regulation of Ca and Mn cellular homeostasis.

In conclusion, our results reveal a functional link between TMEM165 and SPCA1 thereby opening new concepts in  $Ca^{2+}/Mn^{2+}$  Golgi homeostasis regulation, crucial for many fundamental cellular processes such as protein secretion as well as glycosylation. There are indeed growing evidences pointing to dysfunctions of  $Ca^{2+}$  ATPase in colon, lung and breast cancers [26] and future directions in tumor progression and/or metabolic disease mechanisms must take into account the existence of this close link between TMEM165 and SPCA1.

### Abbreviations

ATP2C1, calcium-transporting ATPase type 2C member 1; BSA, bovine serum albumin; CDG, congenital disorders of glycosylation; CQ, chloroquine; DMEM, Dulbecco's modified eagle's medium; GPP130, Golgi phosphoprotein 4; IMDM, Iscove's modified Dulbecco's medium; LAMP2, lysosomal-associated membrane protein 2; Mn, manganese;  $Mn^{2+}$ , manganese, ion (2+);  $MnCl_2$ , manganese (II) chloride tetrahydrate; PAM71, photosynthesis affected mutant 71; PFA, paraformaldehyde; PLA, proximity ligation assay; RT, room temperature; SERCA, sarco/endoplasmic reticulum  $Ca^{2+}$ -ATPase; SPCA1, secretory pathway  $Ca^{2+}$ -ATPase 1; TBS, tris buffer saline; TGN46, *Trans*-Golgi network integral membrane protein 2; TMEM165, transmembrane protein 165; UPF, uncharacterized protein family.

### Author Contribution

Designed the experiments: E.L., M.H., A.K., F.F.; Performed the experiments: E.L., M.H., M.-A.K., D.V., K.K.; Analyzed the data: E.L., M.H., M.-A.K., H.-H.H., A.K. and F.F.; Wrote the paper: C.M.R., A.K. and F.F.

### Funding

This work was supported by grants from Agence Nationale de la Recherche (SOLV-CDG project to FF), EURO-CDG-2 that has received a funding from the European Union's Horizon 2020 research and innovation program under the ERA-NET Cofund action N° 643578 and within the scope of the International Associated Laboratory 'Laboratory for the Research on Congenital Disorders of Glycosylation — from cellular mechanisms to cure — GLYCOLAB4CDG'.

### Acknowledgements

We are indebted to Dr. Dominique Legrand for the Research Federation FRABio (Univ. Lille, CNRS, FR 3688, FRABio, Biochimie Structurale et Fonctionnelle des Assemblages Biomoléculaires) for providing the scientific and technical environment conducive to achieving this work. We thank the Bioluminescence Center of Lille, especially Christian Slomianny and Elodie Richard, for the use of the Leica LSM700 and the Leica LSM780.

### Competing Interests

The Authors declare that there are no competing interests associated with the manuscript.

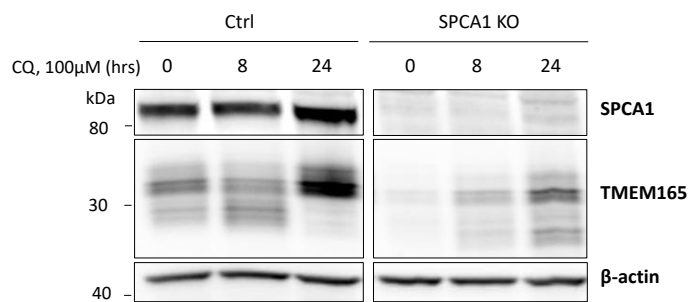
### References

- 1 Powell, J.T. and Brew, K. (1976) Metal ion activation of galactosyltransferase. *J. Biol. Chem.* **251**, 3645–3652 PMID:932001

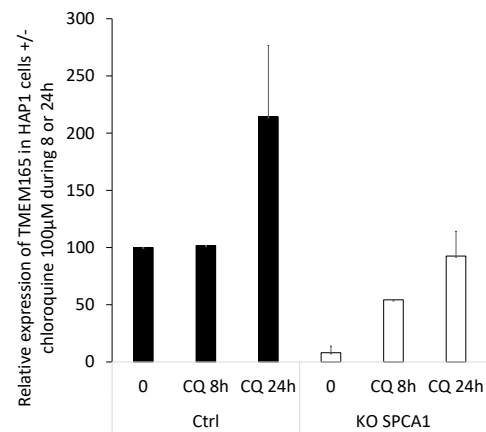
- 2 Demaegd, D., Foulquier, F., Colinet, A.-S., Gremillon, L., Legrand, D., Mariot, P. et al. (2013) Newly characterized Golgi-localized family of proteins is involved in calcium and pH homeostasis in yeast and human cells. *Proc. Natl Acad. Sci. U.S.A.* **110**, 6859–6864 <https://doi.org/10.1073/pnas.1219871110>
- 3 Reinhardt, T.A., Lippolis, J.D. and Sacco, R.E. (2014) The Ca(2+)/H(+) antiporter TMEM165 expression, localization in the developing, lactating and involuting mammary gland parallels the secretory pathway Ca(2+) ATPase (SPCA1). *Biochem. Biophys. Res. Commun.* **445**, 417–421 <https://doi.org/10.1016/j.bbrc.2014.02.020>
- 4 Hu, Z., Bonifas, J.M., Beech, J., Bench, G., Shigihara, T., Ogawa, H. et al. (2000) Mutations in ATP2C1, encoding a calcium pump, cause Hailey–Hailey disease. *Nat. Genet.* **24**, 61–65 <https://doi.org/10.1038/71701>
- 5 Ton, V.-K., Mandal, D., Vahadji, C. and Rao, R. (2002) Functional expression in yeast of the human secretory pathway Ca<sup>2+</sup>, Mn<sup>2+</sup>-ATPase defective in Hailey–Hailey disease. *J. Biol. Chem.* **277**, 6422–6427 <https://doi.org/10.1074/jbc.M110612200>
- 6 Leitch, S., Feng, M., Muend, S., Braiterman, L.T., Hubbard, A.L. and Rao, R. (2011) Vesicular distribution of Secretory Pathway Ca<sup>2+</sup>-ATPase isoform 1 and a role in manganese detoxification in liver-derived polarized cells. *BioMetals* **24**, 159–170 <https://doi.org/10.1007/s10534-010-9384-3>
- 7 Guiltarte, T.R. (2010) Manganese and Parkinson's disease: a critical review and new findings. *Environ. Health Perspect.* **118**, 1071–1080 <https://doi.org/10.1289/ehp.0901748>
- 8 Foulquier, F., Amyere, M., Jaeken, J., Zeevaert, R., Schollen, E., Race, V. et al. (2012) TMEM165 deficiency causes a congenital disorder of glycosylation. *Am. J. Hum. Genet.* **91**, 15–26 <https://doi.org/10.1016/j.ajhg.2012.05.002>
- 9 Jaeken, J. and Péanne, R. (2017) What is new in CDG? *J. Inher. Metab. Dis.* **40**, 569–586 <https://doi.org/10.1007/s10545-017-0050-6>
- 10 Zeevaert, R., de Zegher, F., Sturiale, L., Garozzo, D., Smet, M., Moens, M. et al. (2013) Bone dysplasia as a key feature in three patients with a novel congenital disorder of glycosylation (CDG) type II due to a deep intronic splice mutation in TMEM165. *JIMD Rep.* **8**, 145–152 [https://doi.org/10.1007/8904\\_2012\\_172](https://doi.org/10.1007/8904_2012_172)
- 11 Morelle, W., Potelle, S., Witters, P., Wong, S., Climer, L., Lupashin, V. et al. (2017) Galactose supplementation in patients with TMEM165-CDG rescues the glycosylation defects. *J. Clin. Endocrinol. Metab.* **102**, 1375–1386 <https://doi.org/10.1210/clinem.2016-3443>
- 12 Dulary, E., Potelle, S., Legrand, D. and Foulquier, F. (2017) TMEM165 deficiencies in congenital disorders of glycosylation type II (CDG-II): clues and evidences for roles of the protein in Golgi functions and ion homeostasis. *Tissue Cell* **49**, 150–156 <https://doi.org/10.1016/j.tice.2016.06.006>
- 13 Schneider, A., Steinberger, I., Herdean, A., Gandini, C., Eisenhut, M., Kurz, S. et al. (2016) The evolutionarily conserved protein PHOTOSYNTHESIS AFFECTED MUTANT71 is required for efficient manganese uptake at the thylakoid membrane in Arabidopsis. *Plant Cell* **28**, 892–910 <https://doi.org/10.1105/tpc.15.00812>
- 14 Brandenburg, F., Schoffman, H., Kurz, S., Krämer, U., Keren, N., Weber, A.P.M. et al. (2017) The *Synechocystis* manganese exporter Mnx is essential for manganese homeostasis in cyanobacteria. *Plant Physiol.* **173**, 1798–1810 <https://doi.org/10.1104/pp.16.01895>
- 15 Thines, L., Deschamps, A., Sengottaiyan, P., Savel, O., Stribny, J. and Morsomme, P. (2016) The yeast protein Gdt1p transports Mn<sup>2+</sup> ions and thereby regulates manganese homeostasis in the Golgi. *J. Biol. Chem.* **293**, 8048–8055 <https://doi.org/10.1074/jbc.RA118.002324>
- 16 Colinet, A.-S., Sengottaiyan, P., Deschamps, A., Colsoul, M.-L., Thines, L., Demaegd, D. et al. (2016) Yeast Gdt1 is a Golgi-localized calcium transporter required for stress-induced calcium signaling and protein glycosylation. *Sci. Rep.* **6**, 24282 <https://doi.org/10.1038/srep24282>
- 17 Snyder, N.A., Stefan, C.P., Soroudi, C.T., Kim, A., Evangelista, C. and Cunningham, K.W. (2017) H<sup>+</sup> and Pi byproducts of glycosylation affect Ca<sup>2+</sup> homeostasis and are retrieved from the Golgi complex by homologs of TMEM165 and XPR1. *G3 (Bethesda)* **7**, 3913–3924 <https://doi.org/10.1534/g3.117.300339>
- 18 Dulary, E., Yu, S.-Y., Houdou, M., de Bettignies, G., Decool, V., Potelle, S. et al. (2018) Investigating the function of Gdt1p in yeast Golgi glycosylation. *Biochim. Biophys. Acta* **1862**, 394–402 <https://doi.org/10.1016/j.bbagen.2017.11.006>
- 19 Hoffmann, H.-H., Schneider, W.M., Blumen, V.A., Scull, M.A., Hovnanian, A., Brummelkamp, T.R. et al. (2017) Diverse viruses require the calcium transporter SPCA1 for maturation and spread. *Cell Host Microbe* **22**, 460–470.e5 <https://doi.org/10.1016/j.chom.2017.09.002>
- 20 Potelle, S., Morelle, W., Dulary, E., Duvet, S., Vicogne, D., Spriet, C. et al. (2016) Glycosylation abnormalities in Gdt1p/TMEM165 deficient cells result from a defect in Golgi manganese homeostasis. *Hum. Mol. Genet.* **25**, 1489–1500 <https://doi.org/10.1093/hmg/ddw026>
- 21 Potelle, S., Dulary, E., Climer, L., Duvet, S., Morelle, W., Vicogne, D. et al. (2017) Manganese-induced turnover of TMEM165. *Biochem. J.* **474**, 1481–1493 <https://doi.org/10.1042/BCJ20160910>
- 22 Mukhopadhyay, S. and Linstedt, A.D. (2011) Identification of a gain-of-function mutation in a Golgi P-type ATPase that enhances Mn<sup>2+</sup> efflux and protects against toxicity. *Proc. Natl Acad. Sci. U.S.A.* **108**, 858–863 <https://doi.org/10.1073/pnas.1013642108>
- 23 Houdou, M., Lebredonchel, E., Garat, A., Duvet, S., Legrand, D., Decool, V. et al. (2019) Involvement of thapsigargin- and cyclopiazonic acid-sensitive pumps in the rescue of TMEM165-associated glycosylation defects by Mn<sup>2+</sup>. *FASEB J.* **33**, 2669–2679 <https://doi.org/10.1096/fj.201800387R>
- 24 Audry, M., Jeanneau, C., Imbert, A., Harduin-Lepers, A., Delannoy, P. and Breton, C. (2011) Current trends in the structure-activity relationships of sialyltransferases. *Glycobiology* **21**, 716–726 <https://doi.org/10.1093/glycob/cwq189>
- 25 He, W. and Hu, Z. (2012) The role of the Golgi-resident SPCA Ca<sup>2+</sup>/Mn<sup>2+</sup> pump in ionic homeostasis and neural function. *Neurochem. Res.* **37**, 455–468 <https://doi.org/10.1007/s11064-011-0644-6>
- 26 Dang, D. and Rao, R. (2016) Calcium-ATPases: gene disorders and dysregulation in cancer. *Biochim. Biophys. Acta* **1863**, 1344–1350 <https://doi.org/10.1016/j.bbamcr.2015.11.016>

**Supp Fig. 1**

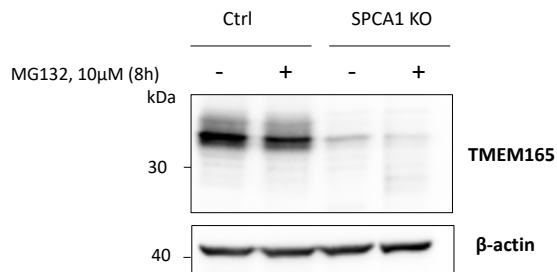
**A.**



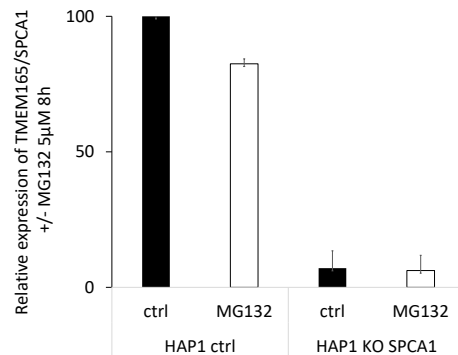
**B.**



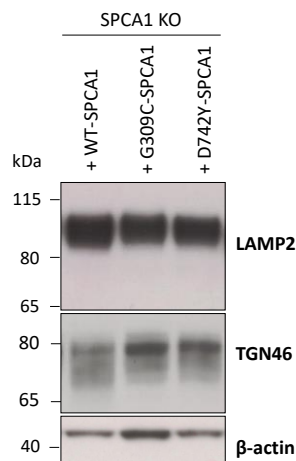
**C.**



**D.**



**E.**



**Supplementary Fig. 1. A.** Kinetics of TMEM165 expression restoration by chloroquine. Expression of TMEM165 in Hap1 control and SPCA1 KO cells with or without chloroquine (CQ) (100µM, 8 or 24h). **B.** Quantification of TMEM165 proteins expression (n=3). **C.** Effect of MG132 on TMEM165 expression in HAP1 KO SPCA1 cells. Expression of TMEM165 in Hap1 control and SPCA1 KO cells with or without MG132 (5µM, 8h). **D.** Quantification of TMEM165 proteins expression (n=3) normalized with beta-actin. **E.** LAMP2 and TGN46 glycosylation profiles in complemented Hap1 SPCA1 KO cells with WT-SPCA1, G309C-SPCA1 and D742Y-SPCA1 assessed by western blot. Total cell lysates were prepared, subjected to SDS-PAGE and western blot with the indicated antibodies.

## 2.3 Conclusion and discussion

### 2.3.1 Proposed model of the link between TMEM165 and SPCA1

Using KO SPCA1 HAP1 cells, we first noticed the abolished expression of TMEM165 in the absence of SPCA1. Then the use of different functional mutated forms of SPCA1 altered in calcium and/or manganese transport, demonstrated that the presence of TMEM165 at the Golgi membrane was dependent on the ability of SPCA1 to import manganese.

In our model, the absence of the  $\text{Ca}^{2+}/\text{Mn}^{2+}$  ATPase pump SPCA1 leads to an increase of the cytosolic manganese concentration, mimicking a high manganese supplementation in the cell medium (**figure 37**), resulting in the specific targeting of TMEM165 to the lysosomes for degradation. The re-expression of a form of SPCA1 with the ability to detoxify the cytosol of a manganese excess leads to the restoration of TMEM165 Golgi localization.

Several studies reinforced the model depicted in this second article that draws a parallel between the absence of SPCA1 and a condition of manganese excess.

A recent publication was submitted by members of our groups (Roy et al., submitted article) about the expression of TMEM165 in Hailey-Hailey disease (HDD) fibroblasts and keratinocytes, expressing one wild type allele and one mutated allele of SPCA1. The results demonstrated that patients cells presented an increased TMEM165 sensitivity to manganese-induced degradation manifested by an accumulation of manganese in SPCA1-depleted cells.

These results are consistent with those obtained in this second publication.

In the first article, we have demonstrated the localization of a cytosolic motif and a luminal motif of highly conserved amino acids responsible for the manganese-sensitivity of TMEM165 (**Results part, article 1**). As TMEM165 represents a manganese sensor that lies in two motifs, one in the cytosolic side and one in the luminal side of the protein; the question is why is the luminal sequence so important? In the model advanced in the discussion of the first article we have shown that mutations in the amino acids of the luminal sequence lead to the impairment of the conformational change of TMEM165 following the manganese binding that would prevent the activation of the degradation process.

The combination of these new findings leads to the proposed model for the link between SPCA1, TMEM165, and its manganese-induced degradation that is summarized in **figure 37**.

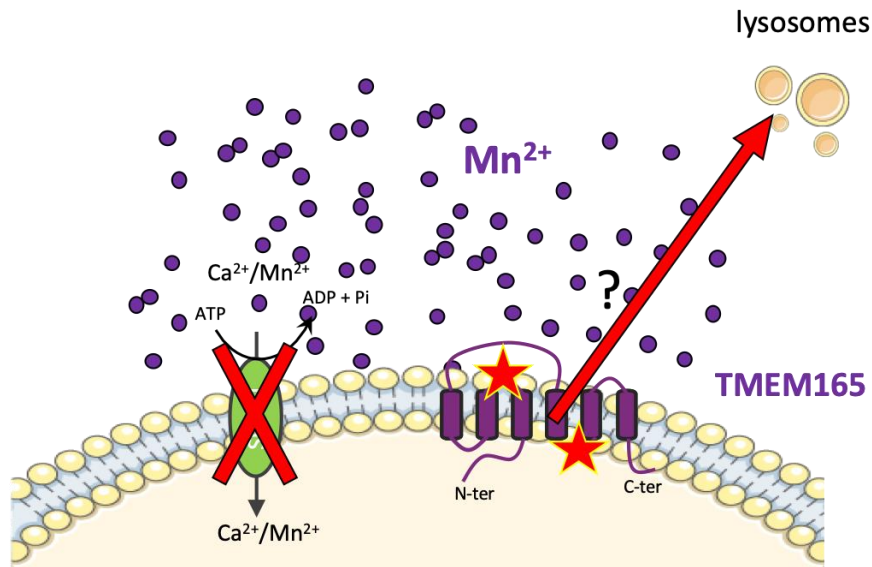
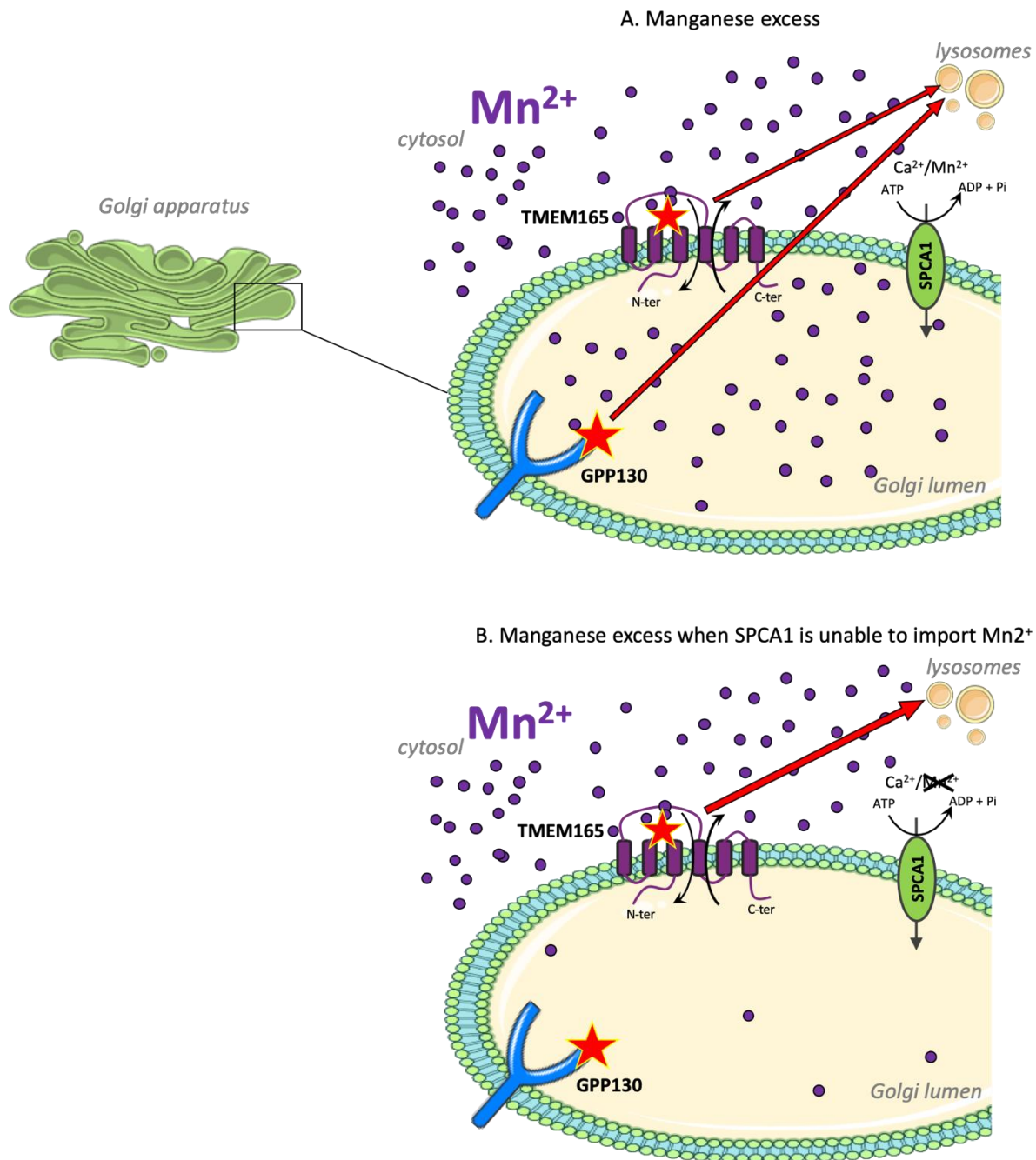


**Figure 37. Hypothetic mechanism explaining the loss of expression of TMEM165 in KO SPCA1 cells.** The red stars symbolize the conserved motifs of the UPF0016 family

### 2.3.2 TMEM165 is a cytosolic manganese sensor

This mutants-based study highlights that TMEM165 represents a cytosolic manganese sensor. Another Golgi protein was already known to be sensitive to lysosomal targeting following an elevation of manganese concentration, GPP130 (result part, article [1] and [4]). However, GPP130 is a luminal manganese sensor (Masuda et al., 2013). In the **figure 2A** of the presented article, the absence of SPCA1 induces a degradation of TMEM165, while preventing GPP130 degradation in high manganese conditions. The manganese-induced degradation of GPP130 is restored only when SPCA1 is present and is able to import manganese **figure 38**. In other words, under high cytosolic manganese concentrations, the massive import of manganese by SPCA1 restores the manganese excess inside the Golgi lumen, responsible of GPP130 degradation.



★ Hypothetic protein manganese sensor sequence localization

**Figure 38. Putative model of TMEM165 and GPP130 as manganese sensors.** TMEM165 manganese-sensitive sequence is localized on the cytosolic side of the protein while the manganese sensor of GPP130 is inside the Golgi lumen. **A.** In manganese excess conditions, both proteins can be targeted to the lysosomal compartment for degradation. **B.** In manganese excess conditions, if SPCA1 is unable to import manganese, GPP130 degradation does not occur.

Questions about the necessity to discard TMEM165 from the Golgi membrane remain.

### 2.3.2 Why TMEM165 has to be degraded?

The manganese-induced degradation of TMEM165 is highly conserved throughout evolution and may have a cellular benefit in certain conditions. Assuming TMEM165 is a  $Mn^{2+}/Ca^{2+}$  exchanger, a manganese excess would compete with  $Ca^{2+}$  for the SPCA1 pump inducing a collapse of the Golgi calcium concentration. The need to discard TMEM165, appear necessary for maintenance of the Golgi  $Ca^{2+}$  and  $Mn^{2+}$  homeostasis. The theory is reinforced by the importance of calcium in the cell regulation mechanisms, confirmed by the observation that a homozygous mutation of SPCA1 is lethal while this is not the case for TMEM165.

### 2.3.3. Perspectives

To consolidate the hypothesis that the loss of TMEM165 in the absence of SPCA1 is due to an elevation of cytosolic manganese concentration, a transfection of manganese-insensitive TMEM165 mutants in KO SPCA1 has to be made. In our first publication, we identified mutants presenting a resistance to elevated manganese concentrations; some of them maintained a Golgi-localization. After transient transfection of these mutants in KO SPCA1 HAP1 cells, the targeting of TMEM165 to the lysosomes should be abolished or delayed as compared to the transfection of the WT-TMEM165. This would reinforce both the idea that TMEM165 is a cytosolic manganese sensor and of the importance of the signature motifs in this mechanism.

# APPENDIX

During my PhD I have contributed to two supplementary publications concerning TMEM165 manganese-induced degradation and the role of SERCA pumps in the restoration of glycosylation in KO TMEM165 cells by manganese.

## Involvement of thapsigargin- and cyclopiazonic acid-sensitive pumps in the rescue of TMEM165-associated glycosylation defects by Mn<sup>2+</sup>

Marine Houdou,<sup>\*</sup> Elodie Lebreton,<sup>\*</sup> Anne Garat,<sup>†</sup> Sandrine Duvet,<sup>\*</sup> Dominique Legrand,<sup>\*</sup> Valérie Decool,<sup>†</sup> André Klein,<sup>\*</sup> Mohamed Ouzzine,<sup>‡</sup> Bruno Gasnier,<sup>§</sup> Sven Potelle,<sup>\*1</sup> and François Foulquier<sup>\*,1,2</sup>

<sup>\*</sup>Centre National de la Recherche Scientifique (CNRS), Unité Mixte de Recherche (UMR) 8576, Unité de Glycobiologie Structurale et Fonctionnelle (UGSF),

<sup>†</sup>Centre Hospitalier Universitaire (CHU) Lille, Institut Pasteur de Lille, Equipe d'Accueil (EA) 4483, Impact de l'Environnement Chimique sur la Santé Humaine (IMPECS), University of Lille, Lille, France;

<sup>‡</sup>UMR 7365, Centre National de la Recherche Scientifique (CNRS)–Université de Lorraine, Biopôle-Faculté de Médecine, Vandoeuvre-les-Nancy, France; and

<sup>§</sup>Neurophotonics Laboratory, CNRS UMR 8250, Paris Descartes University, Sorbonne Paris Cité, Paris, France

<sup>1</sup> These authors contributed equally to this work.

<sup>2</sup> Correspondence: Centre National de la Recherche Scientifique (CNRS),

UMR 8576, Unité de Glycobiologie Structurale et Fonctionnelle (UGSF),

University of Lille, Villeneuve D'Ascq, F-59000 Lille, France. E-mail:

francois.foulquier@univ-lille1.fr

doi: 10.1096/fj.201800387R

### Abstract

Congenital disorders of glycosylation are severe inherited diseases in which aberrant protein glycosylation is a hallmark. Transmembrane protein 165 (TMEM165) is a novel Golgi transmembrane protein involved in type II congenital disorders of glycosylation. Although its biologic function is still a controversial issue, we have demonstrated that the Golgi glycosylation defect due to TMEM165 deficiency resulted from a Golgi Mn<sup>2+</sup> homeostasis defect. The goal of this study was to delineate the cellular pathway by which extracellular Mn<sup>2+</sup> rescues *N*-glycosylation in TMEM165 knockout (KO) cells. We first demonstrated that after extracellular exposure, Mn<sup>2+</sup> uptake by HEK293 cells at the plasma membrane did not rely on endocytosis but was likely done by plasma membrane transporters. Second, we showed that the secretory pathway Ca<sup>2+</sup>-ATPase 1, also known to mediate the influx of cytosolic Mn<sup>2+</sup> into the lumen of the Golgi apparatus, is not crucial for the Mn<sup>2+</sup>-induced rescue glycosylation of lysosomal-associated membrane protein 2 (LAMP2). In contrast, our results demonstrate the involvement of cyclopiazonic acid- and thapsigargin (Tg)-sensitive

pumps in the rescue of TMEM165-associated glycosylation defects by Mn<sup>2+</sup>. Interestingly, overexpression of sarco/endoplasmic reticulum Ca<sup>2+</sup>-ATPase (SERCA) 2b isoform in TMEM165 KO cells partially rescues the observed LAMP2 glycosylation defect. Overall, this study indicates that the rescue of Golgi *N*-glycosylation defects in TMEM165 KO cells by extracellular Mn<sup>2+</sup> involves the activity of Tg and cyclopiazonic acid-sensitive pumps, probably the SERCA pumps.—Houdou, M., Lebretonchel, E., Garat, A., Duvet, S., Legrand, D., Decool, V., Klein, A., Ouzzine, M., Gasnier, B., Potelle, S., Foulquier, F. Involvement of thapsigargin- and cyclopiazonic acid-sensitive pumps in the rescue of TMEM165-associated glycosylation defects by Mn<sup>2+</sup>. *FASEB J.* 33, 2669–2679 (2019). [www.fasebj.org](http://www.fasebj.org)

**Key words:** manganese homeostasis, congenital disorders of glycosylation, Golgi apparatus

**Abbreviations:** BCA, bicinchoninic acid; CDG, congenital disorders of glycosylation; CPA, cyclopiazonic acid; CQ, chloroquine; DPBS, Dulbecco's phosphate-buffered saline; ER, endoplasmic reticulum; ICP-MS, inductively coupled plasma mass spectrometry; KO, knockout; LAMP2, lysosomal-associated membrane protein 2; MBCD, methyl- $\beta$ -cyclodextrin; SERCA, sarco/endoplasmic reticulum Ca<sup>2+</sup>-ATPase; siRNA, small interfering RNA; SPCA1/2, secretory-pathway Ca<sup>2+</sup>-ATPase 1/2; TBS-T, Tris-buffered saline with Tween 20; Tg, thapsigargin; TMEM165, transmembrane protein 165

In 2012, we identified the transmembrane protein 165 (TMEM165) gene as a new gene involved in congenital disorders of glycosylation (CDG) (OMIM entry 614727) (1). TMEM165-CDG patients present a peculiar clinical phenotype, including major skeletal dysplasia, osteoporosis, and dwarfism (2). They also present hyposialylation and hypogalactosylation of their sera *N*-glycoproteins. TMEM165 is a Golgi transmembrane protein belonging to an uncharacterized family of transmembrane proteins named UPF0016 (uncharacterized protein family 0016; Pfam PF01169). Even if TMEM165 is highly conserved during evolution from yeast to human, its biologic function is still a controversial issue. TMEM165 was first described as a Golgi cation antiporter by sequence analogy with other members of the family (3). In addition, we recently demonstrated that the Golgi glycosylation defect due to TMEM165 deficiency in patients and in TMEM165 knockout (KO) cells resulted from a defect in Golgi Mn<sup>2+</sup> homeostasis, thus linking TMEM165 with Mn<sup>2+</sup> homeostasis and suggesting it may import

Mn<sup>2+</sup> into the Golgi stacks (4). This is reinforced by the thylakoid Mn<sup>2+</sup> import via photosynthesis-affected mutant 71 transporter, the *Arabidopsis thaliana* ortholog of TMEM165 (5). In addition, we highlighted that only 1 mM Mn<sup>2+</sup> supplementation was sufficient to rescue a normal glycosylation. Manganese is considered to be a trace element, but it is still essential for several cellular processes. It is involved in the catalytic domain of many enzymes, such as mitochondrial enzymes, RNA and DNA polymerase, and Golgi glycosyltransferases. Although the link between Golgi glycosylation and Mn<sup>2+</sup> has long been known (6), it has only recently been shown that a decrease in cellular Mn<sup>2+</sup> could cause CDG. In addition to our study showing that TMEM165 deficiency was linked with Golgi Mn<sup>2+</sup> homeostasis (4), Park et al. (7) have shown that mutations in SLC39A8, a putative plasma membrane manganese transporter, lead to severe glycosylation defects. The question we address here is how does extracellular Mn<sup>2+</sup> supplementation rescue the glycosylation in TMEM165KO cells? Extracellular Mn<sup>2+</sup> could reach the Golgi lumen one of two ways: first, it might be internalized by endocytosis and subsequently reach the Golgi lumen through endosome-to-*trans*-Golgi network retrograde trafficking (8); and second, it might cross the plasma membrane and eventually the Golgi membrane through unspecific channels or transporters. In the latter case, current knowledge suggests that Mn<sup>2+</sup> supply in the Golgi is achieved via the action of the secretory pathway Ca<sup>2+</sup>-ATPases (SPCA1 and SPCA2) (9–12), which mediates the import of Ca<sup>2+</sup> and Mn<sup>2+</sup> into the Golgi lumen. Thus, the aim of this study was to decipher by which pathways 1 mM MnCl<sub>2</sub> supplementation leads to glycosylation rescue in TMEM165 KO HEK293 cells.

## Material and methods

Anti-TMEM165 and anti- $\beta$ -actin antibodies were purchased from Millipore Sigma (Burlington, MA, USA). Anti-LAMP2 antibodies were purchased from Santa Cruz Biotechnology (Dallas, TX, USA). Anti-SPCA1 antibodies were purchased from Abcam (Cambridge, United Kingdom) for immunofluorescence staining and from Abnova (Taipei City, Taiwan) for Western blot analysis. Anti-GM130 antibody was from BD Biosciences (Franklin Lakes, NJ, USA). Anti-GPP130 antibody was purchased from Covance (Princeton, NJ, USA), and anti-sarco/endoplasmic reticulum Ca<sup>2+</sup>-ATPase (SERCA) 2 antibody was purchased from MilliporeSigma. Polyclonal goat anti-rabbit or goat anti-mouse horseradish peroxidase-conjugated Igs were purchased

from Agilent Technologies (Santa Clara, CA, USA). Polyclonal goat anti-rabbit or goat anti-mouse conjugated with Alexa Fluor were purchased from Thermo Fisher Scientific (Waltham, MA, USA). Manganese (II) chloride tetrahydrate was from Riedel-de-Haën (Seelze, Germany). All other chemicals were from MilliporeSigma, unless otherwise specified.

### **Cell culture, drug treatments, and transfections**

Control and TMEM165 KO HEK293 cells were maintained in DMEM (Lonza, Basel, Switzerland) supplemented with 10% fetal bovine serum (Dutscher, Brumath, France) at 37°C in a humidity saturated 5% CO<sub>2</sub> atmosphere. For drug treatments, cells were incubated either with 1 mM MnCl<sub>2</sub> and/or 10 mM chloroquine (CQ), 300 nM nocodazole, 50 nM Tg, 100 mM cyclopiazonic acid (CPA), 5 mM methyl- $\beta$ -cyclodextrin (MBCD), 500 mM CaCl<sub>2</sub>, 1mM sodium pyruvate for different treatment times. Transfections were performed using Lipofectamine 2000 (Thermo Fisher Scientific) according to the manufacturer's instructions. Human SERCA2b plasmid (pcDNA3.1+) was purchased from Addgene (Cambridge, MA, USA), and human siATP2C1 from Dharmacon (Horizon Discovery, Lafayette, CO, USA).

### **Immunofluorescence staining**

Cells were seeded on coverslips for 12 to 4 h, treated as indicated in each figure, washed twice in PBS (Euromedex, Souffelweyersheim, France), and fixed with 4% paraformaldehyde in PBS pH 7.3, for 30 min at room temperature. Coverslips were then washed 3 times with PBS, and cells were permeabilized with 0.5% Triton X-100 in PBS for 10 min before being washed 3 times with PBS. Coverslips were then incubated for 1 h in blocking buffer [0.2% gelatin, 2% bovin serum albumin, 2% fetal bovine serum (Lonza) in PBS] and then for 1 h with primary antibody diluted either at 1:100 or 1:300 in blocking buffer. After 3 washings with PBS, cells were incubated for 1 h with Alexa Fluor 488- or Alexa Fluor 568-conjugated secondary antibody (Thermo Fisher Scientific) diluted at 1:600 in blocking buffer. After 3 washings with PBS, coverslips were mounted on glass slides with Mowiol. Fluorescence was detected by an inverted Zeiss LSM780 or LSM700 Confocal Microscope. Acquisitions were done using ZEN Pro 2.1 software (Carl Zeiss GmbH, Jena, Germany).

## **Image analyses**

Immunofluorescence images were analyzed using TisGolgi, an in-house made ImageJ plugin (National Institutes of Health, Bethesda, MD, USA; <http://imagej.nih.gov/ij>) developed by the local TisBio (<http://tisbio.wixsite.com/tisbio>) facility.

## **Western blot analysis**

Cells were scraped in Dulbecco's phosphate-buffered saline (DPBS) and then centrifuged at 4000 g, 4°C for 10 min. Supernatant was discarded, and cells were then resuspended in RIPA buffer (Tris/HCl 50 mM pH 7.9, NaCl 120 mM, NP40 0.5%, EDTA 1 mM, Na<sub>3</sub>VO<sub>4</sub> 1mM, NaF 5 mM) supplemented with a protease cocktail inhibitor (Roche Diagnostics, Rotkreuz, Switzerland). Cell lysis was done either by passing the cells several times through a syringe with a 26-gauge needle or by a sonication bath for 2 min followed by incubation on ice for 10min. Cells were centrifuged 20,000 g, 4°C for 30min. Protein concentration contained in the supernatant was estimated with the micro bicinchoninic acid (BCA) Protein Assay Kit (Thermo Fisher Scientific). Ten or 20 mg of total protein lysate was mixed with NuPAGE LDS sample buffer (Thermo Fisher Scientific), pH 8.4, supplemented with 4% b-mercaptoethanol (Fluka; MilliporeSigma). Samples were heated 10 min at 95°C (excepted for TMEM165, SPCA1 and SERCA2), then separated on 4 to 12% Bis-Tris gels (Thermo Fisher Scientific) and transferred to nitrocellulose membrane Hybond ECL (GE Healthcare, Little Chalfont, United Kingdom). Membranes were blocked in blocking buffer [5% milk powder in TBS-T (13 TBS with 0.05% Tween 20)] for 1 h at room temperature, then incubated overnight with the primary antibodies (used at a dilution of 1:1000) in blocking buffer and washed 3 times for 5 min in TBS-T. Membranes were then incubated with peroxidase-conjugated secondary goat anti rabbit or goat anti-mouse antibodies (used at a dilution of 1:10,000 or 1:20,000; Agilent Technologies) in blocking buffer for 1 h at room temperature and later washed 3 times for 5 min in TBST. Signal was detected with chemiluminescence reagent (ECL 2 Western blotting substrate or SuperSignal West Pico Plus Chemiluminescent Substrate; Thermo Fisher Scientific) on imaging film (GE Healthcare).

## Mass spectrometry

Two T75 flasks at 90% confluence, treated as indicated in each figure, were used. Cells were then scraped in DPBS at 4°C and centrifuged at 4000 *g*, 4°C for 5 min. Then, supernatant was discarded, and cells were resuspended in PBS and washed 4 times by centrifugation (4000 *g*, 4°C for 10 min). Before the last wash, an aliquot of the resuspended cells in PBS was kept (1:10) in order to estimate the total protein concentration of the sample. The resting pellets were resuspended in lysis buffer (1% Triton-X100 in BS) after a sonication bath at 4°C for 1 h and centrifuged at 20,000 *g*, 4°C for 10 min. Supernatants were then transferred into new tubes. Next, dithiotreitol (MilliporeSigma) was added to a final concentration of 10 mM and incubated 45 min at 56°C followed by the addition of 50 mM iodoacetamide (Bio-Rad, Hercules, CA, USA) for 1 h at 37°C, protected from light. The reduced and acylated proteins were precipitated with a final concentration of 10% trichloroacetic acid and incubated for 30 min at –20°C. After a centrifugation at 20,000 *g*, 4°C for 10 min, supernatants were discarded. Protein pellets were then washed by the addition of iced acetone and centrifuged at 20,000 *g*, 4°C for 10 min. This step was repeated. Washed protein pellets were dried at room temperature for 30 min. Then trypsin at 2 mg/ml (MilliporeSigma) was added overnight and up to 48 h at 37°C in 50 mM ammonium bicarbonate (MilliporeSigma) with a 5:1 ratio. The reaction was stopped by heating samples 10 min at 100°C. *N*-glycans were released from the proteins by addition of 10 U of PNGase F (Roche Diagnostics) overnight at 37°C. *N*-glycans were then purified by a C18 Sep-Pak chromatography (Water, Guyancourt, France). The column was washed with 100% acetonitrile and 100% 2-propanol, and then equilibrated with 5% acetic acid in water. Samples were loaded onto the C18 Sep-Pak, and the bound peptides were eluted 3 times with 5% acetic acid in water. *N*-glycans in 5% aqueous acetic acid were lyophilized overnight. They were permethylated and spotted onto a matrix-assisted desorption plate and analyzed by matrix-assisted desorption ionization–time of flight mass spectrometry on a 4800 Proteomics Analyzer Mass Spectrometer (Applied Biosystems; Thermo Fisher Scientific), as described by Delannoy *et al.* (13). Each spectrum resulted from the accumulation of 10,000 spectra and shows glycans structures from *m/z* 1500 up to 3000.

## Whole cell Mn measurement

### Sample preparation

After the indicated treatments, cells were washed twice in DPBS at 4°C. Cells were then collected and centrifuged at 4000 g, 4°C for 10 min. Supernatant was discarded, and cells were then resuspended in 1 ml of PBS; 200 µl was kept for protein dosage, and 800 µl was kept for Mn measurement by inductively coupled plasma mass spectrometry (ICP-MS). Both were centrifuged at 4000 g, 4°C for 10 min. The cell pellet for protein dosage was resuspended in RIPA buffer, and cell lysis was performed. Protein concentration contained in the supernatant was estimated with the micro-BCA Protein Assay Kit (Thermo Fisher Scientific). Cell pellet for ICP-MS analysis was resuspended in deionized water and then sonicated for 30 s. A chloroform/methanol/water (ratio 2:1:3) extraction was then done to separate lipids, proteins, and soluble material. The upper phase containing soluble material was kept and dried under nitrogen flux or with a vacuum concentrator (Eppendorf Concentrator 5301). Samples were then dissolved in 500 µl of deionized water.

### **Instrumentation and analysis**

Samples were diluted 50 times with 1.5% (v/v) nitric acid (ultrapure quality 69.5%; Carlo Erba Reagents, Val de Reuil, France) solution in ultrapure water (Purelab Option-Q; Veolia Water, Antony, France) containing 0.1% Triton X-100 (Euromedex), 0.2% butan-1-ol (VWR Chemicals, Fontenay-sous-Bois, France), and 0.5 µg/L rhodium (Merk, Darmstadt, Germany). Assays were performed on an ICP-MS Thermo ICap Q device (Thermo Fisher Scientific). The limit of quantification was 0.2 µg/L.

### **Statistical analysis**

Comparisons between groups were performed by the Student's t test for 2 variables with equal or different variances, depending on the result of the F test.

## **Results**

### **Time course of lysosomal-associated membrane protein 2 glycosylation rescue by Mn<sup>2+</sup>**

Our previous studies demonstrated that supplementation with low Mn<sup>2+</sup> concentrations could completely suppress lysosomal-associated membrane protein 2 (LAMP2) glycosylation defects in TMEM165 KO cells (4). This has, however, been observed for long treatments (48 h). The time course of the Mn<sup>2+</sup> effect was not evaluated. To answer this point, a concentration of 1 µM of MnCl<sub>2</sub> was applied to the cells for increasing times (1–64 h), and

LAMP2 glycosylation was assessed by Western blot analysis (Fig. 1A). The results showed that after Mn<sup>2+</sup> treatment of TMEM165 KO cells, fully glycosylated forms of LAMP2 appear after 8 h of Mn<sup>2+</sup> treatment, yet most LAMP2 remain underglycosylated. Relative quantification of underglycosylated and fully glycosylated LAMP2 (Fig. 1B) indicate that fully glycosylated LAMP2 progressively increases from 10% after 8 h to 97% after 64 h of Mn<sup>2+</sup> treatment. This result is consistent with the slow turnover of LAMP2 estimated to 48 h. In further experiments, cells were treated with 1  $\mu$ M MnCl<sub>2</sub> for 8 and/or 16 h.

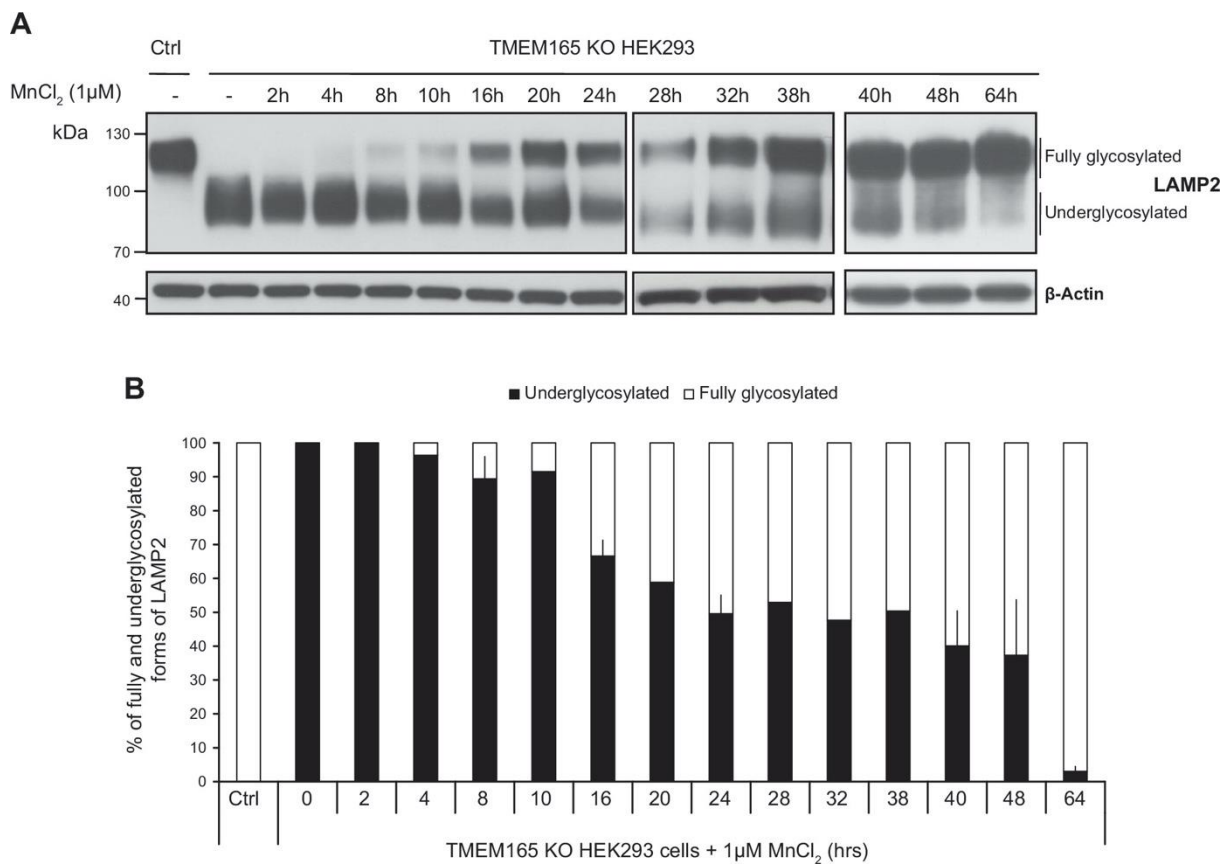


**Figure 1 Time course of Mn<sup>2+</sup>-induced LAMP2 glycosylation rescue.** A) Control and TMEM165 KO HEK293 cells were cultured with 1  $\mu$ M MnCl<sub>2</sub> during indicated times. Cell culture medium was renewed every 16 h. Total cell lysates were prepared, then subjected to SDS-PAGE and Western blot with indicated antibodies. B) Relative quantification of fully and underglycosylated forms of LAMP2 (n = 2)

### Blocking endocytosis in TMEM165 KO cells does not prevent rescue of LAMP2 glycosylation by Mn<sup>2+</sup>

The pathways by which Mn<sup>2+</sup> enters cells after MnCl<sub>2</sub> exposure are unknown. Two different ways are possible, either by permeating membranes using specific and/or unspecific

transporters or via endocytosis and endosome-to-*trans*-Golgi network retrograde trafficking (8). To discriminate between these possibilities, cells were treated with different drugs known to interfere with endocytosis such as CQ (14), a weak base raising the pH of acidic compartments, MBCD, that depletes cholesterol from plasma membrane and nocodazole, a microtubule depolymerizing agent (15) (Fig. 2 and Supplemental Figs. S1 and S2). We first checked the potential effects of these drugs on both the steady-state glycosylation status of LAMP2 in control HEK293 cells and its subcellular localization. No changes in the LAMP2 electrophoresis mobility could be observed in control HEK293 cells after these drug treatments (Supplemental Figs. S1A and S2A), suggesting no major alteration of its glycosylation. Moreover, neither nocodazole nor MBCD nor CQ disrupted the lysosomal localization of LAMP2 (Supplemental Figs. S1B and S2B).

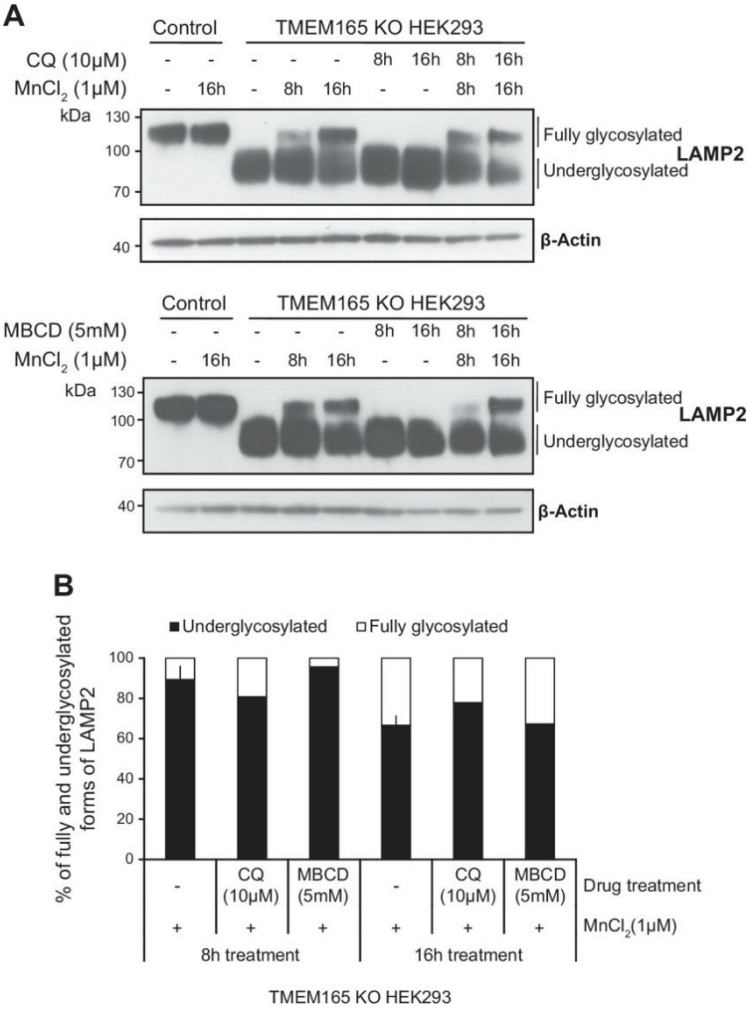


**Figure 2 Mn<sup>2+</sup> entry into TMEM165 KO HEK293 cells does not rely on endocytosis.** A) Control and TMEM165 KO HEK293 cells were cultured with CQ (10 µM) or MBCD (5mM) in combination or not with 1 µM MnCl<sub>2</sub> for 8

or 16 h. Total cell lysates were prepared, then subjected to SDS-PAGE and Western blot with indicated antibodies. B) Relative quantification of fully and underglycosylated forms of LAMP2 (n = 2).

We also checked the effects of those drugs on the morphology of the Golgi apparatus. Immunofluorescence staining of Golgi proteins GPP130 and GM130 were performed, followed by confocal microscopy analyses (Supplemental Figs. S1B and S2B). As already known from the literature, nocodazole fragmented the Golgi apparatus, but CQ and MBCD had no effect on its morphology.

The LAMP2 glycosylation profile in TMEM165 KO HEK293 cells after treatment with or without a combination of those drugs and MnCl<sub>2</sub> was then assessed (Fig. 2 and Supplemental Fig. S2C). The observed LAMP2 mobility in TMEM165 KO cells after 1 μM MnCl<sub>2</sub> treatment was comparable to the one observed in Fig. 1. Ten percent of LAMP2 was found to be normally glycosylated after 8 h of Mn<sup>2+</sup> treatment and 33% after 16 h. Cells were then treated with CQ or MBCD in the presence or absence of 1 μM MnCl<sub>2</sub> for 8 and 16 h (Fig. 2). The results show that CQ and MBCD did not prevent the rescue of LAMP2 glycosylation after Mn<sup>2+</sup> supplementation because 22 and 32% of fully glycosylated forms, respectively, were observed after 16 h treatment. Similar results were obtained with nocodazole (Supplemental Fig. S1C, D).

These results clearly highlight that none of these drugs prevents the rescue of LAMP2 glycosylation by Mn<sup>2+</sup> in TMEM165 KO cells. This suggests that at the extracellular concentration used in our study (1 μM), Mn<sup>2+</sup> enters TMEM165-defective HEK293 cells through plasma membrane transporters rather than by endocytosis.

### **Is Golgi pump SPCA1 involved in Mn<sup>2+</sup>-induced rescue of LAMP2 glycosylation?**

After entering TMEM165-defective cells, cytosolic Mn<sup>2+</sup> should reach the Golgi lumen to correct the glycosylation defects. Besides TMEM165, which acts as a key determinant for Golgi Mn<sup>2+</sup> homeostasis (4), the SPCA pumps (SPCA1 and -2) are known to be the main suppliers of Mn<sup>2+</sup> in the Golgi lumen (11). Because SPCA2 is poorly expressed in our cell line, we tested the contribution of SPCA1 by silencing its gene, ATP2C1 (Fig. 3). The small interfering RNA (siRNA) knockdown was very efficient, as 95% of the protein was depleted compared to untreated cells. Surprisingly, the knockdown of ATP2C1 did not prevent the rescue of LAMP2 glycosylation by Mn<sup>2+</sup>. Thirty-seven percent of LAMP2 was fully glycosylated after 16 h Mn<sup>2+</sup> treatment in siATP2C1-treated cells, a level similar to that observed without ATP2C1

knockdown. SPCA1 is thus not involved in the glycosylation rescue induced by Mn<sup>2+</sup> supplementation in TMEM165 KO HEK293 cells.

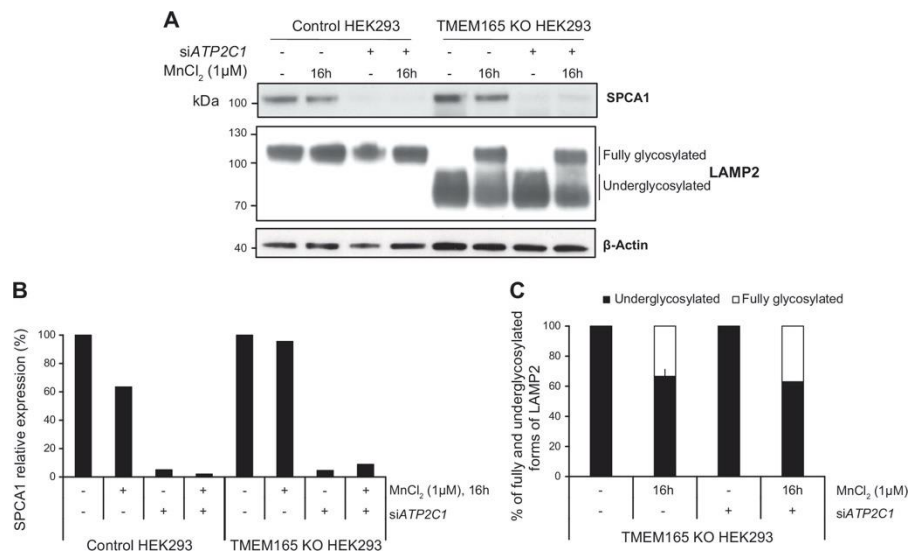


**Figure 3** *ATP2C1* knockdown does not prevent Mn<sup>2+</sup>-induced rescue glycosylation of LAMP2 in TMEM165 KO HEK293 cells. A) Control, TMEM165 KO, and si*ATP2C1* HEK293 cells were cultured with 1 μM MnCl<sub>2</sub> for 16 h. Total cell lysates were prepared, and then subjected to SDS-PAGE and Western blot analyses with indicated antibodies. B) Quantification of SPCA1 protein expression after normalization with actin. C) Relative quantification of fully and underglycosylated forms of LAMP2.

### Golgi glycosylation rescue induced by Mn<sup>2+</sup> supplementation requires Tg and CPA-sensitive pumps

Given the previous results, we next considered whether the endoplasmic reticulum (ER) could play a role in the observed glycosylation rescue. It had indeed been shown that SERCA pumps are able, in certain conditions, to transport Mn<sup>2+</sup> into the ER lumen in addition to Ca<sup>2+</sup> (16–18). We thus hypothesized that SERCA pumps might be involved in the Mn<sup>2+</sup> supplementation effect. To address this point, LAMP2 glycosylation status was evaluated by Western blot analysis in cells treated with CPA or Tg, two specific SERCA inhibitors, in the presence or absence of 1 μM MnCl<sub>2</sub> (Fig. 4). CPA and Tg did not induce any glycosylation defect on LAMP2 in control HEK293 cells; nor did this occur after 8 or 16 h of treatment (Supplemental Fig. S3). Remarkably, in TMEM165 KO HEK293 cells treated with CPA and 1 μM MnCl<sub>2</sub>, the treatment strongly delayed the rescue of LAMP2 glycosylation by Mn<sup>2+</sup>, as only 4% of LAMP2 was fully glycosylated after 8 h and 29% after 16 h of Mn<sup>2+</sup> treatment. To reinforce this result, stronger effects were obtained after Tg treatment (Fig. 4A, B). To confirm these results at the structural level, mass spectrometry of total N-glycans was performed (Fig. 5). TMEM165 KO HEK293 cells were treated or not with 1 μM MnCl<sub>2</sub> and with or without Tg/CPA. Consistent with our

previous studies, a pronounced hypogalactosylation was seen in TMEM165 KO HEK293 cells, with the accumulation of agalactosylated glycan structures detected at m/z 1661, 1835, 2081, and 2326. Consistent with our previous studies, MnCl<sub>2</sub> treatment rescues the general glycosylation defect, as indicated by the decreased abundance of the structures m/z 1835, 2081, and 2326 (54% decrease, Supplemental Fig. S4). Although Tg and CPA treatments in KO TMEM165 cells slightly increase the abnormal agalactosylated glycan structures, such treatments fully prevent the total rescue of TMEM165-associated glycosylation defects by Mn<sup>2+</sup>, as indicated by the remaining high abundance of the structures m/z 1661, 1835, 2081, and 2326 (Supplemental Fig. S4).

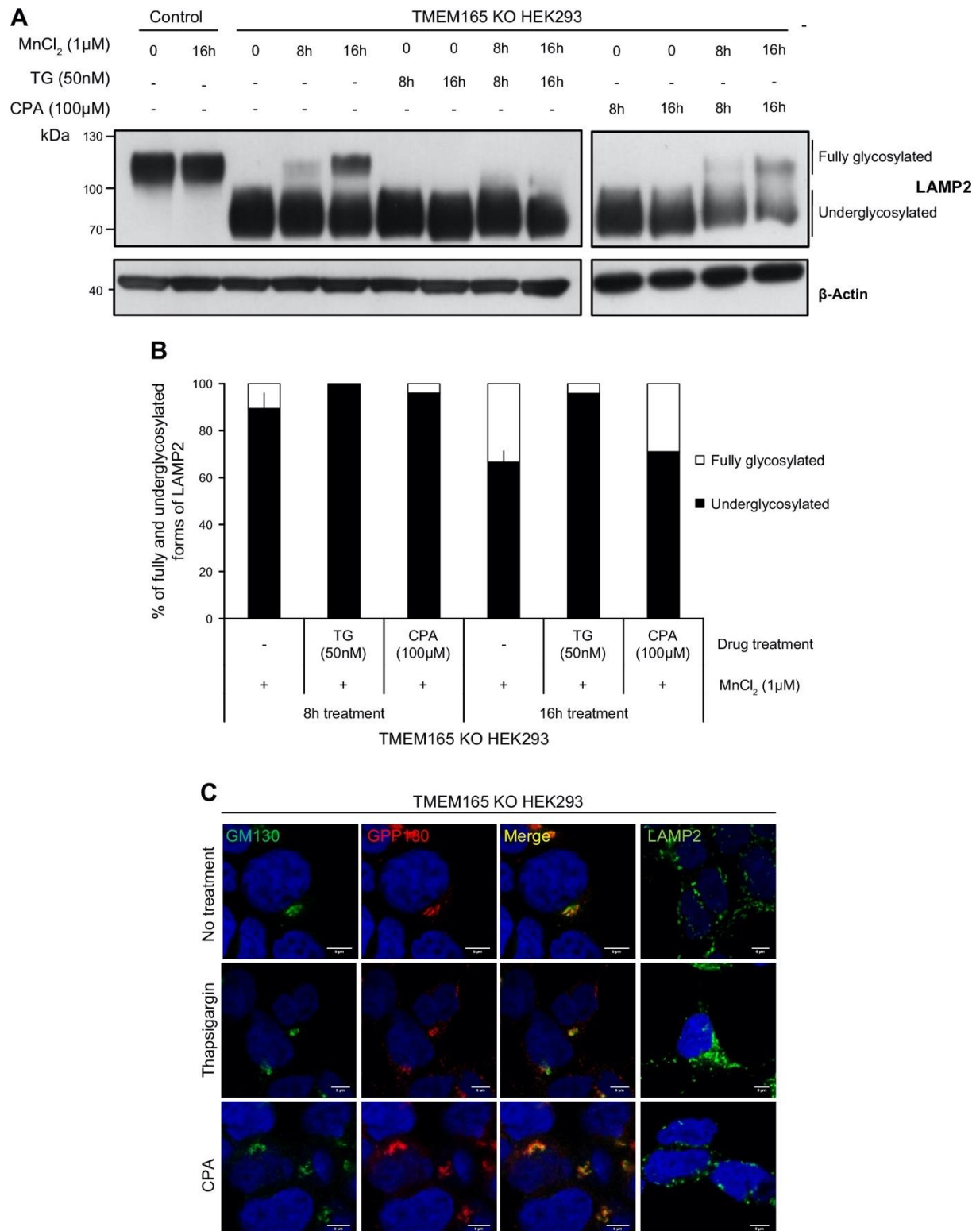


**Figure 4 Involvement of Tg- and CPA-sensitive pumps in Mn<sup>2+</sup>-induced rescue of LAMP2 glycosylation.** A) Control and TMEM165 KO cells were cultured with either Tg (50 nM) or CPA (100 μM), 2 SERCA inhibitors, in combination or not with 1 μM MnCl<sub>2</sub> for 8 or 16 h. Total cell lysates were prepared, then subjected to SDS-PAGE and Western blot with indicated antibodies. B) Relative quantification of fully and underglycosylated forms of LAMP2 (*n* = 2). C) Immunofluorescence analysis. TMEM165 KO HEK293 cells were incubated with either Tg (50 nM) or CPA (100 μM) for 16 h, fixed, permeabilized, and labeled with antibodies against GM130, GPP130, and LAMP2 before confocal microscopy visualization. DAPI staining (blue) was performed, showing nuclei. Scale bars, 5 μm.

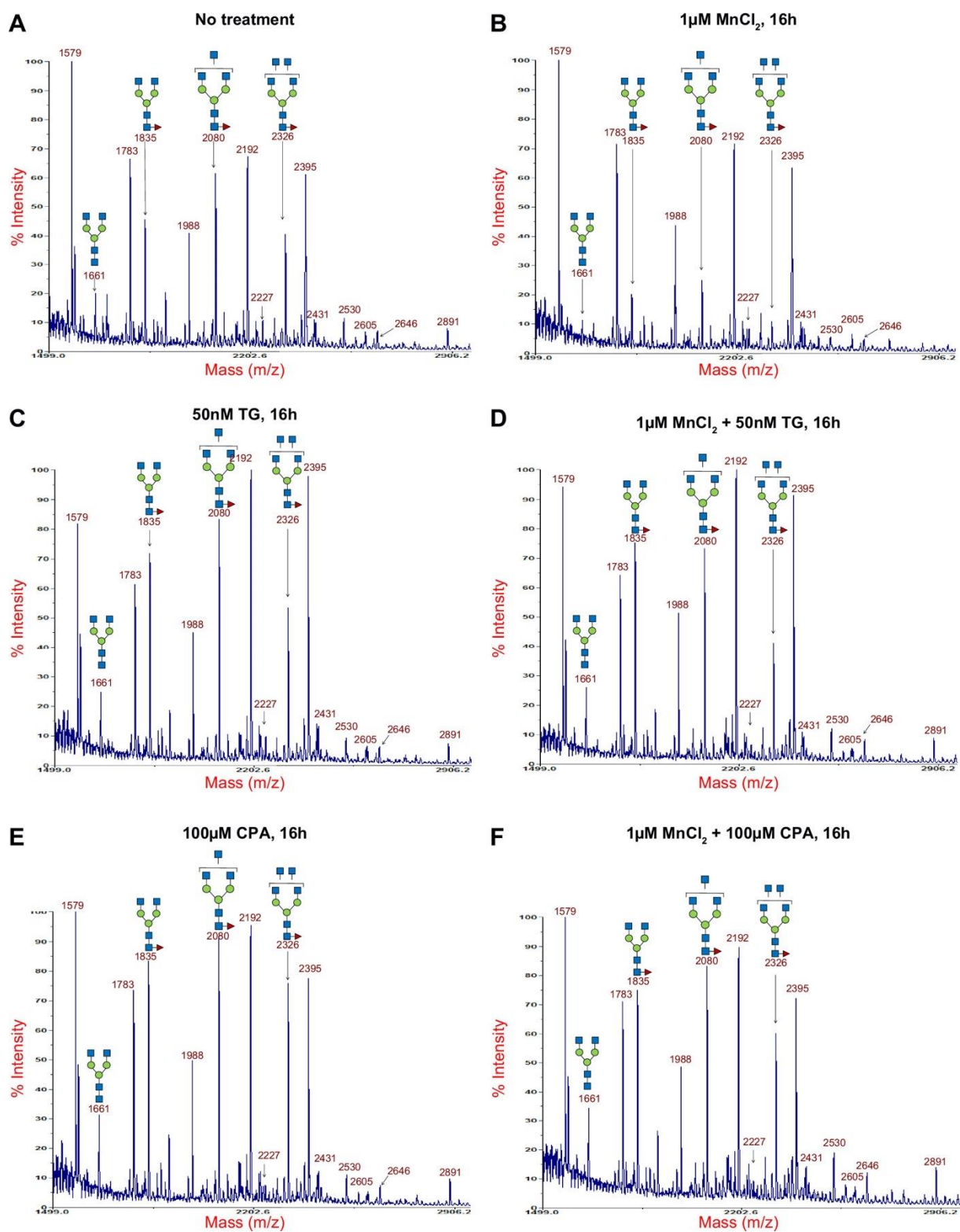


**Figure 5** *N*-glycosylation defects observed in TMEM165 KO HEK293 cells treated with Tg or CPA are not rescued by Mn<sup>2+</sup> supplementation. Matrix-assisted desorption ionization–time of flight mass spectrometry spectra of permethylated *N*-glycans from TMEM165 KO HEK293 cells after different treatments. No treatment (A), TMEM165 KO HEK293 cells treated with 1 μM MnCl<sub>2</sub> for 16 h (B), TMEM165 KO HEK293 cells treated with 50 nM Tg, in combination or not with 1 μM MnCl<sub>2</sub> for 16 h (C, D), TMEM165 KO HEK293 cells treated with 100 μM CPA in combination or not with 1 μM MnCl<sub>2</sub> for 16 h (E, F). Symbols represent sugar residues as follows:

blue square, *N*-acetylglucosamine; green circle, mannose; yellow circle, galactose; purple diamond, sialic acid; red triangle, fucose. Linkages between sugar residues have been removed for simplicity.

To validate these results, we tested whether CPA or Tg treatment acted by indirectly altering Mn<sup>2+</sup> entry into the cells. Therefore, the total cellular Mn concentration in presence and absence of CPA or Tg was evaluated by ICP-MS after MnCl<sub>2</sub> supplementation. The results showed that after Mn<sup>2+</sup> supplementation, the amount of Mn is comparable in cells treated or not with CPA or Tg (Supplemental Fig. S3C). This demonstrated that neither CPA nor Tg prevented the cellular Mn<sup>2+</sup> entry after MnCl<sub>2</sub> supplementation.

In parallel, the effects of CPA and Tg on the morphology of the Golgi apparatus were investigated by confocal immunofluorescence analysis of the Golgi proteins GPP130 and GM130 (Fig. 4C and Supplemental Fig. S3A). No effect was observed on the Golgi apparatus morphology after CPA treatment, and only a slight dilatation of the Golgi was shown after Tg treatment. Moreover, LAMP2 localization was not disrupted by either Tg or CPA.

Overall, these results provide pharmacologic evidence for the involvement of Tg- and CPA-sensitive pumps in the Golgi *N*-glycosylation rescue induced by Mn<sup>2+</sup> supplementation in TMEM165 KO HEK293 cells.

#### **Potential involvement of SERCA pump in the Mn<sup>2+</sup>-induced rescue of LAMP2 glycosylation**

The observed Tg and CPA sensitivity led us to investigate the potential role of ER SERCA pump in the Mn<sup>2+</sup> supplementation effect. Among all SERCA proteins, the SERCA2b isoform is the main form expressed in HEK293 cells. SERCA2b was overexpressed for 48 h in TMEM165 KO HEK293 cells, and LAMP2 glycosylation status was assayed by Western blot analysis. The correct SERCA2b expression was checked by immunofluorescence (data not shown) and by Western blot analyses in both TMEM165 KO and control HEK293 cells (Fig. 6). Compared to untransfected cells, LAMP2 glycosylation profile is slightly restored in TMEM165 KO HEK293 cells overexpressing SERCA2b (Fig. 6). In order to prove that this slight rescue was not due to potential ER/Golgi Ca<sup>2+</sup> homeostasis changes, the overexpressing cells were treated with 500 μM CaCl<sub>2</sub> and 1 mM sodium pyruvate. LAMP2 glycosylation rescue is identical to the one obtained without such treatment and suggests that the observed shift is likely not the cause of the SERCA2b Ca<sup>2+</sup> pumping activity. Taken together, these results suggest the potential involvement of SERCA2b pump in the Mn<sup>2+</sup> rescued glycosylation of LAMP2.

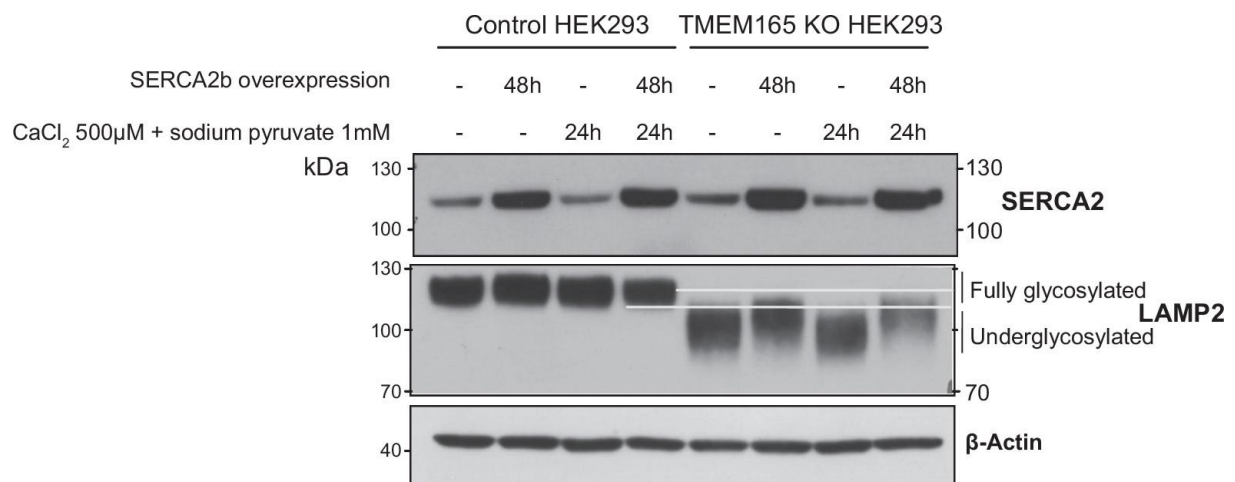


**Figure 6 Potential involvement of SERCA2b pump in Mn<sup>2+</sup> supplementation effect.** Effect of SERCA2b overexpression in control and TMEM165 KO HEK293 cells treated or not with 500 μM CaCl<sub>2</sub> and 1 mM sodium pyruvate on LAMP2 glycosylation. Total cell lysates were prepared, and then subjected to SDS-PAGE and Western blot with indicated antibodies.

## Discussion

TMEM165 deficiency was recently found to lead to a type II CDG associated with strong Golgi glycosylation abnormalities (1). Our previous work has shown that these glycosylation abnormalities in TMEM165 KO cells could result from a lack of Golgi Mn<sup>2+</sup> (4). Many Golgi glycosyltransferases using UDP sugars as a donor substrate, such as UDP-Gal:N-acetylglucosamine β-1,4-galactosyltransferase I (B4GALT1; EC 2.4.1.22) and UDP-Gal:N-acetylglucosamine β-1,4-galactosyltransferase II (B4GALT2; EC 2.4.1.22), are indeed known to require Mn<sup>2+</sup> in their catalytic site to be fully active. Indeed, as it has been well described by Ramakrishnan et al. (19), Mn<sup>2+</sup> first needs to bind the enzyme in a so-called open conformation to then allow the binding of the nucleotide sugar. Once in this enzyme-Mn<sup>2+</sup>-nucleotide sugar conformation, the acceptor substrates bind it, and the catalysis can start. Remarkably, we have demonstrated that 1 μM MnCl<sub>2</sub> supplementation was sufficient to completely suppress the glycosylation defects in TMEM165 KO cells. The underlying mechanism of this glycosylation rescue by Mn<sup>2+</sup> was however unknown.

To address this point, LAMP2 was used as a reporter glycoprotein to finely study the Mn<sup>2+</sup>-induced mechanism of Golgi glycosylation rescue. We have clearly shown that after 8 h 1 μM MnCl<sub>2</sub> treatment, newly synthesized LAMP2 was already fully glycosylated in TMEM165 KO cells. Moreover, and in line with its turnover, half of LAMP2 is fully glycosylated after 24-h treatment, and almost all LAMP2 is fully glycosylated after 64-h treatment. This showed that

LAMP2 could be used to study glycosylation kinetics and that 1  $\mu\text{M}$   $\text{MnCl}_2$  was able to totally suppress the glycosylation defect observed on LAMP2 in TMEM165 KO HEK293 cells.

The first step of this glycosylation rescue induced by 1  $\mu\text{M}$   $\text{MnCl}_2$  is the  $\text{Mn}^{2+}$  uptake at the plasma membrane. This can be done either by endocytosis or through transporters. Using CQ, nocodazole, and MBCD, 3 drugs known to disrupt endocytosis (14), we have demonstrated that none of these drugs prevented the glycosylation rescue after 1  $\mu\text{M}$   $\text{MnCl}_2$  exposure in TMEM165 KO cells, thus suggesting that  $\text{Mn}^{2+}$  does not enter into cells via endocytosis. This can easily be explained by the presence of several plasma membrane transporters known to import  $\text{Mn}^{2+}$ . This includes the divalent metal transporter 1 (DMT1/NRAMP2/SLC11A2) (20, 21), NRAMP1 (22), transferrin, and transporters SLC30A10/ZNT8 (23), SLC39A8/ZIP8 (7) and SLC30A14/ZIP14 (24, 25). As a consequence, we reasonably think that  $\text{Mn}^{2+}$  can use a wide set of transporters to directly enter into cells, thus making the identification of the involved transporters difficult, with possibly different answers depending on the cell type.

Once in the cytosol,  $\text{Mn}^{2+}$  needs to reach the Golgi lumen to suppress the Golgi glycosylation defect induced by a lack of TMEM165. In the absence of TMEM165, it is likely that the  $\text{Mn}^{2+}$  supply in the Golgi is achieved via the action of SPCA pumps (SPCA1 and SPCA2) (9, 11, 26). Overexpression of SPCA1 has indeed been shown to increase  $\text{Mn}^{2+}$  accumulation into the Golgi after high  $\text{Mn}^{2+}$  concentrations exposure (27). Given that SPCA2 is not expressed in HEK cells, we have depleted SPCA1 by siRNA and analyzed the status of LAMP2 glycosylation in TMEM165 KO cells in the presence or absence of 1  $\mu\text{M}$   $\text{MnCl}_2$ . The results unequivocally showed that  $\text{Mn}^{2+}$  supplementation could rescue a normal LAMP2 glycosylation in siATP2C1 TMEM165 KO-treated cells. This demonstrates that somehow SPCA1 is not involved in the glycosylation rescue induced by  $\text{Mn}^{2+}$  in TMEM165 KO cells. However, because 5% of SPCA1 still remains after siRNA treatment, we cannot completely exclude the notion that the remaining SPCA1 is sufficient to efficiently transport  $\text{Mn}^{2+}$  from the cytosol to the Golgi apparatus to rescue glycosylation.

We then investigated the hypothesis that  $\text{Mn}^{2+}$  could reach the ER before being transported to the Golgi compartment. The effects of specific inhibitors of sarcoplasmic reticulum calcium ATPase, Tg, and CPA were investigated. Interestingly, we did demonstrate that  $\text{Mn}^{2+}$  supplementation could not rescue a correct LAMP2 glycosylation in cells treated with CPA (100  $\mu\text{M}$ ) or Tg (50 nM). Importantly, these used concentrations of CPA and Tg did not inhibit the activity of SPCA1. Indeed, Chen et al. (28), recently showed that SPCA1 inhibition by either

CPA or Tg occurred from 182 to 7  $\mu\text{M}$ , respectively. As we demonstrated using ICP-MS, neither CPA nor TG treatment prevented the cellular  $\text{Mn}^{2+}$  entry; our results suggest that the observed Golgi glycosylation rescue induced by  $\text{Mn}^{2+}$  supplementation could come from ER/Golgi uptake via Tg and CPA sensitive proteins. To address the potential involvement of SERCA pumps, SERCA2b (the main isoform expressed in HEK cells) overexpression in TMEM165 KO HEK293 cells was performed. Although partial, the LAMP2 glycosylation profile is clearly enhanced, which suggests the involvement of SERCA2b protein in the  $\text{Mn}^{2+}$  rescued glycosylation of LAMP2.

The importance of SERCA pumps in the observed Golgi glycosylation rescue was quite unexpected, and the molecular mechanisms by which SERCA pumps are involved in the  $\text{Mn}^{2+}$  rescued Golgi glycosylation in TMEM165 KO cells remain unknown. One can expect that under  $\text{Mn}^{2+}$  supplementation, cytosolic  $\text{Mn}^{2+}$  is directly pumped by SERCA into the ER. Such role has already been documented in the literature. Chiesi and Inesi (17) showed in sarcoplasmic reticulum vesicles that a  $\text{Ca}^{2+}$  ATPase could indeed be activated by  $\text{Mn}^{2+}$  and was even able to import  $\text{Mn}^{2+}$  instead of  $\text{Ca}^{2+}$ , but at slower rate. It was also confirmed, many years ago, that SERCA1a was able to transport  $\text{Mn}^{2+}$  instead of  $\text{Ca}^{2+}$  with similar activation energies using the same mechanism but with a much lower affinity (18). Another hypothesis that we cannot exclude would be the crucial importance of ER/Golgi  $\text{Ca}^{2+}$  homeostasis in the  $\text{Mn}^{2+}$ -induced Golgi glycosylation rescue. Some Golgi glycosyltransferases, and particularly the Golgi  $\beta 4\text{GalT1}$  (EC 2.4.1.38) enzyme, possesses 2 metal binding sites. Site I binds  $\text{Mn}^{2+}$  with high affinity, and site II binds diverse metal ions including  $\text{Ca}^{2+}$  (18). It could be possible that a decrease in ER/Golgi  $\text{Ca}^{2+}$  homeostasis completely inhibits, *in cellulo*, the activity of  $\beta 4\text{GalT1}$  even under  $\text{Mn}^{2+}$  supplementation.

Overall, our results shed light on the involvement of Tg- and CPA-sensitive pumps, most likely SERCA pump, in the rescue of TMEM165-associated glycosylation defects by  $\text{Mn}^{2+}$ .

### **Acknowledgments**

The authors are indebted to D. Legrand [Federation of Research Structural and Functional Biochemistry of Biomolecular Assemblies (FRABio), University of Lille] for providing the scientific and technical environment conducive to achieving this work. The authors thank the staff of the BioImagingCenter of Lille, especially C. Slomianny and E. Richard, for the use of the Leica LSM700 and LSM780 devices. The authors are indebted to D. Mouajjah (Centre National

de la Recherche Scientifique Unités Mixte de Recherche 8576, University of Lille) for her helpful assistance in mass spectrometry experiments, and D. Allorge (Centre Hospitalier Universitaire Lille, EA 4483) for her kind assistance in ICP-MS experiments. This work was supported by the French National Research Agency (SOLV-CDG to F.F.) and the Mizutani Foundation for Glycoscience (to F.F.). The authors declare no conflicts of interest.

### Author contributions

S. Potelle and F. Foulquier designed the research; M. Houdou, E. Lebredonchel, and V. Decool performed the experiments; M. Houdou, S. Duvet, and S. Potelle analyzed data; M. Houdou, S. Potelle, and F. Foulquier wrote the manuscript; A. Garat developed and optimized the ICP-MS analysis and kindly gave access to the platform for the experiments; and D. Legrand, A. Klein, M. Ouzzine, and B. Gasnier helped edit the manuscript and provided useful advice.

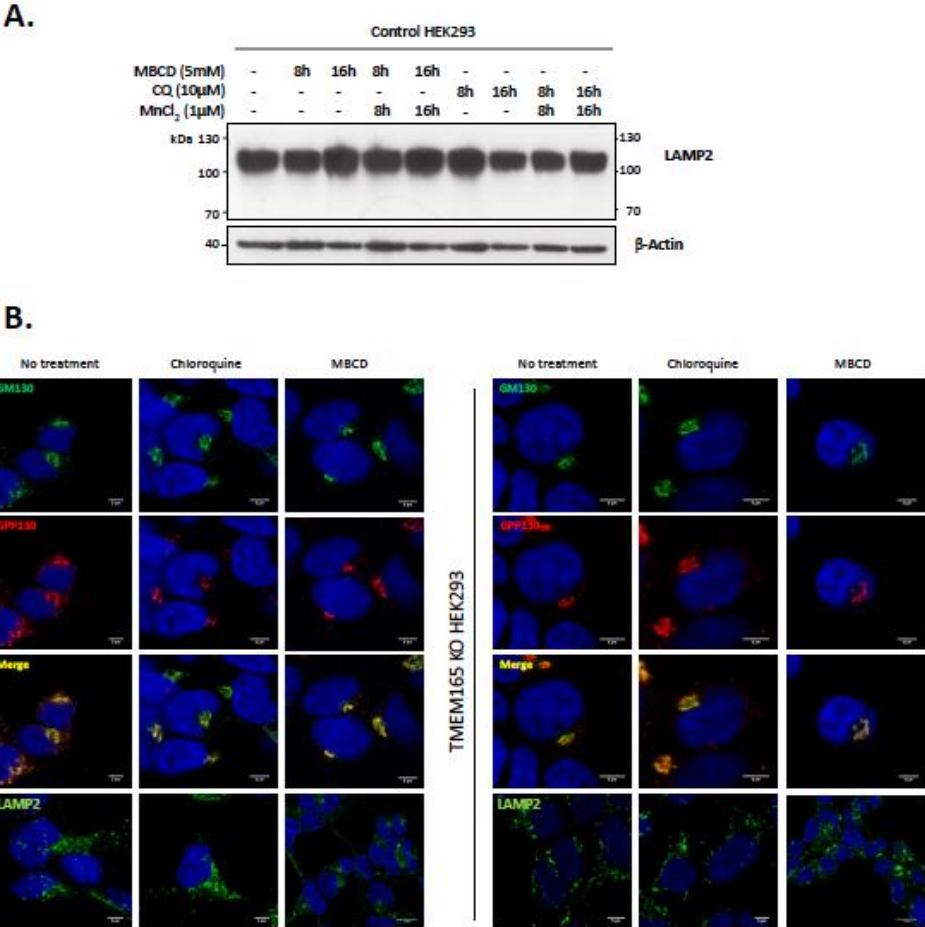
### References

1. Foulquier, F., Amyere, M., Jaeken, J., Zeevaert, R., Schollen, E., Race, V., Bammens, R., Morelle, W., Rosnoblet, C., Legrand, D., Demaegd, D., Buist, N., Cheillan, D., Guffon, N., Morsomme, P., Annaert, W., Freeze, H. H., Van Schaftingen, E., Vikkula, M., and Matthijs, G. (2012) TMEM165 deficiency causes a congenital disorder of glycosylation. *Am. J. Hum. Genet.* 91, 15–26
2. Zeevaert, R., de Zegher, F., Sturiale, L., Garozzo, D., Smet, M., Moens, M., Matthijs, G., and Jaeken, J. (2013) Bone dysplasia as a key feature in three patients with a novel congenital disorder of glycosylation (CDG) type II due to a deep intronic splice mutation in TMEM165. *JIMD Rep.* 8, 145–152
3. Demaegd, D., Foulquier, F., Colinet, A.-S., Gremillon, L., Legrand, D., Mariot, P., Peiter, E., Van Schaftingen, E., Matthijs, G., and Morsomme, P. (2013) Newly characterized Golgi-localized family of proteins is involved in calcium and pH homeostasis in yeast and human cells. *Proc. Natl. Acad. Sci. USA* 110, 6859–6864
4. Potelle, S., Morelle, W., Dulary, E., Duvet, S., Vicogne, D., Spriet, C., Krzewinski-Recchi, M.-A., Morsomme, P., Jaeken, J., Matthijs, G., De Bettignies, G., and Foulquier, F. (2016) Glycosylation abnormalities in Gdt1p/TMEM165 deficient cells result from a defect in Golgi manganese homeostasis. *Hum. Mol. Genet.* 25, 1489–1500
5. Schneider, A., Steinberger, I., Herdean, A., Gandini, C., Eisenhut, M., Kurz, S., Morper, A., Hoecker, N., Röhle, T., Labs, M., Flügge, U.-I., Geimer, S., Schmidt, S. B., Husted, S., Weber, A. P. M., Spetea, C., and Leister, D. (2016) The evolutionarily conserved protein photosynthesis affected mutant71 is required for efficient manganese uptake at the thylakoid membrane in Arabidopsis. *Plant Cell* 28, 892–910
6. Powell, J. T., and Brew, K. (1976) Metal ion activation of galactosyltransferase. *J. Biol. Chem.* 251, 3645–3652
7. Park, J. H., Hogrebe, M., Grüneberg, M., DuChesne, I., von der Heiden, A. L., Reunert, J., Schlingmann, K. P., Boycott, K. M., Beaulieu, C. L., Mhanni, A. A., Innes, A. M., Hörtornagel, K., Biskup, S., Gleixner, E. M., Kurlemann, G., Fiedler, B., Omran, H., Rutsch, F., Wada, Y., Tsiakas, K., Santer, R., Nebert, D. W., Rust, S., and Marquardt, T. (2015) SLC39A8 deficiency: a disorder of manganese transport and glycosylation. *Am. J. Hum. Genet.* 97, 894–903

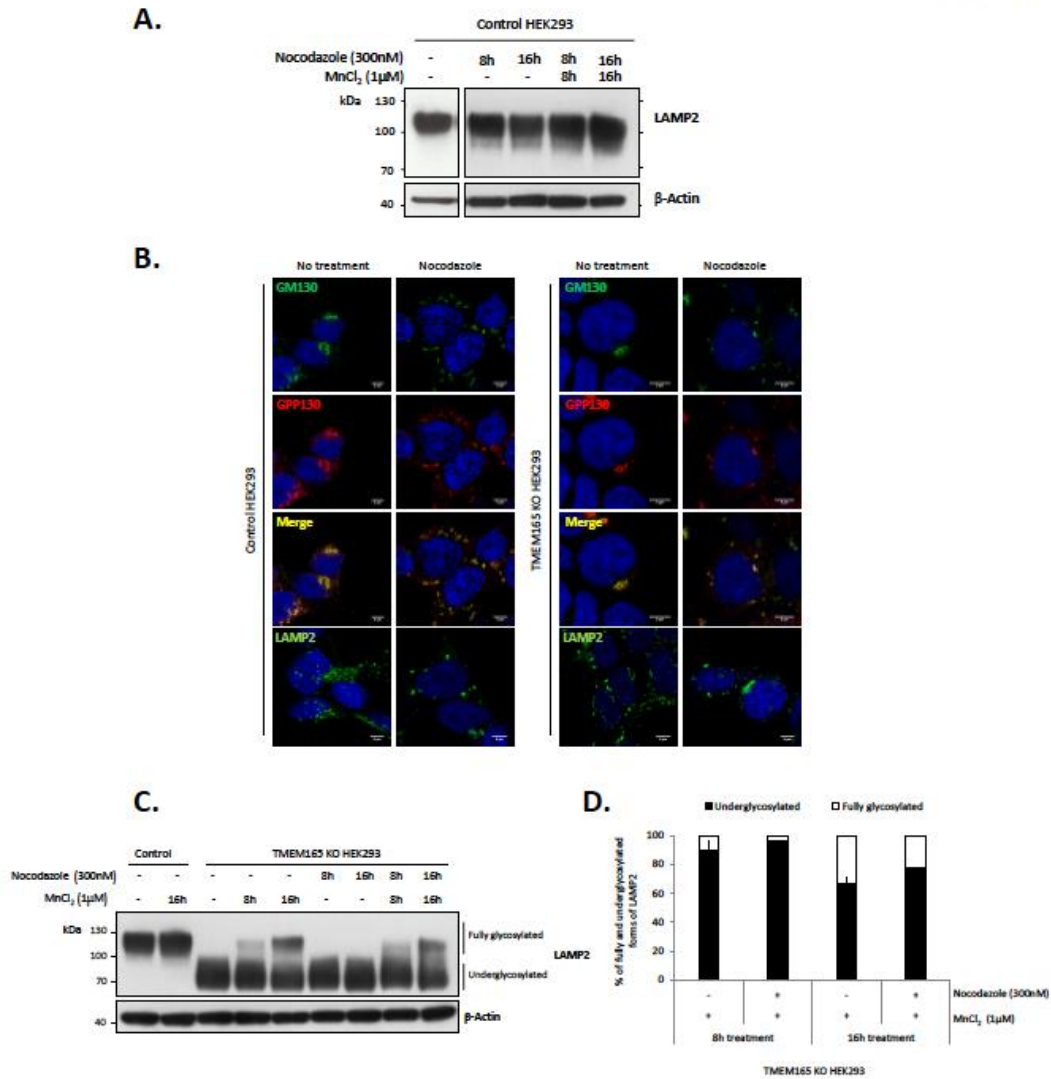
8. Bonifacino, J. S., and Rojas, R. (2006) Retrograde transport from endosomes to the trans-Golgi network. *Nat. Rev. Mol. Cell Biol.* 7, 568–579
9. He, W., and Hu, Z. (2012) The role of the Golgi-resident SPCA Ca<sup>2+</sup>/Mn<sup>2+</sup> pump in ionic homeostasis and neural function. *Neurochem. Res.* 37, 455–468
10. Micaroni, M., Perinetti, G., Berrie, C. P., and Mironov, A. A. (2010) The SPCA1 Ca<sup>2+</sup> pump and intracellular membrane trafficking. *Traffic* 11, 1315–1333; erratum: 12, 789
11. Van Baelen, K., Dode, L., Vanoevelen, J., Callewaert, G., De Smedt, H., Missiaen, L., Parys, J. B., Raeymaekers, L., and Wuytack, F. (2004) The Ca<sup>2+</sup>/Mn<sup>2+</sup> pumps in the Golgi apparatus. *Biochim. Biophys. Acta* 1742, 103–112
12. Roth, J. A. (2006) Homeostatic and toxic mechanisms regulating manganese uptake, retention, and elimination. *Biol. Res.* 39, 45–57
13. Delannoy, C. P., Rombouts, Y., Groux-Degroote, S., Holst, S., Coddeville, B., Harduin-Lepers, A., Wuhrer, M., Ellass-Rochard, E., and Guérardel, Y. (2017) Glycosylation changes triggered by the differentiation of monocytic THP-1 cell line into macrophages. *J. Proteome Res.* 16, 156–169
14. Dutta, D., and Donaldson, J. G. (2012) Search for inhibitors of endocytosis: intended specificity and unintended consequences. *Cell. Logist.* 2, 203–208
15. Bayer, N., Schober, D., Prchla, E., Murphy, R. F., Blaas, D., and Fuchs, R. (1998) Effect of bafilomycin A1 and nocodazole on endocytic transport in HeLa cells: implications for viral uncoating and infection. *J. Virol.* 72, 9645–9655
16. Chiesi, M., and Inesi, G. (1980) Adenosine 59-triphosphate dependent fluxes of manganese and hydrogen ions in sarcoplasmic reticulum vesicles. *Biochemistry* 19, 2912–2918
17. Chiesi, M., and Inesi, G. (1981) Mg<sup>2+</sup> and Mn<sup>2+</sup> modulation of Ca<sup>2+</sup> transport and ATPase activity in sarcoplasmic reticulum vesicles. *Arch. Biochem. Biophys.* 208, 586–592
18. Yonekura, S.-I., and Toyoshima, C. (2016) Mn<sup>2+</sup> transport by Ca<sup>2+</sup>-ATPase of sarcoplasmic reticulum. *FEBS Lett.* 590, 4650; erratum: 2086–2095
19. Ramakrishnan, B., Ramasamy, V., and Qasba, P. K. (2006) Structural snapshots of beta-1,4-galactosyltransferase-I along the kinetic pathway. *J. Mol. Biol.* 357, 1619–1633
20. Au, C., Benedetto, A., and Aschner, M. (2008) Manganese transport in eukaryotes: the role of DMT1. *Neurotoxicology* 29, 569–576
21. Garrick, M. D., Dolan, K. G., Horbinski, C., Ghio, A. J., Higgins, D., Porubcin, M., Moore, E. G., Hainsworth, L. N., Umbreit, J. N., Conrad, M. E., Feng, L., Lis, A., Roth, J. A., Singleton, S., and Garrick, L. M. (2003) DMT1: a mammalian transporter for multiple metals. *Biometals* 16, 41–54
22. Forbes, J. R., and Gros, P. (2003) Iron, manganese, and cobalt transport by Nramp1 (Slc11a1) and Nramp2 (Slc11a2) expressed at the plasma membrane. *Blood* 102, 1884–1892
23. Chen, P., Bowman, A. B., Mukhopadhyay, S., and Aschner, M. (2015) SLC30A10: a novel manganese transporter. *Worm* 4, e1042648
24. Chen, P., Chakraborty, S., Mukhopadhyay, S., Lee, E., Paoliello, M. M. B., Bowman, A. B., and Aschner, M. (2015) Manganese homeostasis in the nervous system. *J. Neurochem.* 134, 601–610
25. Girijashanker, K., He, L., Soleimani, M., Reed, J. M., Li, H., Liu, Z., Wang, B., Dalton, T. P., and Nebert, D. W. (2008) Slc39a14 gene encodes ZIP14, a metal/bicarbonate symporter: similarities to the ZIP8 transporter. *Mol. Pharmacol.* 73, 1413–1423

26. Vandecaetsbeek, I., Vangheluwe, P., Raeymaekers, L., Wuytack, F., and Vanoevelen, J. (2011) The Ca<sup>2+</sup> pumps of the endoplasmic reticulum and Golgi apparatus. *Cold Spring Harb. Perspect. Biol.* 3, a004184
27. Mukhopadhyay, S., and Linstedt, A.D. (2011) Identification of a gain-of function mutation in a Golgi P-type ATPase that enhances Mn<sup>2+</sup> efflux and protects against toxicity. *Proc. Natl. Acad. Sci. USA* 108, 858–863
28. Chen, J., De Raeymaecker, J., Hovgaard, J. B., Smaardijk, S., Vandecaetsbeek, I., Wuytack, F., Møller, J. V., Eggermont, J., De Maeyer, M., Christensen, S. B., and Vangheluwe, P. (2017) Structure/activity relationship of thapsigargin inhibition on the purified Golgi/secretory pathway Ca<sup>2+</sup>/Mn<sup>2+</sup>-transport ATPase (SPCA1a). *J. Biol. Chem.* 292, 6938–6951

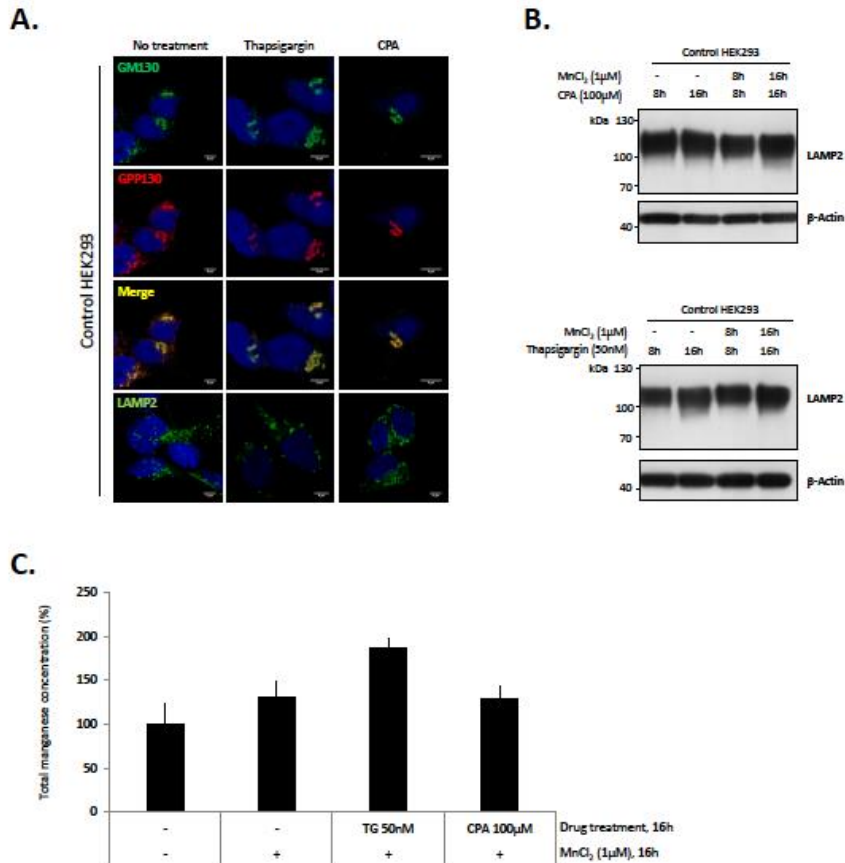
Supplementary figures



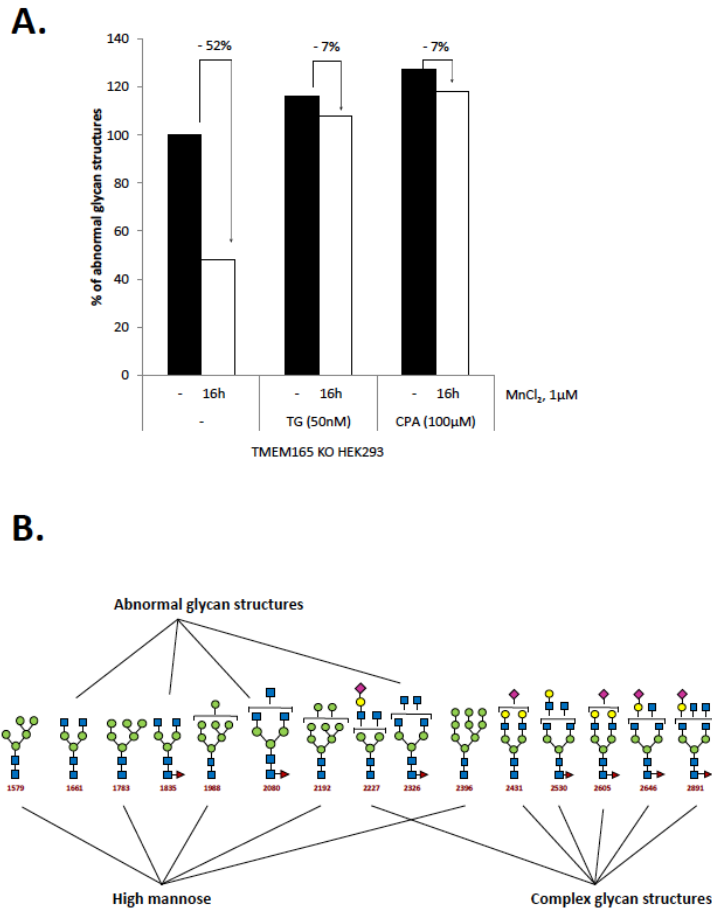
**Supplementary figure 1: Effect of chloroquine (CQ) and methyl-β-cyclodextrin (MBCD) on Golgi morphology, LAMP2 subcellular localization and glycosylation profile.** A. Control HEK293 cells were incubated with CQ (10μM) or MBCD (5mM) for 8h or 16h, in combination or not with 1μM MnCl<sub>2</sub>. Total cell lysates were prepared, subjected to SDS-PAGE and western blot with the indicated antibodies. B. Immunofluorescence analysis. Control and TMEM165 KO HEK293 cells were incubated with CQ (10μM) or MBCD (5mM) for 16h, fixed, permeabilized and labeled with antibodies against GM130, GPP130 and LAMP2 before confocal microscopy visualization. DAPI staining (blue) was performed, showing nuclei.



**Supplementary figure 2: Effect of nocodazole on Golgi morphology, LAMP2 subcellular localization and glycosylation profile.** A. and C. Control and TMEM165 KO HEK293 cells were incubated with nocodazole (300nM) for 8h or 16h, in combination or not with 1μM MnCl<sub>2</sub>. Total cell lysates were prepared, subjected to SDS-PAGE and western blot with the indicated antibodies. B. Immunofluorescence analysis. Control and TMEM165 KO HEK293 cells were incubated with nocodazole (300nM) for 16h, fixed, permeabilized and labeled with antibodies against GM130, GPP130 and LAMP2 before confocal microscopy visualization. DAPI staining (blue) was performed, showing nuclei. D. Relative quantification of fully and underglycosylated forms of LAMP2 (N, number of experiments = 2).



**Supplementary figure 3: Effect of thapsigargin (TG) and cyclopiazonic acid (CPA) on Golgi morphology, LAMP2 subcellular localization and glycosylation profile and manganese uptake.** A. Immunofluorescence analysis. Control cells were incubated with either TG (50nM) or CPA (100µM) for 16h, fixed, permeabilized and labeled with antibodies against GM130, GPP130 and LAMP2 before confocal microscopy visualization. DAPI staining (blue) was performed, showing nuclei. B. Control HEK293 cells were incubated with either TG (50nM) or CPA (100µM) for 8h or 16h, in combination or not with 1µM MnCl<sub>2</sub>. Total cell lysates were prepared, subjected to SDS-PAGE and western blot with the indicated antibodies. C. TMEM165 KO HEK293 cells were cultured with either TG (50nM) or CPA (100µM) in combination with 1µM MnCl<sub>2</sub> for 16h. Total cell lysates were prepared as described in Material and Methods section for ICP-MS analysis and total manganese concentration was measured (N = 2, n, number of samples = 4).



**Supplementary figure 4: Quantification of the abnormal structures found in TMEM165 KO HEK293 cells treated with TG or CPA and with or without Mn<sup>2+</sup>.** A. Quantification of abnormal glycan structures observed in TMEM165 KO HEK293 cells following the different indicated treatments. B. Representative glycan structures taken into account for the quantification (abnormal glycan structures with mass-per-charge ratios (m/z) 1661, 1835, 2080 and 2326; high mannose structures with mass-per-charge ratios (m/z) 1579, 1783, 1988, 2192 and 2396; complex glycan structures mass-per-charge ratios m(z) 2227, 2431, 2530, 2605, 2646 and 2891). Symbols represent sugar residues as follow: blue square, N-acetylglucosamine; green circle, mannose; yellow circle, galactose; purple diamond, sialic acid; red triangle, fucose. Linkages between sugar residues have been removed for simplicity.

## Manganese-induced turnover of TMEM165

Sven Potelle<sup>1</sup>, Eudoxie Dulary<sup>1</sup>, Leslie Climer<sup>2</sup>, Sandrine Duvet<sup>1</sup>, Willy Morelle<sup>1</sup>, Dorothée Vicogne<sup>1</sup>, Elodie Lebredonchel<sup>1</sup>, Marine Houdou<sup>1</sup>, Corentin Spriet<sup>1</sup>, Marie-Ange Krzewinski-Recchi<sup>1</sup>, Romain Peanne<sup>3</sup>, André Klein<sup>1</sup>, Geoffroy de Bettignies<sup>1</sup>, Pierre Morsomme<sup>4</sup>, Gert Matthijs<sup>3</sup>, Thorsten Marquardt<sup>5</sup>, Vladimir Lupashin<sup>2</sup> and François Foulquier<sup>1</sup>

<sup>1</sup>CNRS, UMR 8576 – UGSF – Unité de Glycobiologie Structurale et Fonctionnelle, Université de Lille, Lille F-59000, France;

<sup>2</sup>Department of Physiology and Biophysics, College of Medicine, University of Arkansas for Medical Sciences, Biomed 261-2, Slot 505, 200 South Cedar St., Little Rock, AR 72205, U.S.A.; <sup>3</sup>Center for Human Genetics, KU Leuven, Leuven, Belgium;

<sup>4</sup>Institut des Sciences de la Vie, Université catholique de Louvain, Louvain-la-Neuve B-1348, Belgium;

<sup>5</sup>Klinik und Poliklinik für Kinder- und Jugendmedizin, Universitätsklinikum Münster, Albert-Schweitzer-Campus 1, Gebäude A 1, Münster 48149, Germany

Correspondance: François Foulquier ([francois.foulquier@univ-lille1.fr](mailto:francois.foulquier@univ-lille1.fr))

### Abstract

TMEM165 deficiencies lead to one of the congenital disorders of glycosylation (CDG), a group of inherited diseases where the glycosylation process is altered. We recently demonstrated that the Golgi glycosylation defect due to TMEM165 deficiency resulted from a Golgi manganese homeostasis defect and that Mn<sup>2+</sup> supplementation was sufficient to rescue normal glycosylation. In the present paper, we highlight TMEM165 as a novel Golgi protein sensitive to manganese. When cells were exposed to high Mn<sup>2+</sup> concentrations, TMEM165 was degraded in lysosomes. Remarkably, while the variant R126H was sensitive upon manganese exposure, the variant E108G, recently identified in a novel TMEM165-CDG patient, was found to be insensitive. We also showed that the E108G mutation did not abolish the function of TMEM165 in Golgi glycosylation. Altogether, the present study identified the Golgi protein TMEM165 as a novel Mn<sup>2+</sup>-sensitive protein in mammalian cells and pointed to the crucial importance of the glutamic acid (E108) in the cytosolic ELGDK motif in Mn<sup>2+</sup>-induced degradation of TMEM165.

### Introduction

Manganese is a trace element essential for life. It is involved in the catalytic domain of many enzymes such as Golgi glycosyltransferases, mitochondrial enzymes, and DNA and RNA polymerases. Regulation of its homeostasis is therefore particularly important. Manganese overexposure has been shown to induce neurological symptoms that can result in a Parkinson-like disorder called manganism [1–3]. On the contrary, a decrease in cellular Mn<sup>2+</sup> has recently been shown to cause congenital disorders of glycosylation (CDG). Mutations in SLC39A8, a putative plasma membrane manganese transporter, lead to severe glycosylation

defects [4]. We recently reported that TMEM165 deficiency was also linked with Golgi Mn<sup>2+</sup> homeostasis [5]. Although progress has been made in identifying cellular Mn<sup>2+</sup> transporters in mammals, the mechanisms of Mn<sup>2+</sup> homeostasis are still unclear. Several different transporters have been involved in manganese transport mechanisms, including the divalent metal transporter 1 (DMT1/NRAMP2/SLC11A2) [1,6], NRAMP1 [7], the transferrin receptor, and the transporters SLC30A10/ZNT8 [8], SLC39A8/ZIP8 [4], and SLC30A14/ZIP14 [9,10]. At the cellular level, most of these transporters are localized at the plasma membrane and/or in endosomes. The secretory pathway consisting of the ER, the Golgi and associated vesicles is also crucial in regulating cellular Mn<sup>2+</sup> homeostasis. In addition, the secretory pathway requires luminal Mn<sup>2+</sup> concentration for quality control, proper targeting and processing of proteins. Current knowledge supports that this supply is realized via the action of SPCA1 (secretory pathway Ca-ATPase 1: ATP2C1) and SPCA2 (ATP2C2). SPCA1 is ubiquitously expressed and mediates the import of Ca<sup>2+</sup>/Mn<sup>2+</sup> into the Golgi lumen [11,12]. The tissue expression of SPCA2 is more restricted. However, the importance of the dual transport function in cellular processes is not yet completely deciphered [11]. Overexpression of SPCA1 has been shown to facilitate Mn<sup>2+</sup> accumulation into the Golgi [13] and it was thus proposed that SPCA1 was a way to detoxify cytosolic Mn<sup>2+</sup> accumulation by sequestering it into the secretory pathway.

In 2012, we identified TMEM165 as a novel Golgi transmembrane protein causing CDG [14]. It belongs to an uncharacterized family of membrane proteins named UPF0016 (Uncharacterized Protein Family 0016; Pfam PF01169). We recently demonstrated that the observed Golgi glycosylation defect resulted from Golgi Mn<sup>2+</sup> homeostasis impairment [5]. Based on these results, we hypothesized that TMEM165 could be a novel Golgi Mn<sup>2+</sup> transporter. As studies of Mn<sup>2+</sup> homeostasis in yeasts have indicated that most of the proteins involved in regulating intracellular Mn<sup>2+</sup> concentrations are differentially targeted and/or degraded in response to Mn<sup>2+</sup>, the role of TMEM165 was tested. The aim of the present study was to decipher the impact of high extracellular Mn<sup>2+</sup> concentrations on the subcellular localization and stability of TMEM165. The present study demonstrates that high concentrations of extracellular Mn<sup>2+</sup> lead to a rapid lysosomal degradation of TMEM165. We identified the glutamic acid (E108) in the highly conserved motif ELGDK, oriented toward the cytosol, as being crucial in the Mn-induced degradation of TMEM165.

## Results

### TMEM165 is rapidly and specifically degraded in response to Mn<sup>2+</sup>

Our previous work highlighted a link between TMEM165 and Golgi Mn<sup>2+</sup> homeostasis [5]. As many proteins involved in regulating intracellular Mn<sup>2+</sup> homeostasis are directly impacted in their stability by cellular Mn<sup>2+</sup> homeostasis changes, the effect of Mn<sup>2+</sup> on TMEM165 was tested. For this, a concentration of 500  $\mu$ M of MnCl<sub>2</sub> was first used for different times and the stability of TMEM165 was assessed both by western blot and immunofluorescence experiments. We observed that in response to Mn<sup>2+</sup>, TMEM165 levels were significantly reduced (Figure 1A,B). Interestingly, the same sensitivity to Mn<sup>2+</sup> was observed for Gdt1p, the yeast ortholog of TMEM165 (Figure 1D). The effects of other ions were also tested (Supplementary Figure S1). Remarkably, we observed that TMEM165 degradation only occurred after MnCl<sub>2</sub> exposure, pointing to the specificity of TMEM165 for Mn<sup>2+</sup>. As GPP130 has also been shown to be sensitive to high Mn<sup>2+</sup> concentrations, we compared its time course degradation with TMEM165 (Figure 1A–C). Quantification indicated that TMEM165 loss exceeded 95% after 8 h of Mn<sup>2+</sup> treatment, while only a 40% decrease was seen for GPP130. To further tackle the minimal Mn<sup>2+</sup> concentration able to induce a loss of TMEM165, we analyzed the stability of TMEM165 with low MnCl<sub>2</sub> concentrations (1–50  $\mu$ M). While 100  $\mu$ M MnCl<sub>2</sub> was sufficient to induce GPP130 degradation [15], our results showed that 1–25  $\mu$ M of Mn<sup>2+</sup> was already sufficient to induce a destabilization of TMEM165 (Figure 1B). Altogether these results indicate that TMEM165, compared with GPP130, is more sensitive to manganese and probably suggests the existence of different degradation mechanisms in response to Mn<sup>2+</sup>. The impact of Mn<sup>2+</sup> on TMEM165 was also seen by immunofluorescence where a decrease in TMEM165 fluorescence associated with Golgi was seen (Supplementary Figure S2A, B). We previously demonstrated that TMEM165 could be found at the plasma membrane [14]. To assess the impact of Mn<sup>2+</sup> on the plasma membrane targeted form of TMEM165, surface protein biotinylation was performed in the absence and presence of 500  $\mu$ M of MnCl<sub>2</sub>. Interestingly biotin-labeled cell surface TMEM165 displayed the same sensitivity to Mn<sup>2+</sup> as the cellular TMEM165. This either suggests that the Mn<sup>2+</sup>-induced degradation mechanism is not only dedicated to the Golgi pool of TMEM165 or that less TMEM165 traffics to the plasma membrane from the Golgi when the Golgi pool of TMEM165 has been depleted upon excess manganese exposure (Figure 2A). Previous studies have also demonstrated that in yeast, high environmental Ca<sup>2+</sup> concentrations in *gdt1 $\Delta$*  led to strong N-glycosylation

deficiencies [5]. The impact of Ca<sup>2+</sup> on Mn<sup>2+</sup>-induced degradation of TMEM165 was assessed by western blot and immunofluorescence (Figure 2B, C). Ca<sup>2+</sup> alone had no significant effect on the stability of TMEM165. However, its combined presence with Mn<sup>2+</sup> clearly decreased the Mn<sup>2+</sup>-induced degradation of TMEM165 (80% decrease for the Mn<sup>2+</sup> treatment alone compared with 40% decrease for both Ca<sup>2+</sup> and Mn<sup>2+</sup>; Figure 2B). This was confirmed by confocal microscopy (Figure 2C).

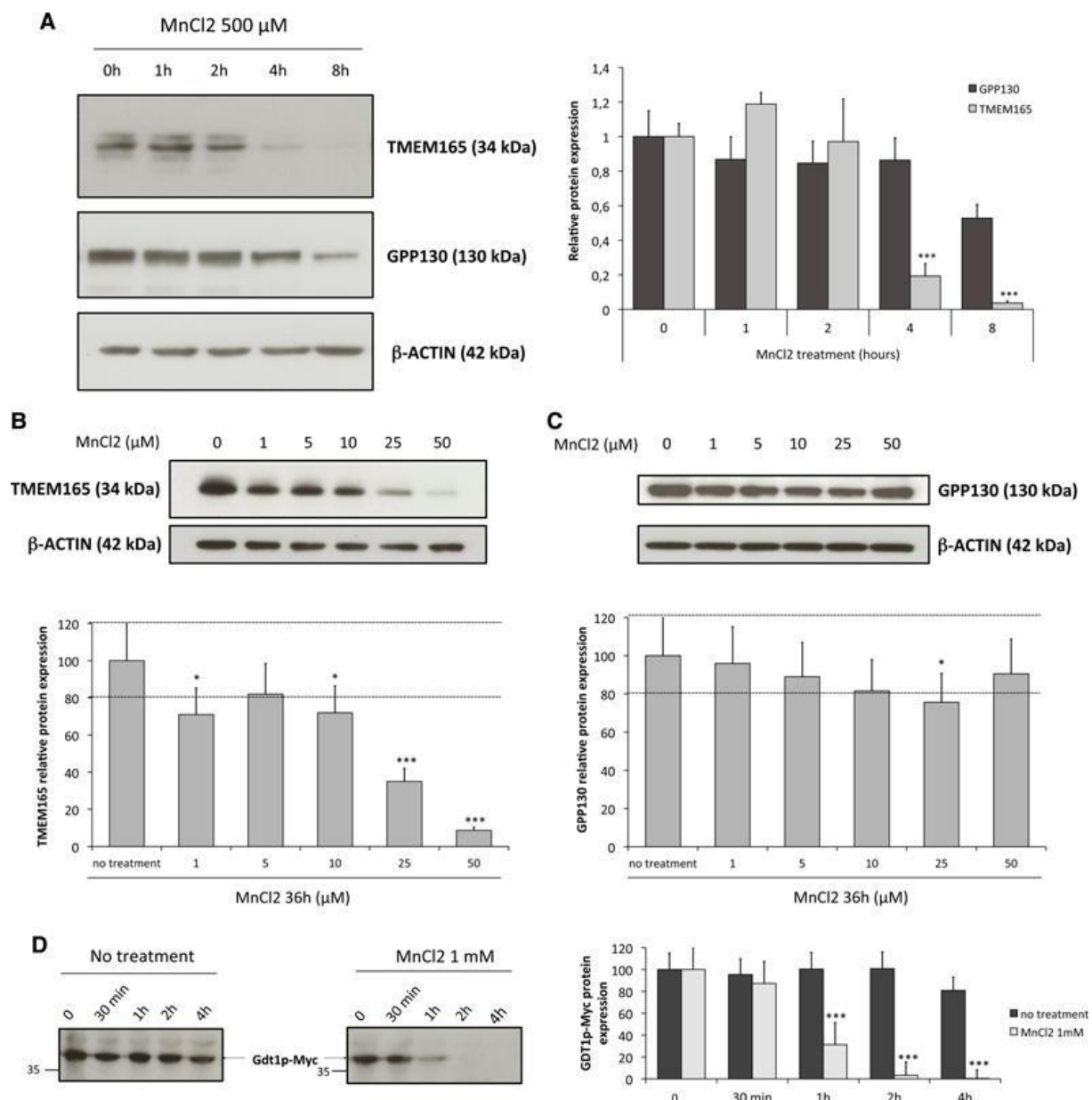


**Figure 1. TMEM is rapidly degraded in response to Mn<sup>2+</sup>.** (A) Steady-state cellular level of TMEM165 and GPP130. HeLa cells were treated with MnCl<sub>2</sub> 500  $\mu$ M for 0–8 h. Total cell lysates were prepared, and subjected to SDS–PAGE and western blot with the indicated antibodies. Right panel shows the quantification of TMEM165 and GPP130 protein levels after normalization with actin [Number of experiments (N) = 2; \*\*\*P-value < 0.001]. (B) Steady-state cellular level of TMEM165. HEK293 cells were treated with MnCl<sub>2</sub> from 0 to 50  $\mu$ M for 36 h. Total cell lysates were prepared, and subjected to SDS–PAGE and western blot with the indicated antibodies. Lower panel shows the quantification of TMEM165 protein levels after normalization with actin (N = 2; \*\*\*P-value < 0.001). (C) Steady-state cellular level of GPP130 in the same experimental conditions as described in (B). (D) *Gdt1 $\Delta$*  yeasts expressing Gdt1p-Myc were cultured in the absence or presence of 1 mM MnCl<sub>2</sub>. Yeast lysates were then subjected to SDS–PAGE and western blot analysis with the indicated antibodies. Right panel shows the quantification of the Gdt1p-Myc protein levels (N = 2; \*\*\*P-value < 0.001).

## Lysosomal degradation of TMEM165

As shown by Mukhopadhyay et al. [16], 500  $\mu\text{M}$   $\text{MnCl}_2$  treatment induces rapid redistribution of GPP130 in vesicles before their lysosomal degradation. At the opposite of GPP130, no redistribution from the Golgi to peripheral punctate structures was observed for TMEM165 in response to high  $\text{Mn}^{2+}$  concentration (Supplementary Figure S2C). This absence of vesicles could be explained by an extremely fast degradation. To test this hypothesis, the stability of TMEM165 in response to  $\text{Mn}^{2+}$  was studied by immunofluorescence in the presence of chloroquine, a lysosomal inhibitor (Figure 3A).

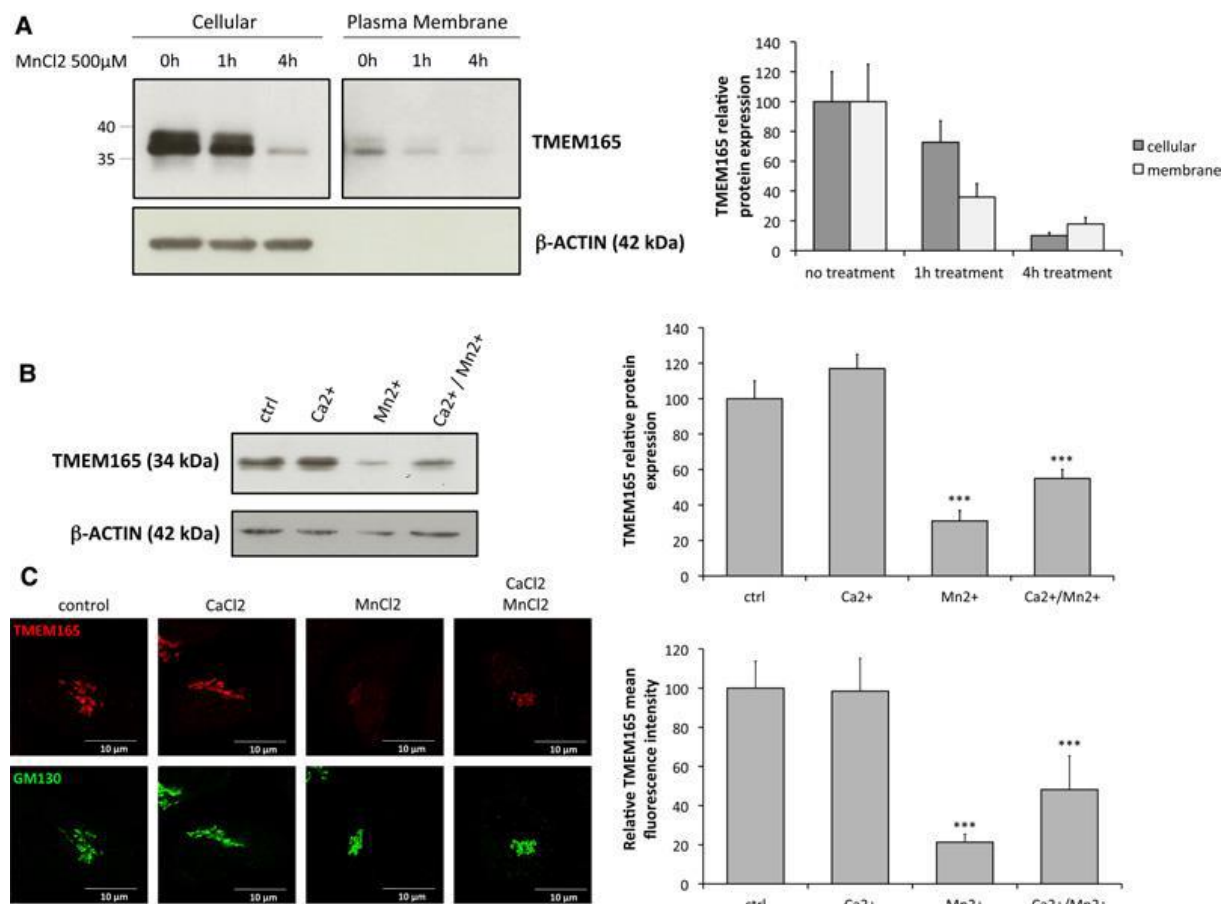


**Figure 2. Plasma membrane TMEM165 is also degraded by  $\text{Mn}^{2+}$  and  $\text{Ca}^{2+}$  compete with  $\text{Mn}^{2+}$  for TMEM165 degradation.** (A) Cell surface biotinylation was performed in the absence and presence of  $\text{MnCl}_2$  500  $\mu\text{M}$ . Samples were prepared as described in the materials and methods section and subjected to SDS-PAGE and western blot with the indicated antibodies. Lower panel shows the quantification of TMEM165 protein levels. The plasma membrane panel is separated from the cellular panel as we had to expose films longer to reveal the bands. (B) HEK293 cells were incubated with 500  $\mu\text{M}$   $\text{MnCl}_2$  and/or 2 mM  $\text{CaCl}_2$  for 4 h, and then subjected to SDS-PAGE and western blot with the indicated antibodies. Right panel shows the quantification of TMEM165 protein levels after normalization with actin (N = 2; \*\*\*P-value < 0.001). (C) HEK293 cells were incubated with 500  $\mu\text{M}$   $\text{MnCl}_2$  and/or 2 mM  $\text{CaCl}_2$  for 4 h, and then fixed and labeled with antibodies against TMEM165 and GM130 before confocal microscopy visualization (N = 2; \*\*\*P-value < 0.001). Right panel shows the quantification of the associated TMEM165 fluorescence intensity (N = 2; n = 50; \*\*\*P-value < 0.001).

Although cells treated with Mn<sup>2+</sup> alone showed a dramatic loss of TMEM165, those treated in the presence of chloroquine exhibited an accumulation of TMEM165 in punctate structures (Figure 3A). Immunofluorescence experiments with LAMP2, a lysosomal marker, confirmed the presence of TMEM165 in LAMP2-positive structures in chloroquine- and Mn<sup>2+</sup>-treated cells. The level of co-localization was determined using Manders' overlap coefficient and revealed a co-localization of TMEM165 with LAMP2 ( $72 \pm 9\%$ ). Same experiments were also done with EEA1 as a specific marker of early endosomes and the quantification revealed no significant co-localization of TMEM165 with EEA1 ( $7 \pm 1\%$ ; data not shown). This result shows that TMEM165 is specifically targeted to lysosomal degradation followed Mn<sup>2+</sup> exposure. To confirm the lysosomal Mn<sup>2+</sup>-induced degradation of TMEM165, an immunoblotting experiment was also performed. As shown in Figure 3B, the Mn-induced degradation of TMEM165 was completely blocked by chloroquine. As chloroquine is known to both shut down endosomal trafficking and inhibit lysosomal proteases, we also tested the effects of leupeptin, a lysosomal protease inhibitor, on the stability of TMEM165 in response to Mn<sup>2+</sup> (Supplementary Figure S3). The experiment confirmed the localization of TMEM165 in LAMP2-positive structure as a co-localization of TMEM165 with LAMP2 ( $62 \pm 1\%$ ) and the absence of co-localization of TMEM165 with EEA1 ( $3 \pm 1\%$ ; data not shown) was observed.

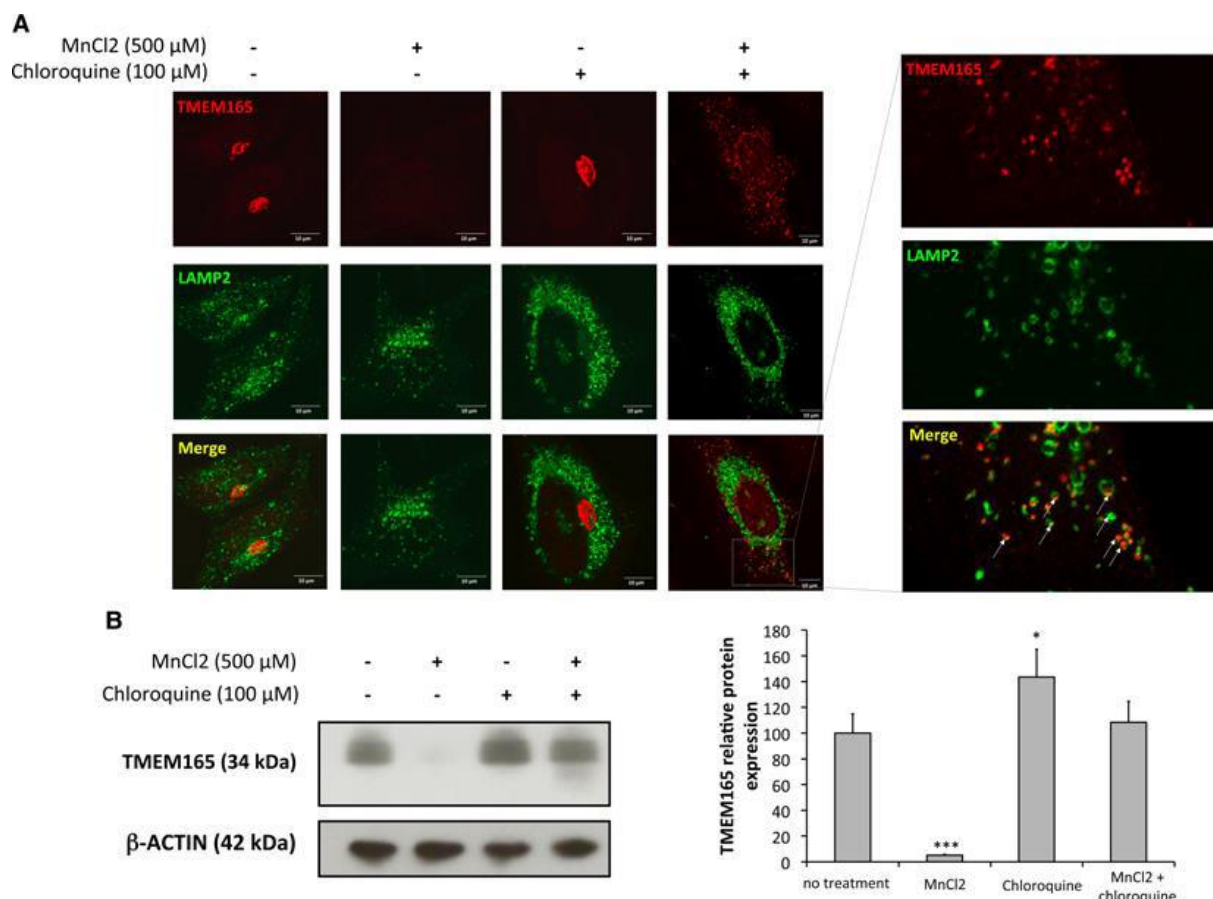


**Figure 3. TMEM165 is targeted to lysosomal degradation after Mn<sup>2+</sup> exposure.** (A) HeLa cells were treated for 8 h with 500 μM MnCl<sub>2</sub> and/or 100 μM chloroquine, and fixed and labeled with antibodies against TMEM165 (upper panels) and LAMP2 (middle panels) before confocal microscopy visualization. (B) Western blot analysis of the same experiment described in (A). Total cell lysates were prepared, and subjected to SDS-PAGE and western blot with the indicated antibodies. Right panel shows the quantification of the TMEM165 protein level after normalization with actin (N = 2; \*\*\*P-value < 0.001).

### The amino acid E108 of the ELGDK motif is involved in Mn<sup>2+</sup>-induced degradation of TMEM165

To gain more insight into the TMEM165 Mn<sup>2+</sup>-induced degradation mechanism, we wondered whether the reported missense mutations (pE108G and pR126H) found in TMEM165-deficient CDG patients could impact the TMEM165 Mn<sup>2+</sup> sensitivity. To test the putative role of these mutations in TMEM165 Mn<sup>2+</sup> responsiveness, immunofluorescence and western blot experiments were performed in the absence and presence of MnCl<sub>2</sub> (Figure 4A,B). The missense mutation c.323 A>G (p.E108G) found in two newly TMEM165 deficient siblings was first tested [17]. As observed for wt-TMEM165, the mutant form is Golgi-localized in fibroblasts for the two siblings. This indicates that the mutation does not disturb the subcellular localization of the mutated form of TMEM165 (Figure 4B). The impact of Mn<sup>2+</sup> treatment was then investigated during an 8 h time course by western blot and

immunofluorescence experiments (Figure 4A, B). As expected, the wild-type (wt) TMEM165 was very sensitive to Mn<sup>2+</sup> exposure (Figure 4A). However, the mutated form of TMEM165 (E108G) remained stable (Figure 4A, B). No changes were observed in localization or stability by immunofluorescence. Quantification of the western blot results indicated that wt-TMEM165 loss exceeded 95% at the 6 h time point, while only 20% loss was observed for the mutated form p.E108G. To demonstrate the distinctive feature of this mutation, fibroblasts from another TMEM165-CDG patient, carrying the R126H mutation, were also tested for Mn<sup>2+</sup> sensitivity by western blot and confocal microscopy (Figure 5). Although the steady-state level of TMEM165, compared with control fibroblasts, is lower in the R126H patients' fibroblasts, our results highlighted that this mutation did not prevent the Mn<sup>2+</sup>-induced TMEM165 (R126H) degradation. It is also important to note that its localization is not altered, neither at the steady-state level nor after chloroquine and Mn<sup>2+</sup> exposure (Supplementary Figure S5). After Mn<sup>2+</sup> and chloroquine exposure, the co-localization between TMEM165 and LAMP2/EEA1 was determined for both control and patient fibroblasts. For control fibroblasts, we observed a co-localization of TMEM165 with LAMP2 (59 ± 5%) and no significant co-localization of TMEM165 with EEA1 (6 ± 1%). For patient fibroblasts (R126H), the results were the same. A co-localization of TMEM165 with LAMP2 (58 ± 11%) but no significant co-localization of TMEM165 with EEA1 (5 ± 1%) was observed. Interestingly, the western blot results showed that the R126H variant is stabilized upon Mn<sup>2+</sup> and chloroquine exposure (Supplementary Figure S5C). This clearly demonstrates that this allele is constitutively able to traffic to the lysosomes upon Mn<sup>2+</sup> exposure. In summary, our results support the evidence that the glutamic acid (E) of the highly conserved ELGDK motif is crucial in mediating the lysosomal degradation of TMEM165 in response to Mn<sup>2+</sup>. To determine whether the E108G mutation could also affect the function of TMEM165, the glycosylation status of LAMP2 was assessed in TMEM165 KO HEK293 cells generated by CRISPR-Cas9 (Figure 4C and Supplementary Figure S4). Both the expression of the wt-TMEM165 and the E108G mutant complemented the observed glycosylation defect. Compared with the expression of the wt TMEM165, the expression of the E108G mutant in rescuing the LAMP2 glycosylation is less efficient. This result suggests, nevertheless, that the E108G mutant remains functional and that the activity of TMEM165 then appears independent of the Mn<sup>2+</sup>-induced degradation mechanism.

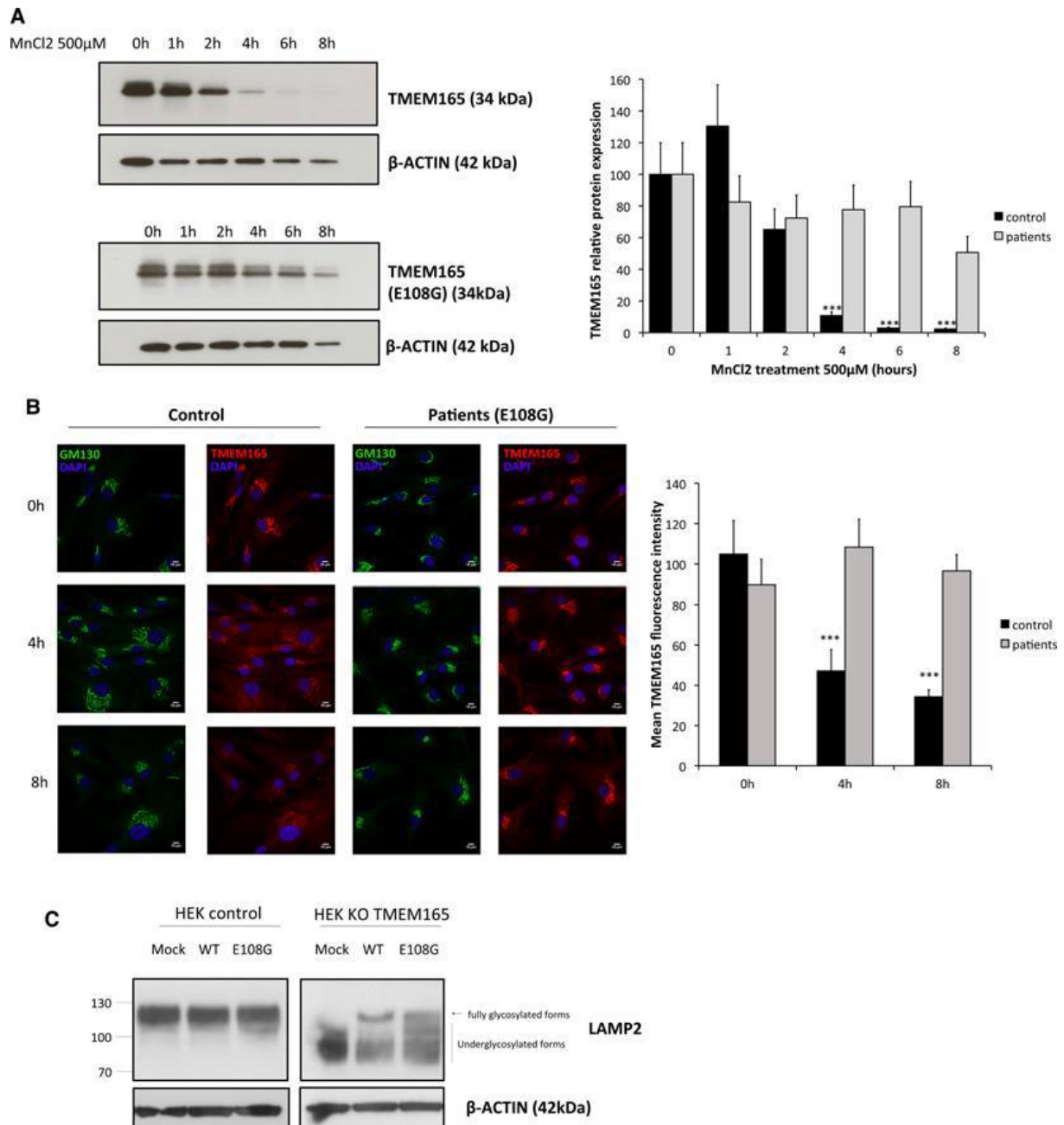


**Figure 4. The glutamic acid (E108) in the ELDGK motif is crucial for Mn<sup>2+</sup> sensitivity.** (A) Healthy skin fibroblasts (upper left) and patients' skin fibroblasts (lower left) carrying E108G mutation were treated with 500 μM MnCl<sub>2</sub> for 0–8 h. Total cell lysates were prepared, and subjected to SDS–PAGE and western blot with the indicated antibodies. Right panel shows the quantification of TMEM165 protein levels after normalization with actin (N = 2; \*\*\*P-value < 0.001). (B) Healthy skin fibroblasts and patients' skin fibroblasts carrying E108G mutation were treated with 500 μM MnCl<sub>2</sub> for 0, 4, and 8 h. Cells were then fixed and labeled with antibodies against TMEM165 and GM130 before confocal microscopy visualization (N = 2; \*\*\*P-value < 0.001). Lower panel shows the quantification of the associated TMEM165 fluorescence intensity (N = 2; n = 30; \*\*\*P-value < 0.001). (C) HEK293 control cells and HEK293 KO TMEM165 cells were transfected with empty-vector, wt or E108G plasmid for 36 h. Total cell lysates were prepared, and subjected to SDS–PAGE and western blot with the indicated antibodies.

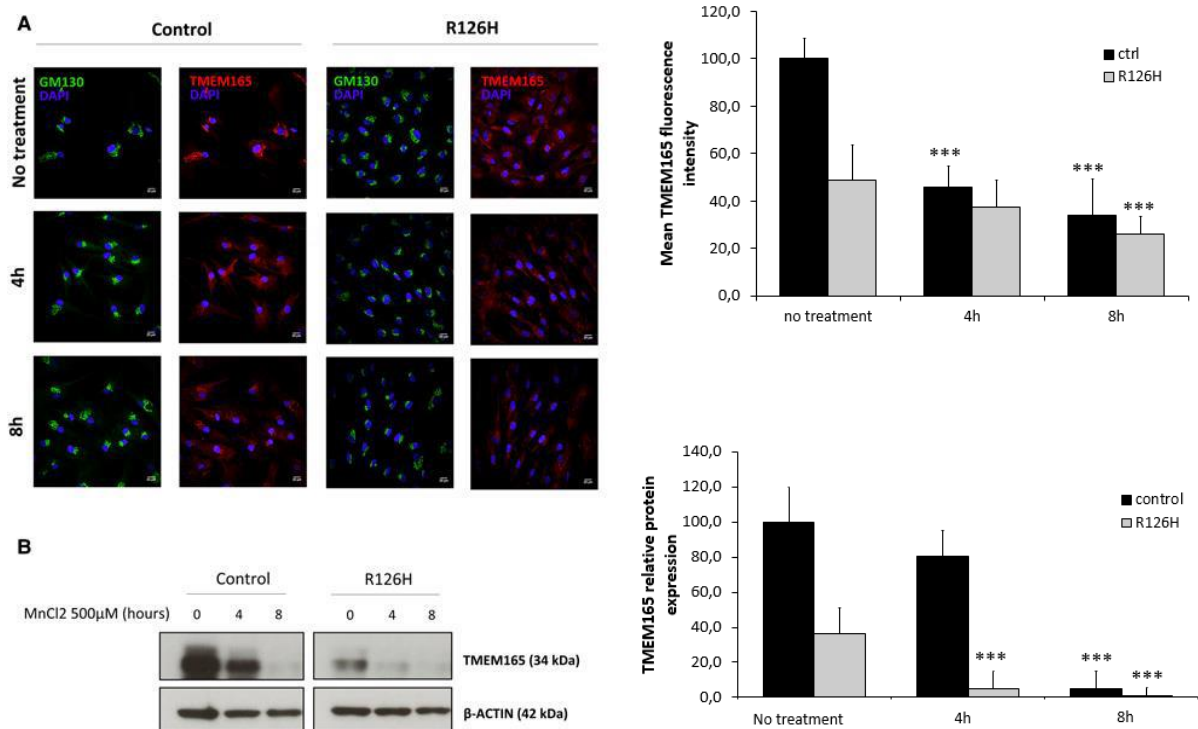


**Figure 5. TMEM165 Mn<sup>2+</sup>-induced degradation also occurs in fibroblasts carrying R126H mutation.** (A) Control skin fibroblasts and patient skin fibroblasts carrying R126H mutation were treated with 500 μM MnCl<sub>2</sub> for 0–8 h and then fixed and labeled with antibodies against TMEM165 and GM130 before confocal microscopy visualization. Right panel shows the quantification of the associated TMEM165 fluorescence intensity [N = 2; number of cells (n) = 30; \*\*\*P-value < 0.001]. (B) Steady-state cellular level of TMEM165. Fibroblasts were treated as described in (A). Total cell lysates were prepared, and subjected to SDS–PAGE and western blot with the indicated antibodies. Right panel shows the quantification of TMEM165 protein levels after normalization with actin (N = 2; \*\*\*P-value < 0.001).

### Validation of a predicted topology of TMEM165

Human TMEM165 encodes a 7-transmembrane spanning protein of 324 amino acids. To validate a predicted topology of TMEM165 and thus the orientation of the ELGDK motif, we used the two available commercial antibodies against TMEM165, each recognizing two differentially oriented epitopes: the Sigma antibodies recognizing the immunogenic sequence (aa176–aa229) and the antibodies provided by Thermo Fischer directed against the immunogenic sequence (aa17–aa45; Figure 6A). The topology was determined by selective membrane permeabilization and immunofluorescence analysis (Figure 6B). Under conditions that allowed antibody access to all cellular compartments, both epitopes were detectable and showed co-localization with the Golgi marker GM130 (Figure 6B). Selective permeabilization of the plasma membrane with low concentrations of digitonin allowed visualization of the cytosolic epitope only recognized by the Sigma antibody. On the basis of these results, we can

propose a model where the loop encompassing the aa 176–229 is cytosolic and where the ELGDK motif is facing the cytosol (Figure 6A).

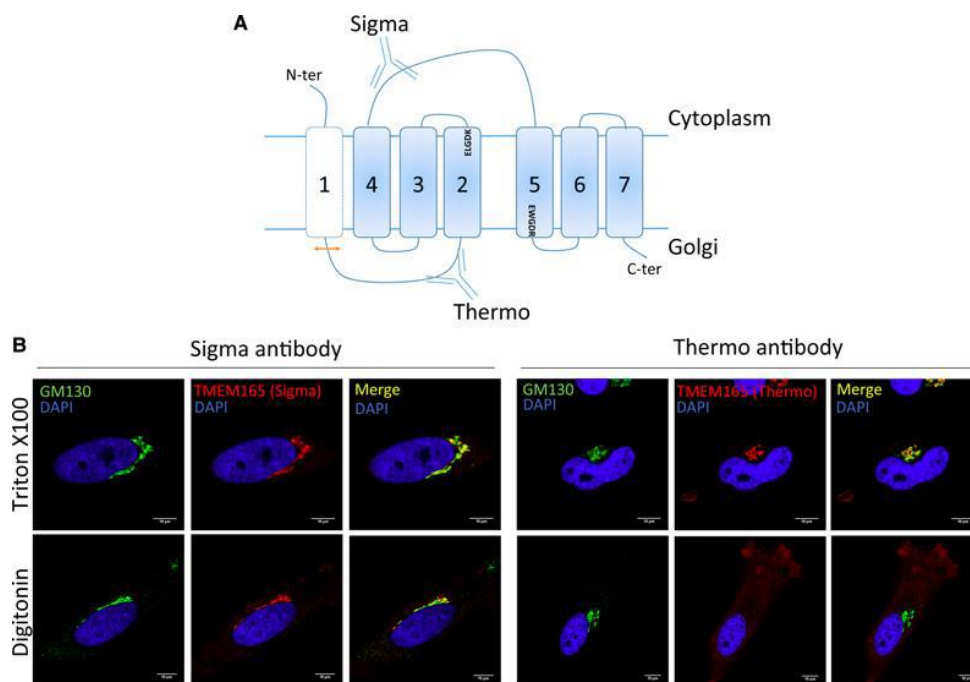


**Figure 6. TMEM165 topology.** (A) Representation of TMEM165 predicted topology. The two anti-TMEM165 antibodies (Sigma–Aldrich and Thermo Fisher Scientific) depicted here recognize two different parts of the protein. The Sigma ones recognize the cytoplasmic loop between the fourth and fifth transmembrane domains. The Thermo ones recognize the short luminal loop between the first and the second transmembrane domain. The red double arrows show the predicted location of the signal sequence cleavage. The first TMD is depicted in white and with a dotted line border as it can be absent from the mature protein. (B) Cells were fixed with PAF 4% and treated as described in the materials and methods section. Selective permeabilization was done by using Triton X-100 or digitonin. Cells were labeled with antibodies against TMEM165 and GM130 before confocal microscopy visualization.

### SPCA1 knockdown does not prevent TMEM165-induced degradation

Since the ELGDK motif is oriented toward the cytosol, we wished to assess whether TMEM165 responded to changes in cytosolic or Golgi luminal Mn<sup>2+</sup>. To tackle this point, we tested the contribution of SPCA1 (known to be one of the major Golgi Mn<sup>2+</sup> importers) in the Mn<sup>2+</sup>-induced degradation of TMEM165. The impacts of knockdown of SPCA1 on the Mn<sup>2+</sup>-induced degradation of TMEM165 were assessed. siRNA depletion of SPCA1 was very efficient as 85% of the protein was depleted compared with untreated cells. Interestingly, knockdown of SPCA1 did not abolish the Mn<sup>2+</sup>-induced degradation of TMEM165 (Figure 7). The results showed that TMEM165 loss exceeded 80% after 8 h of Mn<sup>2+</sup> treatment both in siSPCA1 cells and untreated cells. This highly strengthens the fact that the degradation of TMEM165 is not dependent on Golgi luminal Mn<sup>2+</sup> changes.

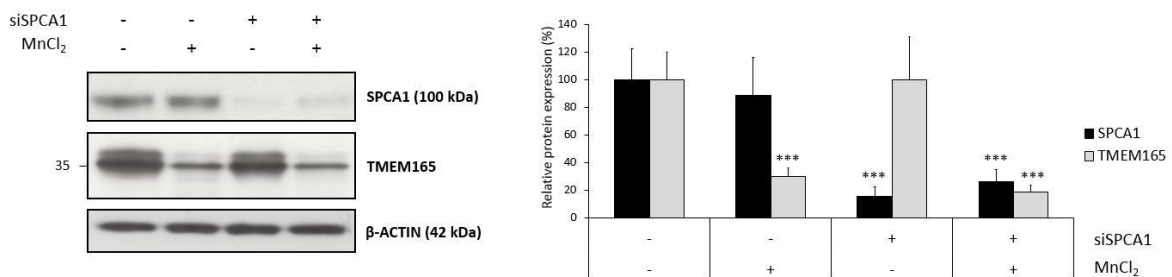


**Figure 7. SPCA1 knockdown does not prevent the Mn-induced degradation of TMEM165.** (A) Steady-state cellular level of TMEM165 and SPCA1 in control and siSPCA1 HeLa cells. Control and siSPCA1 HeLa cells were cultured in the absence or presence of MnCl<sub>2</sub> (500 μM, 8 h); total cell lysates were then prepared, and subjected to SDS-PAGE and western blot with the indicated antibodies. Right panel shows the quantification of TMEM165 and SPCA1 protein levels after normalization with actin (N = 3; \*\*\*P-value < 0.001).

## Discussion

Our previous work has shown that the observed Golgi glycosylation defect due to a lack of Gdt1p/TMEM165 resulted from a Golgi Mn<sup>2+</sup> homeostasis defect, then leading to strong Golgi glycosylation abnormalities. Interestingly, we demonstrated that such defects could totally be suppressed by manganese supplementation, strongly suggesting that TMEM165 could somehow be involved in the Golgi transport of Mn<sup>2+</sup>. It has been shown in yeast that Smf1p and Smf2p, members of the Nramp family of metal transporters, are tightly regulated by different intracellular Mn<sup>2+</sup> concentrations [18–20]. When cells are exposed to toxic Mn<sup>2+</sup> concentrations, Smf1p and Smf2p are targeted to the vacuole for degradation, thus stopping the Mn<sup>2+</sup> cellular entry. To test whether TMEM165 falls under the same regulation, TMEM165 stability for Mn<sup>2+</sup> was tested. Our results showed that TMEM165 was highly sensitive to Mn<sup>2+</sup> as manganese supplementation targets TMEM165 under the way of lysosomal degradation. Although, intriguingly, the molecular mechanisms by which TMEM165 is degraded following Mn<sup>2+</sup> exposure are currently not known, the Mn<sup>2+</sup>-induced degradation of Gdt1p-Myc in yeasts demonstrated that this mechanism is conserved during evolution. Another mammalian Golgi protein GPP130 has been reported to be sensitive to Mn<sup>2+</sup> [16]. While the obtained results are very similar to the one observed for GPP130, several lines of evidences tend to prove that the molecular mechanisms could be different. First, the manganese sensitivity is different as 25 μM manganese is sufficient to engage TMEM165 in the lysosomal degradation pathway, while at this concentration GPP130 is stable. We cannot, however, avoid the fact that this observed difference in manganese sensitivity is coming from the different binding affinities of manganese for these two proteins. Second, the manganese-induced degradation

rate of TMEM165 is faster than that of GPP130, as TMEM165 accumulation was never seen in punctate structures under Mn<sup>2+</sup> supplementation. Because GPP130 and TMEM165 present high sensitivity to manganese, we cannot exclude a functional link between these two Golgi proteins. Interestingly, while the R126H mutation remains Mn<sup>2+</sup> responsive, the glutamic acid (E108) in the highly conserved ELGDK motif was shown to be insensitive to Mn<sup>2+</sup> exposure and then crucial in TMEM165 Mn<sup>2+</sup>-induced degradation. One can suppose that these two mutations act differently on the Mn<sup>2+</sup>-induced degradation mechanisms of TMEM165. Our data also show that the E108G TMEM165 mutant form is able to rescue the glycosylation defect, although less efficiently than the wt-TMEM165 form. This suggests that the Mn<sup>2+</sup>-induced degradation mechanism is independent of the function of TMEM165 in Golgi glycosylation. According to the prediction of TMEM165 membrane topology, this motif is oriented towards the cytosol and located between the second and the third transmembrane domains of TMEM165. Our results show that TMEM165 responds to changes in cytosolic Mn<sup>2+</sup> and not Golgi luminal changes. Although the R126H mutation reduces basal TMEM165 expression, the protein remains Mn responsive.

The other important question is, why is TMEM165 degraded by high cytosolic Mn<sup>2+</sup> concentration? While we currently do not have the answer, our data raise several hypotheses. As a slight fraction of TMEM165 can be found at the plasma membrane, the degradation could be a mechanism to prevent Mn<sup>2+</sup> entry through the plasma membrane. As mammalian cells can, however, transport the metal by other plasma membrane transporters, this hypothesis is not likely. When cells are exposed to high manganese concentrations, the plasma membrane transporters import the dangerous metal in the cytosol where it accumulates and impairs many fundamental cellular processes. It is critical for the cell to detoxify the cytosol. The detoxification is crucial to avoid the impairment of many fundamental cellular processes. It is known that SPCA1, the Golgi P-type ATPase essential to import cytosolic Ca<sup>2+</sup> but also Mn<sup>2+</sup> inside the Golgi lumen, is the major way for eliminating the surplus of cytosolic Mn<sup>2+</sup> from the cell. As TMEM165 is degraded when the manganese level becomes toxic, we can hypothesize that this mechanism participates in detoxification. This is still unclear how TMEM165 participates in such a process, but one can think that TMEM165, in the presence of high Mn<sup>2+</sup> concentration in the Golgi, could transport back the Mn<sup>2+</sup> into the cytosol. In that case, the specific degradation of TMEM165 in response to Mn<sup>2+</sup> would prevent the Mn<sup>2+</sup> from the Golgi to be recaptured back into the cytosol, a mechanism that would definitely

annihilate the efforts made by SPCA1. Overall, our studies highlight TMEM165 as a novel Golgi Mn<sup>2+</sup> sensitive protein in mammalian cells. This discovery sheds light on a novel actor involved in the regulation of intracellular Mn<sup>2+</sup> homeostasis and the pathophysiological mechanisms in TMEM165-CDG patients.

## **Material and methods**

### **Antibodies and other reagents**

Anti-TMEM165 and anti- $\beta$  Actin antibodies were from Sigma–Aldrich (St Louis, MO, U.S.A.). The other anti-TMEM165 antibody was purchased from Thermo Fisher Scientific (Waltham, MA, U.S.A.). Anti-SPCA1 antibody was purchased from Abcam (Cambridge, U.K.). Anti-GM130 antibody was from BD Biosciences (Franklin lakes, NJ, U.S.A.). Anti-GPP130 antibody was purchased from Covance (Princeton, NJ, U.S.A.). Anti-myc (9E10) was purchased from Santa Cruz Biotechnology (Dallas, TX, U.S.A.). Goat anti-rabbit or goat anti-mouse immunoglobulins HRP-conjugated were purchased from Dako (Glostrup, Denmark). Polyclonal goat anti-rabbit or goat anti-mouse conjugated with Alexa Fluor were purchased from Thermo Fisher Scientific (Waltham, MA, U.S.A.). Manganese (II) chloride tetrahydrate was from Riedel-de-Haën (Seelze, Germany). All other chemicals were from Sigma–Aldrich unless otherwise specified.

### **Constructs, vector engineering and mutagenesis**

Plasmids, pcDNA3.1 derivatives expressing either wt-TMEM165 or p.E108G version of TMEM165 (c.A323G mutation), have been generated by Ezyvec (Lille, France). Generation of TMEM165 knockouts HEK293T cells (ATTC) were grown in Dulbecco's Modified Eagle's Medium (DMEM)/F12 medium (Thermo Scientific) supplemented with 10% fetal bovine serum (FBS; Atlas Biologicals). Cells were maintained at 37° and 5% CO<sub>2</sub> in a 90% humidified incubator. HEK293T TMEM165 stable knockouts were generated using the CRISPR technique [21–24]. gRNA sequences were purchased from Genecopoeia (Catalog No. HCP214780-SG01-3). HEK293T cells were transfected with plasmid containing gRNA and a separate plasmid containing Cas9 and mCherry. HEK293 cells were transfected in a 6-well plate at 70% confluence using Lipofectamine 2000 in Opti-MEM (Thermo Scientific). Cells were incubated with the lipid-DNA complexes for 5 h after which the cells were supplemented with DMEM/F12 with FBS at a final concentration of 5%. The medium was changed to DMEM/F12 with 10% FBS 24 h after transfection. Twelve days after transfection, cells were single-cell

sorted and knockout colonies were identified by immunofluorescence and western blot using antibodies to TMEM165 (Sigma). Sequencing of knockouts identified deletions in exon 1.

### **Cell culture and transfections**

All cell lines were maintained in DMEM supplemented with 10% FBS (Lonza, Basel, Switzerland), at 37°C in a humidity-saturated 5% CO<sub>2</sub> atmosphere. Transfections were performed using Lipofectamine 2000® (Thermo Scientific) according to the manufacturer's guidelines. For drug treatments, incubations were done as described in each figure.

### **Immunofluorescence staining**

Cells were seeded on coverslips for 12–24 h, washed once in Dulbecco's Phosphate Buffer Saline (DPBS, Lonza) and fixed either with 4% paraformaldehyde (PAF) in PBS (pH 7.3) for 30 min at room temperature or with ice-cold methanol for 10 min at room temperature. Coverslips were then washed three times with PBS. Only if the fixation had been done with PAF, cells were permeabilized with 0.5% Triton X-100 in PBS for 15 min and then washed three times with PBS. Coverslips were then put in saturation for 1 h in blocking buffer [0.2% gelatin, 2% Bovine Serum Albumin (BSA), 2% FBS (Lonza) in PBS], followed by incubation for 1 h with primary antibody diluted at 1:100 in blocking buffer. After washing with PBS, cells were incubated for 1 h with Alexa 488-, Alexa 568-, or Alexa 700-conjugated secondary antibody (Life Technologies) diluted at 1:600 in blocking buffer. After washing three times with PBS, coverslips were mounted on glass slides with Mowiol. Fluorescence was detected through an inverted Zeiss LSM780 confocal microscope. Acquisitions were done using the ZEN pro 2.1 software (Zeiss, Oberkochen, Germany). For selective membrane permeabilization, we have used digitonin at 5 µg/ml. Stock solution was prepared at 5 mg/ml in absolute ethanol, 0.3 M sucrose 0.1 M KCl, 2.5 mM MgCl<sub>2</sub>, 1 mM EDTA, 10 mM HEPES, pH 6.9. Permeabilization was done at 4°C for 15 min.

### **Image analyses**

Immunofluorescence images were analyzed using TisGolgi, a home-made imageJ (<http://imagej.nih.gov/ij>) plugin developed by TISBio and available upon request. Basically, the program automatically detects and discriminates Golgi and vesicles, based on morphological parameters such as size and sphericity. Then, the program calculates for each

image the number of detected objects, their size and mean fluorescence intensity. Co-localization analyses were done using JACoP plugin and performed according to the guidelines suggested by Bolte et al. [25].

### **Western blotting**

Cells were scraped in DPBS and then centrifuged at 4500 rpm for 3 min. Supernatant was discarded and cells were then resuspended in RIPA buffer [Tris/HCl 50 mM (pH 7.9), NaCl 120 mM, NP40 0.5%, EDTA 1 mM, Na<sub>3</sub> VO<sub>4</sub> 1 mM, NaF 5 mM] supplemented with a protease cocktail inhibitor (Roche Diagnostics, Penzberg, Germany). Cell lysis was done by passing the cells several times through a syringe with a 26G needle. Cells were centrifuged for 30 min at 20 000g. The supernatant containing protein was estimated with the Micro BCA Protein Assay Kit (Thermo Scientific). A 20 µg aliquot of total protein lysate was put in NuPAGE LDS sample buffer (Invitrogen) (pH 8.4) supplemented with 4% β-mercaptoethanol (Fluka). Samples were heated for 10 min at 95°C, then separated on 4–12% Bis–Tris gels (Invitrogen) and transferred to nitrocellulose membrane Hybond ECL (GE Healthcare, Little Chalfont, U.K.). The membranes were blocked in blocking buffer (5% milk powder in TBS-T [1X TBS with 0.05% Tween20]) for 1 h at room temperature, then incubated over night with the primary antibodies (used at a dilution of 1:1000, except for anti-myc, used at 1:200) in blocking buffer, and washed three times for 5 min in TBS-T. The membranes were then incubated with the peroxidase conjugated secondary goat anti-rabbit or goat anti-mouse antibodies (Dako; used at a dilution of 1:10 000) in blocking buffer for 1 h at room temperature and later washed three times for 5 min in TBS-T. Signal was detected with chemiluminescence reagent (ECL 2 Western Blotting Substrate, Thermo Scientific on imaging film (GE Healthcare, Little Chalfont, U.K.).

### **Yeast strains, media and lysis**

Yeast strains originating from BY4741 background were used for the experiments (*gdt1Δ*: Mata his3Δ 1 leu2Δ 0 ura3Δ 0 *gdt1Δ*::KanMX4). Yeasts were cultured at 30°C. Cultures in liquid media are done under light shaking. Rich medium, named YEP medium, contains yeast extract (10 g/l, Difco), Bacto-peptone (20 g/l, Difco); YPD medium is a YEP medium supplemented with 2% D -glucose (Sigma–Aldrich). Before any analysis, a preculture in YPD medium is done and a volume equivalent to 10 OD<sub>600</sub> nm unit is transferred into a bigger volume of YPD medium.

Culture begins at a volume equivalent to 6 OD<sub>600</sub> nm unit until 18 OD<sub>600</sub> nm. MnCl<sub>2</sub> was added at this step at the indicated concentration and yeasts were harvested at the indicated times. Yeasts were centrifuged for 5 min at 3500 g. The supernatant was discarded and the pellet was kept frozen at – 20°C. Yeast lysis was performed as described by Ballou et al [26]. Western blot experiments were done as described above.

### **Cell surface biotinylation**

Cells were plated to reach 70– 80% confluence on the day of the experiment. Cells were kept on ice all the time. Cells were washed four times with PBS+ /+ (containing Ca and Mg), pH8. An aliquot of 1.5 ml PBS+ /+ (pH 8) with 7.5 µl biotin was added per dish [Biotin: EZ Link Sulfo-NHS-SS-Biotin (Life Technologies, Carlsbad, CA, U.S.A.), final concentration of 0.5 mg/ml in DMSO]. Cells were then incubated 30 min in a cold room on slow rocking and then washed three times with PBS+ /+ (pH8). Cells were quenched 15 min with 1.5 ml of PBS+ /+ glycine 100 mM, BSA 0.5% in a cold room on slow rocking and then washed three times with PBS+ /+ glycine. Cells were scraped in 200 µl of lysis buffer [50 mM HEPES (pH 7.2), 100 mM NaCl, 1% Triton X-100, protease inhibitors], incubated 20 min on ice and centrifuged for 15 min at 20 000g at 4°C. The supernatant was kept and the protein concentration was measured. For the pull-down, put the maximum amount of protein, ideally 500 µg in 1 ml final (lysis buffer) + 30 µl streptavidin beads. Incubate 4h at 4°C on a wheel and then centrifuge at 4000g for 1 min at 4°C. Wash three times with 1 ml of lysis buffer (not supplemented with protease inhibitors) and mix well by inverting the tubes 30 times. Centrifuge at 4000g for 1 min at 4°C and remove the supernatant with a flat end tip. Add NuPAGE LDS sample buffer (Invitrogen) pH 8.4 supplemented with 4% β-mercaptoethanol (Fluka). Samples are boiled at 70°C for 10 min (do not boil if one wishes to reveal TMEM165 on western blot afterwards) and then centrifuged at 1000g for 1 min, and the supernatant was collected. Samples were frozen at – 20°C. Samples are ready to load on gel.

### **Statistical analysis**

Comparisons between groups were performed using Student's t -test for two variables with equal or different variances, depending on the result of the F -test.

### **Abbreviations**

BSA, bovine serum albumin; CDG, congenital disorders of glycosylation; DMEM, Dulbecco's Modified Eagle's Medium; DPBS, Dulbecco's Phosphate Buffer Saline; FBS, fetal bovine serum; PAF, paraformaldehyde; SPCA1, secretory pathway Ca-ATPase 1; wt, wild-type.

### **Author Contribution**

F.F. obtained financial support to design this study and he wrote the paper. F.F. and S.P. coordinated the study. S.P. and E.D. performed and analyzed most of the experiments. L.C. and V.L. performed the CRISPR-cas9 TMEM165 cells. M.H. performed the experiment in Figure 7. C.S. provided technical assistance for colocalisation studies. D.V. performed immunofluorescence microscopy experiments. E.L. and A.K. performed and analysed the experiment in Figure 4C. R.P. provided technical assistance on surface biotinylation. S.D., W.M. and M.A.K. provided advices. G.D.B. and P.M. reviewed the yeast results. G.M. reviewed the paper and provided us the R126H deficient CDG patients. T.M. provided us the E108G TMEM165 deficient patients.

### **Funding**

This work was supported by the French National Research Agency [SOLV-CDG to F.F] and the Mizutani Foundation for Glycoscience [to F.F.] and EURO-CDG-2 that has received funding from the European Union's Horizon 2020 research and innovation program under the ERA-NET Cofund action N° 643578. V.L. was supported by the NIH grants [GM083144 and U54 GM105814].

### **Acknowledgements**

We are indebted to Dr Dominique Legrand of the Research Federation FRABio (Univ. Lille, CNRS, FR 3688, FRABio, Biochimie Structurale et Fonctionnelle des Assemblages Biomoléculaires) for providing the scientific and technical environment conducive to achieving this work. We thank the BioImaging Center of Lille, especially Christian Slomianny and Elodie Richard, for the use of the Leica LSM70.

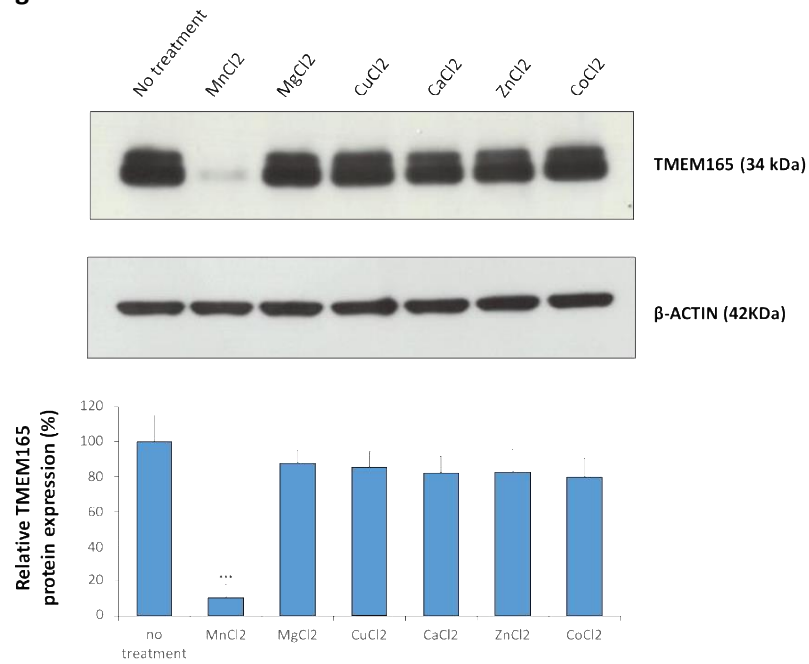
### **Competing Interests**

The Authors declare that there are no competing interests associated with the manuscript.

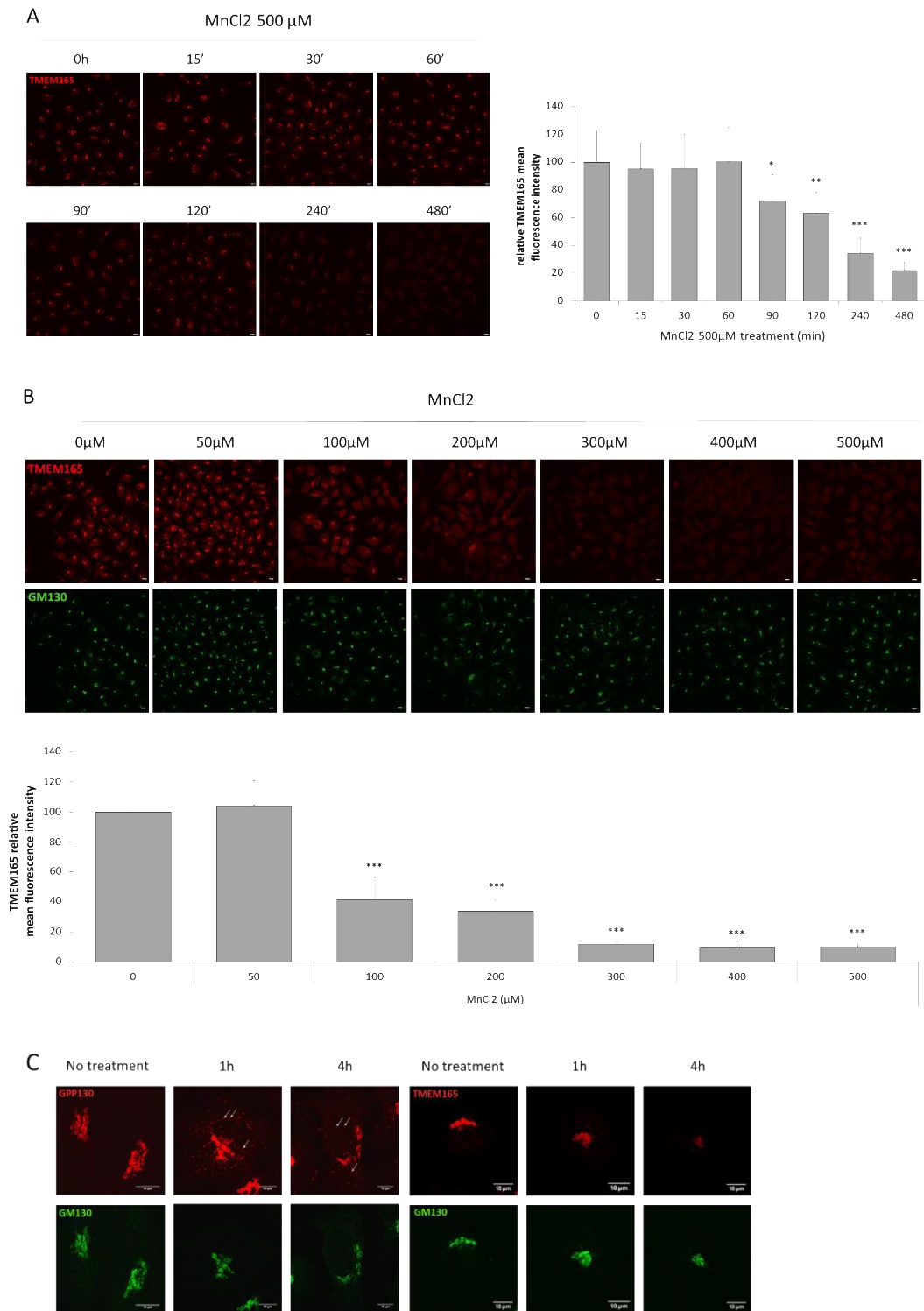
## References

- 1 Au, C., Benedetto, A. and Aschner, M. (2008) Manganese transport in eukaryotes: the role of DMT1. *Neurotoxicology* 29, 569–576 doi:10.1016/j.neuro.2008.04.022
- 2 Perl, D.P. and Olanow, C.W. (2007) The neuropathology of manganese-induced Parkinsonism. *J. Neuropathol. Exp. Neurol.* 66, 675–682 doi:10.1097/nen.0b013e31812503cf
- 3 Squitti, R., Gorgone, G., Panetta, V., Lucchini, R., Bucossi, S., Albini, E. et al. (2009) Implications of metal exposure and liver function in Parkinsonian patients resident in the vicinities of ferroalloy plants. *J. Neural. Transm.* 116, 1281–1287 doi:10.1007/s00702-009-0283-0
- 4 Park, J.H., Högbe, M., Grüneberg, M., DuChesne, I., Heiden, A.L. von der Reunert, J. et al. (2015) SLC39A8 deficiency: a disorder of manganese transport and glycosylation. *Am. J. Hum. Genet.* 97, 894–903 doi:10.1016/j.ajhg.2015.11.003
- 5 Potelle, S., Morelle, W., Dulary, E., Duvet, S., Vicogne, D., Spriet, C. et al. (2016) Glycosylation abnormalities in Gdt1p/TMEM165 deficient cells result from a defect in Golgi manganese homeostasis. *Hum. Mol. Genet.* 25, 1489–1500 doi:10.1093/hmg/ddw026
- 6 Garrick, M.D., Dolan, K.G., Horbinski, C., Ghio, A.J., Higgins, D., Porubcin, M. et al. (2003) DMT1: a mammalian transporter for multiple metals. *Biometals* 16, 41–54 doi:10.1023/A:1020702213099
- 7 Forbes, J.R. and Gros, P. (2003) Iron, manganese, and cobalt transport by Nramp1 (Slc11a1) and Nramp2 (Slc11a2) expressed at the plasma membrane. *Blood* 102, 1884–1892 doi:10.1182/blood-2003-02-0425
- 8 Chen, P., Bowman, A.B., Mukhopadhyay, S. and Aschner, M. (2015) SLC30A10: a novel manganese transporter. *Worm* 4, e1042648 doi:10.1080/21624054.2015.1042648
- 9 Chen, P., Chakraborty, S., Mukhopadhyay, S., Lee, E., Paoliello, M.M.B., Bowman, A.B. et al. (2015) Manganese homeostasis in the nervous system. *J. Neurochem.* 134, 601–610 doi:10.1111/jnc.13170
- 10 Girijashanker, K., He, L., Soleimani, M., Reed, J.M., Li, H., Liu, Z. et al. (2008) Slc39a14 gene encodes ZIP14, a metal/bicarbonate symporter: similarities to the ZIP8 transporter. *Mol. Pharmacol.* 73, 1413–1423 doi:10.1124/mol.107.043588
- 11 Dode, L., Andersen, J.P., Vanoevelen, J., Raeymaekers, L., Missiaen, L., Vilsen, B. et al. (2006) Dissection of the functional differences between human secretory pathway Ca<sup>2+</sup>/Mn<sup>2+</sup>-ATPase (SPCA) 1 and 2 isoenzymes by steady-state and transient kinetic analyses. *J. Biol. Chem.* 281, 3182–3189 doi:10.1074/jbc.M511547200
- 12 He, W. and Hu, Z. (2012) The role of the Golgi-resident SPCA Ca<sup>2+</sup>/Mn<sup>2+</sup> pump in ionic homeostasis and neural function. *Neurochem. Res.* 37, 455–468 doi:10.1007/s11064-011-0644-6
- 13 Mukhopadhyay, S. and Linstedt, A.D. (2011) Identification of a gain-of-function mutation in a Golgi p-type ATPase that enhances Mn<sup>2+</sup> efflux and protects against toxicity. *Proc. Natl Acad. Sci. U.S.A.* 108, 858–863 doi:10.1073/pnas.1013642108
- 14 Foulquier, F., Amyere, M., Jaeken, J., Zeevaert, R., Schollen, E., Race, V. et al. (2012) TMEM165 deficiency causes a congenital disorder of glycosylation. *Am. J. Hum. Genet.* 91, 15–26 doi:10.1016/j.ajhg.2012.05.002
- 15 Masuda, M., Braun-sommargren, M., Crooks, D. and Smith, D.R. (2013) Golgi phosphoprotein 4 (GPP130) is a sensitive and selective cellular target of manganese exposure. *Synapse* 67, 205–215 doi:10.1002/syn.21632
- 16 Mukhopadhyay, S., Bachert, C., Smith, D.R. and Linstedt, A.D. (2010) Manganese-induced trafficking and turnover of the cis-Golgi glycoprotein GPP130. *Mol. Biol. Cell* 21, 1282–1292 doi:10.1091/mbc.E09-11-0985
- 17 Schulte Althoff, S., Grüneberg, M., Reunert, J., Park, J.H., Rust, S., Mühlhausen, C. et al. (2015) TMEM165 deficiency: postnatal changes in glycosylation. *JIMD Rep.* 26, 21–29 doi:10.1007/8904\_2015\_455
- 18 Culotta, V.C., Yang, M. and Hall, M.D. (2005) Manganese transport and trafficking: lessons learned from *Saccharomyces cerevisiae*. *Eukaryot. Cell* 4, 1159–1165 doi:10.1128/EC.4.7.1159-1165.2005
- 19 García-Rodríguez, N., Manzano-López, J., Muñoz-Bravo, M., Fernández-García, E., Muñoz, M. and Wellinger, R.E. (2015) Manganese redistribution by calcium-stimulated vesicle trafficking bypasses the need for P-type ATPase function. *J. Biol. Chem.* 290, 9335–9347 doi:10.1074/jbc.M114.616334
- 20 Reddi, A.R., Jensen, L.T. and Culotta, V.C. (2009) Manganese homeostasis in *Saccharomyces cerevisiae*. *Chem. Rev.* 109, 4722–4732 doi:10.1021/cr900031u
- 21 Bailey Blackburn, J., Pokrovskaya, I., Fisher, P., Ungar, D. and Lupashin, V.V. (2016) COG complex

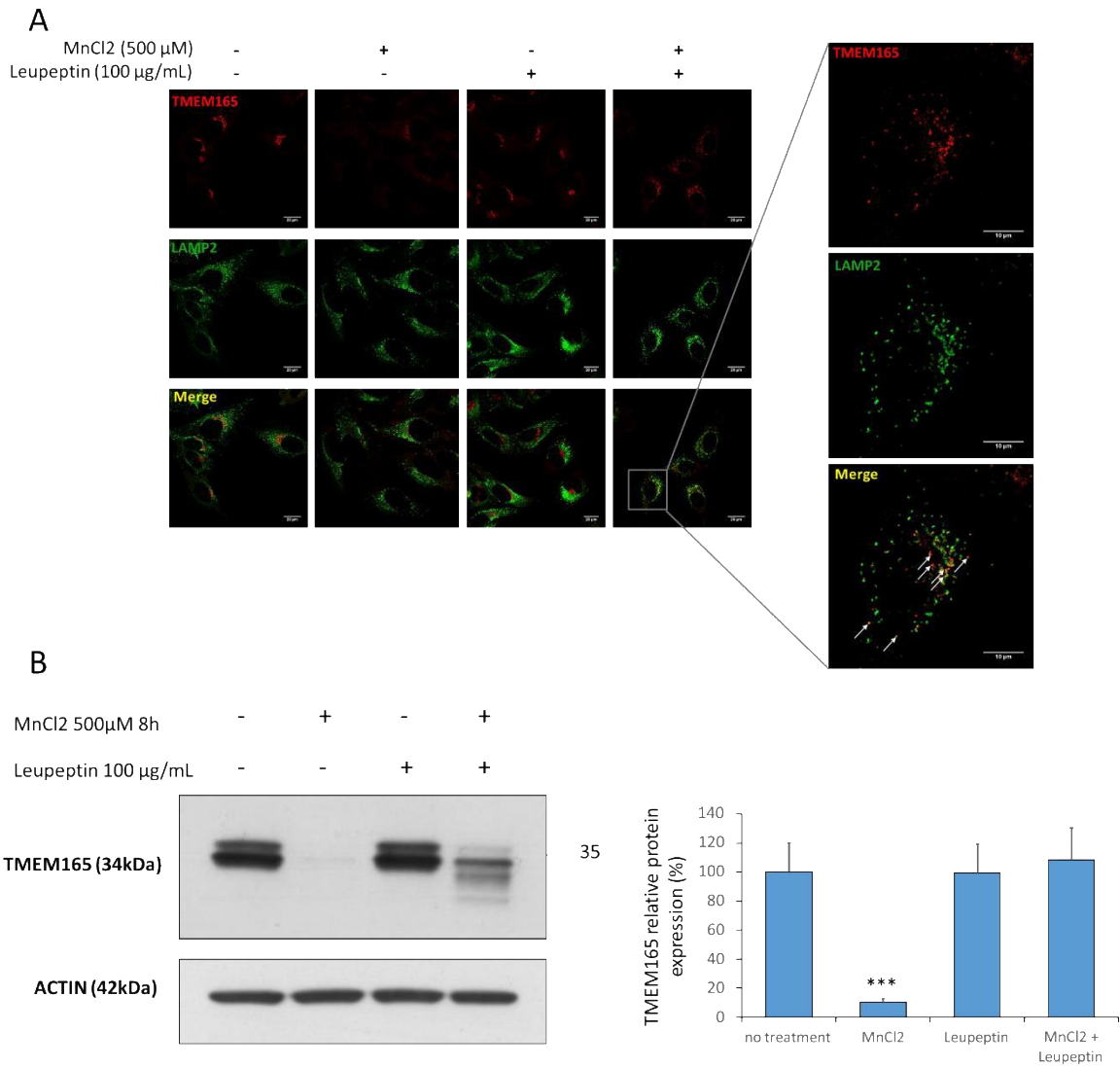
## Supplementary figures



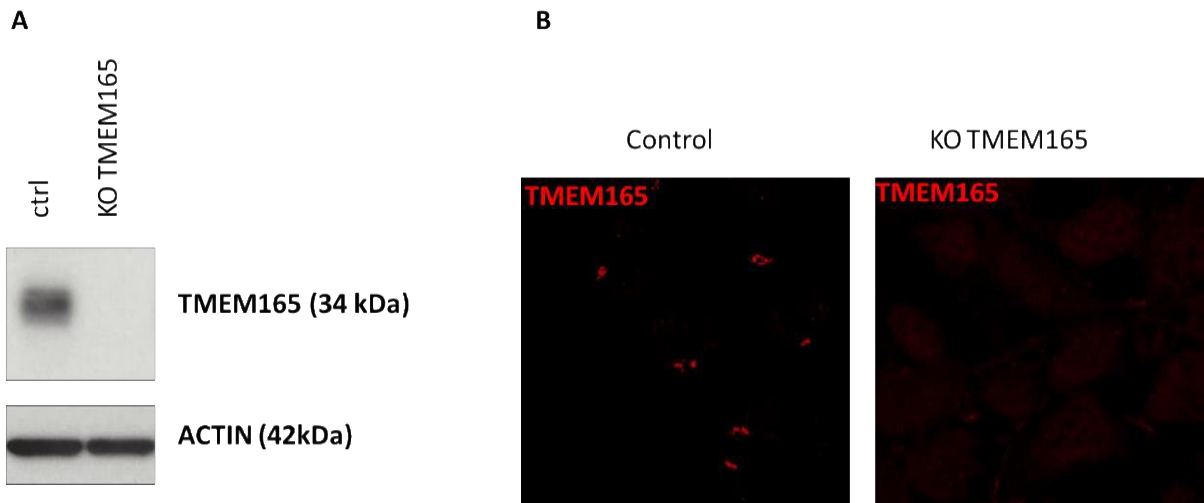
**Supplementary Figure 1. TMEM is specifically degraded in response to Mn<sup>2+</sup>.** Steady state cellular level of TMEM165. HeLa cells were treated with the indicated solution at 500  $\mu$ M for 8h. Total cell lysates were prepared, subjected to SDS-PAGE and Western blot with the indicated antibodies. Lower panel shows the quantification of TMEM165 protein level after normalization with actin (Number of experiments (N) = 3; \*\*\* = P value < 0,001).



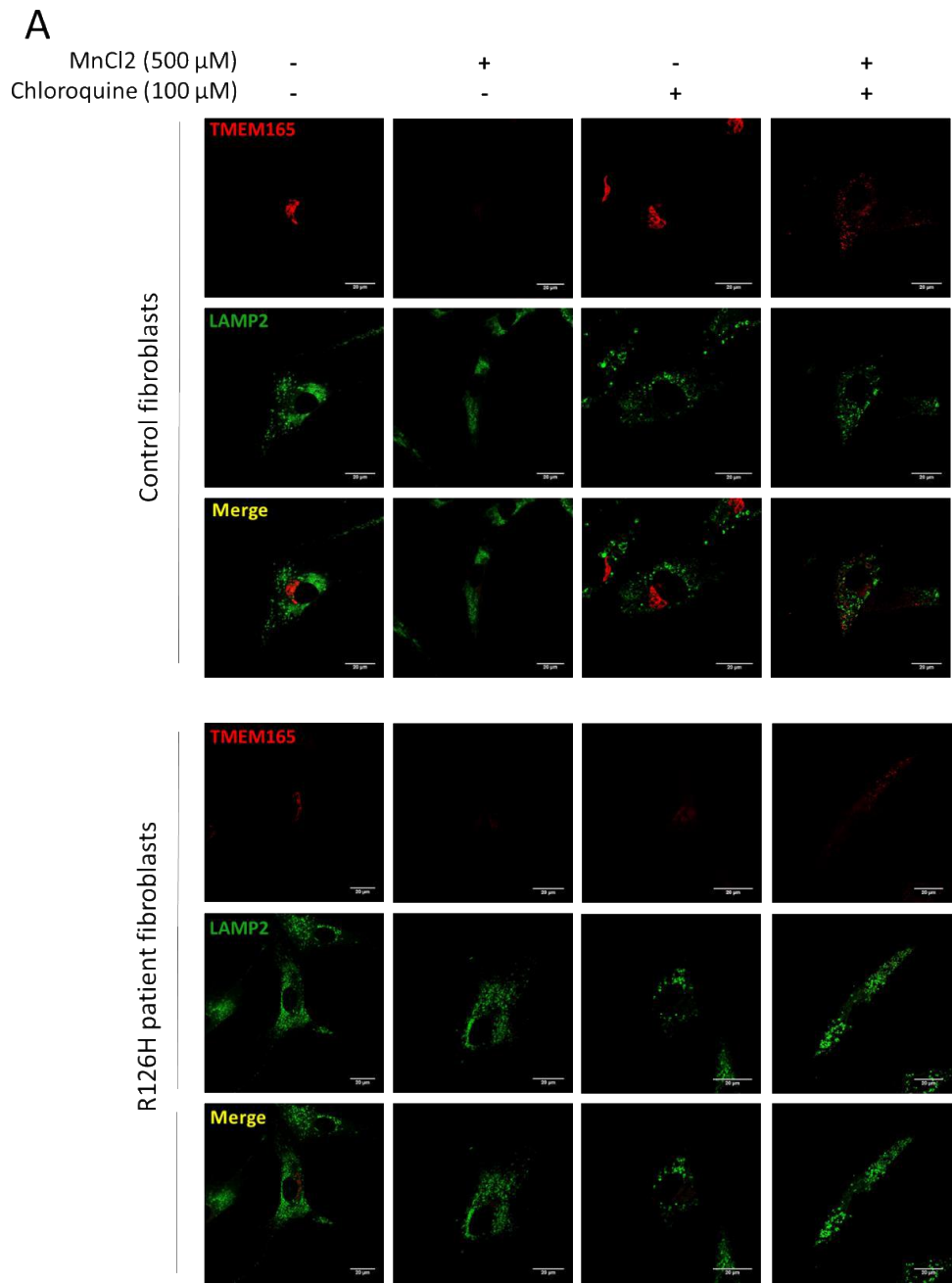
**Supplementary Figure 2. Confirmation of TMEM165 degradation by immunofluorescence experiments (A)** HeLa cells were incubated with MnCl<sub>2</sub> 500  $\mu$ M for 0 to 8h, fixed and labeled with antibodies against TMEM165 before confocal microscopy visualization. Right panel shows the quantification of the associated TMEM165 fluorescence intensity (N = 3; number of cells (n) = 50; \*\*\* = P value < 0,001). **(B)** HeLa cells were treated with MnCl<sub>2</sub> for 8h at different concentrations, then fixed and labeled with antibodies against TMEM165 and GM130 before confocal microscopy visualization. Lower panel shows the quantification of the associated TMEM165 fluorescence intensity (N = 2; n = 50; \*\*\* = P value < 0,001). **(C)** HeLa cells were incubated with MnCl<sub>2</sub> 500  $\mu$ M for 1 and 4h, fixed and labeled with antibodies against TMEM165, GPP130 and GM130 before confocal microscopy visualization. White arrows point to some GPP130 positive vesicles.



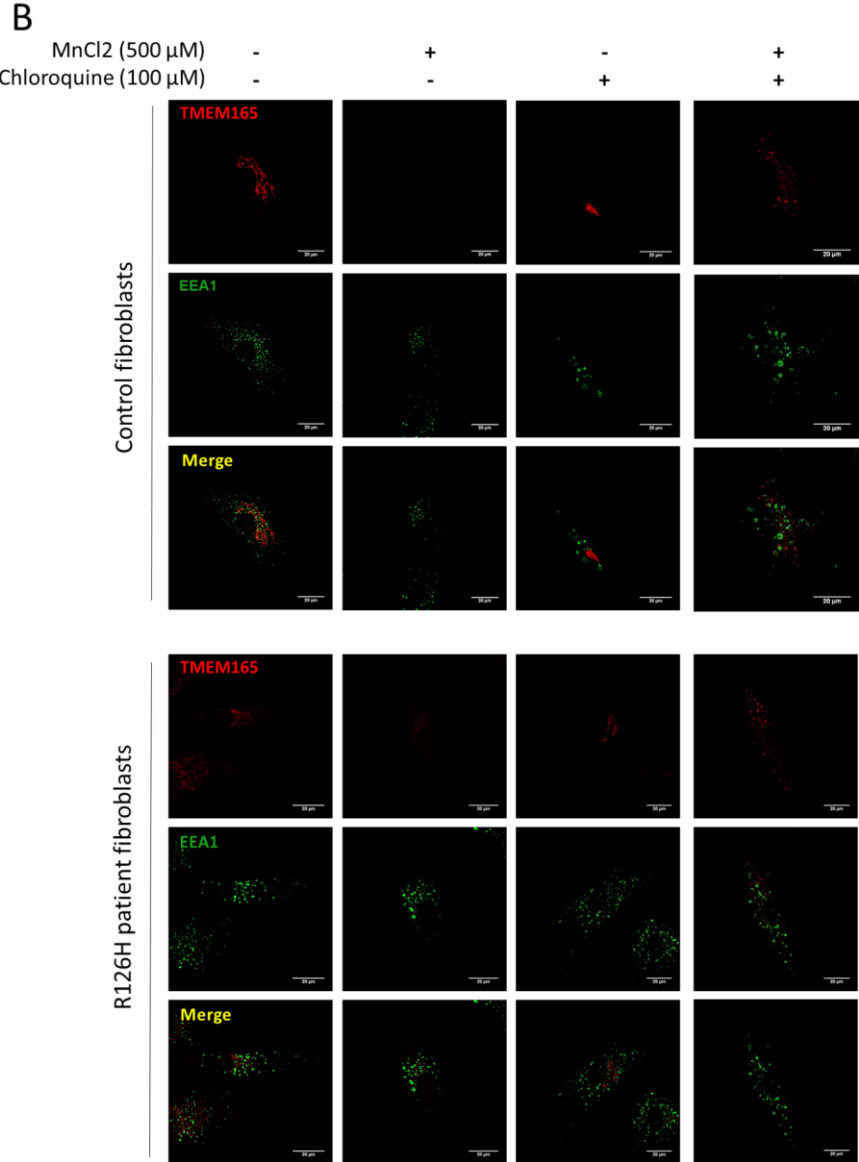
**Supplementary figure 3. Leupeptin also prevents TMEM165 induced lysosomal degradation after Mn<sup>2+</sup> exposure. (A)** HeLa cells were treated for 8h with MnCl<sub>2</sub> 500 μM and/or leupeptin 100 μg/mL, fixed and labeled with antibodies against TMEM165 (upper panels) and LAMP2 (middle panels) before confocal microscopy visualization. For leupeptin, a pretreatment for 24h has been done. **(B)** Western blot analysis of the same experiment described in (A). Total cell lysates were prepared, subjected to SDS-PAGE and Western blot with the indicated antibodies. Right panel shows the quantification of TMEM165 protein level after normalization with actin (N = 2; \*\*\* = P value < 0,001).



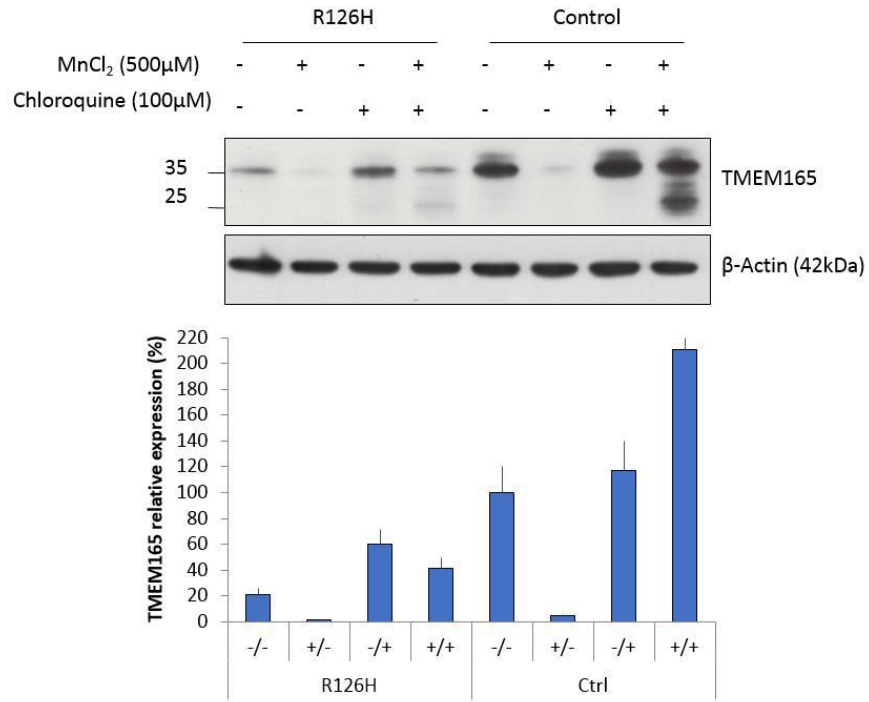
**Supplementary Figure 4. Generation and characterization of knockdown HEK293 cells by crispr-cas9.** (A) Steady-state cellular level of TMEM165. Total cell lysates were prepared, subjected to SDS-PAGE and western blot with the indicated antibodies. (B) Control and knockout HEK293 cells were fixed and labeled with antibodies against TMEM165 before confocal microscopy visualization.



**Supplementary figure 5. The R126H mutation does not affect the TMEM165 lysosomal targeting upon Mn<sup>2+</sup> and chloroquine exposure.** (A) Healthy skin fibroblasts (upper panels) and patients skin fibroblasts (lower panels) carrying R126H mutation were treated for 8h with MnCl<sub>2</sub> 500 μM and/or chloroquine 100 μM, fixed and labeled with antibodies against TMEM165 and LAMP2 before confocal microscopy visualization. (B) Healthy skin fibroblasts (upper panels) and patients skin fibroblasts (lower panels) carrying R126H mutation were treated for 8h with MnCl<sub>2</sub> 500 μM and/or chloroquine 100 μM, fixed and labeled with antibodies against TMEM165 and EEA1 before confocal microscopy visualization. (C) Control and R126H fibroblasts were treated for 8h with MnCl<sub>2</sub> 500 μM and/or chloroquine 100 μM. Total cell lysates were prepared, subjected to SDS-PAGE and Western blot with the indicated antibodies.



Supplementary figure 5. *Continued*



Supplementary figure 5. *Continued*

## GENERAL DISCUSSION

The presented publications in this manuscript were discussed previously. A summary of the contribution of our work to the cellular and molecular characterization of TMEM165 is presented here. Furthermore, our findings will be compared to the models proposed in the literature and perspectives for future research projects will be discussed.

TMEM165/Gdt1 were initially thought to be Golgi  $\text{Ca}^{2+}/\text{H}^{+}$  exchangers, the first eight years of yeast studies have progressively uncovered their function in glycosylation. We are now convinced that TMEM165/Gdt1 have an important role in Golgi manganese homeostasis, supposedly acting as a  $\text{Mn}^{2+}$  importer. According to the tissue, to the subcellular localization and to the ion concentration gradient, the counterion of manganese might be either  $\text{Ca}^{2+}$  or  $\text{H}^{+}$ . Our recent findings, presented in this manuscript will be confronted to previous data and a model, respectively for the function of Gdt1/TMEM165 and the link with the calcium/manganese pump Pmr1/SPCA1, will be proposed.

### 1. Role of Gdt1 and Pmr1 in yeast

As mentioned in chapter 4, in yeast the knockout of Pmr1, a major calcium pump that also imports manganese, induced a glycosylation defect. Interestingly, for Gdt1, the knockout induced a glycosylation defect only under extremely high calcium concentration culture conditions (400-700 nM), conditions under which the wild-type glycosylation was unchanged (Demaegd et al., 2013b) (**table 5**). This indicates that under conditions of calcium excess, calcium would compete with manganese for Pmr1 pumping inside the Golgi lumen. The decrease of the Golgi manganese concentration would impair the galactosyltransferases that require manganese to be fully active, thus explaining the observed glycosylation defect.

Another argument, reinforcing this idea, is the rescue of glycosylation by calcium in KO Pmr1 cells while in KO Gdt1 the addition of calcium is deleterious (**table 5**).

In the initial model, Gdt1 was proposed to be a  $\text{Ca}^{2+}/\text{H}^{+}$  exchanger (Colinet et al., 2016b; Wang et al., 2015c). This model is limited as an isolated decrease of Golgi calcium is not sufficient to explain the glycosylation defect; no direct link between calcium and glycosyltransferases has been demonstrated. The involvement of calcium in the secretory pathway would be the

regulation of the vesicular trafficking that would consequently enhance the manganese redistribution.

Concomitantly, the direct transport of  $Mn^{2+}$  by Gdt1 was advanced to explain the restoration of the glycosylation defect by the  $Mn^{2+}$  supplementation under elevated  $Ca^{2+}$  concentrations (Potelle et al., 2016). In addition, Gdt1 manganese-sensitivity was demonstrated and a potential link between Gdt1 and Pmr1 was hypothesized (Dulary et al., 2018). Moreover, only manganese was able to restore the glycosylation defect observed in the KO Gdt1/Pmr1 strain (Potelle et al., 2016) (table 5).

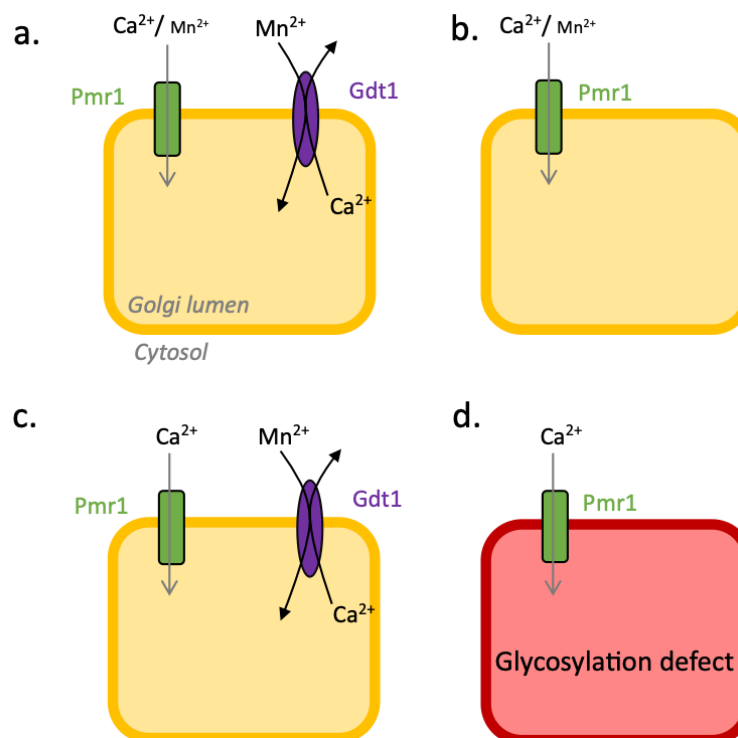


**Figure 39. The proposed model by Dulary and collaborators showing the importance of Pmr1 in the absence of Gdt1 in yeast**

In 2018, Dulary and collaborators studied several strains expressing different forms of Pmr1 with altered transport functions. The glycosylation defect was assessed by an increased electrophoretic mobility of the invertase. When Pmr1 is able to import both calcium and manganese no glycosylation defect was observed in the presence (figure 39a) or in the absence of Gdt1 (figure 39b). When Pmr1 imports calcium solely, the glycosylation defect was only observed in the absence of Gdt1 (figure 39c-d). In other words, Gdt1 is dispensable for the Golgi glycosylation when Pmr1 is able to import manganese. In the yeast model, Pmr1

would be the major importer of manganese inside the Golgi lumen while Gdt1 would be the leak channel of Pmr1 (Dulary et al., 2018) REF.

Although yeast studies have been precursors for human TMEM165 characterization over years, various features have been diverging throughout evolution. The main difference between yeast and human is the linked between Gdt1/TMEM165 and Pmr1/SPCA1 respectively and is summarized in **table 5**.

Name	Differences between Gdt1 /TMEM165 and Pmr1/SPCA1 link in yeast versus human			
	Yeast		Human	
	Gdt1	Pmr1	TMEM165	SPCA1
Induction of a glycosylation defect if KO?	Only under high [Ca <sup>2+</sup> ]	yes	yes	no
Viability of the double KO?	yes		no	
% Loss of Gdt1/TMEM165 in KO Pmr1/SPCA1?	80%		95%	
Gdt1/TMEM165 rescue when Pmr1/Gdt1 import principally Mn <sup>2+</sup> ?	yes		yes	
Gdt1/TMEM165 rescue when Pmr1/Gdt1 import principally Ca <sup>2+</sup> ?	yes		no	
Effect of calcium on the glycosylation defect when KO	worsen	rescue	=	NA
Manganese-induced degradation	yes	no	yes	no
Major Golgi manganese importer	no	yes	yes	no

**Table 5. Comparison of the link between Gdt1/TMEM165 and Pmr1/SPCA1**

## 2. TMEM165 function

The divergent characteristics of Gdt1 and TMEM165 allow us to raise a new model for the human ortholog function.

As the first TMEM165-CDG patients were identified, the link between TMEM165 and glycosylation was established. Mass spectrometry assessed a strong *N*-glycosylation defect in fibroblasts of patients and in TMEM165-depleted cells (Foulquier et al., 2012b; Schulte Althoff et al., 2016). The absence of TMEM165 in humans leads to a severe glycosylation defect whereas in yeast, *gdt1Δ* the defect is observed only under high calcium pressure. However, the glycosylation defect of KO TMEM165 cells was restored by the addition of 1 μM of MnCl<sub>2</sub> to the culture media (Morelle et al., 2017) like in the yeast model (Potelle et al., 2016). Similarly to Gdt1, TMEM165 was shown to be rapidly targeted to the lysosomes for degradation under high manganese concentrations (Potelle et al., 2017) (**Appendix, article 4**).

Surprisingly, in the second presented article of this manuscript, the absence of SPCA1 appears to have the same effect on TMEM165 as the elevation of cytosolic manganese concentration (**results, article 2**).

### 3. TMEM165 and SPCA1

#### 3.1 Current model of the functionality of TMEM165 and SPCA1

SPCA1, the ATP-dependent calcium pump that also imports manganese inside the Golgi lumen is the human ortholog of Pmr1. In the second presented article, a glycosylation defect was not observed in KO SPCA1 HAP1 cells, at the contrary, knockout of Pmr1 presented one (**results, article 2**). Another discrepancy, between yeast and human, is that the double knockout of Pmr1 and Gdt1 only worsen the observed glycosylation defect observed on the yeast invertase, while the double KO of SPCA1 and TMEM165 in HAP1 cell is lethal (Blomen et al., 2015) (**table 5**).

The expression of TMEM165 in the absence of SPCA1 surprisingly, demonstrated an approximately 95% reduction as compared to control cells.

The study of HAP1 cell lines expressing different forms of SPCA1 with a modified ion transport allowed the demonstration that only the forms able to rescue the expression of TMEM165 were those able to import manganese. In addition, the restoration of the expression level of TMEM165 by these transporters was comparable to the level observed in the control cells.

The nature of the counterion is still controversial as Snyder and collaborators showed the necessity of exchanging protons against manganese in the mammary epithelial cells (chapter 4 §4.2.3) (Reinhardt et al., 2014b; Snyder et al., 2019), while a link with calcium exchange is strongly suggested by our studies. In our model (**figure 40**), TMEM165 is the major manganese importer of the Golgi apparatus, which counterion might be either  $\text{Ca}^{2+}$  or  $\text{H}^+$  according to the cell-type and to the available ion gradient.

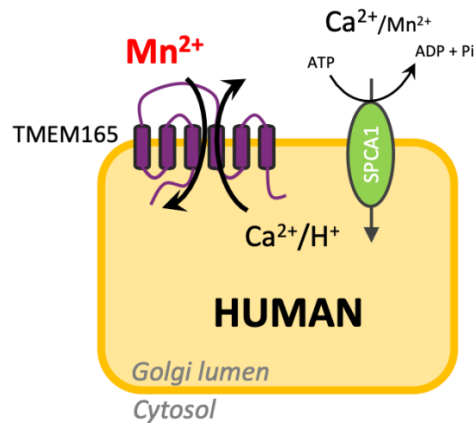


**Figure 40. Current model of the functionality of TMEM165 resulting from our work**

Our hypothesis is consistent with the fact that in plants, PAM71 was assessed to be a  $\text{Ca}^{2+}/\text{Mn}^{2+}$  exchanger in the chloroplast (Schneider et al., 2016). In bacteria, TMEM165 ortholog was also demonstrated to exchange calcium and manganese, with a higher affinity for calcium (Thines et al., 2018).

### 3.2 Putative coupling of TMEM165 and SPCA1 in the late Golgi cisternae

Galactosyltransferases require manganese as cofactor and are localized in the late Golgi cisternae, this is consistent with the *trans*-Golgi localization of TMEM165. We can hypothesize that manganese concentration reaches a peak in the *trans*-Golgi subcompartment.

Golgi apparatus acidity increases from the *cis*-Golgi (6.7) to the *trans*-Golgi (6.3) to reach 6.0 in the TGN and is regulated by the V-ATPase (chapter 2 (§2.5.1)).

On the contrary, the calcium concentration in the secretory pathway decreases from the *cis*-Golgi ( $250\mu\text{M}$ ) to the *trans*-Golgi ( $130\mu\text{M}$ ) (§2.6.1.1). As SPCA1 is more abundant in the late Golgi cisternae, the import of calcium in the early stacks is probably governed by SERCA pumps.

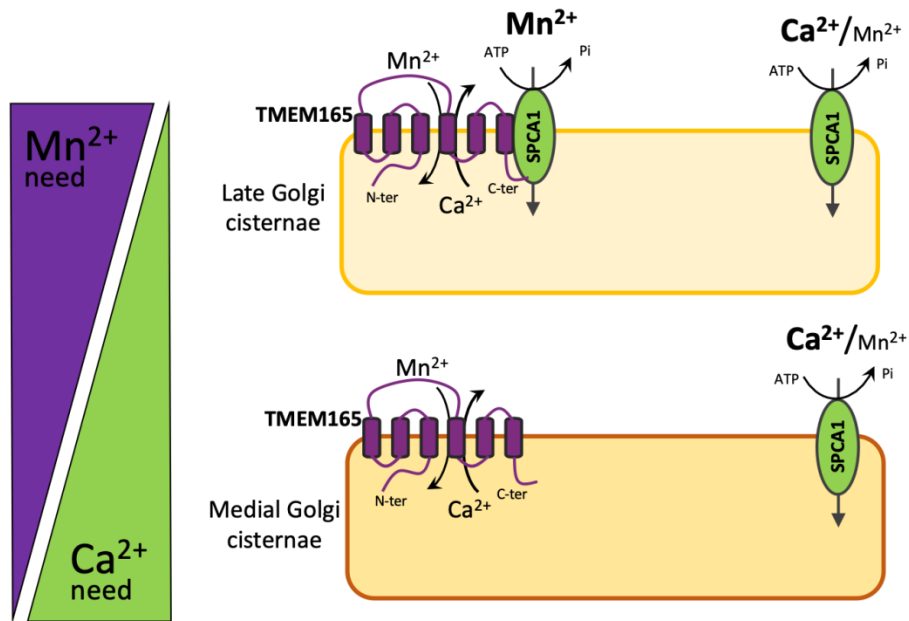


**Figure 41. Putative coupling of TMEM165 and SPCA1 in the late Golgi cisternae**

These hypothesis lead to a model in which, due to their diluted presence in the *medial*-Golgi, TMEM165 and SPCA1 would act independently (**figure 41, lower part**). On the other hand, in the late Golgi stacks TMEM165 is more abundant and would couple to SPCA1 to modulate the activity into a quasi-exclusive manganese importer (**figure 41, upper part**).

#### 4. TMEM165 is a cytosolic manganese sensor

The absence of TMEM165 in KO SPCA1 cells appeared to be due to a continuous degradation (**article 2, discussion**). As the cytosolic manganese detoxification is not accomplished in the absence of SPCA1, the cytosolic manganese concentration increases, resulting in the targeting of TMEM165 to the lysosomes for degradation. Base on this statement, any form of SPCA1 able to pump  $Mn^{2+}$  inside the Golgi lumen restores TMEM165 expression. This indicates that TMEM165 would be a cytosolic sensor of manganese concentration; however, the exact pathway of the degradation remains unknown.

#### 5. Unraveling TMEM165 degradation pathway

Besides the knockdowns of several effectors of protein degradation pathway and vesicular trafficking, the mechanism of TMEM165 manganese-induced degradation remains elusive (**Article 1, discussion**). Moreover, we were not able to reproduce experiments of Lindsted group about the sortilin-mediated degradation of TMEM165 (Mukhopadhyay and Linstedt, 2011; Mukhopadhyay et al., 2010). The hypothesis of a common pathway between TMEM165,

a cytosolic manganese sensor, and GPP130 (**Article 2 figure 4A**) (Masuda et al., 2013), a Golgi luminal manganese sensor (Venkat and Linstedt, 2017) implying sortilin as intermediate effector is hindered. Another argument is the constant degradation of TMEM165 in the absence of SPCA1, while Linstedt group demonstrated the inhibition of GPP130 manganese-induced degradation when silencing SPCA1 (Mukhopadhyay and Linstedt, 2011). This discrepancy suggests the degradation of TMEM165 through a different pathway than GPP130 that has probably not been discovered yet. In the literature, a zinc transporter SLC39A14, ZIP14, able transport manganese, was demonstrated to be degraded in the presence of high manganese concentrations (Thompson and Wessling-Resnick, 2019). Mutations in the gene encoding this transporter are also linked to a manganese-related disease. This indicates that manganese transporters may be regulated by a negative feedback loop in high manganese concentration conditions.

Furthermore, a transporter SLC10A7 (chapter 3 §3.4.3; 3.3.1.1), also involved in a skeletal dysplasia, is proposed to be implied in the glycosylation processes in a very specific manner (Dubail et al., 2018). Our research group is currently studying the link between this transporter, calcium, and glycosylation. Hopefully, this will clarify and complete our Golgi calcium homeostasis understanding.

To further understand the regulation of cellular calcium and manganese, the future studies should be larger taking in account the respective roles of every transporter.

We have seen that TMEM165 represents a manganese sensor whose degradation pathway remains elusive. Several questions remain unanswered: which amino acids constitute this sensor and which were involved in the glycosylation function of TMEM165? And finally, would the manganese-sensitivity and the glycosylation function of TMEM165 be linked?

## 6. Amino acids implicated in the glycosylation function of TMEM165 and in manganese sensitivity

It appeared essential to unravel the position and the nature of the amino acids of TMEM165 that might be involved in the cation binding, and thus in the glycosylation function and manganese sensitivity of this protein. Sequence alignment of various species, including yeast, attests to a high level of conservation of TMEM165 throughout evolution (chapter 4 §4.1.1) (Demaegd et al., 2014).

The steady-state glycosylation status of KO TMEM165 HEK293 cells complemented with mutated forms of TMEM165 was compared to other conserved amino acids outside of these motifs. Mutants in amino acids contained in the two signature motifs, especially the charged amino acids, were shown to be essential for the glycosylation function of TMEM165. This is consistent with the implication of the glutamic acids residues of these motifs in calcium transport in yeast (Colinet et al., 2017).

The study of the sensitivity of these mutants to lysosomal degradation demonstrated that most of the mutants, that presented a partial or a total resistance to manganese-induced degradation, were altered on the polar amino acids of the two motifs. The degradation delay might be due either to an authentic resistance or to a subcellular mislocalization of the protein. These results, discussed in article 1, are consistent with the hypothesis of TMEM165 as a cytosolic manganese sensor and attest the importance of the two motifs in the function and manganese sensitivity of TMEM165.

In this study, an unexpected increased electrophoretic mobility was observed for a particular mutant, T73G-TMEM165, indicating a decrease of the apparent molecular weight of the protein compared to the wild type form. The threonine residue at position 73 is hypothesized to be *O*-glycosylated; a mutation of this amino acid would lead to a loss of a glycan structure lowering the weight of the T73-TMEM165 mutant. Another possibility is the creation of a proteolytic site following the mutation of T73 into a G73. We have obtained a cell line devoid of complex *O*-glycosylation, KO COSMC HEK293, in which the addition of galactose to the GalNAc residue is inhibited, impairing the *O*-glycans structures from Core 1 biosynthesis. Our research group now aims to transfect T73-TMEM165 mutant in the KO COSMC cells to analyze the electrophoretic mobility. In addition to this, experiments with specific protease inhibitors would shed light on the nature of the T73G-TMEM165 apparent molecular weight shift. The shorter form could be due to the loss of a post-translational modification and/or the induction of a conformational change caused by the mutation with the apparition of a cleavage site.

Another challenge is our understanding on the molecular mechanism by which the supplementation of 1  $\mu$ M of  $MnCl_2$  (Morelle et al., 2017) is able to rescue the Golgi glycosylation defect in the absence of TMEM165. Although the mechanism remains enigmatic, some hypotheses arose.

### 7. TMEM165-depleted cells glycosylation restoration pathway by manganese

Manganese might enter the cell by membrane manganese transporters, endocytosis vesicles undergoing a retrograde trafficking in the TGN, or direct membrane crossing. Snyder, in his thesis in 2018, hypothesizes that the restoration of the glycosylation defect observed in KO TMEM165 by manganese would be due to the transport of  $Mn^{2+}$  into the Golgi lumen by SPCA1 (Snyder, 2018). In 2019, Houdou and collaborators assessed that the silencing of SPCA1 in KO TMEM165 HEK293 cells does not affect the glycosylation restoration. In addition, a potential role of particular isoforms of SERCA pumps in the secretory pathway manganese supply was assessed (**Appendix, article 3**). Based on the two hypothesis we have to take into account that (i) SERCA pumps have already been shown to transport manganese under certain conditions (Chiesi and Inesi, 1981; Yonekura and Toyoshima, 2016), and/or (ii) the rescue might be due to the remaining expressed SPCA1 after RNA silencing.

### 8. Potential role of TMEM165 in the bone phenotype

According to databases (Genecards, Uniprot), TMEM165 expression is ubiquitous as it is present in the immune system, musculoskeletal system, reproductive organs, heart, digestive system blood cells and various glands, consistent with the phenotype observed in patients. In addition, TMEM165 is overexpressed in cancer affecting different organs.

TMEM165-CDG is one of the rare CDG subtypes affecting the four classes of glycoconjugates: *N*-glycosylation, *O*-glycosylation, proteoglycans, and glycolipids. However, homozygous mutations are not lethal, the existence of patients mutations with a residual activity might be an explanation. In most tissues, the manganese import is not regulated only by TMEM165 but a whole group of manganese transporters that might compensate and correct the manganese defect.

At bone level, the smaller stature and the craniofacial dysmorphia observed in KO TMEM165 zebrafish experiments were demonstrated to originate from the alteration of the chondroitin sulfate proteoglycan biosynthesis of the cartilage, a process with considerable manganese needs (Zeevaert et al., 2012). The animals also presented a defect in osteoblasts and chondrocytes differentiation (Bammens et al., 2015). This would explain the skeletal dysplasia and dwarfism observed in the severest phenotypes among TMEM165-CDG patients.

TMEM165-CDG patients are currently treated by oral galactose supplementation that mainly rescues the *N*-glycosylation defect in KO TMEM165 *via* an unknown mechanism (Morelle et al., 2017). As the efficiency of the manganese supplementation at low doses for a CDG subtype, SLC39A8-CDG, presenting a manganese depletion, was assessed (Park et al., 2018), our work brings new insights on TMEM165 functions and opens a window for manganese treatment as a novel therapeutic approach. A clinical trial using manganese as a treatment for TMEM165-CDG is being conducted and the evaluation is still ongoing.

- Aebi, M. (2013). N-linked protein glycosylation in the ER. *Biochim. Biophys. Acta BBA - Mol. Cell Res.* *1833*, 2430–2437.
- Ahuja, S., and Whorton, M.R. (2019). Structural basis for mammalian nucleotide sugar transport. *ELife* *8*.
- Albesa-Jové, D., Giganti, D., Jackson, M., Alzari, P.M., and Guerin, M.E. (2014). Structure-function relationships of membrane-associated GT-B glycosyltransferases. *Glycobiology* *24*, 108–124.
- Amado, M., Almeida, R., Carneiro, F., Levery, S.B., Holmes, E.H., Nomoto, M., Hollingsworth, M.A., Hassan, H., Schwientek, T., Nielsen, P.A., et al. (1998). A family of human beta3-galactosyltransferases. Characterization of four members of a UDP-galactose:beta-N-acetyl-glucosamine/beta-nacetyl-galactosamine beta-1,3-galactosyltransferase family. *J. Biol. Chem.* *273*, 12770–12778.
- Anagianni, S., and Tuschl, K. (2019). Genetic Disorders of Manganese Metabolism. *Curr. Neurol. Neurosci. Rep.* *19*, 33.
- Appenzeller-Herzog, C., and Hauri, H.-P. (2006). The ER-Golgi intermediate compartment (ERGIC): in search of its identity and function. *J. Cell Sci.* *119*, 2173–2183.
- Arnold, S.M., Fessler, L.I., Fessler, J.H., and Kaufman, R.J. (2000). Two homologues encoding human UDP-glucose:glycoprotein glucosyltransferase differ in mRNA expression and enzymatic activity. *Biochemistry* *39*, 2149–2163.
- Aschner, M. (2006). The transport of manganese across the blood-brain barrier. *Neurotoxicology* *27*, 311–314.
- Aschner, M., Erikson, K.M., and Dorman, D.C. (2005). Manganese dosimetry: species differences and implications for neurotoxicity. *Crit. Rev. Toxicol.* *35*, 1–32.
- Avila, D.S., Puntel, R.L., and Aschner, M. (2013). Manganese in health and disease. *Met. Ions Life Sci.* *13*, 199–227.
- Aydemir, T.B., and Cousins, R.J. (2018). The Multiple Faces of the Metal Transporter ZIP14 (SLC39A14). *J. Nutr.* *148*, 174–184.
- Bailey Blackburn, J., Pokrovskaya, I., Fisher, P., Ungar, D., and Lupashin, V.V. (2016). COG Complex Complexities: Detailed Characterization of a Complete Set of HEK293T Cells Lacking Individual COG Subunits. *Front. Cell Dev. Biol.* *4*, 23.
- Baker, M.G., Simpson, C.D., Stover, B., Sheppard, L., Checkoway, H., Racette, B.A., and Seixas, N.S. (2014). Blood Manganese as an Exposure Biomarker: State of the Evidence. *J. Occup. Environ. Hyg.* *11*, 210–217.
- Bammens, R., Mehta, N., Race, V., Foulquier, F., Jaeken, J., Tiemeyer, M., Steet, R., Matthijs, G., and Flanagan-Steet, H. (2015a). Abnormal cartilage development and altered N-glycosylation in Tmem165-deficient zebrafish mirrors the phenotypes associated with TMEM165-CDG. *Glycobiology* *25*, 669–682.
- Bammens, R., Mehta, N., Race, V., Foulquier, F., Jaeken, J., Tiemeyer, M., Steet, R., Matthijs, G., and Flanagan-Steet, H. (2015b). Abnormal cartilage development and altered N-glycosylation in Tmem165-deficient zebrafish mirrors the phenotypes associated with TMEM165-CDG. *Glycobiology* *25*, 669–682.
- Banfield, D.K. (2011). Mechanisms of Protein Retention in the Golgi. *Cold Spring Harb. Perspect. Biol.* *3*, a005264–a005264.

- Barinaga-Rementeria Ramirez, I., and Lowe, M. (2009). Golgins and GRASPs: Holding the Golgi together. *Semin. Cell Dev. Biol.* *20*, 770–779.
- Barré, L., Venkatesan, N., Magdalou, J., Netter, P., Fournel-Gigleux, S., and Ouzzine, M. (2006). Evidence of calcium-dependent pathway in the regulation of human beta1,3-glucuronosyltransferase-1 (GlcAT-I) gene expression: a key enzyme in proteoglycan synthesis. *FASEB J. Off. Publ. Fed. Am. Soc. Exp. Biol.* *20*, 1692–1694.
- Bashyal, B.P., Fleet, G.W.J., Gough, M.J., and Smith, P.W. (1987). Synthesis of the  $\alpha$ -Mannosidase inhibitors swainsonine [(1S, 2R, 8R, 8aR)-1,2,8-trihydroxyoctahydroindolizine] and 1,4-dideoxy-1,4-imino-d-mannitol from mannose. *Tetrahedron* *43*, 3083–3093.
- Beznoussenko, G.V., Parashuraman, S., Rizzo, R., Polishchuk, R., Martella, O., Di Giandomenico, D., Fusella, A., Spaar, A., Sallèse, M., Capestrano, M.G., et al. (2014). Transport of soluble proteins through the Golgi occurs by diffusion via continuities across cisternae. *ELife* *3*, e02009.
- Blackburn, J.B., Kudlyk, T., Pokrovskaya, I., and Lupashin, V.V. (2018). More than just sugars: Conserved oligomeric Golgi complex deficiency causes glycosylation-independent cellular defects. *Traffic* *19*, 463–480.
- Blackburn, J.B., D'Souza, Z., and Lupashin, V.V. (2019). Maintaining order: COG complex controls Golgi trafficking, processing, and sorting. *FEBS Lett.* *593*, 2466–2487.
- Blank, B., and von Blume, J. (2017). Cab45—Unraveling key features of a novel secretory cargo sorter at the trans-Golgi network. *Eur. J. Cell Biol.* *96*, 383–390.
- Blobel, G., and Dobberstein, B. (1975). Transfer of proteins across membranes. I. Presence of proteolytically processed and unprocessed nascent immunoglobulin light chains on membrane-bound ribosomes of murine myeloma. *J. Cell Biol.* *67*, 835–851.
- Blomen, V.A., Májek, P., Jae, L.T., Bigenzahn, J.W., Nieuwenhuis, J., Staring, J., Sacco, R., van Diemen, F.R., Olk, N., Stukalov, A., et al. (2015). Gene essentiality and synthetic lethality in haploid human cells. *Science* *350*, 1092–1096.
- Blommaert, E., Péanne, R., Cherepanova, N.A., Rymen, D., Staels, F., Jaeken, J., Race, V., Keldermans, L., Souche, E., Corveleyn, A., et al. (2019). Mutations in MAGT1 lead to a glycosylation disorder with a variable phenotype. *Proc. Natl. Acad. Sci. U. S. A.* *116*, 9865–9870.
- Boix, E., Zhang, Y., Swaminathan, G.J., Brew, K., and Acharya, K.R. (2002). Structural basis of ordered binding of donor and acceptor substrates to the retaining glycosyltransferase, alpha-1,3-galactosyltransferase. *J. Biol. Chem.* *277*, 28310–28318.
- Boncompain, G., and Weigel, A.V. (2018). Transport and sorting in the Golgi complex: multiple mechanisms sort diverse cargo. *Curr. Opin. Cell Biol.* *50*, 94–101.
- Bonifacino, J.S., and Glick, B.S. (2004). The mechanisms of vesicle budding and fusion. *Cell* *116*, 153–166.
- Bowman, E.J., Siebers, A., and Altendorf, K. (1988). Bafilomycins: a class of inhibitors of membrane ATPases from microorganisms, animal cells, and plant cells. *Proc. Natl. Acad. Sci.* *85*, 7972–7976.
- Brasil, S., Pascoal, C., Francisco, R., Marques-da-Silva, D., Andreotti, G., Videira, P., Morava, E., Jaeken, J., and dos Reis Ferreira, V. (2018). CDG Therapies: From Bench to Bedside. *Int. J. Mol. Sci.* *19*, 1304.
- Braunger, K., Pfeffer, S., Shrimal, S., Gilmore, R., Berninghausen, O., Mandon, E.C., Becker, T., Förster,

- F., and Beckmann, R. (2018). Structural basis for coupling protein transport and N-glycosylation at the mammalian endoplasmic reticulum. *Science* *360*, 215–219.
- Breton, C., Šnajdrová, L., Jeanneau, C., Koča, J., and Imberty, A. (2006). Structures and mechanisms of glycosyltransferases. *Glycobiology* *16*, 29R–37R.
- Bretscher, M.S., and Munro, S. (1993). Cholesterol and the Golgi apparatus. *Science* *261*, 1280–1281.
- Brown, D., Paunescu, T.G., Breton, S., and Marshansky, V. (2009). Regulation of the V-ATPase in kidney epithelial cells: dual role in acid-base homeostasis and vesicle trafficking. *J. Exp. Biol.* *212*, 1762–1772.
- Brunet, S., and Sacher, M. (2014). In *Sickness and in Health: The Role of TRAPP and Associated Proteins in Disease*. *Traffic* *15*, 803–818.
- Brynedal, B., Wojcik, J., Esposito, F., Debailleul, V., Yaouanq, J., Martinelli-Boneschi, F., Edan, G., Comi, G., Hillert, J., and Abderrahim, H. (2010). MGAT5 alters the severity of multiple sclerosis. *J. Neuroimmunol.* *220*, 120–124.
- Callewaert, G., Parys, J.B., De Smedt, H., Raeymaekers, L., Wuytack, F., Vanoevelen, J., Van Baelen, K., Simoni, A., Rizzuto, R., and Missiaen, L. (2003). Similar Ca(2+)-signaling properties in keratinocytes and in COS-1 cells overexpressing the secretory-pathway Ca(2+)-ATPase SPCA1. *Cell Calcium* *34*, 157–162.
- Cantagrel, V., and Lefeber, D.J. (2011). From glycosylation disorders to dolichol biosynthesis defects: a new class of metabolic diseases. *J. Inherit. Metab. Dis.* *34*, 859–867.
- Caramelo, J.J., and Parodi, A.J. (2015). A sweet code for glycoprotein folding. *FEBS Lett.* *589*, 3379–3387.
- Carlsson, S.R., Roth, J., Piller, F., and Fukuda, M. (1988). Isolation and characterization of human lysosomal membrane glycoproteins, h-lamp-1 and h-lamp-2. Major sialoglycoproteins carrying polylectosaminoglycan. *J. Biol. Chem.* *263*, 18911–18919.
- Carmona, A., Zogzas, C.E., Roudeau, S., Porcaro, F., Garrevoet, J., Spiers, K.M., Salomé, M., Cloetens, P., Mukhopadhyay, S., and Ortega, R. (2019). SLC30A10 Mutation Involved in Parkinsonism Results in Manganese Accumulation within Nanovesicles of the Golgi Apparatus. *ACS Chem. Neurosci.* *10*, 599–609.
- Chalmin, E., Vignaud, C., Salomon, H., Farges, F., Susini, J., and Menu, M. (2006). Minerals discovered in paleolithic black pigments by transmission electron microscopy and micro-X-ray absorption near-edge structure. *Appl. Phys. A* *83*, 213–218.
- Chen, P., Bornhorst, J., and Aschner, M. (2018). Manganese metabolism in humans. *Front. Biosci. Landmark Ed.* *23*, 1655–1679.
- Chen, W., Unligil, U.M., Rini, J.M., and Stanley, P. (2001). Independent Lec1A CHO glycosylation mutants arise from point mutations in N-acetylglucosaminyltransferase I that reduce affinity for both substrates. Molecular consequences based on the crystal structure of GlcNAc-TI. *Biochemistry* *40*, 8765–8772.
- Cheng, P.W., and DeVries, A. (1986). Mucin biosynthesis. Enzymic properties of human-tracheal epithelial GDP-L-fucose:beta-D-galactoside alpha-(1----2)-L-fucosyltransferase. *Carbohydr. Res.* *149*, 253–261.
- Cheung, P., and Dennis, J.W. (2007). Mgat5 and Pten interact to regulate cell growth and polarity. *Glycobiology* *17*, 767–773.

- Chiesi, M., and Inesi, G. (1981). Mg<sup>2+</sup> and Mn<sup>2+</sup> modulation of Ca<sup>2+</sup> transport and ATPase activity in sarcoplasmic reticulum vesicles. *Arch. Biochem. Biophys.* *208*, 586–592.
- Clayton, P.T. (2017). Inherited disorders of transition metal metabolism: an update. *J. Inherit. Metab. Dis.* *40*, 519–529.
- Climer, L.K., Hendrix, R.D., and Lupashin, V.V. (2018). Conserved Oligomeric Golgi and Neuronal Vesicular Trafficking. *Handb. Exp. Pharmacol.* *245*, 227–247.
- Colinet, A.-S., Sengottaiyan, P., Deschamps, A., Colsoul, M.-L., Thines, L., Demaegd, D., Duchêne, M.-C., Foulquier, F., Hols, P., and Morsomme, P. (2016a). Yeast Gdt1 is a Golgi-localized calcium transporter required for stress-induced calcium signaling and protein glycosylation. *Sci. Rep.* *6*.
- Colinet, A.-S., Sengottaiyan, P., Deschamps, A., Colsoul, M.-L., Thines, L., Demaegd, D., Duchêne, M.-C., Foulquier, F., Hols, P., and Morsomme, P. (2016b). Yeast Gdt1 is a Golgi-localized calcium transporter required for stress-induced calcium signaling and protein glycosylation. *Sci. Rep.* *6*, 24282.
- Colinet, A.-S., Thines, L., Deschamps, A., Flémal, G., Demaegd, D., and Morsomme, P. (2017). Acidic and uncharged polar residues in the consensus motifs of the yeast Ca<sup>2+</sup> transporter Gdt1p are required for calcium transport. *Cell. Microbiol.* *19*.
- Crossgrove, J., and Zheng, W. (2004). Manganese toxicity upon overexposure. *NMR Biomed.* *17*, 544–553.
- Daran, J.M., Dallies, N., Thines-Sempoux, D., Paquet, V., and Francois, J. (1995). Genetic and Biochemical Characterization of the UGP1 Gene Encoding the UDP-Glucose Pyrophosphorylase from *Saccharomyces cerevisiae*. *Eur. J. Biochem.* *233*, 520–530.
- De Praeter CM, Gerwig, G.J., Bause, E., Nuytinck, L.K., Vliegenthart, J.F., Breuer, W., Kamerling, J.P., Espeel, M.F., Martin, J.J., De Paepe AM, null, et al. (2000). A novel disorder caused by defective biosynthesis of N-linked oligosaccharides due to glucosidase I deficiency. *Am. J. Hum. Genet.* *66*, 1744–1756.
- Demaegd, D., Foulquier, F., Colinet, A.-S., Gremillon, L., Legrand, D., Mariot, P., Peiter, E., Van Schaftingen, E., Matthijs, G., and Morsomme, P. (2013a). Newly characterized Golgi-localized family of proteins is involved in calcium and pH homeostasis in yeast and human cells. *Proc. Natl. Acad. Sci.* *110*, 6859–6864.
- Demaegd, D., Foulquier, F., Colinet, A.-S., Gremillon, L., Legrand, D., Mariot, P., Peiter, E., Van Schaftingen, E., Matthijs, G., and Morsomme, P. (2013b). Newly characterized Golgi-localized family of proteins is involved in calcium and pH homeostasis in yeast and human cells. *Proc. Natl. Acad. Sci.* *110*, 6859–6864.
- Demaegd, D., Colinet, A.-S., Deschamps, A., and Morsomme, P. (2014). Molecular evolution of a novel family of putative calcium transporters. *PLoS One* *9*, e100851.
- Dennis, J.W., Nabi, I.R., and Demetriou, M. (2009). Metabolism, Cell Surface Organization, and Disease. *Cell* *139*, 1229–1241.
- Dodonova, S.O., Aderhold, P., Kopp, J., Ganeva, I., Röhling, S., Hagen, W.J.H., Sinning, I., Wieland, F., and Briggs, J.A.G. (2017). 9Å structure of the COPI coat reveals that the Arf1 GTPase occupies two contrasting molecular environments. *ELife* *6*.
- Dröscher, A. (1998). Camillo Golgi and the discovery of the Golgi apparatus. *Histochem. Cell Biol.* *109*,

425–430.

Dubail, J., Huber, C., Chantepie, S., Sonntag, S., Tüysüz, B., Mihci, E., Gordon, C.T., Steichen-Gersdorf, E., Amiel, J., Nur, B., et al. (2018). SLC10A7 mutations cause a skeletal dysplasia with amelogenesis imperfecta mediated by GAG biosynthesis defects. *Nat. Commun.* *9*, 3087.

Dulary, E., Potelle, S., Legrand, D., and Foulquier, F. (2017). TMEM165 deficiencies in Congenital Disorders of Glycosylation type II (CDG-II): Clues and evidences for roles of the protein in Golgi functions and ion homeostasis. *Tissue Cell* *49*, 150–156.

Dulary, E., Yu, S.-Y., Houdou, M., de Bettignies, G., Decool, V., Potelle, S., Duvet, S., Krzewinski-Recchi, M.-A., Garat, A., Matthijs, G., et al. (2018). Investigating the function of Gdt1p in yeast Golgi glycosylation. *Biochim. Biophys. Acta BBA - Gen. Subj.* *1862*, 394–402.

Dunlop, M.H., Ernst, A.M., Schroeder, L.K., Toomre, D.K., Lavieu, G., and Rothman, J.E. (2017). Land-locked mammalian Golgi reveals cargo transport between stable cisternae. *Nat. Commun.* *8*, 432.

Edvardson, S., Ashikov, A., Jalas, C., Sturiale, L., Shaag, A., Fedick, A., Treff, N.R., Garozzo, D., Gerardy-Schahn, R., and Elpeleg, O. (2013). Mutations in SLC35A3 cause autism spectrum disorder, epilepsy and arthrogryposis. *J. Med. Genet.* *50*, 733–739.

Eisenhut, M., Hoecker, N., Schmidt, S.B., Basgaran, R.M., Flachbart, S., Jahns, P., Eser, T., Geimer, S., Husted, S., Weber, A.P.M., et al. (2018). The Plastid Envelope CHLOROPLAST MANGANESE TRANSPORTER1 Is Essential for Manganese Homeostasis in Arabidopsis. *Mol. Plant* *11*, 955–969.

Elbein, A.D., Tropea, J.E., Mitchell, M., and Kaushal, G.P. (1990). Kifunensine, a potent inhibitor of the glycoprotein processing mannosidase I. *J. Biol. Chem.* *265*, 15599–15605.

Erikson, K.M., and Aschner, M. (2019). Manganese: Its Role in Disease and Health. *Met. Ions Life Sci.* *19*.

Farquhar, M.G., and Palade, G.E. (1981). The Golgi apparatus (complex)-(1954-1981)-from artifact to center stage. *J. Cell Biol.* *91*, 77s–103s.

Ferrara, C., Grau, S., Jäger, C., Sondermann, P., Brünker, P., Waldhauer, I., Hennig, M., Ruf, A., Rufer, A.C., Stihle, M., et al. (2011). Unique carbohydrate-carbohydrate interactions are required for high affinity binding between FcγRIII and antibodies lacking core fucose. *Proc. Natl. Acad. Sci. U. S. A.* *108*, 12669–12674.

Ferreira, K.N. (2004). Architecture of the Photosynthetic Oxygen-Evolving Center. *Science* *303*, 1831–1838.

Ferreira, C.R., Altassan, R., Marques-Da-Silva, D., Francisco, R., Jaeken, J., and Morava, E. (2018). Recognizable phenotypes in CDG. *J. Inherit. Metab. Dis.* *41*, 541–553.

Foulquier, F. (2009). COG defects, birth and rise! *Biochim. Biophys. Acta* *1792*, 896–902.

Foulquier, F., Ungar, D., Reynders, E., Zeevaert, R., Mills, P., García-Silva, M.T., Briones, P., Winchester, B., Morelle, W., Krieger, M., et al. (2007). A new inborn error of glycosylation due to a Cog8 deficiency reveals a critical role for the Cog1-Cog8 interaction in COG complex formation. *Hum. Mol. Genet.* *16*, 717–730.

Foulquier, F., Amyere, M., Jaeken, J., Zeevaert, R., Schollen, E., Race, V., Bammens, R., Morelle, W., Rosnoble, C., Legrand, D., et al. (2012a). TMEM165 Deficiency Causes a Congenital Disorder of Glycosylation. *Am. J. Hum. Genet.* *91*, 15–26.

- Foulquier, F., Amyere, M., Jaeken, J., Zeevaert, R., Schollen, E., Race, V., Bammens, R., Morelle, W., Rosnoble, C., Legrand, D., et al. (2012b). TMEM165 deficiency causes a congenital disorder of glycosylation. *Am. J. Hum. Genet.* *91*, 15–26.
- Freeze, H.H., and Elbein, A.D. (2009). Glycosylation Precursors. In *Essentials of Glycobiology*, A. Varki, R.D. Cummings, J.D. Esko, H.H. Freeze, P. Stanley, C.R. Bertozzi, G.W. Hart, and M.E. Etzler, eds. (Cold Spring Harbor (NY): Cold Spring Harbor Laboratory Press), p.
- Friedman, B.J., Freeland-Graves, J.H., Bales, C.W., Behmardi, F., Shorey-Kutschke, R.L., Willis, R.A., Crosby, J.B., Trickett, P.C., and Houston, S.D. (1987). Manganese balance and clinical observations in young men fed a manganese-deficient diet. *J. Nutr.* *117*, 133–143.
- Fujita, M., Gao, X.-D., and Kinoshita, T. (2015). Glycan-Mediated Protein Transport from the Endoplasmic Reticulum. In *Sugar Chains*, T. Suzuki, K. Ohtsubo, and N. Taniguchi, eds. (Tokyo: Springer Japan), pp. 21–34.
- Fukuda, M. (1991). Lysosomal membrane glycoproteins. Structure, biosynthesis, and intracellular trafficking. *J. Biol. Chem.* *266*, 21327–21330.
- Furbee, B. (2009). Manganese. In *Clinical Neurotoxicology*, (Elsevier), pp. 293–301.
- Gallegos-Gómez, M.-L., Greotti, E., López-Méndez, M.-C., Sánchez-Vázquez, V.-H., Arias, J.-M., and Guerrero-Hernández, A. (2018). The Trans Golgi Region is a Labile Intracellular Ca<sup>2+</sup> Store Sensitive to Emetine. *Sci. Rep.* *8*, 17143.
- Gandini, C., Schmidt, S.B., Husted, S., Schneider, A., and Leister, D. (2017). The transporter SynPAM71 is located in the plasma membrane and thylakoids, and mediates manganese tolerance in *Synechocystis* PCC6803. *New Phytol.* *215*, 256–268.
- Garrick, M.D., Dolan, K.G., Horbinski, C., Ghio, A.J., Higgins, D., Porubcin, M., Moore, E.G., Hainsworth, L.N., Umbreit, J.N., Conrad, M.E., et al. (2003). DMT1: a mammalian transporter for multiple metals. *Biometals Int. J. Role Met. Ions Biol. Biochem. Med.* *16*, 41–54.
- Garrick, M.D., Singleton, S.T., Vargas, F., Kuo, H.-C., Zhao, L., Knöpfel, M., Davidson, T., Costa, M., Paradkar, P., Roth, J.A., et al. (2006). DMT1: Which metals does it transport? *Biol. Res.* *39*.
- Gil, G.-C., Velandar, W.H., and Van Cott, K.E. (2009). N-glycosylation microheterogeneity and site occupancy of an Asn-X-Cys sequon in plasma-derived and recombinant protein C. *PROTEOMICS* *9*, 2555–2567.
- Glick, B.S., and Luini, A. (2011). Models for Golgi traffic: a critical assessment. *Cold Spring Harb. Perspect. Biol.* *3*, a005215.
- Glick, B.S., and Nakano, A. (2009). Membrane Traffic Within the Golgi Apparatus. *Annu. Rev. Cell Dev. Biol.* *25*, 113–132.
- Gonzalez, A., Valeiras, M., Sidransky, E., and Tayebi, N. (2014). Lysosomal integral membrane protein-2: A new player in lysosome-related pathology. *Mol. Genet. Metab.* *111*, 84–91.
- Götting, C., Müller, S., Schöttler, M., Schön, S., Prante, C., Brinkmann, T., Kuhn, J., and Kleesiek, K. (2004). Analysis of the DXD motifs in human xylosyltransferase I required for enzyme activity. *J. Biol. Chem.* *279*, 42566–42573.
- Griesemer, M., Young, C., Robinson, A.S., and Petzold, L. (2014). BiP clustering facilitates protein folding in the endoplasmic reticulum. *PLoS Comput. Biol.* *10*, e1003675.

- Gunter, T.E., Gerstner, B., Gunter, K.K., Malecki, J., Gelein, R., Valentine, W.M., Aschner, M., and Yule, D.I. (2013). Manganese transport via the transferrin mechanism. *Neurotoxicology* 34, 118–127.
- Hadley, B., Maggioni, A., Ashikov, A., Day, C.J., Haselhorst, T., and Tiralongo, J. (2014). Structure and function of nucleotide sugar transporters: Current progress. *Comput. Struct. Biotechnol. J.* 10, 23–32.
- Hadley, B., Litfin, T., Day, C.J., Haselhorst, T., Zhou, Y., and Tiralongo, J. (2019). Nucleotide Sugar Transporter SLC35 Family Structure and Function. *Comput. Struct. Biotechnol. J.* 17, 1123–1134.
- Haijes, H.A., Jaeken, J., Foulquier, F., and van Hasselt, P.M. (2018). Hypothesis: lobe A (COG1-4)-CDG causes a more severe phenotype than lobe B (COG5-8)-CDG. *J. Med. Genet.* 55, 137–142.
- Hansske, B., Thiel, C., Lübke, T., Hasilik, M., Höning, S., Peters, V., Heidemann, P.H., Hoffmann, G.F., Berger, E.G., von Figura, K., et al. (2002). Deficiency of UDP-galactose:N-acetylglucosamine beta-1,4-galactosyltransferase I causes the congenital disorder of glycosylation type IIId. *J. Clin. Invest.* 109, 725–733.
- Harischandra, D.S., Jin, H., Anantharam, V., Kanthasamy, A., and Kanthasamy, A.G. (2015).  $\alpha$ -Synuclein protects against manganese neurotoxic insult during the early stages of exposure in a dopaminergic cell model of Parkinson's disease. *Toxicol. Sci. Off. J. Soc. Toxicol.* 143, 454–468.
- He, W., and Hu, Z. (2012). The role of the Golgi-resident SPCA  $\text{Ca}^{2+}/\text{Mn}^{2+}$  pump in ionic homeostasis and neural function. *Neurochem. Res.* 37, 455–468.
- Hediger, M.A., Romero, M.F., Peng, J.-B., Rolfs, A., Takanaga, H., and Bruford, E.A. (2004). The ABCs of solute carriers: physiological, pathological and therapeutic implications of human membrane transport proteins. *Pflügers Arch. Eur. J. Physiol.* 447, 465–468.
- Heesen, S. te, Lehle, L., Weissmann, A., and Aebi, M. (1994). Isolation of the ALG5 Locus Encoding the UDP-Glucose:Dolichyl-Phosphate Glucosyltransferase from *Saccharomyces cerevisiae*. *Eur. J. Biochem.* 224, 71–79.
- Helenius, A., and Aebi, M. (2004). Roles of N-linked glycans in the endoplasmic reticulum. *Annu. Rev. Biochem.* 73, 1019–1049.
- Hempel, A., Camerman, N., Mastropaolo, D., and Camerman, A. (1993). Glucosidase inhibitors: structures of deoxynojirimycin and castanospermine. *J. Med. Chem.* 36, 4082–4086.
- Hennet, T. (2002). The galactosyltransferase family. *Cell. Mol. Life Sci. CMLS* 59, 1081–1095.
- Herscovics, A., and Orlean, P. (1993). Glycoprotein biosynthesis in yeast. *FASEB J.* 7, 540–550.
- Hinsdale, M.E. (2014). Xylosyltransferase I, II (XYLT1,2). In *Handbook of Glycosyltransferases and Related Genes*, N. Taniguchi, K. Honke, M. Fukuda, H. Narimatsu, Y. Yamaguchi, and T. Angata, eds. (Tokyo: Springer Japan), pp. 873–883.
- Hiraoka, S., Furuichi, T., Nishimura, G., Shibata, S., Yanagishita, M., Rimoin, D.L., Superti-Furga, A., Nikkels, P.G., Ogawa, M., Katsuyama, K., et al. (2007). Nucleotide-sugar transporter SLC35D1 is critical to chondroitin sulfate synthesis in cartilage and skeletal development in mouse and human. *Nat. Med.* 13, 1363–1367.
- Hoffmann, H.-H., Schneider, W.M., Blomen, V.A., Scull, M.A., Hovnanian, A., Brummelkamp, T.R., and Rice, C.M. (2017). Diverse Viruses Require the Calcium Transporter SPCA1 for Maturation and Spread. *Cell Host Microbe* 22, 460-470.e5.

- Honke, K. (2014). Globoside Alpha-1,3-N-Acetylgalactosaminyltransferase 1 (GBGT1). In Handbook of Glycosyltransferases and Related Genes, N. Taniguchi, K. Honke, M. Fukuda, H. Narimatsu, Y. Yamaguchi, and T. Angata, eds. (Tokyo: Springer Japan), pp. 455–461.
- Houdou, M., Lebredonchel, E., Garat, A., Duvet, S., Legrand, D., Decool, V., Klein, A., Ouzzine, M., Gasnier, B., Potelle, S., et al. (2019). Involvement of thapsigargin- and cyclopiazonic acid-sensitive pumps in the rescue of TMEM165-associated glycosylation defects by Mn<sup>2+</sup>. *FASEB J. Off. Publ. Fed. Am. Soc. Exp. Biol.* *33*, 2669–2679.
- Inamori, K., Willer, T., Hara, Y., Venzke, D., Anderson, M.E., Clarke, N.F., Guicheney, P., Bönnemann, C.G., Moore, S.A., and Campbell, K.P. (2014). Endogenous glucuronyltransferase activity of LARGE or LARGE2 required for functional modification of  $\alpha$ -dystroglycan in cells and tissues. *J. Biol. Chem.* *289*, 28138–28148.
- Institute of Medicine (US) Panel on Micronutrients (2001). Dietary Reference Intakes for Vitamin A, Vitamin K, Arsenic, Boron, Chromium, Copper, Iodine, Iron, Manganese, Molybdenum, Nickel, Silicon, Vanadium, and Zinc (Washington (DC): National Academies Press (US)).
- Jaeken, J. (2011). Congenital disorders of glycosylation (CDG): it's (nearly) all in it! *J. Inher. Metab. Dis.* *34*, 853–858.
- Jaeken, J., Schachter, H., Carchon, H., De Cock, P., Coddeville, B., and Spik, G. (1994). Carbohydrate deficient glycoprotein syndrome type II: a deficiency in Golgi localised N-acetylglucosaminyltransferase II. *Arch. Dis. Child.* *71*, 123–127.
- Jaeken, J., Hennet, T., Matthijs, G., and Freeze, H.H. (2009). CDG nomenclature: time for a change! *Biochim. Biophys. Acta* *1792*, 825–826.
- Jansen, J.C., Timal, S., van Scherpenzeel, M., Michelakakis, H., Vicogne, D., Ashikov, A., Moraitou, M., Hoischen, A., Huijben, K., Steenbergen, G., et al. (2016a). TMEM199 Deficiency Is a Disorder of Golgi Homeostasis Characterized by Elevated Aminotransferases, Alkaline Phosphatase, and Cholesterol and Abnormal Glycosylation. *Am. J. Hum. Genet.* *98*, 322–330.
- Jansen, J.C., Cirak, S., van Scherpenzeel, M., Timal, S., Reunert, J., Rust, S., Pérez, B., Vicogne, D., Krawitz, P., Wada, Y., et al. (2016b). CCDC115 Deficiency Causes a Disorder of Golgi Homeostasis with Abnormal Protein Glycosylation. *Am. J. Hum. Genet.* *98*, 310–321.
- Jansen, J.C., Wolthuis, D., Van Scherpenzeel, M., Ratziu, V., Drenth, J.P.H., and Lefeber, D.J. (2018). NAFLD Phenotype in Patients With V-ATPase Proton Pump Assembly Defects. *Cell. Mol. Gastroenterol. Hepatol.* *5*, 415-417.e1.
- Jiang, Y.-M., Mo, X.-A., Du, F.-Q., Fu, X., Zhu, X.-Y., Gao, H.-Y., Xie, J.-L., Liao, F.-L., Pira, E., and Zheng, W. (2006). Effective treatment of manganese-induced occupational Parkinsonism with p-aminosalicylic acid: a case of 17-year follow-up study. *J. Occup. Environ. Med.* *48*, 644–649.
- Johswich, A., Longuet, C., Pawling, J., Abdel Rahman, A., Ryczko, M., Drucker, D.J., and Dennis, J.W. (2014). N-glycan remodeling on glucagon receptor is an effector of nutrient sensing by the hexosamine biosynthesis pathway. *J. Biol. Chem.* *289*, 15927–15941.
- Joshi, H.J., Hansen, L., Narimatsu, Y., Freeze, H.H., Henrissat, B., Bennett, E., Wandall, H.H., Clausen, H., and Schjoldager, K.T. (2018). Glycosyltransferase genes that cause monogenic congenital disorders of glycosylation are distinct from glycosyltransferase genes associated with complex diseases. *Glycobiology* *28*, 284–294.

- Kakuda, S., Shiba, T., Ishiguro, M., Tagawa, H., Oka, S., Kajihara, Y., Kawasaki, T., Wakatsuki, S., and Kato, R. (2004). Structural basis for acceptor substrate recognition of a human glucuronyltransferase, GlcAT-P, an enzyme critical in the biosynthesis of the carbohydrate epitope HNK-1. *J. Biol. Chem.* *279*, 22693–22703.
- Kaneko, Y., Nimmerjahn, F., and Ravetch, J.V. (2006). Anti-inflammatory activity of immunoglobulin G resulting from Fc sialylation. *Science* *313*, 670–673.
- Kaufman, R.J., Swaroop, M., and Murtha-Riel, P. (1994). Depletion of Manganese within the Secretory Pathway Inhibits O-Linked Glycosylation in Mammalian Cells. *Biochemistry* *33*, 9813–9819.
- Keith M. Erikson, M.A. (2019). 4. Ironing out the Brain. In *Essential Metals in Medicine: Therapeutic Use and Toxicity of Metal Ions in the Clinic*, (Berlin, Boston: De Gruyter), pp. 87–122.
- Kellokumpu, S. (2019). Golgi pH, Ion and Redox Homeostasis: How Much Do They Really Matter? *Front. Cell Dev. Biol.* *7*, 93.
- Kiyoshi, M., Tsumoto, K., Ishii-Watabe, A., and Caaveiro, J.M.M. (2017). Glycosylation of IgG-Fc: a molecular perspective. *Int. Immunol.* *29*, 311–317.
- Kizuka, Y., and Oka, S. (2014). Beta-1,3-Glucuronyltransferase 1 (Glucuronosyltransferase P); Beta-1,3-Glucuronyltransferase 2 (B3GAT1,2). In *Handbook of Glycosyltransferases and Related Genes*, N. Taniguchi, K. Honke, M. Fukuda, H. Narimatsu, Y. Yamaguchi, and T. Angata, eds. (Tokyo: Springer Japan), pp. 835–847.
- Kornak, U., Reynders, E., Dimopoulou, A., van Reeuwijk, J., Fischer, B., Rajab, A., Budde, B., Nürnberg, P., Foulquier, F., Lefeber, D., et al. (2008). Impaired glycosylation and cutis laxa caused by mutations in the vesicular H<sup>+</sup>-ATPase subunit ATP6V0A2. *Nat. Genet.* *40*, 32–34.
- Kranz, C., Denecke, J., Lehrman, M.A., Ray, S., Kienz, P., Kreissel, G., Sagi, D., Peter-Katalinic, J., Freeze, H.H., Schmid, T., et al. (2001). A mutation in the human MPDU1 gene causes congenital disorder of glycosylation type If (CDG-If). *J. Clin. Invest.* *108*, 1613–1619.
- Kubota, T., Shiba, T., Sugioka, S., Furukawa, S., Sawaki, H., Kato, R., Wakatsuki, S., and Narimatsu, H. (2006). Structural basis of carbohydrate transfer activity by human UDP-GalNAc: polypeptide alpha-N-acetylgalactosaminyltransferase (pp-GalNAc-T10). *J. Mol. Biol.* *359*, 708–727.
- Kumar, K.K., Lowe, E.W., Aboud, A.A., Neely, M.D., Redha, R., Bauer, J.A., Odak, M., Weaver, C.D., Meiler, J., Aschner, M., et al. (2015). Cellular manganese content is developmentally regulated in human dopaminergic neurons. *Sci. Rep.* *4*, 6801.
- Kundra, R., and Kornfeld, S. (1999). Asparagine-linked Oligosaccharides Protect Lamp-1 and Lamp-2 from Intracellular Proteolysis. *J. Biol. Chem.* *274*, 31039–31046.
- Kurokawa, K., Osakada, H., Kojidani, T., Waga, M., Suda, Y., Asakawa, H., Haraguchi, T., and Nakano, A. (2019). Visualization of secretory cargo transport within the Golgi apparatus. *J. Cell Biol.* *218*, 1602–1618.
- Lacampagne, A., Fauconnier, J., and Richard, S. (2008). Récepteur de la ryanodine et dysfonctionnement myocardique. *Médecine/Sciences* *24*, 399–406.
- Lairson, L.L., Henrissat, B., Davies, G.J., and Withers, S.G. (2008). Glycosyltransferases: structures, functions, and mechanisms. *Annu. Rev. Biochem.* *77*, 521–555.
- Lastra, G.C., Thompson, S.J., Lemonidis, A.S., and Elson, C.J. (1998). Changes in the galactose content

of IgG during humoral immune responses. *Autoimmunity* 28, 25–30.

Lau, K.S., Partridge, E.A., Grigorian, A., Silvescu, C.I., Reinhold, V.N., Demetriou, M., and Dennis, J.W. (2007). Complex N-Glycan Number and Degree of Branching Cooperate to Regulate Cell Proliferation and Differentiation. *Cell* 129, 123–134.

Lavieu, G., Zheng, H., and Rothman, J.E. (2013). Stapled Golgi cisternae remain in place as cargo passes through the stack. *ELife* 2, e00558.

Li, J., Rancour, D.M., Allende, M.L., Worth, C.A., Darling, D.S., Gilbert, J.B., Menon, A.K., and Young, W.W. (2001). The DXD motif is required for GM2 synthase activity but is not critical for nucleotide binding. *Glycobiology* 11, 217–229.

Li, L.-H., Tian, X.-R., Jiang, Z., Zeng, L.-W., He, W.-F., and Hu, Z.-P. (2013). The Golgi Apparatus: Panel Point of Cytosolic Ca<sup>2+</sup> Regulation. *Neurosignals* 21, 272–284.

Lide, D.R. (2004). *CRC Handbook of Chemistry and Physics*, 85th Edition (CRC Press).

Liu, Q. (2017). TMBIM-mediated Ca<sup>2+</sup> homeostasis and cell death. *Biochim. Biophys. Acta Mol. Cell Res.* 1864, 850–857.

Liu, S.D., Chalouni, C., Young, J.C., Junttila, T.T., Sliwkowski, M.X., and Lowe, J.B. (2015). Afucosylated antibodies increase activation of FcγRIIIa-dependent signaling components to intensify processes promoting ADCC. *Cancer Immunol. Res.* 3, 173–183.

Lühn, K., Wild, M.K., Eckhardt, M., Gerardy-Schahn, R., and Vestweber, D. (2001). The gene defective in leukocyte adhesion deficiency II encodes a putative GDP-fucose transporter. *Nat. Genet.* 28, 69–72.

Maeda, Y. (2011). [pH homeostasis of the Golgi apparatus by GPHR, a novel anion channel]. *Nihon Yakurigaku Zasshi Folia Pharmacol. Jpn.* 137, 212–216.

Makaraci, P., and Kim, K. (2018). trans -Golgi network-bound cargo traffic. *Eur. J. Cell Biol.* 97, 137–149.

Makhoul, C., Gosavi, P., and Gleeson, P.A. (2018). The Golgi architecture and cell sensing. *Biochem. Soc. Trans.* 46, 1063–1072.

Malhotra, R., Wormald, M.R., Rudd, P.M., Fischer, P.B., Dwek, R.A., and Sim, R.B. (1995). Glycosylation changes of IgG associated with rheumatoid arthritis can activate complement via the mannose-binding protein. *Nat. Med.* 1, 237–243.

Mandon, E.C., Trueman, S.F., and Gilmore, R. (2013). Protein translocation across the rough endoplasmic reticulum. *Cold Spring Harb. Perspect. Biol.* 5.

Manya, H., Chiba, A., Yoshida, A., Wang, X., Chiba, Y., Jigami, Y., Margolis, R.U., and Endo, T. (2004). Demonstration of mammalian protein O-mannosyltransferase activity: coexpression of POMT1 and POMT2 required for enzymatic activity. *Proc. Natl. Acad. Sci. U. S. A.* 101, 500–505.

Marquardt, T., Lühn, K., Srikrishna, G., Freeze, H.H., Harms, E., and Vestweber, D. (1999). Correction of Leukocyte Adhesion Deficiency Type II With Oral Fucose. *Blood* 94, 3976–3985.

Marshansky, V., and Futai, M. (2008). The V-type H<sup>+</sup>-ATPase in vesicular trafficking: targeting, regulation and function. *Curr. Opin. Cell Biol.* 20, 415–426.

Masuda, M., Braun-sommargren, M., Crooks, D., and Smith, D.R. (2013). Golgi Phosphoprotein 4 (GPP130) is a Sensitive and Selective Cellular Target of Manganese Exposure. *Synap. N. Y. N* 67, 205–

215.

Maxel, T., Smidt, K., Petersen, C.C., Honoré, B., Christensen, A.K., Jeppesen, P.B., Brock, B., Rungby, J., Palmfeldt, J., and Larsen, A. (2019). The zinc transporter Zip14 (SLC39a14) affects Beta-cell Function: Proteomics, Gene expression, and Insulin secretion studies in INS-1E cells. *Sci. Rep.* *9*, 8589.

Mergler, D., and Baldwin, M. (1997). Early Manifestations of Manganese Neurotoxicity in Humans: An Update. *Environ. Res.* *73*, 92–100.

Mestrom, Przepis, Kowalczykiewicz, Pollender, Kumpf, Marsden, Bento, Jarzębski, Szymańska, Chruściel, et al. (2019). Leloir Glycosyltransferases in Applied Biocatalysis: A Multidisciplinary Approach. *Int. J. Mol. Sci.* *20*, 5263.

Meusser, B., Hirsch, C., Jarosch, E., and Sommer, T. (2005). ERAD: the long road to destruction. *Nat. Cell Biol.* *7*, 766–772.

Mi, Y., Coonce, M., Fiete, D., Steirer, L., Dveksler, G., Townsend, R.R., and Baenziger, J.U. (2016). Functional Consequences of Mannose and Asialoglycoprotein Receptor Ablation. *J. Biol. Chem.* *291*, 18700–18717.

Micaroni, M. (2012). Calcium around the Golgi apparatus: implications for intracellular membrane trafficking. *Adv. Exp. Med. Biol.* *740*, 439–460.

Micaroni, M., Giacchetti, G., Plebani, R., Xiao, G.G., and Federici, L. (2016). ATP2C1 gene mutations in Hailey–Hailey disease and possible roles of SPCA1 isoforms in membrane trafficking. *Cell Death Dis.* *7*, e2259–e2259.

Milatovic, D., Gupta, R.C., Yin, Z., Zaja-Milatovic, S., and Aschner, M. (2011). Manganese. In *Reproductive and Developmental Toxicology*, (Elsevier), pp. 439–450.

Minamida, S., Aoki, K., Natsuka, S., Omichi, K., Fukase, K., Kusumoto, S., and Hase, S. (1996). Detection of UDP-D-xylose: alpha-D-xyloside alpha 1-->3xylosyltransferase activity in human hepatoma cell line HepG2. *J. Biochem. (Tokyo)* *120*, 1002–1006.

Missiaen, L., Raeymaekers, L., Dode, L., Vanoevelen, J., Van Baelen, K., Parys, J.B., Callewaert, G., De Smedt, H., Segaert, S., and Wuytack, F. (2004). SPCA1 pumps and Hailey–Hailey disease. *Biochem. Biophys. Res. Commun.* *322*, 1204–1213.

Mkhikian, H., Grigorian, A., Li, C.F., Chen, H.-L., Newton, B., Zhou, R.W., Beeton, C., Torossian, S., Tatarian, G.G., Lee, S.-U., et al. (2011). Genetics and the environment converge to dysregulate N-glycosylation in multiple sclerosis. *Nat. Commun.* *2*, 334.

Mkhikian, H., Mortales, C.-L., Zhou, R.W., Khachikyan, K., Wu, G., Haslam, S.M., Kavarian, P., Dell, A., and Demetriou, M. (2016). Golgi self-correction generates bioequivalent glycans to preserve cellular homeostasis. *ELife* *5*.

Molinari, M. (2003). Role of EDEM in the Release of Misfolded Glycoproteins from the Calnexin Cycle. *Science* *299*, 1397–1400.

Molinari, F., Foulquier, F., Tarpey, P.S., Morelle, W., Boissel, S., Teague, J., Edkins, S., Futreal, P.A., Stratton, M.R., Turner, G., et al. (2008). Oligosaccharyltransferase-subunit mutations in nonsyndromic mental retardation. *Am. J. Hum. Genet.* *82*, 1150–1157.

Morel, N., Poëa-Guyon, S., Ammar, M.-R., and Vitale, N. (2014). La V-ATPase : un senseur de pH contrôlant la fusion membranaire. *Médecine/Sciences* *30*, 631–633.

- Morelle, W., Potelle, S., Witters, P., Wong, S., Climer, L., Lupashin, V., Matthijs, G., Gadomski, T., Jaeken, J., Cassiman, D., et al. (2017a). Galactose Supplementation in Patients With TMEM165-CDG Rescues the Glycosylation Defects. *J. Clin. Endocrinol. Metab.* *102*, 1375–1386.
- Morelle, W., Potelle, S., Witters, P., Wong, S., Climer, L., Lupashin, V., Matthijs, G., Gadomski, T., Jaeken, J., Cassiman, D., et al. (2017b). Galactose Supplementation in Patients With TMEM165-CDG Rescues the Glycosylation Defects. *J. Clin. Endocrinol. Metab.* *102*, 1375–1386.
- Moremen, K., Trimble, R.B., and Herscovics, A. (1994). Glycosidases of the asparagine-linked oligosaccharide processing pathway. *Glycobiology* *4*, 113–125.
- Mukhopadhyay, S., and Linstedt, A.D. (2011). Identification of a gain-of-function mutation in a Golgi P-type ATPase that enhances Mn<sup>2+</sup> efflux and protects against toxicity. *Proc. Natl. Acad. Sci.* *108*, 858–863.
- Mukhopadhyay, S., Bachert, C., Smith, D.R., and Linstedt, A.D. (2010a). Manganese-induced trafficking and turnover of the cis-Golgi glycoprotein GPP130. *Mol. Biol. Cell* *21*, 1282–1292.
- Mukhopadhyay, S., Bachert, C., Smith, D.R., and Linstedt, A.D. (2010b). Manganese-induced Trafficking and Turnover of the cis-Golgi Glycoprotein GPP130. *Mol. Biol. Cell* *21*, 1282–1292.
- Muroi, M., Shiragami, N., Nagao, K., Yamasaki, M., and Takatsuki, A. (1993). Folimycin(Concanamycin A), a Specific Inhibitor of V-ATPase, Blocks Intracellular Translocation of the Glycoprotein of Vesicular Stomatitis Virus before Arrival to the Golgi Apparatus. *Cell Struct. Funct.* *18*, 139–149.
- Murray, B.W., Takayama, S., Schultz, J., and Wong, C.H. (1996). Mechanism and specificity of human alpha-1,3-fucosyltransferase V. *Biochemistry* *35*, 11183–11195.
- Muthana, S.M., Campbell, C.T., and Gildersleeve, J.C. (2012). Modifications of glycans: biological significance and therapeutic opportunities. *ACS Chem. Biol.* *7*, 31–43.
- Nabi, I.R., Shankar, J., and Dennis, J.W. (2015). The galectin lattice at a glance. *J. Cell Sci.* *128*, 2213–2219.
- Nebert, D.W., and Liu, Z. (2019). SLC39A8 gene encoding a metal ion transporter: discovery and bench to bedside. *Hum. Genomics* *13*, 51.
- Need, A.C., Shashi, V., Hitomi, Y., Schoch, K., Shianna, K.V., McDonald, M.T., Meisler, M.H., and Goldstein, D.B. (2012). Clinical application of exome sequencing in undiagnosed genetic conditions. *J. Med. Genet.* *49*, 353–361.
- Neelamegham, S., and Liu, G. (2011). Systems glycobiology: biochemical reaction networks regulating glycan structure and function. *Glycobiology* *21*, 1541–1553.
- Nelson, M., Huggins, T., Licorish, R., Carroll, M.A., and Catapane, E.J. (2010). Effects of p-Aminosalicylic acid on the neurotoxicity of manganese on the dopaminergic innervation of the cilia of the lateral cells of the gill of the bivalve mollusc, *Crassostrea virginica*. *Comp. Biochem. Physiol. Toxicol. Pharmacol. CBP* *151*, 264–270.
- Ng, B.G., and Freeze, H.H. (2018). Perspectives on Glycosylation and Its Congenital Disorders. *Trends Genet.* *TIG* *34*, 466–476.
- Ng, B.G., Buckingham, K.J., Raymond, K., Kircher, M., Turner, E.H., He, M., Smith, J.D., Eroshkin, A., Szybowska, M., Losfeld, M.E., et al. (2013). Mosaicism of the UDP-galactose transporter SLC35A2 causes a congenital disorder of glycosylation. *Am. J. Hum. Genet.* *92*, 632–636.

- Nilsson, J., Halim, A., Larsson, E., Moslemi, A.-R., Oldfors, A., Larson, G., and Nilsson, J. (2014). LC-MS/MS characterization of combined glycogenin-1 and glycogenin-2 enzymatic activities reveals their self-glycosylation preferences. *Biochim. Biophys. Acta BBA - Proteins Proteomics* 1844, 398–405.
- Numata, M., and Orlowski, J. (2001). Molecular cloning and characterization of a novel (Na<sup>+</sup>,K<sup>+</sup>)/H<sup>+</sup> exchanger localized to the trans-Golgi network. *J. Biol. Chem.* 276, 17387–17394.
- Oda, Y., Hosokawa, N., Wada, I., and Nagata, K. (2003). EDEM as an acceptor of terminally misfolded glycoproteins released from calnexin. *Science* 299, 1394–1397.
- Ohtsubo, K., Takamatsu, S., Minowa, M.T., Yoshida, A., Takeuchi, M., and Marth, J.D. (2005). Dietary and genetic control of glucose transporter 2 glycosylation promotes insulin secretion in suppressing diabetes. *Cell* 123, 1307–1321.
- Okajima, T., Nakamura, Y., Uchikawa, M., Haslam, D.B., Numata, S.I., Furukawa, K., Urano, T., and Furukawa, K. (2000). Expression cloning of human globoside synthase cDNAs. Identification of beta 3Gal-T3 as UDP-N-acetylgalactosamine:globotriaosylceramide beta 1,3-N-acetylgalactosaminyltransferase. *J. Biol. Chem.* 275, 40498–40503.
- O’Neal, S.L., and Zheng, W. (2015a). Manganese Toxicity Upon Overexposure: a Decade in Review. *Curr. Environ. Health Rep.* 2, 315–328.
- O’Neal, S.L., and Zheng, W. (2015b). Manganese Toxicity Upon Overexposure: a Decade in Review. *Curr. Environ. Health Rep.* 2, 315–328.
- Oot, R.A., Couoh-Cardel, S., Sharma, S., Stam, N.J., and Wilkens, S. (2017). Breaking up and making up: The secret life of the vacuolar H<sup>+</sup> -ATPase. *Protein Sci. Publ. Protein Soc.* 26, 896–909.
- Orlean, P. (1990). Dolichol phosphate mannose synthase is required in vivo for glycosyl phosphatidylinositol membrane anchoring, O mannosylation, and N glycosylation of protein in *Saccharomyces cerevisiae*. *Mol. Cell. Biol.* 10, 5796–5805.
- Paesold-Burda, P., Maag, C., Troxler, H., Foulquier, F., Kleinert, P., Schnabel, S., Baumgartner, M., and Hennet, T. (2009). Deficiency in COG5 causes a moderate form of congenital disorders of glycosylation. *Hum. Mol. Genet.* 18, 4350–4356.
- Palma, A.S., Morais, V.A., Coelho, A.V., and Costa, J. (2004). Effect of the manganese ion on human alpha3/4 fucosyltransferase III activity. *Biometals Int. J. Role Met. Ions Biol. Biochem. Med.* 17, 35–43.
- Parekh, R.B., Dwek, R.A., Sutton, B.J., Fernandes, D.L., Leung, A., Stanworth, D., Rademacher, T.W., Mizuochi, T., Taniguchi, T., and Matsuta, K. (1985). Association of rheumatoid arthritis and primary osteoarthritis with changes in the glycosylation pattern of total serum IgG. *Nature* 316, 452–457.
- Park, J.H., Hoglebe, M., Grüneberg, M., DuChesne, I., von der Heiden, A.L., Reunert, J., Schlingmann, K.P., Boycott, K.M., Beaulieu, C.L., Mhanni, A.A., et al. (2015). SLC39A8 Deficiency: A Disorder of Manganese Transport and Glycosylation. *Am. J. Hum. Genet.* 97, 894–903.
- Park, J.H., Hoglebe, M., Fobker, M., Brackmann, R., Fiedler, B., Reunert, J., Rust, S., Tsiakas, K., Santer, R., Grüneberg, M., et al. (2018). SLC39A8 deficiency: biochemical correction and major clinical improvement by manganese therapy. *Genet. Med.* 20, 259–268.
- Parker, J.L., and Newstead, S. (2019). Gateway to the Golgi: molecular mechanisms of nucleotide sugar transporters. *Curr. Opin. Struct. Biol.* 57, 127–134.
- Parker, J.L., Corey, R.A., Stansfeld, P.J., and Newstead, S. (2019). Structural basis for substrate

specificity and regulation of nucleotide sugar transporters in the lipid bilayer. *Nat. Commun.* *10*, 4657.

Paroutis, P., Touret, N., and Grinstein, S. (2004). The pH of the Secretory Pathway: Measurement, Determinants, and Regulation. *Physiology* *19*, 207–215.

Parys, J.B., and Vervliet, T. (2020). New Insights in the IP3 Receptor and Its Regulation. *Adv. Exp. Med. Biol.* *1131*, 243–270.

Patterson, G.H., Hirschberg, K., Polishchuk, R.S., Gerlich, D., Phair, R.D., and Lippincott-Schwartz, J. (2008). Transport through the Golgi apparatus by rapid partitioning within a two-phase membrane system. *Cell* *133*, 1055–1067.

Peanne, R., Legrand, D., Duvet, S., Mir, A.-M., Matthijs, G., Rohrer, J., and Foulquier, F. (2011). Differential effects of lobe A and lobe B of the Conserved Oligomeric Golgi complex on the stability of  $\beta$ 1,4-galactosyltransferase 1 and  $\alpha$ 2,6-sialyltransferase 1. *Glycobiology* *21*, 864–876.

Pedersen, P.L., and Carafoli, E. (1987). Ion motive ATPases. I. Ubiquity, properties, and significance to cell function. *Trends Biochem. Sci.* *12*, 146–150.

Pedersen, L.C., Dong, J., Taniguchi, F., Kitagawa, H., Krahn, J.M., Pedersen, L.G., Sugahara, K., and Negishi, M. (2003). Crystal structure of an alpha 1,4-N-acetylhexosaminyltransferase (EXTL2), a member of the exostosin gene family involved in heparan sulfate biosynthesis. *J. Biol. Chem.* *278*, 14420–14428.

Peotter, J., Kasberg, W., Pustova, I., and Audhya, A. (2019). COPII-mediated trafficking at the ER/ERGIC interface. *Traffic* *20*, 491–503.

Peres, T.V., Parmalee, N.L., Martinez-Finley, E.J., and Aschner, M. (2016). Untangling the Manganese- $\alpha$ -Synuclein Web. *Front. Neurosci.* *10*.

Persson, M., Letts, J.A., Hosseini-Maaf, B., Borisova, S.N., Palcic, M.M., Evans, S.V., and Olsson, M.L. (2007). Structural effects of naturally occurring human blood group B galactosyltransferase mutations adjacent to the DXD motif. *J. Biol. Chem.* *282*, 9564–9570.

Pizzo, P., Lissandron, V., and Pozzan, T. (2010). The trans-golgi compartment: A new distinct intracellular Ca store. *Commun. Integr. Biol.* *3*, 462–464.

Pokrovskaya, I.D., Willett, R., Smith, R.D., Morelle, W., Kudlyk, T., and Lupashin, V.V. (2011). Conserved oligomeric Golgi complex specifically regulates the maintenance of Golgi glycosylation machinery. *Glycobiology* *21*, 1554–1569.

Potelle, S., Morelle, W., Dulary, E., Duvet, S., Vicogne, D., Spriet, C., Krzewinski-Recchi, M.-A., Morsomme, P., Jaeken, J., Matthijs, G., et al. (2016). Glycosylation abnormalities in Gdt1p/TMEM165 deficient cells result from a defect in Golgi manganese homeostasis. *Hum. Mol. Genet.* *25*, 1489–1500.

Potelle, S., Dulary, E., Climer, L., Duvet, S., Morelle, W., Vicogne, D., Lebredonchel, E., Houdou, M., Spriet, C., Krzewinski-Recchi, M.-A., et al. (2017). Manganese-induced turnover of TMEM165. *Biochem. J.* *474*, 1481–1493.

Preuss, D., Mulholland, J., Franzusoff, A., Segev, N., and Botstein, D. (1992). Characterization of the *Saccharomyces* Golgi complex through the cell cycle by immunoelectron microscopy. *Mol. Biol. Cell* *3*, 789–803.

Qasba, P.K., Ramakrishnan, B., and Boeggeman, E. (2008). Structure and function of beta -1,4-galactosyltransferase. *Curr. Drug Targets* *9*, 292–309.

- Quadri, M., Federico, A., Zhao, T., Breedveld, G.J., Battisti, C., Delnooz, C., Severijnen, L.-A., Di Toro Mammarella, L., Mignarri, A., Monti, L., et al. (2012). Mutations in SLC30A10 cause parkinsonism and dystonia with hypermanganesemia, polycythemia, and chronic liver disease. *Am. J. Hum. Genet.* *90*, 467–477.
- Quelhas, D., Jaeken, J., Fortuna, A., Azevedo, L., Bandeira, A., Matthijs, G., and Martins, E. (2018). RFT1-CDG: Absence of Epilepsy and Deafness in Two Patients with Novel Pathogenic Variants. In *JIMD Reports*, Volume 43, E. Morava, M. Baumgartner, M. Patterson, S. Rahman, J. Zschocke, and V. Peters, eds. (Berlin, Heidelberg: Springer Berlin Heidelberg), pp. 111–116.
- Rabouille, C., and Linstedt, A.D. (2016). GRASP: A Multitasking Tether. *Front. Cell Dev. Biol.* *4*.
- Rahil-Khazen, R., Bolann, B.J., Myking, A., and Ulvik, R.J. (2002). Multi-element analysis of trace element levels in human autopsy tissues by using inductively coupled atomic emission spectrometry technique (ICP-AES). *J. Trace Elem. Med. Biol. Organ Soc. Miner. Trace Elem. GMS* *16*, 15–25.
- Reinhardt, T.A., Lippolis, J.D., and Sacco, R.E. (2014a). The Ca<sup>2+</sup>/H<sup>+</sup> antiporter TMEM165 expression, localization in the developing, lactating and involuting mammary gland parallels the secretory pathway Ca<sup>2+</sup> ATPase (SPCA1). *Biochem. Biophys. Res. Commun.* *445*, 417–421.
- Reinhardt, T.A., Lippolis, J.D., and Sacco, R.E. (2014b). The Ca(2+)/H(+) antiporter TMEM165 expression, localization in the developing, lactating and involuting mammary gland parallels the secretory pathway Ca(2+) ATPase (SPCA1). *Biochem. Biophys. Res. Commun.* *445*, 417–421.
- Reynders, E., Foulquier, F., Leão Teles, E., Quelhas, D., Morelle, W., Rabouille, C., Annaert, W., and Matthijs, G. (2009). Golgi function and dysfunction in the first COG4-deficient CDG type II patient. *Hum. Mol. Genet.* *18*, 3244–3256.
- Rip, J.W., Rugar, C.A., Ravi, K., and Carroll, K.K. (1985). Distribution, metabolism and function of dolichol and polyprenols. *Prog. Lipid Res.* *24*, 269–309.
- Rivera-Mancía, S., Ríos, C., and Montes, S. (2011). Manganese accumulation in the CNS and associated pathologies. *Biometals Int. J. Role Met. Ions Biol. Biochem. Med.* *24*, 811–825.
- Rivinoja, A., Hassinen, A., Kokkonen, N., Kauppila, A., and Kellokumpu, S. (2009). Elevated Golgi pH impairs terminal N-glycosylation by inducing mislocalization of Golgi glycosyltransferases. *J. Cell. Physiol.* *220*, 144–154.
- Rivinoja, A., Pujol, F.M., Hassinen, A., and Kellokumpu, S. (2012). Golgi pH, its regulation and roles in human disease. *Ann. Med.* *44*, 542–554.
- Rizzo, R., Parashuraman, S., Mirabelli, P., Puri, C., Lucocq, J., and Luini, A. (2013). The dynamics of engineered resident proteins in the mammalian Golgi complex relies on cisternal maturation. *J. Cell Biol.* *201*, 1027–1036.
- Rosnoblet, C., Legrand, D., Demaegd, D., Hacine-Gherbi, H., de Bettignies, G., Bammens, R., Borrego, C., Duvet, S., Morsomme, P., Matthijs, G., et al. (2013). Impact of disease-causing mutations on TMEM165 subcellular localization, a recently identified protein involved in CDG-II. *Hum. Mol. Genet.* *22*, 2914–2928.
- Roth, J., and Zuber, C. (2017). Quality control of glycoprotein folding and ERAD: the role of N-glycan handling, EDEM1 and OS-9. *Histochem. Cell Biol.* *147*, 269–284.
- Rothman, J.E., and Wieland, F.T. (1996). Protein sorting by transport vesicles. *Science* *272*, 227–234.

- Rujano, M.A., Cannata Serio, M., Panasyuk, G., Péanne, R., Reunert, J., Rymen, D., Hauser, V., Park, J.H., Freisinger, P., Souche, E., et al. (2017). Mutations in the X-linked ATP6AP2 cause a glycosylation disorder with autophagic defects. *J. Exp. Med.* *214*, 3707–3729.
- Rutishauser, U. (1975). Cell-to-cell binding induced by different lectins. *J. Cell Biol.* *65*, 247–257.
- Rymen, D., Peanne, R., Millón, M.B., Race, V., Sturiale, L., Garozzo, D., Mills, P., Clayton, P., Asteggiano, C.G., Quelhas, D., et al. (2013). MAN1B1 deficiency: an unexpected CDG-II. *PLoS Genet.* *9*, e1003989.
- Sacher, M., Shahrzad, N., Kamel, H., and Milev, M.P. (2019). TRAPPopathies: An emerging set of disorders linked to variations in the genes encoding transport protein particle (TRAPP)-associated proteins. *Traffic* *20*, 5–26.
- Saito, F., Sakamoto, I., Kanatani, A., and Chiba, Y. (2016). Manganese ion concentration affects production of human core 3 O-glycan in *Saccharomyces cerevisiae*. *Biochim. Biophys. Acta* *1860*, 1809–1820.
- Schapiro, F.B., and Grinstein, S. (2000). Determinants of the pH of the Golgi Complex. *J. Biol. Chem.* *275*, 21025–21032.
- Schneider, A., Steinberger, I., Herdean, A., Gandini, C., Eisenhut, M., Kurz, S., Morper, A., Hoecker, N., Rühle, T., Labs, M., et al. (2016). The Evolutionarily Conserved Protein PHOTOSYNTHESIS AFFECTED MUTANT71 Is Required for Efficient Manganese Uptake at the Thylakoid Membrane in *Arabidopsis*. *Plant Cell* *28*, 892–910.
- Schulte Althoff, S., Grüneberg, M., Reunert, J., Park, J.H., Rust, S., Mühlhausen, C., Wada, Y., Santer, R., and Marquardt, T. (2015). TMEM165 Deficiency: Postnatal Changes in Glycosylation. In *JIMD Reports*, Volume 26, E. Morava, M. Baumgartner, M. Patterson, S. Rahman, J. Zschocke, and V. Peters, eds. (Berlin, Heidelberg: Springer Berlin Heidelberg), pp. 21–29.
- Schulte Althoff, S., Grüneberg, M., Reunert, J., Park, J.H., Rust, S., Mühlhausen, C., Wada, Y., Santer, R., and Marquardt, T. (2016). TMEM165 Deficiency: Postnatal Changes in Glycosylation. *JIMD Rep.* *26*, 21–29.
- Shaper, N.L., Shaper, J.H., Meuth, J.L., Fox, J.L., Chang, H., Kirsch, I.R., and Hollis, G.F. (1986). Bovine galactosyltransferase: identification of a clone by direct immunological screening of a cDNA expression library. *Proc. Natl. Acad. Sci. U. S. A.* *83*, 1573–1577.
- Shima, D.T., Cabrera-Poch, N., Pepperkok, R., and Warren, G. (1998). An ordered inheritance strategy for the Golgi apparatus: visualization of mitotic disassembly reveals a role for the mitotic spindle. *J. Cell Biol.* *141*, 955–966.
- Shinkawa, T., Nakamura, K., Yamane, N., Shoji-Hosaka, E., Kanda, Y., Sakurada, M., Uchida, K., Anazawa, H., Satoh, M., Yamasaki, M., et al. (2003). The absence of fucose but not the presence of galactose or bisecting N-acetylglucosamine of human IgG1 complex-type oligosaccharides shows the critical role of enhancing antibody-dependent cellular cytotoxicity. *J. Biol. Chem.* *278*, 3466–3473.
- Shrimal, S., Ng, B.G., Losfeld, M.-E., Gilmore, R., and Freeze, H.H. (2013). Mutations in STT3A and STT3B cause two congenital disorders of glycosylation. *Hum. Mol. Genet.* *22*, 4638–4645.
- Smith, R.D., and Lupashin, V.V. (2008). Role of the conserved oligomeric Golgi (COG) complex in protein glycosylation. *Carbohydr. Res.* *343*, 2024–2031.
- Snyder, N.A. (2018). Identification and analysis of Golgi transporters that provide homeostasis for

glycosylation and other Golgi processes. Johns Hopkins University.

Snyder, N.A., Stefan, C.P., Soroudi, C.T., Kim, A., Evangelista, C., and Cunningham, K.W. (2017). H<sup>+</sup> and Pi Byproducts of Glycosylation Affect Ca<sup>2+</sup> Homeostasis and Are Retrieved from the Golgi Complex by Homologs of TMEM165 and XPR1. *G3 Bethesda Md* 7, 3913–3924.

Snyder, N.A., Palmer, M.V., Reinhardt, T.A., and Cunningham, K.W. (2019). Milk biosynthesis requires the Golgi cation exchanger TMEM165. *J. Biol. Chem.* 294, 3181–3191.

Spahn, P.N., Hansen, A.H., Kol, S., Voldborg, B.G., and Lewis, N.E. (2017). Predictive glycoengineering of biosimilars using a Markov chain glycosylation model. *Biotechnol. J.* 12.

Steimle, B.L., Smith, F.M., and Kosman, D.J. (2019). The solute carriers ZIP8 and ZIP14 regulate manganese accumulation in brain microvascular endothelial cells and control brain manganese levels. *J. Biol. Chem.*

Suda, T., Kamiyama, S., Suzuki, M., Kikuchi, N., Nakayama, K.-I., Narimatsu, H., Jigami, Y., Aoki, T., and Nishihara, S. (2004). Molecular cloning and characterization of a human multisubstrate specific nucleotide-sugar transporter homologous to *Drosophila* fringe connection. *J. Biol. Chem.* 279, 26469–26474.

Sun, S., and Zhang, H. (2015). Identification and Validation of Atypical N-Glycosylation Sites. *Anal. Chem.* 87, 11948–11951.

Sundaramoorthy, V., Sultana, J.M., and Atkin, J.D. (2015). Golgi fragmentation in amyotrophic lateral sclerosis, an overview of possible triggers and consequences. *Front. Neurosci.* 9, 400.

Sun-Wada, G.-H., and Wada, Y. (2015). Role of vacuolar-type proton ATPase in signal transduction. *Biochim. Biophys. Acta BBA - Bioenerg.* 1847, 1166–1172.

Suzuki, T. (2016). Catabolism of N-glycoproteins in mammalian cells: Molecular mechanisms and genetic disorders related to the processes. *Mol. Aspects Med.* 51, 89–103.

Suzuki, T., Seko, A., Kitajima, K., Inoue, Y., and Inoue, S. (1993). Identification of Peptide:N-Glycanase Activity in Mammalian-Derived Cultured Cells. *Biochem. Biophys. Res. Commun.* 194, 1124–1130.

Suzuki, T., Huang, C., and Fujihira, H. (2016). The cytoplasmic peptide:N-glycanase (NGLY1) — Structure, expression and cellular functions. *Gene* 577, 1–7.

Tannous, A., Pisoni, G.B., Hebert, D.N., and Molinari, M. (2015). N-linked sugar-regulated protein folding and quality control in the ER. *Semin. Cell Dev. Biol.* 41, 79–89.

Tempel, W., Karaveg, K., Liu, Z.-J., Rose, J., Wang, B.-C., and Moremen, K.W. (2004). Structure of mouse Golgi alpha-mannosidase IA reveals the molecular basis for substrate specificity among class 1 (family 47 glycosylhydrolase) alpha1,2-mannosidases. *J. Biol. Chem.* 279, 29774–29786.

Thines, L., Deschamps, A., Sengottaiyan, P., Savel, O., Stribny, J., and Morsomme, P. (2018). The yeast protein Gdt1p transports Mn<sup>2+</sup> ions and thereby regulates manganese homeostasis in the Golgi. *J. Biol. Chem.* 293, 8048–8055.

Thompson, K.J., and Wessling-Resnick, M. (2019). ZIP14 is degraded in response to manganese exposure. *Biometals Int. J. Role Met. Ions Biol. Biochem. Med.*

Tsutsui, Y., Ramakrishnan, B., and Qasba, P.K. (2013). Crystal structures of  $\beta$ -1,4-galactosyltransferase 7 enzyme reveal conformational changes and substrate binding. *J. Biol. Chem.* 288, 31963–31970.

- Tu, L., and Banfield, D.K. (2010). Localization of Golgi-resident glycosyltransferases. *Cell. Mol. Life Sci.* *67*, 29–41.
- Tuschl, K., Clayton, P.T., Gospe, S.M., Gulab, S., Ibrahim, S., Singhi, P., Aulakh, R., Ribeiro, R.T., Barsottini, O.G., Zaki, M.S., et al. (2012). Syndrome of hepatic cirrhosis, dystonia, polycythemia, and hypermanganesemia caused by mutations in SLC30A10, a manganese transporter in man. *Am. J. Hum. Genet.* *90*, 457–466.
- Tuschl, K., Meyer, E., Valdivia, L.E., Zhao, N., Dadswell, C., Abdul-Sada, A., Hung, C.Y., Simpson, M.A., Chong, W.K., Jacques, T.S., et al. (2016). Mutations in SLC39A14 disrupt manganese homeostasis and cause childhood-onset parkinsonism-dystonia. *Nat. Commun.* *7*, 11601.
- Umana, P., Jean-Mairet, J., Moudry, R., Amstutz, H., and Bailey, J. (1999). Umana P, Jean-Mairet J, Moudry R, Amstutz H, Bailey J Engineered glycoforms of an antineuroblastoma IgG1 with optimized antibody-dependent cellular cytotoxic activity. *Nat Biotechnol* *17*: 176-180. *Nat. Biotechnol.* *17*, 176–180.
- Ungar, D., Oka, T., Brittle, E.E., Vasile, E., Lupashin, V.V., Chatterton, J.E., Heuser, J.E., Krieger, M., and Waters, M.G. (2002). Characterization of a mammalian Golgi-localized protein complex, COG, that is required for normal Golgi morphology and function. *J. Cell Biol.* *157*, 405–415.
- Valcke, M., Bourgault, M.-H., Haddad, S., Bouchard, M., Gauvin, D., and Levallois, P. (2018). Deriving A Drinking Water Guideline for A Non-Carcinogenic Contaminant: The Case of Manganese. *Int. J. Environ. Res. Public. Health* *15*.
- Van Damme, T., Gardeitchik, T., Mohamed, M., Guerrero-Castillo, S., Freisinger, P., Guillemyn, B., Kariminejad, A., Dalloyaux, D., van Kraaij, S., Lefeber, D.J., et al. (2017). Mutations in ATP6V1E1 or ATP6V1A Cause Autosomal-Recessive Cutis Laxa. *Am. J. Hum. Genet.* *100*, 216–227.
- Varki, A. (2017). Biological roles of glycans. *Glycobiology* *27*, 3–49.
- Varki, N.M., and Varki, A. (2007). Diversity in cell surface sialic acid presentations: implications for biology and disease. *Lab. Investig. J. Tech. Methods Pathol.* *87*, 851–857.
- Venkat, S., and Linstedt, A.D. (2017). Manganese-induced trafficking and turnover of GPP130 is mediated by sortilin. *Mol. Biol. Cell* mbc.E17-05-0326.
- de Vries, T., Storm, J., Rotteveel, F., Verdonk, G., van Duin, M., van den Eijnden, D.H., Joziase, D.H., and Bunschoten, H. (2001). Production of soluble human 3-fucosyltransferase (FucT VII) by membrane targeting and in vivo proteolysis. *Glycobiology* *11*, 711–717.
- Wandall, H.H., Hassan, H., Mirgorodskaya, E., Kristensen, A.K., Roepstorff, P., Bennett, E.P., Nielsen, P.A., Hollingsworth, M.A., Burchell, J., Taylor-Papadimitriou, J., et al. (1997). Substrate specificities of three members of the human UDP-N-acetyl-alpha-D-galactosamine:Polypeptide N-acetylgalactosaminyltransferase family, GalNAc-T1, -T2, and -T3. *J. Biol. Chem.* *272*, 23503–23514.
- Wang, L., Yu, H., Yang, G., Zhang, Y., Wang, W., Su, T., Ma, W., Yang, F., Chen, L., He, L., et al. (2015a). Correlation between bone mineral density and serum trace element contents of elderly males in Beijing urban area. *Int. J. Clin. Exp. Med.* *8*, 19250–19257.
- Wang, T.T., Maamary, J., Tan, G.S., Bournazos, S., Davis, C.W., Krammer, F., Schlesinger, S.J., Palese, P., Ahmed, R., and Ravetch, J.V. (2015b). Anti-HA Glycoforms Drive B Cell Affinity Selection and Determine Influenza Vaccine Efficacy. *Cell* *162*, 160–169.

- Wang, Y., Wang, J., Cheng, J., Xu, D., and Jiang, L. (2015c). Genetic interactions between the Golgi Ca<sup>2+</sup>/H<sup>+</sup> exchanger Gdt1 and the plasma compartment membrane calcium channel Cch1/Mid1 in the regulation of calcium homeostasis, stress response and virulence in *Candida albicans*. *FEMS Yeast Res.*
- Washburn, N., Schwab, I., Ortiz, D., Bhatnagar, N., Lansing, J.C., Medeiros, A., Tyler, S., Mekala, D., Cochran, E., Sarvaiya, H., et al. (2015). Controlled tetra-Fc sialylation of IVIg results in a drug candidate with consistent enhanced anti-inflammatory activity. *Proc. Natl. Acad. Sci. U. S. A.* *112*, E1297-1306.
- Welch, L.G., and Munro, S. (2019). A tale of short tails, through thick and thin: investigating the sorting mechanisms of Golgi enzymes. *FEBS Lett.* *593*, 2452–2465.
- Willer, T., Inamori, K.-I., Venzke, D., Harvey, C., Morgensen, G., Hara, Y., Beltrán Valero de Bernabé, D., Yu, L., Wright, K.M., and Campbell, K.P. (2014). The glucuronyltransferase B4GAT1 is required for initiation of LARGE-mediated  $\alpha$ -dystroglycan functional glycosylation. *ELife* *3*.
- Willett, R., Ungar, D., and Lupashin, V. (2013). The Golgi puppet master: COG complex at center stage of membrane trafficking interactions. *Histochem. Cell Biol.* *140*, 271–283.
- Willett, R., Blackburn, J.B., Climer, L., Pokrovskaya, I., Kudlyk, T., Wang, W., and Lupashin, V. (2016). COG lobe B sub-complex engages v-SNARE GS15 and functions via regulated interaction with lobe A sub-complex. *Sci. Rep.* *6*, 29139.
- Witkos, T.M., Chan, W.L., Joensuu, M., Rhiel, M., Pallister, E., Thomas-Oates, J., Mould, A.P., Mironov, A.A., Biot, C., Guerardel, Y., et al. (2019). GORAB scaffolds COPI at the trans-Golgi for efficient enzyme recycling and correct protein glycosylation. *Nat. Commun.* *10*, 127.
- Wu, X., Steet, R.A., Bohorov, O., Bakker, J., Newell, J., Krieger, M., Spaapen, L., Kornfeld, S., and Freeze, H.H. (2004). Mutation of the COG complex subunit gene COG7 causes a lethal congenital disorder. *Nat. Med.* *10*, 518–523.
- Yada, T., Gotoh, M., Sato, T., Shionyu, M., Go, M., Kaseyama, H., Iwasaki, H., Kikuchi, N., Kwon, Y.-D., Togayachi, A., et al. (2003). Chondroitin sulfate synthase-2. Molecular cloning and characterization of a novel human glycosyltransferase homologous to chondroitin sulfate glucuronyltransferase, which has dual enzymatic activities. *J. Biol. Chem.* *278*, 30235–30247.
- Yin, Z., Jiang, H., Lee, E.-S.Y., Ni, M., Erikson, K.M., Milatovic, D., Bowman, A.B., and Aschner, M. (2010). Ferroportin is a manganese-responsive protein that decreases manganese cytotoxicity and accumulation. *J. Neurochem.* *112*, 1190–1198.
- Yonekura, S.-I., and Toyoshima, C. (2016). Mn<sup>2+</sup> transport by Ca<sup>2+</sup> -ATPase of sarcoplasmic reticulum. *FEBS Lett.* *590*, 4650.
- Yuste-Checa, P., Medrano, C., Gámez, A., Desviat, L.R., Matthijs, G., Ugarte, M., Pérez-Cerdá, C., and Pérez, B. (2015). Antisense-mediated therapeutic pseudoexon skipping in TMEM165-CDG. *Clin. Genet.* *87*, 42–48.
- Zeevaert, R., Foulquier, F., Jaeken, J., and Matthijs, G. (2008). Deficiencies in subunits of the Conserved Oligomeric Golgi (COG) complex define a novel group of Congenital Disorders of Glycosylation. *Mol. Genet. Metab.* *93*, 15–21.
- Zeevaert, R., Foulquier, F., Cheillan, D., Cloix, I., Guffon, N., Sturiale, L., Garozzo, D., Matthijs, G., and Jaeken, J. (2009). A new mutation in COG7 extends the spectrum of COG subunit deficiencies. *Eur. J. Med. Genet.* *52*, 303–305.

- Zeevaert, R., de Zegher, F., Sturiale, L., Garozzo, D., Smet, M., Moens, M., Matthijs, G., and Jaeken, J. (2012). Bone Dysplasia as a Key Feature in Three Patients with a Novel Congenital Disorder of Glycosylation (CDG) Type II Due to a Deep Intronic Splice Mutation in TMEM165. *JIMD Rep.* 8, 145–152.
- Zeevaert, R., de Zegher, F., Sturiale, L., Garozzo, D., Smet, M., Moens, M., Matthijs, G., and Jaeken, J. (2013). Bone Dysplasia as a Key Feature in Three Patients with a Novel Congenital Disorder of Glycosylation (CDG) Type II Due to a Deep Intronic Splice Mutation in TMEM165. *JIMD Rep.* 8, 145–152.
- Zhang, S., Zhou, Z., and Fu, J. (2003). Effect of manganese chloride exposure on liver and brain mitochondria function in rats. *Environ. Res.* 93, 149–157.
- Zhao, N., and Enns, C.A. (2013). N-linked glycosylation is required for transferrin-induced stabilization of transferrin receptor 2, but not for transferrin binding or trafficking to the cell surface. *Biochemistry* 52, 3310–3319.
- Zhou, Q., and Qiu, H. (2019). The Mechanistic Impact of N-Glycosylation on Stability, Pharmacokinetics, and Immunogenicity of Therapeutic Proteins. *J. Pharm. Sci.* 108, 1366–1377.
- Zhou, D., Dinter, A., Gutiérrez Gallego, R., Kamerling, J.P., Vliegenthart, J.F., Berger, E.G., and Hennet, T. (1999). A beta-1,3-N-acetylglucosaminyltransferase with poly-N-acetyllactosamine synthase activity is structurally related to beta-1,3-galactosyltransferases. *Proc. Natl. Acad. Sci. U. S. A.* 96, 406–411.
- Zhu, X., and Kaverina, I. (2013). Golgi as an MTOC: making microtubules for its own good. *Histochem. Cell Biol.* 140, 361–367.
- Zofková, I., Nemcikova, P., and Matucha, P. (2013). Trace elements and bone health. *Clin. Chem. Lab. Med.* 0, 1–7.
- Zofkova, I., Davis, M., and Blahos, J. (2017). Trace elements have beneficial, as well as detrimental effects on bone homeostasis. *Physiol. Res.* 66, 391–402.
- Zogzas, C.E., and Mukhopadhyay, S. (2018). Putative metal binding site in the transmembrane domain of the manganese transporter SLC30A10 is different from that of related zinc transporters. *Metallomics* 10, 1053–1064.
- (1997). *The Golgi Apparatus* (Birkhäuser Basel).
- (2015). *Essentials of Glycobiology* (Cold Spring Harbor (NY): Cold Spring Harbor Laboratory Press).
- (2018). *Chemical glycobiology. Part B: Monitoring glycans and their interactions* (Cambridge: Academic Press).
- (2019). *Introduction to human nutrition* (Hoboken, NJ: Wiley).